



University of
**Southern
Queensland**

MECHANICAL, SETTING AND DURABILITY PROPERTIES OF HYBRID ALKALINE CEMENTS

A Thesis submitted by

Liqiang Wang

For the award of

Doctor of Philosophy

2024

ABSTRACT

Hybrid alkaline cement (HAC) is composed of a significant proportion of supplementary cementitious materials (SCMs) such as fly ash (FA) and/or granulated blast furnace slag (GBFS), a minor proportion of ordinary Portland cement (OPC), and alkali activators. A series of HACs were prepared with 10-30% OPC and 90-70%SCM using 0-8% alkali activator and curing at room temperature. The samples were then characterized using compressive strength, setting time, X-Ray Powder Diffraction (XRD), Scanning Electron Microscopy (SEM), ^1H Low-field NMR technology, isothermal conduction calorimetry, and thermogravimetric analysis (TG). The effects of type and dosage of activator used, and the ratio of raw materials on the mechanical, setting and durability properties of different HACs were studied. The results indicated that the setting times of HACs decreases with increasing alkali activator dosage. The HACs with high proportion of SCMs, cured at ambient temperature and activated by appropriate dosage of alkali activator perform similar or higher compressive strength than OPC. The compressive strength of HACs increases with the increasing of Na_2O dosage. By selecting the type of alkali activators and adjusting their dosage, controlling the proportion of OPC in HAC system, HAC can be prepared at ambient temperature, which is useful for engineering application. The durability properties of HAC concrete are indeed crucial for its application in the construction industry. The results indicate that HAC concrete demonstrates significantly greater resistance to harsh environmental conditions compared to OPC concrete, exhibiting robust performance in both early and later stages of development. HAC concrete exhibits clear advantages over OPC in terms of resistance to chloride corrosion, sulfate penetration and alkali–silica reaction (ASR)-induced expansions.

CERTIFICATION OF THESIS

I Liqiang Wang declare that the PhD Thesis entitled *Mechanical, Setting and Durability Properties of Hybrid Alkaline Cements* is not more than 100,000 words in length including quotes and exclusive of tables, figures, appendices, bibliography, references, and footnotes.

This Thesis is the work of Liqiang Wang except where otherwise acknowledged, with the majority of the contribution to the papers presented as a Thesis by Publication undertaken by the student. The work is original and has not previously been submitted for any other award, except where acknowledged.

Date: 25/01/2024

Endorsed by:

Hao Wang
Principle Supervisor

Zuhua Zhang
Associate Supervisor

Student and supervisors' signatures of endorsement are held at the University.

STATEMENT OF CONTRIBUTION

Papers 1:

Liqiang Wang, Zhang Zuhua, Lili Xue, Hao Wang. (2021). A review of recent progress in hybrid alkaline cement. Fourth International Conference on Chemically Activated Materials, Hefei, China, from 27 to 29 August 2021. Oral presentation.

Student contributed 80% to this paper. Collectively Zuhua Zhang, Lili Xue and Hao Wang contributed the remainder.

Papers 2:

Liqiang Wang, Zuhua Zhang, Hao Wang. (2024). Synthesis and mechanical properties of hybrid alkaline cements based on slag and Portland cement. Construction and Building Materials (submitted).

Student contributed 80% to this paper. Collectively Zuhua Zhang and Hao Wang contributed the remainder.

Papers 3:

Liqiang Wang, Zuhua Zhang, Hao Wang. (2024). The factors affecting setting properties of hybrid alkaline cement based on Portland cement and ground blast furnace slag. Composites Part B (submitted).

Student contributed 80% to this paper. Collectively Zuhua Zhang and Hao Wang contributed the remainder.

Papers 4:

Liqiang Wang, Zuhua Zhang, Hao Wang. (2024). Durability of hybrid alkaline cement based on Portland cement and ground blast furnace slag. Cement and Concrete Composites (submitted).

Student contributed 80% to this paper. Collectively Zuhua Zhang and Hao Wang

contributed the remainder.

Book chapters 1:

Liqiang Wang, Zuhua Zhang. (2024): Chapter 7: Research on the characteristics of functionalized Geopolymers, Geopolymer monograph. (In edition)

Student contributed 60% to this book chapters. Collectively Zuhua Zhang contributed the remainder.

ACKNOWLEDGEMENTS

I would like to thank all the people who have helped me throughout this research. In particular, I want to acknowledge my supervisors, Prof. Hao Wang, Dr. Zuhua, Zhang and Mr. Zhou. This is an amazing supervisor team with strong academic background on materials science, alkaline activated material, geopolymer chemistry, project management and engineering experiences. Zuhua Zhang gave a lot of assistances in the experimental environments and discussions on the research. Hao Wang gave me a lot of knowledge and advice on research and experimental methods. Mr. Zhou facilitated the projects of Jiaxing College and Jiaxing Longding Large Concrete Component Co., Ltd., and provided me with great assistance during the project implementation process. He provided the raw materials, testing equipment, testing site, and human resources required during the testing process, with his help, the project was successfully completed. Their advice, encouragement, and selfless assistances are valuable resources for promoting the success of this research.

At the same time, I would like to express my special gratitude to my classmate Lili Xue who taught me many methods related to experimental operations. She is also a staff member in the architectural engineering laboratory of Jiaxing University, and she provides many experimental equipment and instruments. I also participated in the development of many experimental plans and methods, and with her help, my experiment at Jiaxing College was successfully completed.

The support of the scholarships of both Jiaxing University and USQ are acknowledged. I would like to take this opportunity to express my gratitude to my wife Li Ma. During my studying for a PhD at USQ, she provided me with great help and encouragement, and made many sacrifices for our family. Thank you for your help and support on my life path over the past 16 years.

TABLE OF CONTENTS

ABSTRACT.....	i
CERTIFICATION OF THESIS.....	ii
STATEMENT OF CONTRIBUTION.....	iii
ACKNOWLEDGEMENTS.....	v
TABLE OF CONTENTS.....	vi
LIST OF TABLES.....	x
LIST OF FIGURES.....	xi
CHAPTER 1: INTRODUCTION.....	1
CHAPTER 2: LITERATURE REVIEW.....	5
2.1 Hybrid alkaline cement.....	5
2.2 Mechanical properties of HAC.....	6
2.3 Setting properties of HAC.....	7
2.4 Durability of HAC.....	9
2.5 Research gap.....	12
2.6 Aims and objectives of the research.....	13
CHAPTER 3: PAPER 1 – A REVIEW OF RECENT PROGRESS IN HYBRID ALKALINE CEMENT.....	14
3.1 Introduction.....	14
3.2 Hybrid alkaline cement system.....	15
3.2.1 Activators.....	15
3.2.2 Precursors.....	17
3.2.3 Chemical admixtures.....	17
3.3 Reaction mechanisms in HAC.....	18
3.3.1 OPC hydration vs Alkali Activation of SCMs.....	18
3.3.2 Reaction mechanisms in HAC.....	18
3.4 Properties of hybrid alkaline cement.....	20

3.4.1 Rheology.....	20
3.4.2 Setting time.....	20
3.4.3 Application.....	22
3.4.4 Durability.....	23
3.5 Conclusion.....	24
3.6 Perspectives for future research.....	24
CHAPTER 4: RESEARCH PLAN AND METHODOLOGY.....	26
4.1 Introduction.....	26
4.2 Research flow chart.....	26
4.3 Materials.....	27
4.3.1 Precursors.....	27
4.3.2 Alkali activator.....	28
4.3.3 Other materials.....	29
4.4 Procedures.....	29
4.4.1 XRD/XRF analysis for the phase determination.....	29
4.4.2 SEM analysis.....	30
4.4.3 ¹ H NMR analysis.....	30
4.4.4 TGA analysis.....	30
4.4.5 Hydration heat analysis.....	30
4.4.6 Procedures for mechanical testing.....	31
4.4.7 Setting time.....	31
4.4.8 Procedures for chloride permeability measurement.....	32
4.4.9 Procedures for sulphate attack resistance test.....	32
4.4.10 Resistance to the alkali-silica reaction.....	34
CHAPTER 5: PAPER 2 – SYNTHESIS AND MECHANICAL PROPERTIES OF HYBRID ALKALINE CEMENTS BASED ON SLAG AND PORTLAND CEMENT.....	35
5.1 Introduction.....	35
5.2 Experimental.....	37

5.3 Testing procedure.....	38
5.4 Results and discussion.....	38
5.4.1 Compressive strength.....	38
5.4.2 XRD analysis.....	41
5.4.3 ¹ H NMR analysis.....	45
5.4.4 Scanning Electron Microscopy analysis.....	48
5.5 Conclusions.....	53
CHAPTER 6: PAPER 3 – THE FACTORS AFFECTING SETTING PROPERTIES OF HYBRID ALKALINE CEMENT BASED ON PORTLAND CEMENT AND GROUND BLAST FURNACE SLAG.....	55
6.1 Introduction.....	55
6.2 Experimental.....	56
6.3 Testing procedure.....	57
6.4 Results and discussion.....	57
6.4.1 Setting time.....	57
6.4.2 Hydration heat analysis.....	60
6.4.3 ¹ H NMR analysis.....	63
6.4.4 TGA analysis of hydration products.....	67
6.4.5 SEM analysis of hydration products.....	72
6.5 Conclusions.....	76
CHAPTER 7: PAPER 4 – DURABILITY OF HYBRID ALKALINE CEMENT BASED ON PORTLAND CEMENT AND GROUND BLASET FURNACE SLAG.....	78
7.1 Introduction.....	78
7.2 Experimental.....	81
7.3 Testing procedure.....	82
7.4 Results and discussion.....	82
7.4.1 Compressive strength.....	83
7.4.2 Resistance to chloride penetration.....	85

7.4.3 Sulphate attack resistance.....	90
7.4.4 Alkali-aggregate reaction.....	95
7.5 Conclusions.....	102
CHAPTER 8: CONCLUSIONS AND RECOMMENDATIONS.....	104
8.1 Conclusions.....	104
8.2 Cautions in the development and applications of HACs.....	106
8.2.1 Fast initial setting of fresh HAC.....	106
8.2.2 Workability of HAC fresh concrete.....	107
8.3 Recommendations for the future research.....	107
8.3.1 Research on physics and chemistry of raw material.....	107
8.3.2 Research on rheology properties of HACs.....	108
8.3.3 Research on long term performance of HACs.....	109
8.3.4 Research on standardisation for HACs.....	109
REFERENCES.....	111
APPENDIX A ELEMENTAL DISTRIBUTION MAPPING OF HAC MORTAR BARS IN NaOH AT 80°C FOR 14 DAYS.....	120
APPENDIX B MECHANICAL STRENGTH PREPARATION AND TEST FOR HAC PAST.....	139
APPENDIX C ¹ H NMR TESTING OF ALL BINDER SYSTEMS DURING THE SETTING PERIOD.....	141
APPENDIX D POOR WORKABILITY OF HAC FRESH CONCRETE.....	142
APPENDIX E DURABILITY OF HAC ON COMPRESSIVE STRESSIV STRENGTH	143
APPENDIX F DURABILITY OF HAC TO CHLORIDE PENETRATION.....	145
APPENDIX G DURABILILTY OF HAC TO SULFHATE ATTACK.....	146
APPENDIX H DURABILITY OF HAC TO ALKALI-AGGREGATE REACTION.....	148

LIST OF TABLES

Table 3-1 Overview of hybrid alkaline cement system.....	16
Table 3-2 The influence factors on rheological properties of HAC.....	20
Table 3-3 Mix proportions of HAC.....	21
Table 3-4 The different precursors' setting time.....	21
Table 3-5 The different precursors' setting time.....	22
Table 4-1 Chemical composition of OPC and GBFS, determined by X-ray fluorescence.....	28
Table 4-2 Solid sodium silicate specifications.....	29
Table 5-1 Comparison of the three methods (Illustrated by fly ash).....	36
Table 5-2 Composition of HAC paste systems (wt.%).....	37
Table 6-1 Composition of binder systems (wt.%).....	56
Table 6-2 Elemental ratios of HACs with different dosage of Na ₂ O at initial setting time.....	75
Table 7-1 Composition of concrete systems.....	82
Table 7-2 Composition of mortar bar systems.....	82
Table 7-3 Total charge passed values of OPC and HACs at 28 days.....	87
Table 7-4 Total charge passed values of OPC and HACs at 91 days.....	87
Table 7-5 Sulphate attack resistance of OPC and HACs.....	93

LIST OF FIGURES

Figure 2-1 Comparison of the three methods (Illustrated by fly ash).....	6
Figure 3-1 (a) Flow curves of different admixtures (b) relative table (Criado, Palomo et al. 2009).....	17
Figure 3-2 (a) Evolution of the degree of hydration of tricalcium silicate vs. time (Roussel 2011) (b) C-S-H gel structure (García-Lodeiro, Maltseva et al. 2012).....	18
Figure 3-3 (a) Conceptual model for AAFA alkali activation (Garcia-Lodeiro, Donatello et al. 2016) (b) N-A-S-H gel structure (García-Lodeiro, Maltseva et al. 2012).....	18
Figure 3-4 Heat flow and cumulative heat of OPC, FA and M (HAC) systems with (a) and (b) W (water); (c) and (d) D1; (e) and (f) D2 (Garcia-Lodeiro, Fernandez-Jimenez et al. 2013).....	19
Figure 3-5 Activation models for HAC in D1 and D2 (Garcia-Lodeiro, Fernandez-Jimenez et al. 2013).....	19
Figure 3-6 (a) Yield stress of AAFA suspensions at different testing temperatures (b) relative table (Palacios, Alonso et al. 2019).....	20
Figure 3-7 Setting times of different proportions of HC.....	21
Figure 3-8 Schematic diagram of manufacturing process and stages of ternary hybrid cement (Qu, Martin et al. 2016).....	22
Figure 3-9 Structure and appearance of mortars exposed in Na ₂ SO ₄ solution...	23
Figure 3-10 Evolution of mortar bar expansion during the AAR test (S. Donatello1 2014).....	23
Figure 3-11 Evolution of PC and hybrid cement mortar strengths following immersion in aggressive solutions (S. Donatello1 2014).....	24
Figure 3-12 Visual changes in (a) hybrid alkaline cement and (b) control PC pastes after temperature exposure.....	24
Figure 4-1 Research flow chart of this thesis.....	28
Figure 4-2 XRD patterns of OPC and GBFS.....	28
Figure 4-3 HAC paste specimens preparation and mechanical test.....	31

Figure 4-4 HAC concrete specimens preparation and mechanical test.....	31
Figure 4-5 Initial setting time and final setting time test for HAC paste.....	32
Figure 4-6 Rapid chloride permeability test for HAC concrete.....	32
Figure 4-7 Sulphate attack resistance test.....	33
Figure 4-8 Resistance to the alkali-silica reaction test.....	34
Figure 5-1 Compressive strength of binder systems activated with 5% Na ₂ O....	39
Figure 5-2 Compressive strength of OPC and HACs activated by different dosage of alkali activator.....	41
Figure 5-3 XRD patterns of binders with different proportion of precursors, (a) 1 day of curing; (b) 7 days of curing; (c) 28 days of curing. A:C ₃ S; B:C ₂ S; C:Calcite; H: Hydrocaluminte; Ge:hydrated Gehlenite(C ₂ ASH ₈).....	43
Figure 5-4 XRD patterns of HACs with different dosage of Na ₂ O, (a) 1 day of curing; (b)7 days of curing; (c)28 days of curing. A:C ₃ S; B:C ₂ S; C:Calcite; H: Hydrocaluminte; Ge:hydrated Gehlenite(C ₂ ASH ₈).....	44
Figure 5-5 T ₂ vs. intensity during hydration of binders with different ratio of OPC (a) 1day;(b) 7 day; (c) 28day.....	45
Figure 5-6 T ₂ vs. intensity during hydration of binders with different dosage of Na ₂ O (a) 1day;(b) 7 day; (c) 28day.....	48
Figure 5-7 SEM images of binder systems activated with 5% Na ₂ O for 1 day....	48
Figure 5-8 SEM images of binder systems activated with 5% Na ₂ O for 7 days..	49
Figure 5-9 SEM images of binder systems activated with 5% Na ₂ O for 28 days.	49
Figure 5-10 SEM images of HACs with different dosage of Na ₂ O curing for 1 day.	50
Figure 5-11 SEM images of HACs with different dosage of Na ₂ O curing for 7 days.....	51
Figure 5-12 SEM images of HACs with different dosage of Na ₂ O curing for 28 days.....	52
Figure 6-1 (a) setting time of binder systems; (b) setting time of HACs with different dosage of Na ₂ O content.....	58
Figure 6-2 (a) Heat flow; (b) Cumulative heat of binders with different ratio of OPC.....	61

Figure 6-3 (a) Heat flow; (b) Cumulative heat of HACs with different dosage of alkali activator.....	62
Figure 6-4 T_2 vs. intensity during hydration of binders (a) 90GBFS-10OPC;(b) 80GBFS-20OPC; (c)70GBFS-30OPC; (d) 100OPC; (e)100GBFS.....	65
Figure 6-5 T_2 vs. intensity during hydration of HACs with different dosage of alkali activator.....	67
Figure 6-6 (a)TG and (b)DTG of hydrated binder systems at initial setting time.	68
Figure 6-7 (a)TG and (b)DTG of hydrated binder systems at final setting time..	68
Figure 6-8 (a)TG and (b)DTG of hydrated HACs activated by different dosage of alkali activator at initial setting time.....	70
Figure 6-9 (a)TG and (b)DTG of hydrated HACs activated by different dosage of alkali activator at final setting time.....	71
Figure 6-10 SEM images of binder systems activated with 5% Na_2O at initial setting.....	73
Figure 6-11 SEM images of binder systems activated with 5% Na_2O at final setting.....	73
Figure 6-12 SEM images of HACs with different dosage of Na_2O at initial setting.	74
Figure 6-13 SEM images of HACs with different dosage of Na_2O at final setting.	75
Figure 7-1 Compressive strength of HAC systems activated with 5% Na_2O	83
Figure 7-2 Compressive strength of OPC and HACs activated by different dosage of alkali activator.....	85
Figure 7-3 T_2 vs signal intensity of binders with ratio of OPC before and after chloride penetration.....	89
Figure 7-4 T_2 vs signal intensity of HACs with different dosage of Na_2O content before and after chloride penetration.....	90
Figure 7-5 XRD patterns of binders with different ratio of OPC before and after sulphate attack. (a) before; (b) after. A: C_3S ; B: C_2S ; C:Calcite; E:ettrigite; H: Hydrocaluminte; Ge:hydrated Gehlenite(C_2ASH_8).....	94
Figure 7-6 XRD patterns of HACs with different dosage of Na_2O content before	

and after sulphate attack. (a) before; (b) after. A:C ₃ S; B:C ₂ S; C:Calcite; E:ettrigite; H: Hydrocaluminte; Ge:hydrated Gehlenite(C ₂ ASH ₈).....	95
Figure 7-7 Longitudinal expansions of the mortar bars with different ratio of OPC in 1N NaOH at 80°C.....	97
Figure 7-8 Mortar bars of HAC with different dosage of Na ₂ O content in solution of 1N NaOH at 80°C.....	99
Figure 7-9 SEM images of mortar bars with different ratio of OPC in 1N NaOH at 80°C for 14 days.....	100
Figure 7-10 Element distribution in the matrix of mortar bars with different ratio of OPC.....	101
Figure 7-11 SEM images of HAC mortar bars with different Na ₂ O content in 1N NaOH at 80°C for 14 days.....	101
Figure 7-12 Element distribution in the matrix of HAC mortar bars with different Na ₂ O content.....	102
Figure 8-1 Key Knowledge Concept Map.....	110
Figure A-1 Elemental distribution mapping of HAC mortar bars with 0% Na ₂ O content.....	122
Figure A-2 Elemental distribution mapping of HAC mortar bars with 2% Na ₂ O content.....	124
Figure A-3 Elemental distribution mapping of HAC mortar bars with 4% Na ₂ O content.....	126
Figure A-4 Elemental distribution mapping of HAC mortar bars with 5% Na ₂ O content.....	128
Figure A-5 Elemental distribution mapping of HAC mortar bars with 8% Na ₂ O content.....	130
Figure A-6 Elemental distribution mapping of 80GBFS-20OPC mortar bars with 5% Na ₂ O content.....	132
Figure A-7 Elemental distribution mapping of 70GBFS-30OPC mortar bars with 5% Na ₂ O content.....	134
Figure A-8 Elemental distribution mapping of 100OPC mortar bars with 5% Na ₂ O content.....	136
Figure A-9 Elemental distribution mapping of 100GBFS mortar bars with 5%	

Na ₂ O content.....	138
Figure B- 1 Mechanical strength preparation and test for HAC past.....	140
Figure C- 1 ¹ H NMR testing of all binder systems during the setting period.....	141
Figure D- 1 Poor workability of HAC fresh concrete.....	142
Figure E- 1 Durability of hybrid alkaline cement on compressive strength.....	144
Figure F- 1 Durability of hybrid alkaline cement to chloride penetration.....	145
Figure G- 1 Durability of hybrid alkaline cement to sulphate attack.....	147
Figure H- 1 Durability of hybrid alkaline cement to alkali-aggregate reaction....	149

CHAPTER 1: INTRODUCTION

Ground blast furnace slag (GBFS) is a by-product of the iron industry, and the production of 1 ton of iron releases approximately 0.5 ton of GBFS. The utilization of GBFS as a supplementary cementitious material is considered a sustainable approach to address energy shortages and reduce greenhouse gas emissions, providing an eco-efficient alternative to ordinary Portland Cement (OPC). While GBFS has been successfully utilized as supplementary cementitious materials (SCMs) in blended cement, achieving replacement ratios of 70-80% with OPC, challenges are encountered with high replacement ratios. Blended cement compositions with a high proportion of GBFS may experience issues such as low early-age strength, uncontrolled setting times, and compromised durability properties in aggressive environments. These challenges highlight the importance of carefully optimizing the composition of blended cement to ensure the desired performance characteristics are maintained.

Hybrid Alkaline Cement (HAC) consists of a high proportion of SCMs, such as FA and or GBFS, a low proportion of OPC and alkali activator. The applications of HAC as pavement and masonry blocks have been reported. Hybrid alkaline cement (HAC) stands out as a promising alternative to Ordinary Portland Cement (OPC) due to its comparable or superior performance, reduced need for alkali activators compared to alkali-activated materials (AAM), and the ability to cure at ambient temperatures. The lower dependence on alkali activators contributes to the economic and safety aspects of HAC application. Moreover, the capacity to harden at ambient temperatures distinguishes HAC from alkali-activated fly ash, which typically requires moderately high curing temperatures (60°C to 90°C) in alkali-activated materials (AAM). These characteristics position HAC as an environmentally friendly and economically viable option in the construction industry. HAC emerges as a promising alternative to OPC due to its unique properties. Unlike OPC, HAC requires an alkali activator for pozzolanic reactions, but it demands less activator compared to alkali-activated materials. This makes HAC both safer and more economical. With comparable performance to OPC and the ability to cure at ambient temperatures, HAC stands out as an eco-efficient and cost-effective building material.

The factors influencing the compressive strength of HAC are not fully

understood, necessitating further research for a comprehensive understanding and improved application in construction. The incorporation of a chemical activator enhances the hydration kinetics and augments the mechanical strength of HAC. However, for HAC formulations aiming for high mechanical strength, exceeding 60 MPa, challenges arise in terms of poor workability characterized by rapid setting and elevated viscosity. The characteristics of poor workability, rapid setting, and high viscosity in HAC formulations with high mechanical strength, exceeding 60MPa, pose challenges in effectively pumping or casting the material. The ideal initial setting time of fresh concrete significantly influences its mixing and pumping process, as well as impacting its strength, durability, and surface quality. The durability of HAC is crucial for its successful application in the construction industry. Despite its potential, there are limited reports on the practical engineering applications of this new generation of binders. Several challenges need to be addressed, including the instability of raw materials, rapid setting times, high viscosity, cost implications associated with alkali activators, and the absence of industry norms. The concerns about the durability properties of HAC concrete have garnered widespread attention, emphasizing the need for further research and development in this area.

(1) this study investigates the development of mechanical strength in HAC under various influencing factors, along with changes in its gel phase and mineral phase. Additionally, it examines the trend of capillary water or gel water during HAC hydration. The study explores the impact of raw material mix proportions and alkali activator dosage on the mechanical strength development of HAC, providing a theoretical basis for the compressive strength development patterns of HAC under different parameters, and further offering a reference for the design and application of HAC..

(2) setting time, particularly the initial setting time, affects the workability of HAC and has a significant important on the quality after hardening. This study uses the heat of hydration testing method to study the exothermic behavior during the HAC hydration process. It employs ^1H NMR technology to investigate the changes in capillary water and gel water during hydration and analyzes the product phases after initial and final setting. This provides a theoretical foundation for understanding the effects of different parameters on the setting and hardening of HAC.

(3) this study employs several accelerated testing methods to study the impact

of various factors on the durability of HAC. It analyzes the phases and rates of formation of erosion products under different influencing factors. Mechanistic studies on durability can provide a theoretical basis for the application of HAC in extreme corrosive environments.

In Chapter 3, the literature review discussed greenhouse gas emissions and energy consumption in OPC and concrete industry. To address these issues, three methods were introduced. The first method involves the partial replacement (usually below 25%) of OPC with supplementary cementitious materials (SCMs). Another option is to develop alkali-activated material (AAM), which is an OPC-free solid material. The third option is a new type of binder known as HAC. As a new generation of low-carbon binder, this section provides an overview of HAC systems and discusses fundamental reaction mechanisms and engineering properties associated with HAC.

The literature review highlighted some of the issues in the application of HAC concrete and outlined the importance of developing more comprehensive and better understanding of the factors, such as raw materials, alkali activators on mechanical, setting and durability properties of HAC system.

In Chapter 4, the raw materials used in this research were reviewed, and some other materials and alkali activator used in this research was outlined. The characterization procedures for the materials and the HAC system were described. In particular, the test methods for HAC paste, mortar and concrete were introduced in detail.

Chapter 5 explored the factors affecting the mechanical properties of HAC systems. The effect of the ration of raw materials, the type and dosage of alkali activator on mechanical properties were studied. By adjusting the ratio of raw materials, and activated by alkali activator, HACs exhibit different mechanical strength, especially at early age. The type and dosage of alkali activator played an important role on mechanical properties of HAC systems. By selecting suitable alkali activators and adjusting the dosage of them, HAC can be prepared with different mechanical properties.

In Chapter 6, the factors affecting the setting properties of HAC systems were investigated. The composition of the precursors, the type and dosage of alkali activator on the effect of setting properties of HAC paste were explored. when HAC

was designed with high mechanical strength, HAC often suffers from poor workability with fast setting and high viscosity, which make it difficult to pump or cast. The proportion of OPC in HAC system had a significant impact on the setting time. The setting times of HACs decreases with the increasing of alkali activator dosage. With the increasing of Na_2O content, while the compressive of HACs increases with the increasing of Na_2O dosage. By selecting the type of alkali activators and adjusting the dosage of them, associated adjust the proportion of OPC in HAC system, HAC can be prepared at possible temperature in practical engineering.

Chapter 7 investigates the effect of the ratio of OPC and the dosage of alkali activator on durability properties of hybrid alkaline cement concrete. After understanding the mechanical and setting properties of HAC paste and mortars, durability of HAC concrete is of vital importance for its application in the construction industry. Chloride ions could cause corrosion of steel bars in concrete, which can cause oxidation and localized damage to the passivation film of the steel bars. Sulfate ions penetrate and react with Ca and Al species in cement, forming expansion products such as ettringite. HAC suffers from higher alkalis content than OPC, which increases the risk of potential alkali-silica reaction (ASR)-induced expansions. To study the durability issues faced by the application of HAC in the construction industry, the effect of dosage of Na_2O content on compressive strength, chloride permeability, sulphate attack resistance and resistance to the alkali-silica reaction of hybrid alkaline cement concrete are investigated. The outcome proved that by adding an appropriate dosage of alkali activator, HAC concrete exhibits much stronger resistance in aggressive environment than OPC concrete, both at early age and later ages.

In Chapter 8, the conclusions of the research undertaken in this thesis are drawn. Some issues that need to be noted in HAC production and engineering applications are mentioned. Perspectives for future research and application are presented for HAC production.

CHAPTER 2: LITERATURE REVIEW

2.1 Hybrid alkaline cement

At present, ordinary Portland Cement (OPC) stands as the cornerstone of construction materials. Its benefits are manifold, boasting high mechanical strength, adaptable workability, widespread availability, extensive use, commendable fire resistance, straightforward maintenance, and the continual evolution of polymer admixtures. With a rich history spanning over 160 years, OPC demonstrates outstanding performance and exceptional value for investment (Garcia-Lodeiro et al., 2012, Palomo et al., 2013a, Fernandez-Jimenez et al., 2013a, Provis et al., 2015a, Zhang et al., 2014). Nevertheless, the production of ordinary Portland Cement (OPC) has raised significant environmental and energy concerns (Monteiro et al., 2017, Cao et al., 2021). Numerous efforts have been made to decrease the production of OPC. One of the primary strategies involves implementing partial substitution of OPC with supplementary cementitious materials (SCMs) (Samad and Shah, 2017, Juenger et al., 2015, Lothenbach et al., 2011b, Cao et al., 2021, Fu et al., 2020). Another avenue is the development of alternative binders, such as alkali-activated materials (AAM), which offer a solid, OPC-free alternative (Provis and Bernal, 2014, Provis et al., 2015b, Shi et al., 2011a). Lastly, the concept of HAC has been introduced (Fernandez-Jimenez et al., 2013b, García-Lodeiro et al., 2012, Palomo et al., 2013b, Palomo et al., 2007)

HAC comprises a substantial portion of supplementary cementitious materials (SCMs) like fly ash (FA) and/or granulated blast furnace slag (GBFS), alongside a minimal proportion of OPC and alkali activators. The research group led by Prof. Palomo has reported the utilization of HAC in applications such as pavement construction and manufacturing masonry blocks (Fernandez-Jimenez et al., 2013a). HAC demonstrates performance comparable to OPC while requiring less alkali activator than alkali-activated materials (AAM) (Fernandez-Jimenez et al., 2013b, García-Lodeiro et al., 2012, Palomo et al., 2013b, Donatello et al., 2013b). Additionally, it can solidify at ambient temperatures, whereas AAM typically necessitates curing temperatures as high as 60°C to 90°C (Fernández-Jiménez and Palomo, 2007, Garcia-Lodeiro et al., 2016b). In comparison to OPC, HACs rely on alkali activators to initiate their pozzolanic reaction. However, when compared to

AAMs, HACs require a lower dosage of alkali activator, enhancing their safety and economic feasibility in various applications. A comprehensive overview of the disparities among these three binders is presented in Figure 2-1 (Garcia-Lodeiro et al., 2016b).

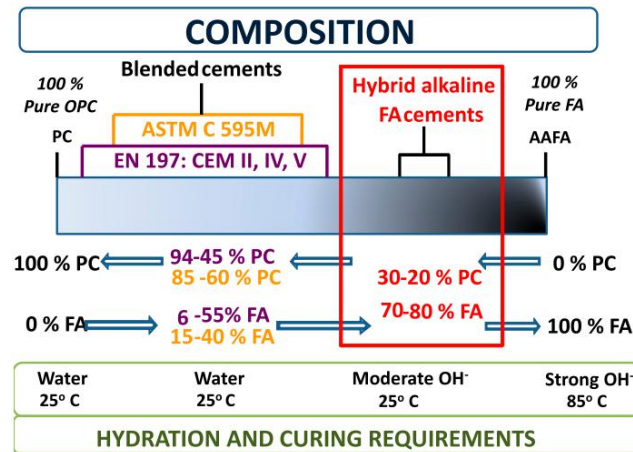


Figure 2-1 Comparison of the three methods (Illustrated by fly ash).

2.2 Mechanical properties of HAC

The complete understanding of the mechanical strength development mechanism of HAC is still lacking, and a systematic study of the factors influencing the compressive strength of HAC has yet to be conducted. Mahya Askarian et al. (Askarian et al., 2018) conducted research on one-part hybrid OPC-geopolymer concrete, examining various ratios of raw materials. Their findings highlighted the crucial impact of Na_2O content dosage on workability, setting time, and mechanical properties of the concrete. Salaheddine Alahrache et al. (Alahrache et al., 2016b) examined the strength development of hybrid alkaline cements (HACs) comprising 30% OPC and 70% fly ash (FA), activated using various activators including Na_2CO_3 , Na_2SiO_3 , K_2SiO_3 , $\text{Na}_2\text{Oxalate}$, and $\text{K}_3\text{Citrate}$. Their study concluded that the choice of alkali activator notably influences the strength development of HACs. Some research (Garcia-Lodeiro et al., 2016b, Garcia-Lodeiro et al., 2013b, A. Palomo, 2007) have proposed descriptive models for the hydration of low-Ca hybrid alkaline cement (HAC) systems. These models encompass both the conventional hydration processes of ordinary Portland cement (OPC) and the alkali activation of fly ash. The findings suggest that N–A–S–H and C–S–H gels, initially formed at early ages, evolve into C–A–S–H structures as the material ages. Martin T. Palou et al. (Palou et al., 2016)

investigated the influence of curing temperature on blended cements. Their study revealed that raising the curing temperature accelerated the initial hydration rate; however, the hydration rate at later ages was diminished. Escalante-Garcia et al. (Escalante-Garcia and Sharp, 2000) reported that the impact of curing temperature on the hydration rate of blended cements varies depending on the alterations in cement components.

The effects of raw materials and alkali activators on the microstructural evolution and strength development mechanisms of HAC systems are not yet understood.. Previous research has predominantly concentrated on low-Ca HAC systems, with compressive strength typically remaining low in both early and late stages, often below 50 MPa (Palomo, 2007, Donatello et al., 2013a, Mejia et al., 2015, Alahrache et al., 2016b, Garcia-Lodeiro et al., 2017, Askarian et al., 2018). It is widely acknowledged that the alkali activator plays a pivotal role in alkali-activated materials (Alahrache et al., 2016b, Garcia-Lodeiro et al., 2016b, Sedira and Castro-Gomes, 2020). Studying the impact of alkali activator dosage on the mechanical properties of HAC is imperative. Additionally, the curing conditions represent a crucial parameter for alkali-activated materials, particularly in terms of compressive strength development, especially during the early stages (Qu et al., 2016). Analyzing the microstructure of HACs with varying alkali activator and precursor dosages is advantageous for gaining precise insights into their mechanical strength development. Such investigations are crucial for offering guidance in the design and application of HACs in construction. Understanding the mechanical strength development mechanisms of different HAC systems is essential for providing valuable references in construction design and application.

2.3 Setting properties of HAC

Ordinary Portland Cement (OPC) has long been a cornerstone of construction, playing an undeniable role in human history. However, its production poses significant energy and environmental challenges, requiring temperatures as high as 1,450°C and relying on raw materials that disrupt natural landscapes and ecosystems. Due to greenhouse emission concerns, there is a global push to find more environmentally sustainable alternatives to OPC (Shi et al., 2019a, Palacios et al., 2008). Blending cement with a high ratio of substitutive materials often

encounters challenges such as low early-age strength and unpredictable setting times (Beushausen et al., 2012).

Hybrid alkaline cement (HAC) is widely recognized as a new generation of low-carbon binders. It typically comprises a high proportion of supplementary cementitious materials (SCMs), a low proportion of ordinary Portland cement (OPC), and is activated by suitable alkali activators. HAC effectively combines the benefits of both alkaline activated materials (AAM) and blended cement. It demonstrates comparable or even superior mechanical strength and exceptional durability performance (Garcia-Lodeiro et al., 2013b, Xue et al., 2021b, Fernandez-Jimenez et al., 2013a, S. Donatello¹, 2014). The addition of a chemical activator indeed accelerates the hydration kinetics and boosts the mechanical strength of HAC. However, when HAC is formulated to achieve high mechanical strength (greater than 60MPa) for specific applications, it often encounters challenges in workability. Issues such as rapid setting and high viscosity make it difficult to pump or cast. For instance, in a HAC paste consisting of 70% fly ash and 30% OPC activated by $\text{Na}_2\text{O} \cdot n\text{SiO}_3$ and NaOH, the initial and final setting times are 13 and 31 minutes, respectively. In comparison, the initial and final setting times for OPC typically range around 138 and 196 minutes, respectively (Suwan et al., 2014). The optimal initial setting time of fresh concrete plays a crucial role in its mixing and pumping process. It also significantly affects its strength, durability, and surface quality.

Li et al.(Li et al., 2019) investigated a method to control setting time by adjusting the composition of alkali activator ions and the extent of silicate polymerization in alkaline-activated slag. They varied the dosage and alkali modulus of the alkali activator and concluded that appropriately designed activators can achieve both desired setting time and satisfactory compressive strength. Chang et al.(Chang, 2003) investigated the setting properties of slag activated by sodium silicate and observed that the pH value of the reaction solution, as well as the dosage and alkali modulus of the alkali activator, significantly influence these properties. Pilehvar et al.(Pilehvar et al., 2020) noted that the setting times of both ordinary Portland cement (OPC) and alkali-activated materials (AAM) paste decreased with increasing temperature. This phenomenon was attributed to the accelerated hydration of OPC and geopolymerization of AAM at higher temperatures. Furthermore, other studies have found that the ratio of raw materials in hybrid

alkaline cement (HAC) systems significantly influences their setting characteristics (Balun and Karatas, 2023). As of now, the factors influencing the setting characteristics of hybrid alkaline cement (HAC) systems remain non-comprehensive. Previous research has predominantly concentrated on low-calcium-based HAC systems, with limited reports on HAC systems exhibiting high mechanical strength and controlled setting times (Millan-Corrales et al., 2020, Fernandez-Jimenez et al., 2019, Alahrache et al., 2016b, Donatello et al., 2013a, Qu et al., 2016, Askarian et al., 2018, Sanchez-Herrero et al., 2019).

2.4 Durability of HAC

Hybrid alkaline cements (HACs) are composed of a significant proportion of supplementary cementitious materials (SCMs), a reduced amount of ordinary Portland cement (OPC), and are activated by chemical activators at either ambient or elevated temperatures (A. Palomo, 2007, Garcia-Lodeiro et al., 2012, Palomo et al., 2013a). Indeed, they are widely recognized as a new generation of low-carbon binders for the construction industry (Shi et al., 2019b, Xue et al., 2021b, Shi et al., 2011b). The production of these new types of binders aims to reduce energy consumption and lower carbon dioxide emissions. Meanwhile, hybrid alkaline cements (HACs) exhibit outstanding compressive strength, particularly in early stages, and can cure at ambient temperatures. However, reports regarding the practical engineering applications of these new binders remain scarce. Numerous challenges persist, including the instability of raw materials, rapid setting times, high viscosity, cost implications associated with alkali activators, and the absence of industry standards (Shi et al., 2011b, Shi et al., 2019b). Indeed, the durability properties of HAC concrete have attracted significant attention and concern within the construction industry.

Chloride ions are known to induce corrosion in steel reinforcement bars embedded in concrete structures. This corrosion process can lead to oxidation and localized damage to the passivation film of the steel bars, compromising the structural integrity of the concrete (Wang et al., 2019). Sulfate ions have the ability to penetrate concrete and react with calcium (Ca) and aluminum (Al) species present in the cement matrix. This reaction results in the formation of expansive products such as ettringite ($\text{Ca}_6[\text{Al}(\text{OH})_6]_2(\text{SO}_4)_3 \cdot 26\text{H}_2\text{O}$) and gypsum ($\text{CaSO}_4 \cdot 2\text{H}_2\text{O}$) (Yang et al.,

2022, Alexander et al., 2013). Alkali-activated materials (AAMs) typically contain higher levels of alkalis compared to Portland clinkers. This elevated alkali content heightens the risk of potential alkali-silica reaction (ASR)-induced expansions in concrete structures (Fernández-Jiménez et al., 2007, Provis et al., 2015a).

Alkali-activated materials (AAMs) typically exhibit stronger resistance to sulfate attack and chloride corrosion compared to ordinary Portland cement (OPC). This is attributed to the three-dimensional structure of N-A-S-H or C-A-S-H gel in AAMs, which is more compact and less susceptible to ingress of harmful ions than the two-dimensional structure of C-A-H gel in OPC (Monticelli et al., 2016b, Monticelli et al., 2016a, Babaei and Castel, 2016, Tennakoon et al., 2017). In alkali-activated materials (AAMs), the penetration of chloride ions is notably influenced by the Na_2O content. Increasing the dosage of Na_2O tends to decrease chloride penetration into the material (Chi, 2012, Lee and Lee, 2016). Some researchers posit that the superior sulfate resistance of alkali-activated materials (AAMs) may be attributed to the absence of calcium hydroxide ($\text{Ca}(\text{OH})_2$) in the activation products of AAMs (Donatello et al., 2013b, S. Donatello¹, 2014, Janotka et al., 2014, Bačuvčík et al., 2018). Indeed, the question of whether alkali-silica reaction (ASR)-induced expansion occurs in alkali-activated materials (AAMs) has been a topic of ongoing debate and controversy in the research community. San Nicolas et al. (San Nicolas et al., 2014) conducted a study on high-calcium based alkali-activated materials (AAM) concretes aged for seven years. Their research revealed that slag-based AAMs exhibit excellent durability as they age, and no evidence of alkali-silica reaction (ASR)-induced expansions was found. Shi et al. (Shi et al., 2015b) assert that alkali-aggregate reaction (AAR) can lead to destructive expansion in alkali-activated material (AAM) mortars and concretes. They further note that AAR is influenced by factors such as the dosage and type of alkali activators, the nature of precursors used, and the testing methods employed.

Up to now, research on chloride penetration in HAC has been relatively limited. Rivera, et al. (Rivera et al., 2014) suggested that chloride penetration is significantly influenced by the raw materials used in hybrid alkaline cement (HAC) systems. Typically, HACs based on high-calcium materials exhibit higher resistance to chloride penetration compared to those based on low-calcium materials. This difference is attributed to variations in the composition of C-S-H/C-A-S-H gel and N-A-S-H gel

produced in the two types of HAC systems. The coexistence of C-S-H/C-A-S-H gel is denser and deeper than N-A-S-H gel, resulting in increased chloride penetration resistance. Moreover, the denser gels are associated with enhanced mechanical strength in high-calcium materials based HACs. Garcia-Lodeiro et al. (Garcia-Lodeiro et al., 2016a) highlighted that chloride content in hybrid alkaline cement (HAC) systems, particularly those blended with fly ash, bottom ash, and OPC clinker, exceeded existing standards. This elevated chloride concentration could potentially lead to corrosion of steel bars in concrete, especially in scenarios where HACs are utilized in marine or offshore structures. Hence, there is a pressing need for systematic and comprehensive studies to understand the factors influencing chloride penetration in HAC systems.

Indeed, several studies have reported the remarkable durability of hybrid alkaline cement (HAC) binders in diverse aggressive environments. These include resistance to high temperatures, sulfate attack, chloride penetration, and alkali-aggregate reaction (Fernandez-Jimenez et al., 2013a, S. Donatello¹, 2014, Zhang et al., 2017, Donatello et al., 2013b). The binders produced through alkaline activation of 80% fly ash and 20% OPC have been shown to exhibit superior durability performance in aggressive environments. This includes resistance to high temperatures, sulfate attack, chloride penetration, and alkali aggregate reactionn (S. Donatello¹, 2014, Donatello et al., 2013b). HAC mortars, composed of a blend of 12% OPC + 88% GBFS + alkali activator, demonstrate higher mechanical strength compared to controlled OPC mortars when subjected to exposure to aggressive media such as 0.1-N HCl, sodium sulfates and seawater (Fernandez-Jimenez et al., 2013a). The excellent resistance of HAC to sulfate attack is evidenced by the strength retention of HAC-mortar over a period of five years. Studies report that when HACs are exposed to aggressive media, their performance is entirely comparable to that of conventional Portland cements.

Up to now, only a few studies have demonstrated the excellent sulfate resistance of HAC concrete. Donatello et al. (Donatello et al., 2013b) demonstrated the good sulfate resistance of HAC pastes and mortars under a series of aggressive solutions. HAC binders, formed with 80% fly ash and 20% Portland cement clinker, activated by Na_2SO_4 , were immersed in seawater and 4.4% Na_2SO_4 solutions for 90 days. HAC mortars demonstrated satisfactory resistance to seawater and Na_2SO_4

solutions, surpassing current requirements for sulfate-resistant cement (Donatello et al., 2013b, S. Donatello, 2014). Some researchers have investigated the sulfate resistance of HAC mortars over extended periods, and the results indicate that HAC mortars demonstrate superior resistance to sulfate attack compared to reference PC mortars over long ages (Janotka et al., 2014, Zhang et al., 2017, Bačuvčík et al., 2018). Fernández-Jiménez et al. (Fernandez-Jimenez et al., 2013a) examined the durability aspects of HACs in aggressive solutions and concluded that HAC binders, consisting of a blend of 12% Portland clinker, 88% blast furnace slag, and alkali activator, demonstrate good sulfate resistance in a 4.4% Na_2SO_4 solution. To date, studies on alkali-silica reaction (ASR)-induced expansion in hybrid alkaline cements (HACs) are limited. Some researchers argue that ASR-induced expansion is unlikely to occur in HACs because the alkalis from the chemical activator are bound within the alkali activation products (Garcia-Lodeiro et al., 2016b, Palomo et al., 2019). Donatello et al. (Donatello et al., 2013b) investigated the alkali-silica reaction (ASR)-induced expansion of ordinary Portland cement (OPC) and HAC based on fly ash using the ASTM C1260 method. The results revealed that the ASR-induced expansion of both binders was less than 0.1% over the 16-day testing period, which meets the 16 days limit specified by ASTM C1260. However, as the testing progressed, distinctions in expansion became apparent. HAC mortar bars exhibited greater stability in dimensional expansion compared to the ordinary Portland cement (OPC) mortar bars. Angulo-Ramírez et al. (Angulo-Ramirez et al., 2018) reported on the alkali-silica reaction (ASR)-induced expansion of ordinary Portland cement (OPC), Portland blended cement, and hybrid alkaline cement (HAC) based on 80% GBFS and 20% OPC. They concluded that blended cement exhibited the smallest expansion due to alkali-silica reaction. HAC showed expansion of less than 0.1% over 16 days of testing, and less than 0.2% over 30 days of testing. OPC, on the other hand, displayed the largest dimensional expansion, exceeding both the 16 days and 30 days limits.

2.5 Research gap

Mechanical, setting and durability characteristics of OPC and AAMs pastes, mortars and concrete have been studied in depth. While, studies on these properties of HAC are limited. However, it is of great importance for a better understanding of

these behaviors of HAC based cements and concretes in view of its potential engineering applications.

To summarize, the following research gaps of HAC have not been explored:

- (1) the relationships between mechanical properties and the ratio of raw materials, the type and dosage of activator;
- (2) the factors affecting setting properties of hybrid alkaline cement based on ordinary Portland cement and ground blast furnace slag.
- (3) the influence of the raw materials, type and dosage of alkali activators on durability properties of HAC concrete.

2.6 Aims and objectives of the research

This research is intended to solve some of the challenges in HAC application. The aims of this project include:

- (1) investigating the relationship between the mechanical development mechanism and raw materials, as well as the type and dosage of alkali activators in hybrid alkaline cement (HAC) systems;
- (2) exploring the fundamental setting behavior of fresh HAC paste and mortar, and investigating the main factors that affect the setting time of HACs;
- (3) investigation the relationship between durability performances of HACs in aggressive environments and the ratio of OPC and the dosage of alkali activator;
- (4) development of HACs with high mechanical strength, good workability and long-term durability performances.

The knowledge garnered from this research is poised to make a significant contribution to advancements in both scientific understanding and technological applications. By furnishing key parameters for the manufacturing and application of hybrid alkaline cements (HACs) in the construction industry, this research will facilitate their adoption and utilization. A comprehensive understanding of the development of mechanical, setting, and durability properties of HACs will bridge the gap between theoretical research and engineering applications. This will not only enhance the efficacy and reliability of HACs in real-world construction scenarios but also pave the way for further innovations and improvements in this burgeoning field.

CHAPTER 3: PAPER 1 – A REVIEW OF RECENT PROGRESS IN HYBRID ALKALINE CEMENT

Note: this chapter is based on the manuscript entitled “A review of recent progress in hybrid alkaline cement”, by Liqiang Wang, Lili Xue, Zuhua Zhang and Hao Wang, published in CAM2021, 2021.

3.1 Introduction

Greenhouse gas emission and energy shortage have led the world to seek for more eco-efficient materials to replace ordinary Portland cement (OPC)(Zhang et al., 2017, Shi et al., 2019b, Biernacki et al., 2017). The first option is partial replacement (normally less than 30%) of OPC with supplementary cementitious materials (SCMs), such as fly ash, slag and limestone (Samad and Shah, 2017, Juenger et al., 2015, Lothenbach et al., 2011b, Skibsted and Snellings, 2019). Another option is to develop alternative binders, e.g. alkali activated material (AAM), which is an OPC-free solid material (Provis and Bernal, 2014, Provis et al., 2015b, Shi et al., 2011a). The third option is a new type of binder known as blended or hybrid alkaline cement (HAC) (Fernandez-Jimenez et al., 2013b, García-Lodeiro et al., 2012, Palomo et al., 2013b, Palomo et al., 2007). Palomo introduced HAC in 2007. HAC is composed of a significant amount of supplementary cementitious materials (SCMs) like fly ash and slag, a minimal proportion of Ordinary Portland Cement (OPC), and alkali activators. The applications of HAC as pavement and masonry blocks have been reported by the research group of Prof. Palomo. HAC possesses comparable performance as OPC (Fernandez-Jimenez et al., 2013b, García-Lodeiro et al., 2012, Palomo et al., 2013b, Donatello et al., 2013b); and needs less alkali activator than AAM and can harden at ambient temperature (in case of alkali activated fly ash, a curing temperature high up 60°C to 90°C is needed in alkali activated materials) (Garcia-Lodeiro et al., 2016c).

HACs have shown satisfactory performances in building structures, road paving and waste solid (Fernandez-Jimenez et al., 2013a, Al-Kutti et al., 2018); Nevertheless, the widespread adoption of this technology has not yet occurred, attributed to both technical and non-technical factors, including the cost associated with activators, fast setting time, hard controlled rheology and unknown performance

of durability.

This paper reviews HAC system: including activators, precursors and chemical admixtures, rheology, setting time properties and some durability aspects. This paper also discusses the needs for future research and development to support the application of HACs in construction materials industry.

3.2 Hybrid alkaline cement system

3.2.1 Activators

HACs needs the help of alkali activator to active its Pozzolanic reaction. While compared with AAMs, HAC needs less alkali activator, which will make it more safety and economical in application. Alkali activators play an important part in rheology, setting time, mechanical and durability properties, and also influence hydration mechanisms and main production in the HAC. The combination of Na_2SiO_3 with NaOH is widely acknowledged as the most effective activator in HAC technology. This formulation is recognized for yielding high strength and other beneficial properties (A. Palomo, 2007, Garcia-Lodeiro et al., 2013b, Sedira and Castro-Gomes, 2020, Rios et al., 2020, Barboza-Chavez et al., 2020, Askarian et al., 2018, Angulo-Ramirez et al., 2018). The concentration and quantity of activator employed in each scenario largely hinge on the CaO content in the cement blend and the specific reactivity of supplementary cementitious materials (SCMs) (Palomo et al., 2013a).

Alkali activator usually the most expensive component in HAC system, which makes it hard to application. The productions of activators from waste glass (Vinai and Soutsos, 2019, Liu et al., 2019, Toniolo et al., 2018, Torres-Carrasco et al., 2015), and the use of alkali activator obtained from red mud and car batteries recycling , have been reported with some success.

The use of near-neutral salts such as Na_2SO_4 (Donatello et al., 2013a, Donatello et al., 2014, Millan-Corrales et al., 2020, Qu et al., 2020, Garcia-Lodeiro et al., 2018b, Garcia-Lodeiro et al., 2018a, du Toit et al., 2018, Fernandez-Jimenez et al., 2019, Garcia-Lodeiro et al., 2016b), $\text{Na}_2\text{SO}_4 + \text{CaSO}_4$ (Palomo et al., 2019, Sanchez-Herrero et al., 2019, Garcia-Lodeiro et al., 2017), Na_2CO_3 (Garcia-Lodeiro et al., 2013a, Garcia-Lodeiro et al., 2016b, Alahrache et al., 2016b), K_2CO_3 (Askarian et al., 2018) and Na_2O xalate (Alahrache et al., 2016b) were used as alkali activators

Table 3- 1 Overview of hybrid alkaline cement system.

Composition	Activator	Compressive strength (MPa)						Setting time(min)		Ref
		1d	2d	3d	7d	28d	91d	Initial	Final	
70%FA+30%OPC	NaOH+SS n=1.5	-	12.91	-	-	36.94	-	-	-	(A. Palomo, 2007)
78%FA+18%OPC	4%Na ₂ SO ₄	-	-	-	-	22.8±1.4	-	85	290	(Donatello et al., 2013a)
40%BFS+40%MK+20%CK	Na ₂ CO ₃	-	32	-	-	-	-	-	-	(Garcia-Lodeiro et al., 2015)
70%FA+30%OPC		-	-	-	-	51.7	-	-	-	(Mejia et al., 2015)
70%FA+30%OPC	2%(K,Na) ₂ SiO ₃	4.8±0.5	-	8.4±0.1	10.1±0.4	19.0±0.6	28.0±0.5	90	270	
70%FA+30%OPC	3%Na ₂ CO ₃	3.6±0.2	-	6.8±0.2	7.4±0.4	14.8±0.1	18.9±0.2	150	318	(Alahache et al., 2016b)
70%FA+30%OPC	8%Na ₂ O	4.6±0.1	-	4.4±0.2	10.3±0.1	18.0±0.3	25.0±0.1	318	360	
70%FA+30%OPC	3%K ₃ Citrate	0.5±0.1	-	0.6±0.1	0.8±0.1	9.3±1.8	29.1±0.1	198	678	
40%BF,FA+60%OPC		-	-	-	-	32.5	-	-	-	(Garcia-Lodeiro et al., 2016a)
32.5%BFS+32.5%FA+30%OPC	5%	-	-	-	-	35	40	202	327	(Qu et al., 2016)
80%FA+20%OPC	Na ₂ SO ₄ +CaSO ₄	-	18	-	-	30	-	-	-	(Garcia-Lodeiro et al., 2017)
60%FA+40%OPC	Na ₂ SO ₄ +CaSO ₄	-	25	-	-	53	-	-	-	
80%GBFS+20%OPC	NaOH+SS n=1.0	-	-	-	-	-	-	-	-	(Angulo-Ramirez et al., 2018)
81%FA+9%SLAG+10%OPC	7.5% K ₂ CO ₃	13.2±1.9	-	-	26.7±0.4	33.4±0.6	-	86	139	
72%FA+8%SLAG+20%OPC	7.5% K ₂ CO ₃	17.8±1.1	-	-	31.3±0.8	39.7±0.8	-	61	102	(Askarian et al., 2018)
63%FA+7%SLAG+30%OPC	7.5% K ₂ CO ₃	25.3±0.3	-	-	45.6±0.5	50.3±1.3	-	44	107	
70%FA+30%OPC	5%Na ₂ SO ₄	-	-	-	32.5	-	-	-	-	(du Toit et al., 2018)
80%BT+20%OPC	5%Na ₂ SO ₄	-	12.76±0.8	-	-	30.94±2.49	-	-	-	(Garcia-Lodeiro et al., 2018a)
70%BT+30%OPC	5%Na ₂ SO ₄	-	14.61±2.3	-	-	37.64±2.2	-	-	-	
60%BT+40%OPC	5%Na ₂ SO ₄	-	-	-	-	53	-	-	-	(Garcia-Lodeiro et al., 2018b)
50%M-FA+50%OPC	Liquid 5%Na ₂ SO ₄	-	23.82±0.41	-	37.90±0.54	51.32±0.62	-	101	132	(Fernandez-Jimenez et al., 2019)
50%AM-FA+50%OPC	Solid 5%Na ₂ SO ₄	-	30.33±0.5	-	41.32±0.29	52.53±1.70	-	149	204	
48%FA+48 %OPC	1.5%gypsum 2.5% 5%Na ₂ SO ₄		10.8±0.2	-	22.2±0.5	40.0±1.1	47.7+1.6	83	193	(Sanchez-Herrero et al., 2019)
10%LIMESTON+55%FA+30%OPC	5%Na ₂ SO ₄	-	-	30.32	-	49.06	51.30	-	-	(Millan-Corrales et al., 2020)

has received certain advances.

3.2.2 Precursors

The HAC systems most frequently studied include:

Fly ash –OPC blends

Blast furnace slag –OPC blends

Limestone –fly ash–OPC blends

Bottom fly ash–metakaolin–OPC blends

Phosphorous slag –OPC blends

Steel mill and blast furnace slag –OPC blends

Fly ash – blast furnace slag –OPC blends

Multi-constituent cement blends(Abdelrahman and Subaihi, 2020, Donatello et al., 2013a)

Fly ash and blast furnace slag are the most used SCMs in HAC both in research and engineering, especially fly ash (Shi et al., 2011b, Garcia-Lodeiro et al., 2016b, Garcia-Lodeiro et al., 2016a, Mejia et al., 2015, Palomo et al., 2013a, Fernandez-Jimenez et al., 2013a, Garcia-Lodeiro et al., 2012).

3.2.3 Chemical admixtures

Rheology and setting properties are hard to control in the application HACs. it has become important and crucial to find suitable admixtures in the wide application of HAC. It is observed that the admixtures that used in OPC pastes, mortars have weak effects both in AAM and HAC products. The huge drop on yield stress in fly ash based AAM is found when Melamine-derivative synthetic polymers are added because of their inherent stability in alkaline media as shown in Figure 3- 1.

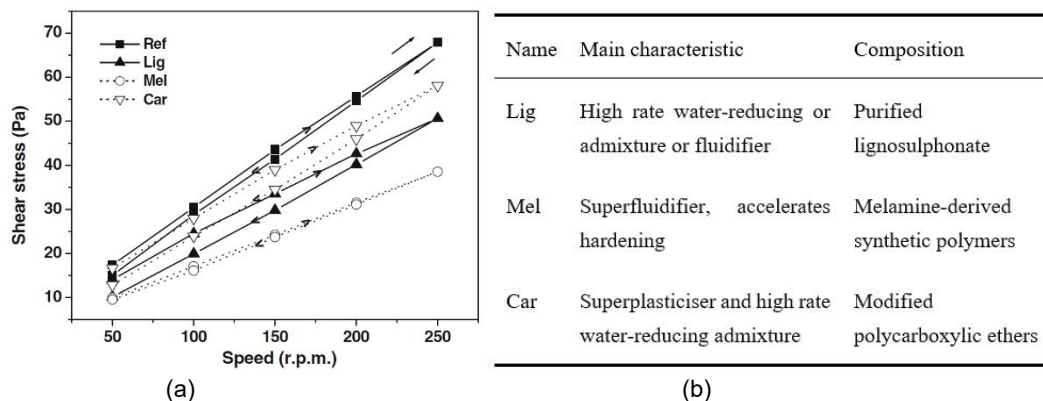


Figure 3- 1 (a) Flow curves of different admixtures (b) relative table (Criado, Palomo et al. 2009).

3.3 Reaction mechanisms in HAC

3.3.1 OPC hydration vs Alkali Activation of SCMs

The evolution of OPC paste from a flowable material to a hardened solid occurs in several stages Figure 3-2(a) Calcium silicate hydrate (C-S-H) gel is the main product in OPC hydration Figure 3-2 (b), and the chemical reactions start very slowly, allowing for the safe casting of concrete before setting (Roussel, 2011).

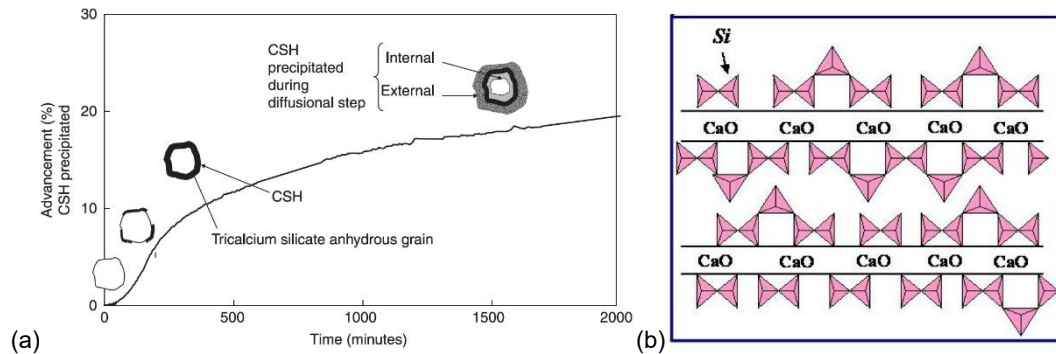


Figure 3-2 (a) Evolution of the degree of hydration of tricalcium silicate vs. time (Roussel 2011) (b) C-S-H gel structure (García-Lodeiro, Maltseva et al. 2012).

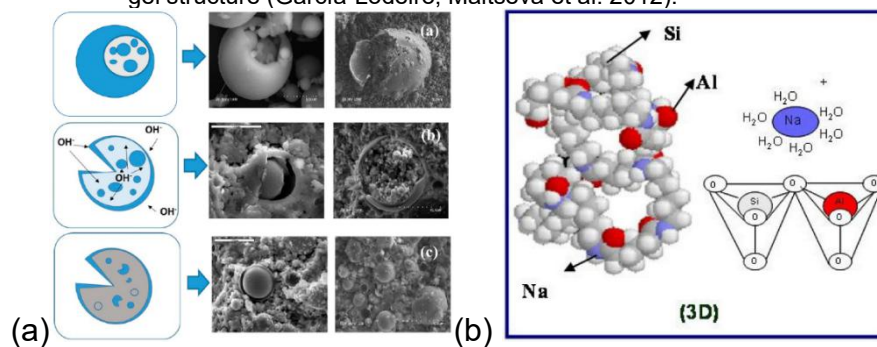


Figure 3-3 (a) Conceptual model for AAFA alkali activation (Garcia-Lodeiro, Donatello et al. 2016) (b) N-A-S-H gel structure (García-Lodeiro, Maltseva et al. 2012).

However, in AAM the alkali activation (in case of alkaline activated fly ash (AAFA)), process is proposed consists of three different stages: (a) Destruction-Coagulation; (b) Coagulation-Condensation; and (c) Condensation-Crystallization Figure 3-3 (a). As shown in Figure 3-3 (b), the reaction product in AAM is an amorphous alkaline aluminosilicate hydrate, which is known as N-A-S-H.

3.3.2 Reaction mechanisms in HAC

The reaction products of HAC systems are complicated. They may include OPC hydration, OPC activation with alkali activators and alkali activation of SCMs.

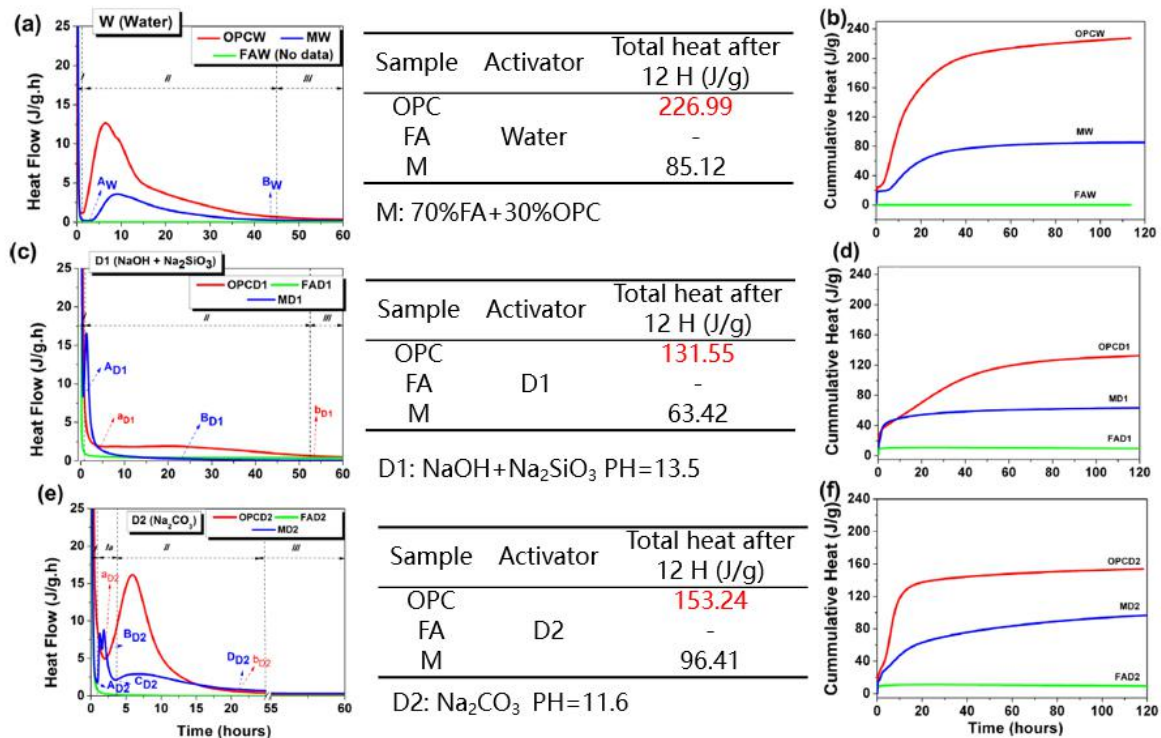


Figure 3-4 Heat flow and cumulative heat of OPC, FA and M (HAC) systems with (a) and (b) W (water); (c) and (d) D1; (e) and (f) D2 (Garcia-Lodeiro, Fernandez-Jimenez et al. 2013).

From the heat flow of OPC, fly ash and HAC in different solutions, it is obtained that (1) in alkaline solution, both OPC and HAC hydration have been accelerated. (2) In higher PH solution, the hydration is more quickly, especially for OPC hydration. The high rate of OPC hydration will bring fast setting and increase the shear stress of the HAC paste, mortar and concrete.

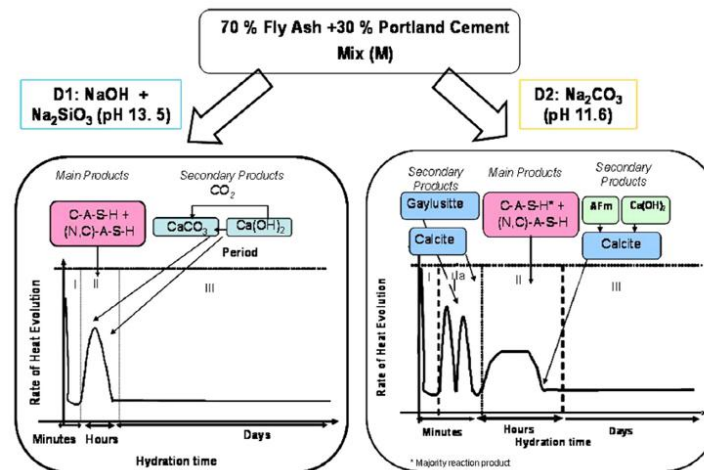


Figure 3-5 Activation models for HAC in D1 and D2 (Garcia-Lodeiro, Fernandez-Jimenez et al. 2013).

The main products both in D1 and D2 are C-A-S-H and (N,C)-A-S-H. Generally speaking, the alkali activators used in HACs influence the reaction kinetics and the final products. Correspondently, the type of activator influences the

rheological properties of HAC, Na_2SiO_3 tends to bring fast setting, high viscosity, and fast increasing of shear stress.

3.4 Properties of hybrid alkaline cement

3.4.1 Rheology

HAC is made from complex compositions, which contain OPC, SCMs, alkali activators, admixtures etc. Furthermore, the rheological properties of HAC changed with time, due to the hydration of OPC, together with the alkaline activation reaction. In addition to HAC design, the rheological properties as influenced by the synergic effect of the following factors in Table 3-2:

Table 3-2 The influence factors on rheological properties of HAC.			
SCMs	Activator	Admixtures	Mixing conditions
Chemical composition Mineralogical composition Particle size distribution Solid volume fraction, etc.	Nature Concentration $\text{Na}_2\text{O}/\text{SiO}_2$	Superplasticizers Retarders, etc.	Time energy Temperature, etc.

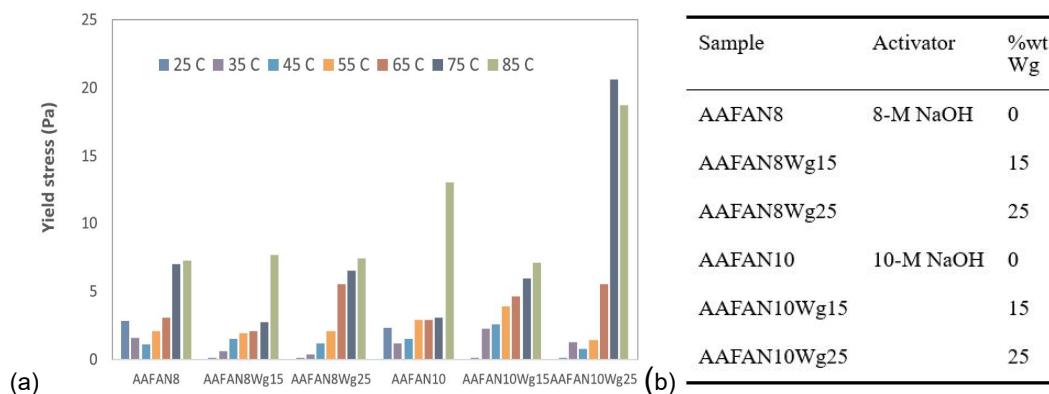


Figure 3-6 (a) Yield stress of AAFAN suspensions at different testing temperatures (b) relative table (Palacios, Alonso et al. 2019).

Rheology properties of AAM and HAC are influenced by the type and dosage of alkali activator. And the yield stress and viscosity of these binder paste increased as the temperature increased as shown in Figure 3-6.

3.4.2 Setting time

The ratio of OPC in HAC systems effects the setting properties significantly. Increasing the ratio of OPC in HAC system, the initial setting time decreased dramatically. The fast setting made HAC hard to cast and mix. Decreasing the ratio of OPC in HAC system, setting time increased. The binder systems were presented in Table 3-3, and the setting properties are shown in Figure 3-7. Conclusion can be

made that increasing the ratio of OPC in HAC systems, setting time decreased dramatically.

Table 3-3 Mix proportions of HAC.

Mix No	Designation	OPC	Fly ash	Slag	Activator	W/B	Superplasticiser
1	GP60	60%	36%	4%	3%	0.30	1.5%
2	GP40	40%	54%	6%	4.50%	0.30	1.5%
3	GP30	30%	63%	7%	5.25%	0.30	1.5%
4	GP20	20%	72%	8%	6%	0.30	1.5%
5	GP10	10%	81%	9%	6.75%	0.30	1.5%
6	GP0	0%	90%	10%	7.50%	0.30	1.5%

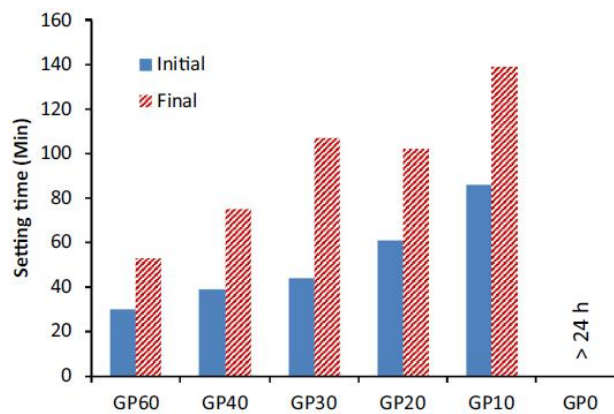


Figure 3-7 Setting times of different proportions of HC.

With the help of alkali activator, the pH value rose in the solution, the speed of dissolution of SCMs accelerated. That led to substantially higher reactivity, shorter setting time and greater early age strength. Differences were observed in setting behaviour depending on whether the supplementary material was slag or fly ash(Palomo et al., 2013a).

Table 3-4 The different precursors' setting time.

Binder	Composition	Activator	W/B	setting time	
				Initial	End
1	20%OPC+80%FA	No	0.38	<18h	-
2	20%OPC+80%FA	Yes	0.38	1h47min	4h12min
3	20%OPC+80%BSAGE	No	0.26	6h12min	9h12min
4	20%OPC+80%BSAGE	Yes	0.26	1h25min	2h8min

The particle size and the liquid or solid activator also influence the setting time of hybrid alkaline cement. It can be found that grinding the ash (from mainly 45 μ m to 10 μ m) enhanced its reactivity, and shorted its setting time. Liquid alkali activator

accelerated the reaction rate in HAC system, and brought faster setting compared with solid alkali activator.

Table 3-5 The different precursors' setting time.

Binder	Composition	Activator 5%Na ₂ SO ₄	W/B	setting time	
				Initial	End
1	100%OPC	No	0.35	2h30min	4h50min
2	50%OPC+50%O-FA	Liquid	0.35	2h6min	3h31min
3	50%OPC+50%M-FA	Liquid	0.35	1h41min	2h16min
4	50%OPC+50%AM-FA	Solid	0.35	2h29min	3h24min

O-FA: Original FA, M-FA: Grinding FA (particle size form mainly 45μm to 10μm), AM-FA: M-FA+ solid activator. The activator is 5% of Na₂SO₄ (%FA weight)

3.4.3 Application

The applications of HAC as industrial pavers and blocks have been reported by the research group of Prof. Palomo (Fernandez-Jimenez et al., 2013b), the compressive strength of HAC is relatively low (30-40MPa). In a subsequent industrial trial, the concrete made with this type of binder was successfully used in the manufacture of precast blocks and pavers.

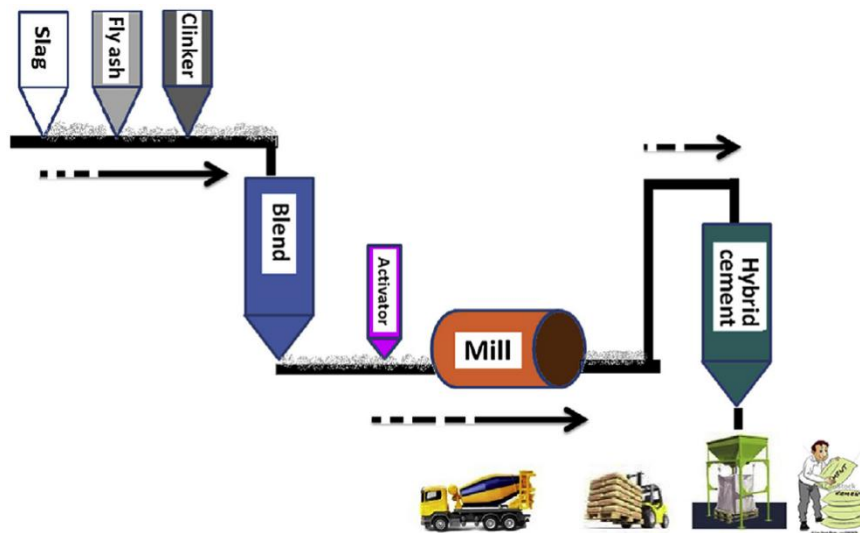


Figure 3-8 Schematic diagram of manufacturing process and stages of ternary hybrid cement (Qu, Martin et al. 2016).

The production of HAC in Latin-American cement plant was reported(Qu et al., 2016). The HAC system consists of 30% OPC, 32.5% bottom fly ash, 32.5% fly ash and 5% solid activator.

3.4.4 Durability

The durability of hybrid alkaline cements (HACs) in aggressive environments, such as sulphate attack, alkali aggregate reaction, high temperature, chloride penetration, carbonation, have always been the focus of global research (Fernandez-Jimenez et al., 2013a, S. Donatello1, 2014, Zhang et al., 2017, Donatello et al., 2013b). The products and reaction kinetics in HAC systems are different from the hydration of OPC, and the corrosion mechanism and evaluation methods are also different.

Excellent resistance of HAC to a sulphate attack is demonstrated by the 5-years strength of HAC-mortar. It is reported that when HAC are exposed to aggressive media, their behaviour is wholly comparable to the performance of conventional Portland cements. The HAC perform even better than OPC in seawater. No differential pattern seemed to be present.



(a) OPC mortar immersed 4 years in Na_2SO_4

(b) HAC mortar immersed 5 years in Na_2SO_4

Figure 3-9 Structure and appearance of mortars exposed in Na_2SO_4 solution.

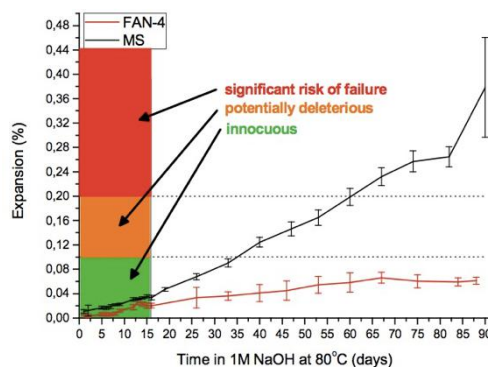


Figure 3-10 Evolution of mortar bar expansion during the AAR test (S. Donatello1 2014).

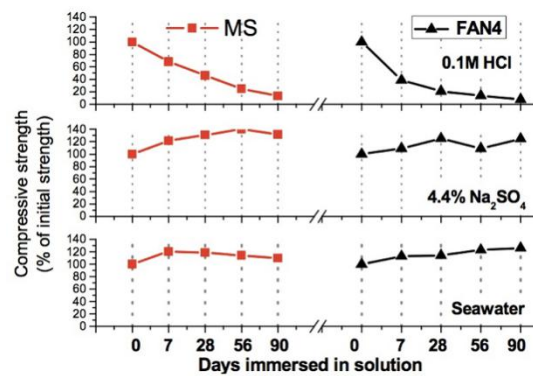


Figure 3- 11 Evolution of PC and hybrid cement mortar strengths following immersion in aggressive solutions (S. Donatello1 2014).

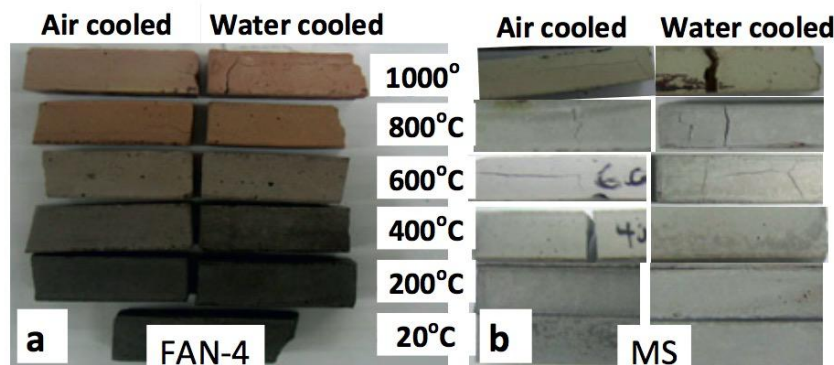


Figure 3- 12 Visual changes in (a) hybrid alkaline cement and (b) control PC pastes after temperature exposure.

3.5 Conclusion

The recent progress in hybrid alkaline cement can be summarized as follows:

- (1) HAC is considered an eco-efficient material due to its high content of supplementary cementitious materials (SCMs).
- (2) HAC demonstrates mechanical performance comparable to that of Ordinary Portland Cement (OPC).
- (3) the type of alkali activator significantly influences reaction kinetics and the formation of secondary reaction products .
- (4) HAC exhibits poor workability characterized by rapid setting and high viscosity. .
- (5) HAC demonstrates similar or even superior durability compared to OPC.

3.6 Perspectives for future research

(1) currently reported applications of HAC focus on achieving compressive strengths of 30-40 MPa. There are few reported applications of HAC in high-strength concrete members exceeding 60 MPa.

(2) The challenge lies in HAC's poor workability characterized by fast setting and

high viscosity. Given the necessity to study new binders and simulate broader application conditions, there is an increasing importance in exploring the fundamental rheological parameters of fresh concrete, both from scientific and technological perspectives.

(3)it is also necessary to explore methods and standards suitable for testing the durability aspects and long-term durability performance of HAC.

CHAPTER 4: RESEARCH PLAN AND METHODOLOGY

4.1 Introduction

From the previous chapter, it is clearly that the production and application of HAC faces several challenges. To be a fundamental construction material, HAC needs to possess high mechanical strength, flexible workability and good resistance performance in virous environment. As a new generation of low carbon binders, HACs differ from OPC in many aspects. The effect of raw materials and curing conditions on the microstructural evolution of HAC systems and relevant properties are not well understood. Understanding microstructural evolution and the relationship to relevant properties, and building up references database are important in designing and application of HACs in construction.

The research plan and methodology for this thesis are presented in this chapter. HAC is used to describe binders consists of a high proportion of GBFS, a low proportion of OPC and alkali activator. All samples are prepared under room temperature refer to 20-25°C, humidity 40-60%, normal atmospheric pressure. The *alkali activator* refers to the solid activators include $\text{Na}_2\text{SiO}_3 \cdot 9\text{H}_2\text{O}$. The *raw materials* refer to amorphous materials that are generally in a powder form. In this thesis the raw materials include ordinary Portland cement (OPC), P II 52.5 and Ground blast furnace slag (GBFS).

4.2 Research flow chart

This research is intended to solve some of the challenges in HAC application. The aims of this project include:

(1) understanding the relationship between the mechanical development mechanism and the raw materials, as well as the type and dosage of alkali activators in HAC systems;

(2) to fully understand the setting and hardening mechanisms of HAC, and to clarify the main factors affecting its initial and final setting time;

(3) to study the erosion mechanisms of HAC in various complex environments and analyze the impact of raw material composition and activator dosage on erosion products ;

(4) development of HACs with high mechanical strength, good workability and long-term durability performances.

The knowledge established in this research will significantly advance industry applications for sustainable development. It provides essential parameters for the production and use of HACs in construction. Understanding the development of mechanical, setting, and durability properties will help bridge the gap between theoretical research and practical engineering applications. The materials used and the methods adopted in this research are described in the following sections of this chapter.

The research flow chart shown in Figure 4- 1 provides an outline for this thesis.

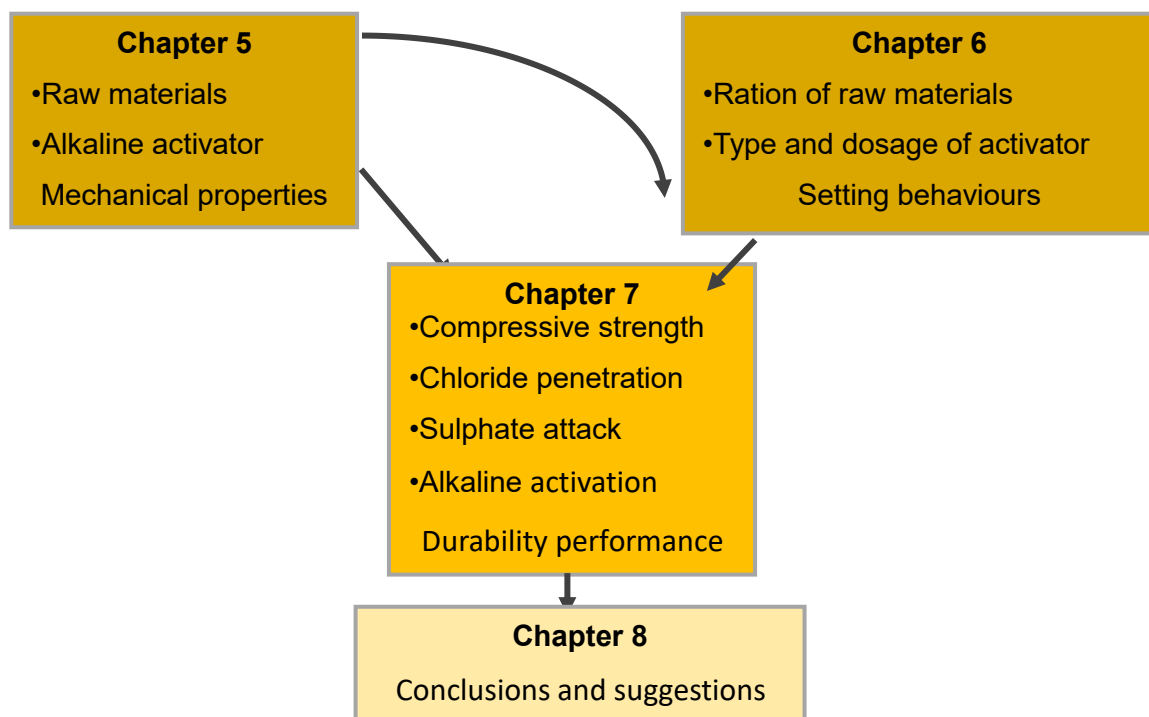


Figure 4- 1 Research flow chart of this thesis.

4.3 Materials

4.3.1 Precursors

The precursors used in this research were: (a) ordinary Portland cement (OPC), P II 52.5, (b) Ground blast furnace slag (GBFS), S95 grade, with specific gravity of 2910kg/m³, and a specific surface area of 388m²/kg. These raw materials were provided by a local company. Their chemical composition was measured using X-ray fluorescence (XRF). The phase analysis of raw materials was conducted by X-ray Diffraction (XRD). The XRD patterns of OPC, GBFS and FA are shown in Figure 4- 2.

Table 4- 1 Chemical composition of OPC and GBFS, determined by X-ray fluorescence.

Type	OPC	GBFS
SiO ₂	20.99	31.43
Al ₂ O ₃	5.36	15.22
Fe ₂ O ₃	3.81	0.71
CaO	61.36	37.79
MgO	1.38	9.62
SO ₃	2.4	1.2
K ₂ O	0.65	0.43
TiO ₂	0.27	0.67
Na ₂ O	0.13	0.52

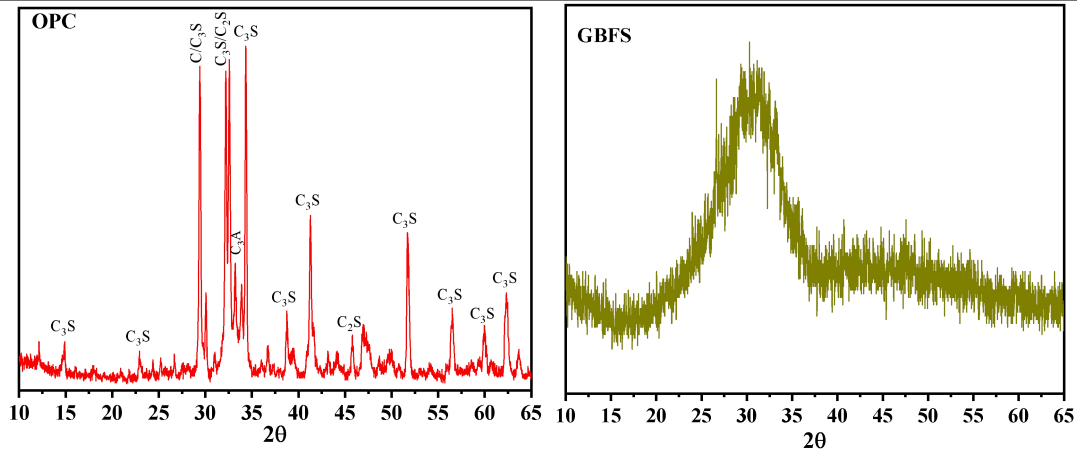


Figure 4- 2 XRD patterns of OPC and GBFS.

4.3.2 Alkali activator

Alkali activator is a key component in HAC system. The alkali activator not only provides alkaline reaction environment for the hydration of HAC solid parts, but also it has the greatest impact on the costs for production of this kind of binder. The use of alkali activator usually produces HAC uncompetitive in price compared to OPC. HAC systems activated by different types of alkali activators show different performances on mechanical, setting and durability properties (Alahrache et al., 2016b, Garcia-Lodeiro et al., 2016b, Sedira and Castro-Gomes, 2020). The production of alkali activator also causes some environment issues, if it has been manufactured at high purity for use in other industry sectors. The type and dosage of alkali activator will greatly affect the economic and environmental impact in the production of HAC.

The alkali activator Na₂SiO₃·9H₂O is a commercial sodium silicate in solid condition, with 32.4 wt.% SiO₂, 13.5 wt.% Na₂O and 54.1 wt.% H₂O, to reach the

desired overall molar ratios. The chemical composition is shown in Table 4-2. Analysis of pure $\text{Na}_2\text{SiO}_3 \cdot 9\text{H}_2\text{O}$, purchased by a chemical product from a store in Jiaxing.

Table 4- 2 Solid sodium silicate specifications.

Solid sodium Silicate	D–Grade TM
SiO_2 (wt.%)	32.4
Na_2O (wt.%)	13.5
H_2O (wt.%)	54.1
$\text{SiO}_2/\text{Na}_2\text{O}$ mass ratio	0.97
$\text{SiO}_2/\text{Na}_2\text{O}$ molar ratio	1.0

4.3.3 Other materials

4.3.3.1 Sand

The sand used in chapter 4 is standard sand for cement strength testing according to ISO standard. The sand used in chapter 6 chloride ion content is less than 0.06%. The fineness modulus is 1.5, and the mud content is less than 1% and provided by a local company.

3.3.3.2 Aggregate

The aggregate used is crushed stone, granite, with a maximum particle size of 35mm, needle and flake particle content less than 7%, crushing index 4.5-5, and mud content less than 0.2%.

4.4 Procedures

4.4.1 XRD/XRF analysis for the phase determination

In this research, the mineral composition of binder paste powder at different curing at 1day, 7 and 28 days was monitored by XRD. And the binder paste powder after sulphate attack was also monitored by XRD. Analysis was got through an acceleration voltage of 60KV and 80mA current XRD-7000 diffractometer with Ceramic X-ray tube and Cu target. The samples were scanned at the rate of $2.5^\circ/\text{min}$ between the angel 5° to $80^\circ 2\theta$.

4.4.2 SEM analysis

Scanning Electron Microscopy (SEM) was used to monitor the microstructural evolution and phase composition of binder paste hydration products. To determine the reaction products of binders with different ratio of raw materials, and HACs with different dosage of alkali content. SEM with an accelerating voltage of 10 kV and working distance of 10mm was carried out using a Phenom Pro X. An IONSPUTTERE 1045 was used to coat with gold on polished specimens. The chemical compositions are determined by a link-energy dispersive X-ray (EDX) detector.

4.4.3 ^1H NMR analysis

A low-field ^1H nuclear magnetic resonance (NMR) instrument (MAGMED-PM-1030; MAGMET Analytical Instrument Corporation, Jiangsu, China) was used for the ^1H NMR experiments at room temperature with a constant magnetic field of 10 MHz and a 30 mm coil. ^1H NMR technology was used to explore pore structure of all binder systems curing at 1 day, 7 and 28 days and after chloride penetration. ^1H NMR technology was also used to explore the setting properties of all binder systems during the setting period.

4.4.4 TGA analysis

TGA and DTG of hydrated products of binder systems at initial and final setting time were carried out under N_2 -atmosphere on a STA-409PC instrument heated from 30 $^\circ\text{C}$ to 1000 $^\circ\text{C}$ at a heating rate of 10 $^\circ\text{C}/\text{min}$.

4.4.5 Hydration heat analysis

The early heat flow and cumulative heat of binders with different ratio of OPC and different dosage of Na_2O content are tested by isothermal conduction calorimetry for 72 hours on a THERMOMETRIC TAM air calorimeter. The binder systems that studied included 70%-100%GBFS blended 30%-0% OPC which were hydrated with solid alkali activator $\text{Na}_2\text{SiO}_3 \cdot 9\text{H}_2\text{O}$. 100OPC hydrated by the same w/b ratio as control system. Superplasticizer and retarder are excluded in order to obtain accurate test results. Each one of the sample weights about 5g.

4.4.6 Procedures for mechanical testing

In chapter 4, the compressive strength is measured on 40 mm cubic mortar specimens. Three parallel mortar specimens were tested at different ages (1,7 and 28 days) and an average of results was presented. The compression loading rate was 2.4 KN/s.



Figure 4-3 HAC paste specimens preparation and mechanical test.

In chapter 6, concrete specimens are measured to obtain compressive strength in accordance to standard procedure of was measured on 100 mm cubic concrete specimens. Triplicate parallel concrete specimens are tested at different ages (7, 28, 91 and 180 days) and an average of results are presented. The compression loading rate was 0.5 KN/s.



Figure 4-4 HAC concrete specimens preparation and mechanical test.

4.4.7 Setting time

The setting times (initial setting and the final setting) of all the binders were tested in accordance to Chinese standard specified in GBT 1346–2011 (Test methods for water requirement of normal consistency, setting time and soundness of the Portland cement).

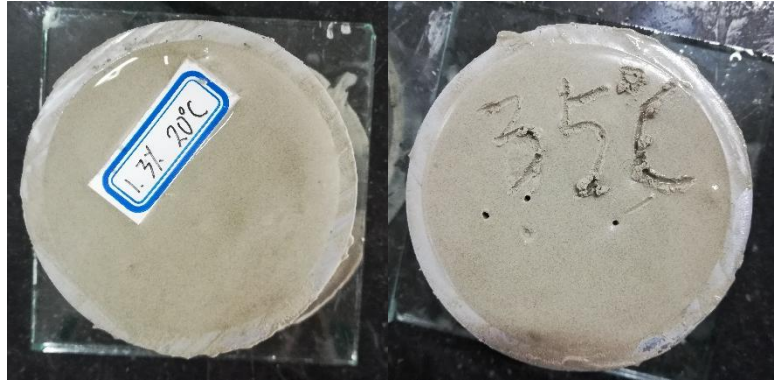


Figure 4-5 Initial setting time and final setting time test for HAC paste.

4.4.8 Procedures for chloride permeability measurement

A measure to test concrete's resistance to chloride ion penetration is conducted by the rapid chloride permeability test (RCPT) according to ASTM C 1202 (ASTM, 2012). The specimens used for RCPT have a thickness of 50 ± 2 mm and a diameter of 100 ± 1 mm. The specimens are conducted vacuum saturation treatment one day before the test, and then installed in a sealed experimental tank, with storage tanks on both sides. Inject a solution containing 0.3N NaOH into the anode chamber and a solution containing 3% NaCl into the cathode chamber of the storage tank. Cure the prepared HAC concrete specimens under standard conditions, and perform the chloride ion penetration test at curing times of 28 days and 91 days.. A 60 volts potential drop is applied on the two electrodes installed on each side of the specimen. The total charge passed during the first 6 hours of measure is indicated as the RCPT value.

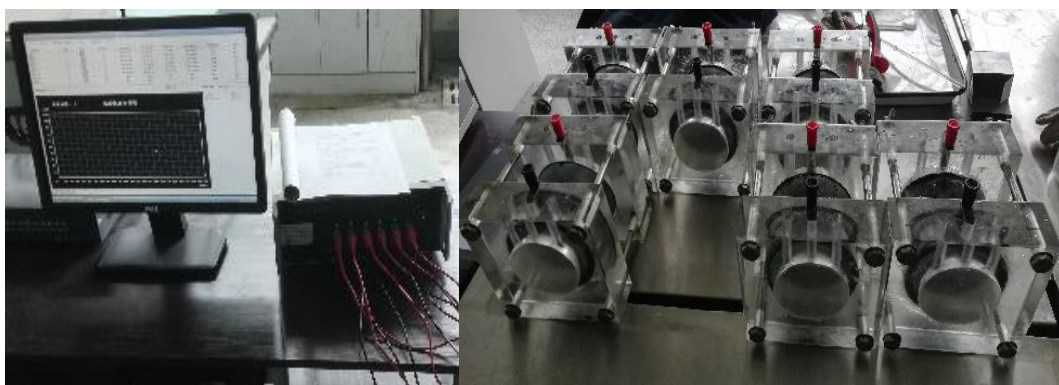


Figure 4-6 Rapid chloride permeability test for HAC concrete.

4.4.9 Procedures for sulphate attack resistance test

A test to measure HAC and OPC concrete's ability of resistance to sulphate attack is conducted on 100 mm cubic concrete specimens at the age of 28 days.

Before testing, the specimens were dried at $80 \pm ^\circ\text{C}$ for 48 hours to ensure thorough drying. The specimens of HAC and OPC concretes are placed in sodium sulfate solution. In order to maintain a stable pH value of the solution, this experiment requires testing the pH value of the solution once every 15 cycles to maintain it between 6 and 8, and the pH value of the solution can be pleasantly adjusted by 1mol/L of sulfuric acid solution. For the convenience of the drying -and-wetting cycles, an automatic drying-and-wetting cycle equipment is used in this study. An automatic drying-and-wetting cycle is 16h of immersion in sodium sulfate solution, 6h of drying, and 2h of cooling, that is 24 hours for one cycle.



Figure 4- 7 Sulphate attack resistance test.

The Weight loss (W , %) of 100 mm cube specimens are measured according to Eq. (3-1). Three parallel specimens are tested and an average of results are presented.

$$W = (W_t - W_0) \cdot 100 / W_0 \quad (4-1)$$

Where W_t (g) is the weight of specimen measured over 150 times of sulphate attack cycles; W_0 (g) is the initial weight of the specimen tested after 28 days of standard curing.

The reduction in compressive strength (C , %) of 100 mm cube specimens after 150 times of sulphate attack cycles is tested according to Eq. (3-2), the specimens cured in distilled water with the same age are used as control.

$$C = (C_0 - C_t) \cdot 100 / C_0 \quad (4-2)$$

where C_t (MPa) is the compressive strength of 100 mm cube specimen tested after 150 times of sulphate attack cycles; C_0 (MPa) is the compressive strength of the specimen tested at the same ages curing in distilled water.

When the times of sulphate attack reached 150, the specimens are examined for appearance, weight and compressive strength and microscopic analysis.

4.4.10 Resistance to the alkali-silica reaction

A measure to test mortar bar's resistance to the alkali-silica reaction is evaluated in accordance to procedures of ASTM C1260 (Astm, 2007). Three types of binder systems are evaluated. The system 1 (blended cement) contains 90% GBFS) and 10% OPC, and the second (HAC) with the same precursors but in addition of an alkali activator. The alkali activator is a commercial sodium silicate solid: $\text{Na}_2\text{SiO}_3 \cdot 9\text{H}_2\text{O}$, and is expressed by the wt.% of Na_2O relative to the quality of the binders, and the solid chemical activator is blended into ground together with the binders. The third system, 100% OPC is used as reference. For all the above systems, mortar bars with the same ratio of binder to sand equals 1 to 2.25, that is 400 g of binder, 900 g of sand and a water/binder ratio of 0.47. For each case, Triplicate parallel specimens are made. The initial longitudinal length is measured for the sample after 24 hours of standard curing. Soon after, the samples are immersed in 80°C water for 24 hours, and longitudinal length are measured again. Later, the samples are placed in 80°C NaOH (1N) solution, and longitudinal length are measured at 3d, 5d, 16d, 30d, and 35d.



Figure 4-8 Resistance to the alkali-silica reaction test.

CHAPTER 5: PAPER 2 – SYNTHESIS AND MECHANICAL PROPERTIES OF HYBRID ALKALINE CEMENTS BASED ON SLAG AND PORTLAND CEMENT

5.1 Introduction

Currently, ordinary Portland Cement (OPC) serves as the fundamental construction material. The production of OPC brought many environmental and energy issues (Monteiro et al., 2017, Cao et al., 2021). To reduce the production of OPC, many efforts were made. Firstly, partial replacement of OPC with SCMs was applied (Samad and Shah, 2017, Juenger et al., 2015, Lothenbach et al., 2011b, Cao et al., 2021, Fu et al., 2020). Another option is to develop alternative binders, e.g. alkali activated material (AAM), which is an OPC-free solid material (Provis and Bernal, 2014, Provis et al., 2015b, Shi et al., 2011a). Finally, the concept of hybrid alkaline cement (HAC) was introduced (Fernandez-Jimenez et al., 2013b, García-Lodeiro et al., 2012, Palomo et al., 2013b, Palomo et al., 2007)

HAC consists of a high proportion of SCMs, such as FA and or GBFS, a low proportion of OPC and alkali activators. The applications of HAC as pavement and masonry blocks have been reported by the research group of Prof. Palomo (Fernandez-Jimenez et al., 2013a). HAC possesses comparable performance as OPC (Fernandez-Jimenez et al., 2013b, García-Lodeiro et al., 2012, Palomo et al., 2013b, Donatello et al., 2013b), needs less alkali activator than AAM and can harden at ambient temperature (a curing temperature high up 60°C to 90°C is needed in alkali activated materials) (Fernández-Jiménez and Palomo, 2007, Garcia-Lodeiro et al., 2016b). Compared with OPC, HACs needs the help of alkali activator to active its Pozzolanic reaction. While compared with AAMs, HAC needs less dosage of alkali activator, which will make it more safety and economical in application. The differences of these three binders were shown in Table 5-1.

Table 5- 1 Comparison of the three methods (Illustrated by fly ash).

Option	Binders	Composition	Alkali activator	Curing condition
0	OPC	100%OPC	0	25°C
1	Partial replacement	25%FA+75%OPC	0	25°C
2	AAM	100%FA	Strong OH ⁻	60°C to 90°C
3	HAC	70%-80%FA+20%-30%OPC	Moderate OH ⁻	25°C

However, the mechanical strength development mechanism of HAC is not fully understood, and the factors affecting the compressive strength of HAC have not been systematically studied. Mahya Askarian et al.(Askarian et al., 2018) investigated one-part hybrid OPC-geopolymer concrete with different ration of raw materials. It was found that the dosage of Na₂O content plays an important role on the workability, setting time, and mechanical properties. Salaheddine Alahrache et al. (Alahrache et al., 2016b) studied the strength development of the HACs based on 30% OPC, 70%FA activated by different activators (Na₂CO₃, Na₂SiO₃, K₂SiO₃, Na₂Oxalate and K₃Citrate), concluding that the alkali activator has an obvious impact on strength development. Some research (Garcia-Lodeiro et al., 2016b, Garcia-Lodeiro et al., 2013b, A. Palomo, 2007) presents descriptive models for low-Ca HAC systems hydration, which involve both typical OPC hydration and alkali activation of fly ash, and it is concluded that the early hydration products are N–A–S–H and C–S–H gels, which gradually evolve into C–A–S–H structures as hydration progresses. Martin T. Palou et al.(Palou et al., 2016) studied the effect of curing temperature on blended cements, and concluding that increasing the curing temperature accelerated the initial hydration rate, however the hydration rate at later age was reduced. Escalante-Garcia et al.(Escalante-Garcia and Sharp, 2000) reported that the curing temperature effect the hydration rate of blended cements varies with the changes in cement components.

By now, the effect of raw materials and alkali activators on the microstructural evolution of HAC systems and relevant strength development mechanism are not well understood. The previous studies mainly focused on low-Ca HAC systems, and the compressive strength is generally low in both early and late stages (normally below 50 MPa)(A. Palomo, 2007, Donatello et al., 2013a, Mejia et al., 2015, Alahrache et al., 2016b, Garcia-Lodeiro et al., 2017, Askarian et al., 2018). As is well known that alkali activator is a key parameter of alkali-activated materials (Alahrache et al., 2016b, Garcia-Lodeiro et al., 2016b, Sedira and Castro-Gomes, 2020). The

influence of the dosage of alkali activator on HAC mechanical properties need to be studied. Besides, the curing condition is also an important parameter of alkali-activated materials for compressive strength development especially at early age(Qu et al., 2016). And the microanalysis of HACs with different dosage of alkali activator and precursors are beneficial to understand their mechanical strength development precisely. To provide reference for design and application of HACs in construction, it is essential to understand the mechanical strength development mechanism of different HACs system.

In this study, a series of HACs was prepared with 10%-30% OPC, 90%-70% GBFS, 0-8% alkali activator and curing at room temperature. The effects of type and dosage of activator used, and the ration of raw materials on the mechanical properties of different HACs will be studied.

5.2 Experimental

The binder systems were prepared in Table 5-2. The systems include Partial replacement system (NO.1), HAC systems (NO. 2 to 9), OPC system (NO. 12) and AAM system (NO. 13). The OPC system hydrated by water was prepared as reference. All systems were mixed with the same water-to-solids ratio (w/s) of 0.4.

The activators (wt.% of binders) used was $\text{Na}_2\text{SiO}_3 \cdot 9\text{H}_2\text{O}$ in solid condition and blended into ground together with the binders.

Table 5-2 Composition of HAC paste systems (wt.%).

NO.	System	GBFS	OPC	Activator
1	90GBFS-10OPC	90	10	-
2	90GBFS-10OPC	90	10	1
3	90GBFS-10OPC	90	10	2
4	90GBFS-10OPC	90	10	3
5	90GBFS-10OPC	90	10	4
6	90GBFS-10OPC	90	10	5
7	90GBFS-10OPC	90	10	6
8	90GBFS-10OPC	90	10	7
9	90GBFS-10OPC	90	10	8
10	80GBFS-20OPC	80	20	5
11	70GBFS-30OPC	70	30	5
12	100OPC	-	100	-
13	100GBFS	100	-	5

The samples were cured in standard curing condition (at 20 ± 2 °C and RH >

95 %) in accordance with ISO 1920-3-2004.

5.3 Testing procedure

The testing procedure are introduced in chapter 3 section 3.4.

5.4 Results and discussion

5.4.1 Compressive strength

This section presents the compressive strength results for all the systems detailed in Table 5-2. These systems were cured at room temperature and tested at intervals of 1 day, 7 days, and 28 days, using varying dosage of alkaline activator. . In this study, the compressive strength of HAC pastes were evaluated by the ratio of raw materials and the dosage of alkali activator.

The highest mechanical strength results at early ages were obtained in systems with higher GBFS content, indicating that a 5% dosage of Na_2O activator is adequate for early activation of GBFS. Systems 10 and 11 showed a significantly slower strength increase in the initial stages (1–7 days), a behavior characteristic of replaced cements, as observed by Barnett et al. (Barnett et al., 2006). It has been reported that GBFS particles act as nucleation sites, promoting the formation of C–S–H gel, densifying the cementitious matrix, and reducing porosity. Additionally, GBFS improves fluidity, further decreasing porosity (Bijen, 1996, Escalante-García et al., 2003). The systems with higher dosages of Na_2O exhibit increased strengths. This is confirmed by previous investigations, which indicate that a highly alkaline environment is necessary to achieve greater mechanical strengths (Xue et al., 2021a). However, excessive Na_2O content resulted in the development of cracks in the HAC, leading to a decrease in compressive strength as shown in Figure 5-2. It is crucial to incorporate an appropriate dosage of alkali activator in the design and application of HAC.

5.4.1.1 Effect of the ratio of OPC

The compressive strength results showed in Figure 5-1 are the binders described in Table 5-2, activated with 5% Na_2O content, cured at room temperature and tested at 1 day, 7, and 28 days.

System6 (90GBFS-10OPC) demonstrates superior mechanical strength

outcomes: 1d 36.2MPa, 7d 64.3 MPa and 28d 82.8 MPa, higher than OPC at the same periods which is 1d 25.9 MPa, 7d 61.4 MPa and 28d 71.2 MPa. The result assures that HAC system with high proportion (90%) of SCMs exhibits even higher compressive strength than OPC. The result also proves that by adjusting the proportion of raw materials and adding an appropriate dosage of alkali activator, high-strength HAC can be obtained. Systems 4 to 7 exhibit higher compressive strength compared to system 13 at 28 days. This indicates that the HAC shows higher compressive strength than AAM with the same type and dosage of alkali activator. The main reason for this phenomenon is that the hydration of OPC in the HAC system increases the pH value of the reaction solution (Garcia-Lodeiro et al., 2016b), resulting in a more complete final reaction compared to the AAM system. The hydration reaction of OPC is slower than the alkali activation reaction, which may be the reason why the early strength of system 10 and 11 (especially 1-day strength) is lower than that of system 13.

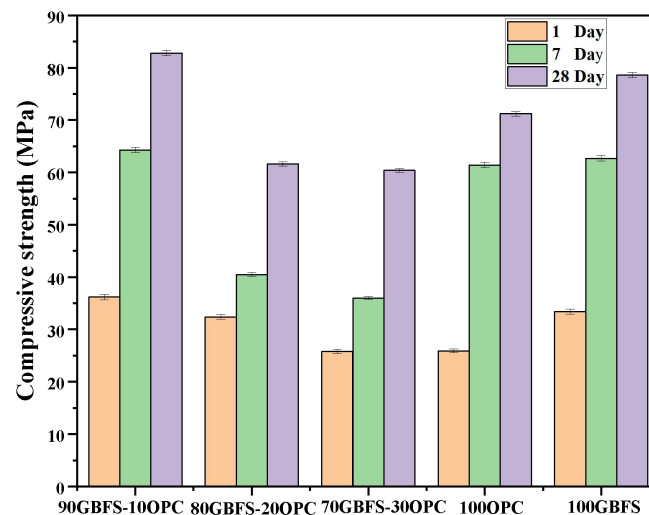


Figure 5- 1 Compressive strength of binder systems activated with 5% Na₂O.

5.4.1.2 Effect of dosage of alkali activator

The compressive strength results showed in Figure 5-2. are the system 1 to 9, activated by different dosage of Na₂SiO₃ · 9H₂O, cured at room temperature and tested at 1day, 7, and 28 days. OPC sample and system 1 (90GBFD-10OPC or call blended cement) hydrated by only water were taken and used as references.

As it is shown in Figure 5-2, blended cement (BC) provides the lowest compressive strength in all the specimens at 1 day, 7 and 28 days, especially at early age (6.8 MPa at 1d). The main reason is that the hydration reaction rate of BC

hydrated by only water is relatively slow, associated with higher porosity, reduced mechanical strength and stiffness compared to OPC concretes (Menéndez et al., 2003, Hoshino et al., 2006, Whittaker et al., 2014, Hlobil et al., 2016, Durdziński et al., 2017). The slow hydration reaction rate of blended cement (Macphee et al., 1988, Pane and Hansen, 2005, Kocaba et al., 2012) produces the reduced reactivity of GBFS compared to OPC (Escalante-Garcia and Sharp, 2001). GBFS particles blended with OPC react only after activation due to the production of OH^- produced from OPC hydration (Roy, 1982). Due to the relatively low proportion of OPC in this experiment, the reaction process relatively slow, which result in the low compressive strength at early age. The hydration reactions of OPC and GBFS occur simultaneously and interact with each other (Richardson and Groves, 1992, Chen and Brouwers, 2007), resulting in a very complex combination of different hydration products. Since GBFS contains relatively lower content of calcium than OPC (Lothenbach et al., 2011a), the calcium-silicate-hydrates (C-S-H gel), the most significant hydration products of OPC exhibit a lower calcium-to-silicate ratio (C/S) in blended cement compared to OPC (Richardson and Groves, 1992, Königsberger and Carrette, 2020).

The compressive strength of HAC systems shows an increase with the rising dosage of alkali activator, followed by a decrease with the increment of Na_2O content. When the Na_2O content dosage reaches 4%, HAC demonstrates a compressive strength of 47.4 MPa at 7 days, showing a 36% increase when the Na_2O content dosage reaches 5%. The compressive strength of the HAC system exhibits an increasing trend with the rising dosage of Na_2O content, which is more pronounced in the early age and less apparent in the later stages. The compressive strength of HAC reaches 64.3 MPa with a 5% dosage of Na_2O content at 7 days. Subsequently, there is a further 29% increase, reaching 82.8 MPa, in compressive strength from 7 to 28 days. This surpasses the compressive strength of OPC concrete samples at all tested ages. However, the compressive strength of HAC decreases with the increasing dosage of Na_2O content, especially when the dosage exceeds 5%. In comparison between HAC samples with alkali content of 5% and 8%, the compressive strength of HAC exhibits a decrease of 25% at 7 days and further decreases by 27% at 28 days. The compressive strength of HAC displays a decreasing trend with the increasing dosage of Na_2O content. This trend is less

apparent in the early age and becomes more noticeable in the later stages.

With the increasing dosage of alkali activator, the pH value in the reaction solution increases gradually, thereby accelerating the dissolution of GBFS in alkaline solution and increasing the reaction rate. When the dosage of Na_2O reaches 4%, HAC exhibits a compressive strength equivalent to OPC at 28 days. Upon reaching a dosage of 5% Na_2O content, the compressive strength of HAC reaches its peak, subsequently declining as the activator dosage increases. The main reason for this phenomenon is that an excessive amount of Na_2O causes HAC samples to expand and crack, resulting in a decrease in the compressive strength of HAC. Observably, by adding an appropriate dosage of alkali activator, HAC exhibits higher compressive strength than OPC, both at early age and later age.

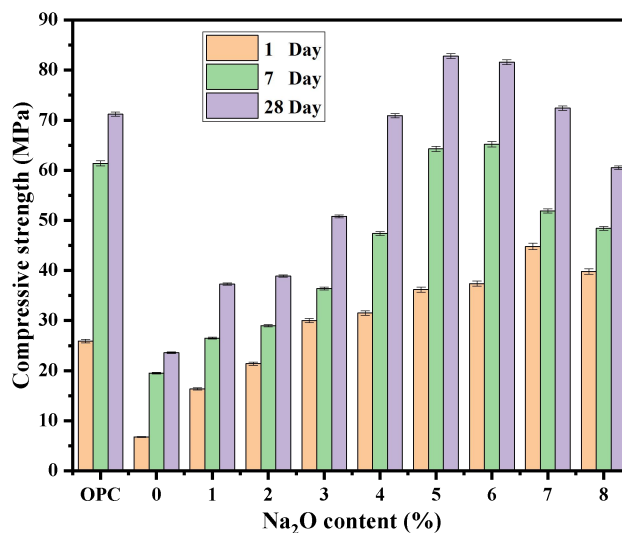


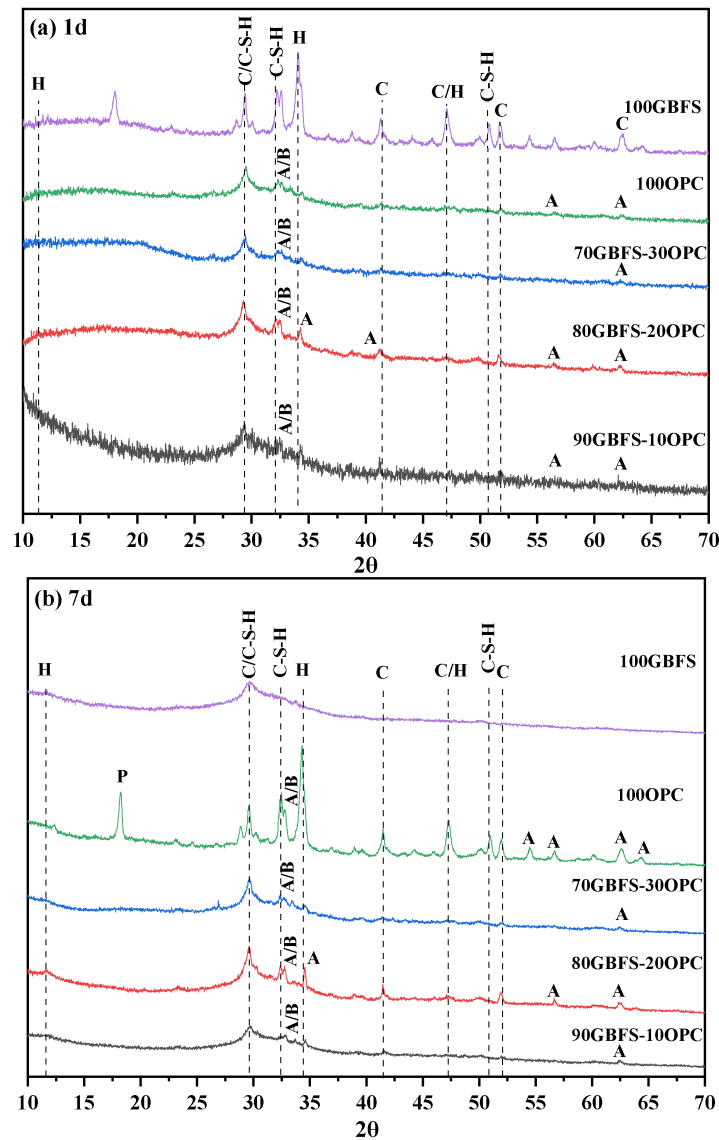
Figure 5-2 Compressive strength of OPC and HACs activated by different dosage of alkali activator.

5.4.2 XRD analysis

X-ray diffraction (XRD) technique was used to study the reaction products of all binders. XRD patterns for binders with different ratio of raw materials, and Na_2O content ranging from 0 to 8%, curing at 1 day, 7 and 28 days were shown in Figure 5-3 and Figure 5-4. Analysis of the variations in the diffractograms over time and by varying the ratio of raw materials and Na_2O content revealed in the following.

A diffraction peak at around 11.6° (2θ) is possibly due to the presence of hydrocalumite, which is prone to be produce with a high proportion of GBFS (S. Donatello¹, Taylor et al., 2010, Qiu et al., 2015), and activated with Na_2SiO_3 and NaOH (Shi et al., 2003, Haha et al., 2011). Peaks corresponding to portlandite and ettringite are not observed neither in HACs curing at 1day, 7days nor 28 days. This

phenomenon is similar to what has been reported in other researches (Angulo-Ramirez et al., 2017), and due to the small proportion of OPC in HAC system and inhibition or delay of hydration rate in OPC as a consequence of high alkalinity in the solution (Puertas et al., 2011). Hydrated gehlenite has also been detected as a hydrated product of GBFS activated with Na_2SiO_3 and NaOH (Shi et al., 2003). A corresponding peak at $29.4^\circ 2\theta$ is likely due to the presence of calcite, attributed to the carbonation of portlandite, as high pH solutions tend to induce carbonation (Garcia-Lodeiro et al., 2013a, Cao et al., 2021).



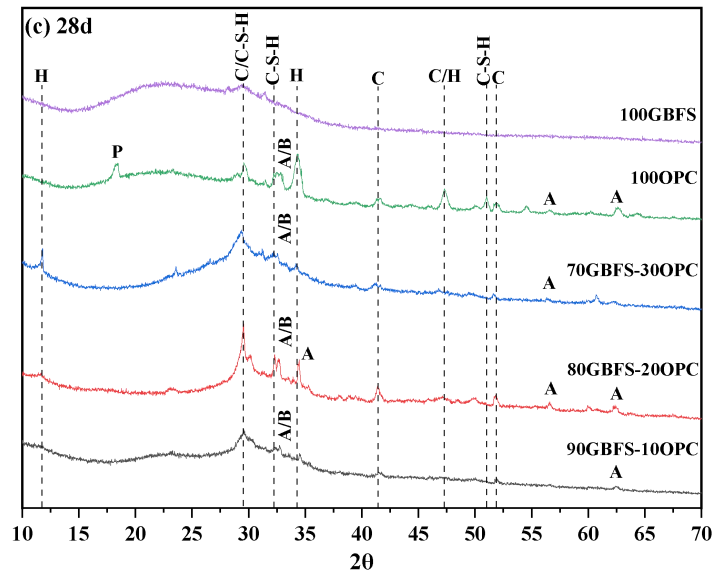
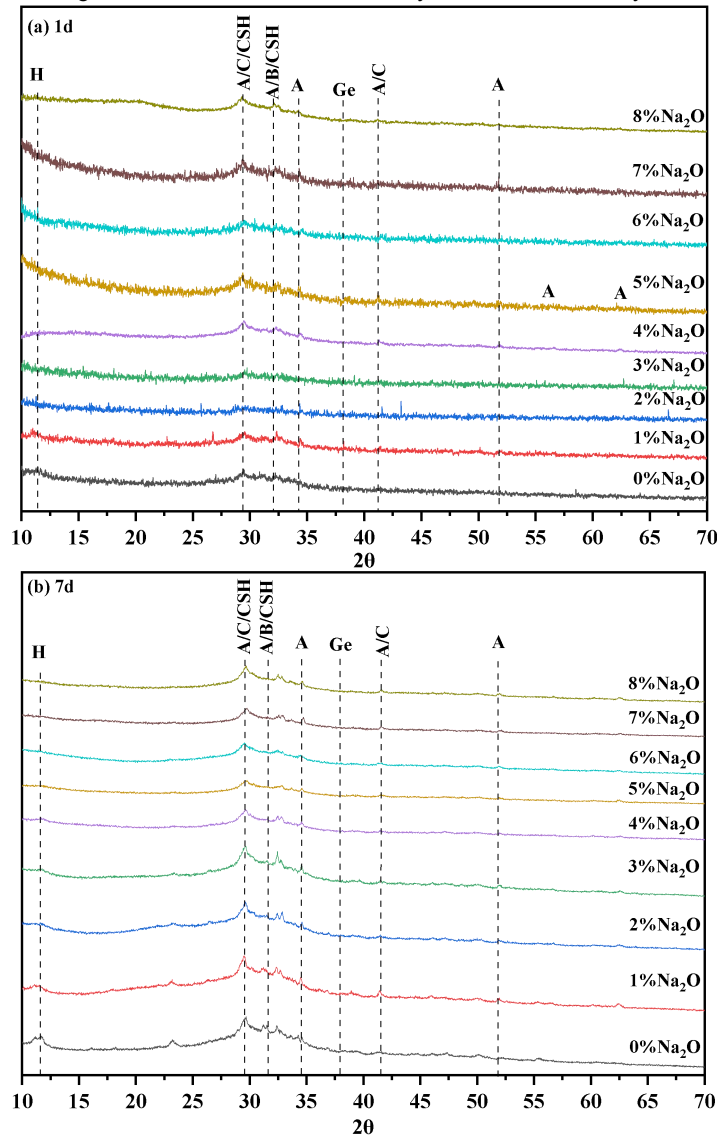


Figure 5-3 XRD patterns of binders with different proportion of precursors, (a) 1 day of curing; (b) 7 days of curing; (c) 28 days of curing. A: C_3S ; B: C_2S ; C: Calcite; H: Hydrocaluminte; Ge: hydrated Gehlenite (C_2ASH_6).



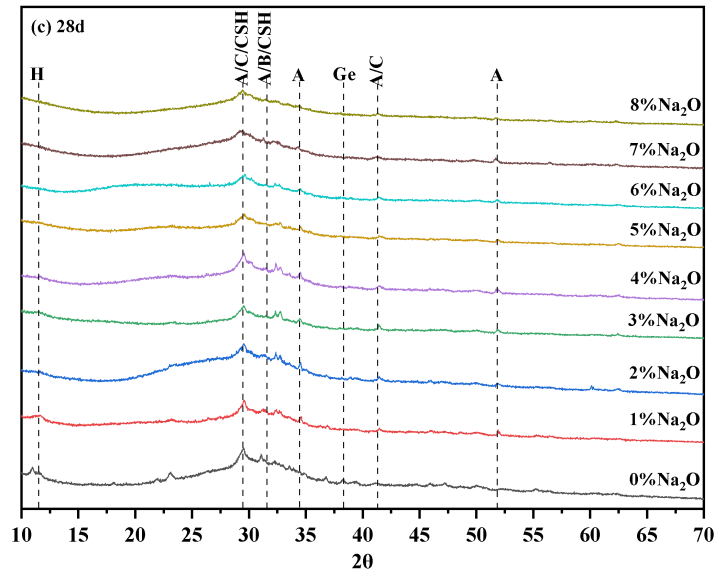


Figure 5-4 XRD patterns of HACs with different dosage of Na_2O , (a) 1 day of curing; (b) 7 days of curing; (c) 28 days of curing. A: C_3S ; B: C_2S ; C: Calcite; H: Hydrocaluminte; Ge: hydrated Gehlenite (C_2ASH_8).

Crystalline phases alite (C_3S) and belite (C_2S), which come from the unreacted OPC, are detected in HAC and OPC samples. The quantity of C_3S and C_2S is decreased gradually with the increasing curing time and dosage of alkali activator in HAC systems. At the same time, the quantity of crystalline hydration products such as hydrocaluminte, hydrated gehlenite and calcite is increased with the prolong of curing time and increasing of Na_2O content. This may be the main reason for the continuous development of the compressive strength of the samples with increasing age and alkali content, and the result is consistent with the increasing density of particles in the SEM image of the sample.

All the diffraction patterns contain a wide diffuse halo from 29.4° to 50.1° (2θ), which is generally associated with the formation of a mixture of C-S-H (the main hydration product of OPC) and or C-A-S-H (the main product of alkali activated GBFS) gels (Garcia-Lodeiro et al., 2013a, Angulo-Ramirez et al., 2017). The mixture gels of C-S-H and C-A-S-H has been proved in previous studies (Xue et al., 2021a, Garcia-Lodeiro et al., 2013b, Donatello et al., 2014, Alahrache et al., 2016b, Garcia-Lodeiro et al., 2011). The gels of C-S-H and C-A-S-H and the mixture of them are all XRD amorphous, and their presence will be confirmed by BSEM.

It is observed that HACs with different dosage of Na_2O content consistently exhibit the same reflection peaks. Moreover, the XRD patterns of the main reaction products of HACs with different dosage of Na_2O content did not show significant changes at 1 day, 7 days, and 28 days. Generally speaking, the compressive strength of HACs activated with different dosage of Na_2O content is not determined

by the types of reaction products, but more closely related to their quantity.

5.4.3 ^1H NMR analysis

^1H NMR technology was used to explore pore structure of all binder systems curing at 1 day, 7 and 28 days. In this ^1H NMR analysis, the signal intensity of water in all binders are tested. And, the relationship between water mass and signal intensity has to been established. The development of transverse relaxation time of T_2 vs signal intensity is evaluated by the different ratio of raw materials in the binder systems, and the dosage of Na_2O content in HACs.

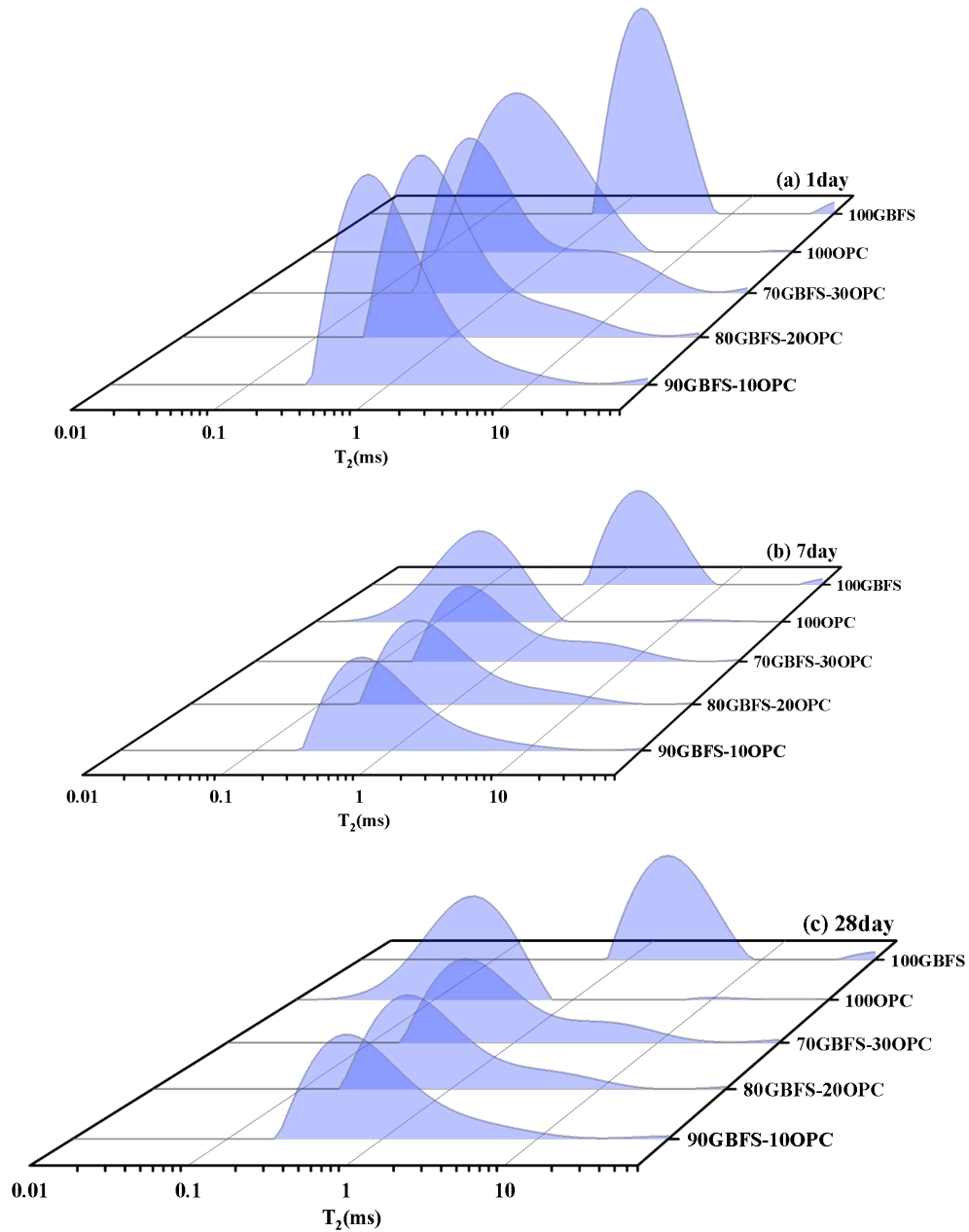
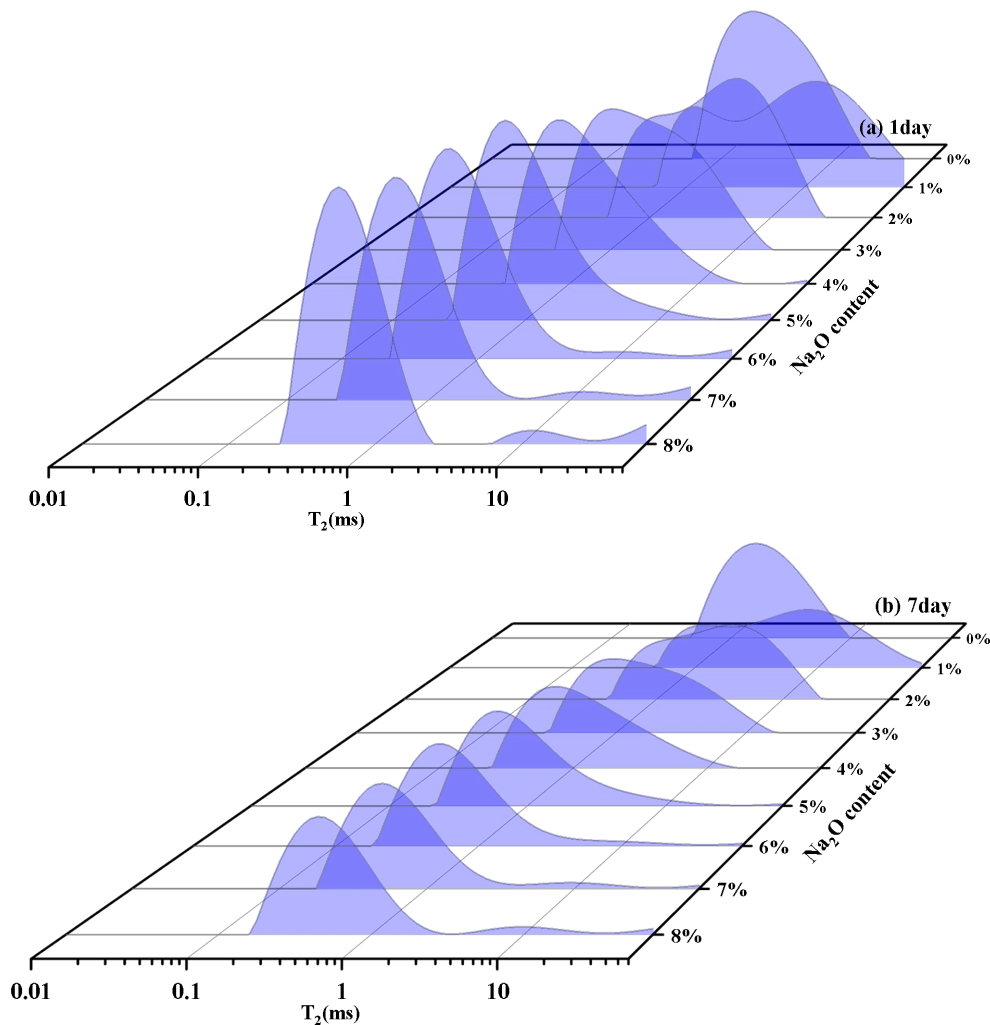


Figure 5-5 T_2 vs. intensity during hydration of binders with different ratio of OPC (a) 1day;(b) 7 day; (c) 28day.

T_2 vs. intensity during curing days of binder systems with different ratio of OPC on pore structure distribution is shown in Figure 5-5(a, b and c), and different ratio of OPC present different pore structure distribution. All of the binders present the signal intensity peaks of T_2 shifted left gradually with time, attributed to the majority of water migrating to smaller pores, and show compressive strength increases with the prolong of curing age. AAM (100GBFS) presents signal intensity peak of T_2 at 1.8ms for the first day, indicating that the water mainly exists in the form of capillary pore water. OPC shows signal intensity peak of T_2 at 0.4ms, and HACs at 0.5-0.7ms for the first day, which indicated that some water is converted into gel pore water in the first day. With the increasing curing time, AAM (100GBFS) presents signal intensity peak of T_2 at 1.7ms for 7 days, but with intensity peak decreasing significant declined. OPC shows signal intensity peak of T_2 at 0.2ms, indicating that lots of water is converted into gel pore water in the first day. HACs present nearly the same pore structure distribution, 90GBFS-10OPC shows the signal intensity peaks of T_2 shifted left the most with time, attributed to the highest compressive strength increases with time. OPC shows signal intensity peak of $T_2 < 0.2$ ms, which indicating that the water is converted into smaller gel pore water with the hydration. The T_2 vs. intensity curves for 7 and 28 days did not exhibit significant changes in HACs and GBFS. This suggests that the compressive strength increases more rapidly in the early curing days and more gradually in the later age.

The influence of the dosage of Na_2O content in HACs on pore structure distribution is shown in Figure 5-6(a, b and c), and the increasing dosage of alkali activator in HACs exhibit different pore structure distributions. As shown in Figure 5-6(a), BC (90GBFS-10OPC hydrated by only water) exhibits signal intensity peak of T_2 at around 2.0ms for 1 day, which indicated that the water mainly exists in the form of capillary pore water, thus presents the lowest compressive strength at 1 day. The curves of BC shifted to left with the increasing curing day, but the speed is very slow. After 28 days, the intensity peak of T_2 moved left slowly to around 1.0ms, signals are found on the intensity curve at $T_2 < 1.0$ ms, which suggests that some water has infiltrated into the gel pores, leading to the formation of hydration products. The outcome may explain reason why BC with high proportion of OPC presents compressive strength increasing slowly. The intensity peaks shifted to the left and weakened with curing time as the dosage of Na_2O content increased in HACs. As

shown in Figure 5-6(a and b) Two intensity peaks were detected in HACs with Na_2O content ranged from 1% to 3%. An intensity peak at $T_2 < 1.0\text{ms}$ suggests the formation of hydration products. The other peak at $T_2 > 1.0\text{ms}$, indicating a proportion of water was trapped in larger pores. The results meant that larger pores were produced in HACs with small dosage of alkali activator. As Na_2O content continues to increase the intensity peaks shifted to left over time, and the rate of leftward movement increases with the increase of Na_2O content, and this is more pronounced in the early stages and less prominent in the later stages. Meanwhile, it should notice that the intensity peaks do not decrease continuously with the increase of Na_2O content. The intensity peaks show the lowest with an Na_2O content of 5% after 1 day 7, and 28 days, which indicated that the most suitable pore structure distribution were produced. Correspondingly, the compressive strength of HACs exhibits an increasing trend with the rising dosage of alkali activator, followed by a decrease with the increment of Na_2O content, as shown in Figure 5-2.



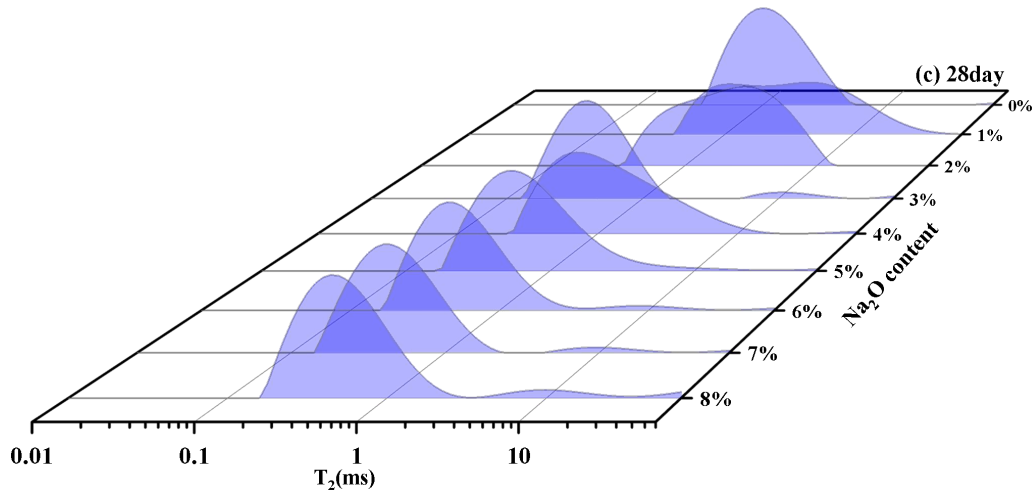


Figure 5-6 T_2 vs. intensity during hydration of binders with different dosage of Na_2O (a) 1day;(b) 7 day; (c) 28day.

5.4.4 Scanning Electron Microscopy analysis

Scanning Electron Microscopy (SEM) analysis was conducted on HACs with varying ratios of OPC and different dosages of Na_2O content, cured at 1 day, 7 and 28 days were shown in Figure 5-7 to Figure 5-12. Analysis of the variations in the micrographs over time and by varying the ratio of OPC and Na_2O content revealed in the following.

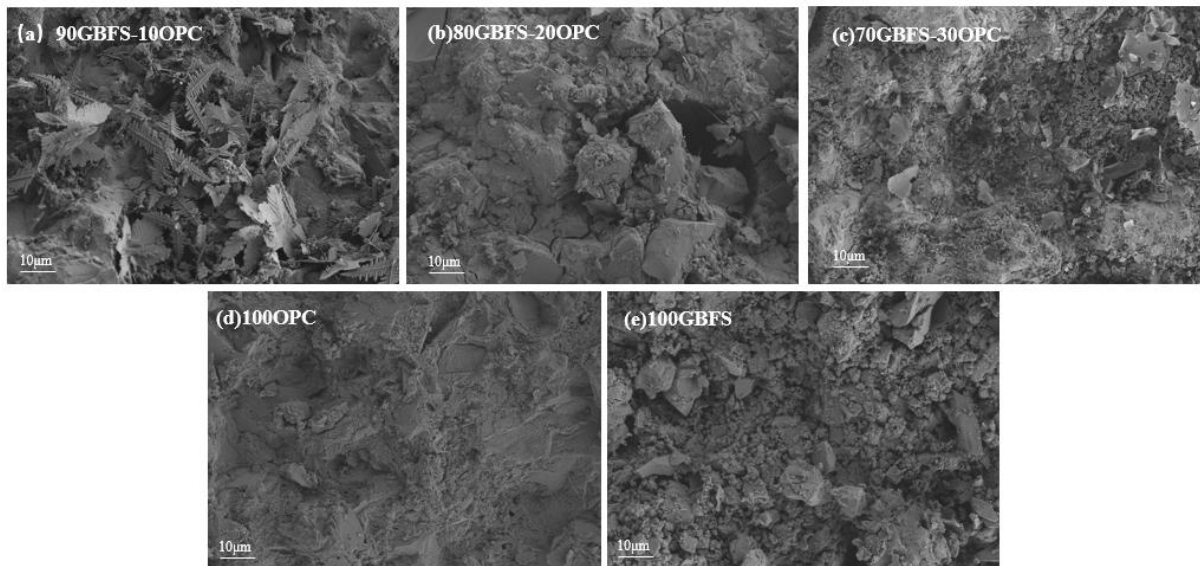


Figure 5-7 SEM images of binder systems activated with 5% Na_2O for 1 day.

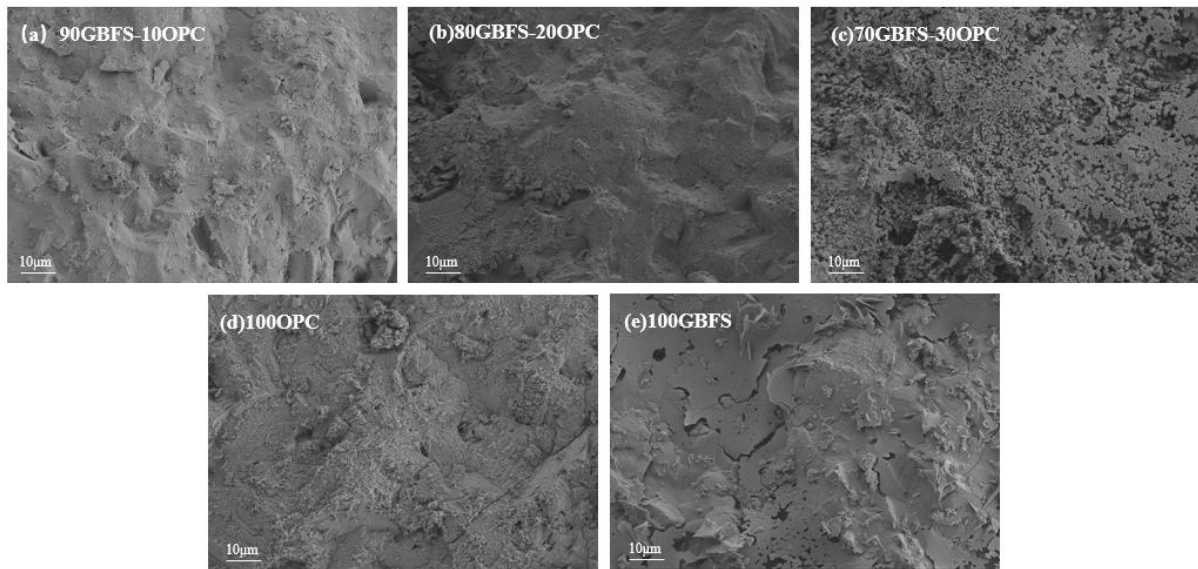


Figure 5-8 SEM images of binder systems activated with 5% Na₂O for 7 days.

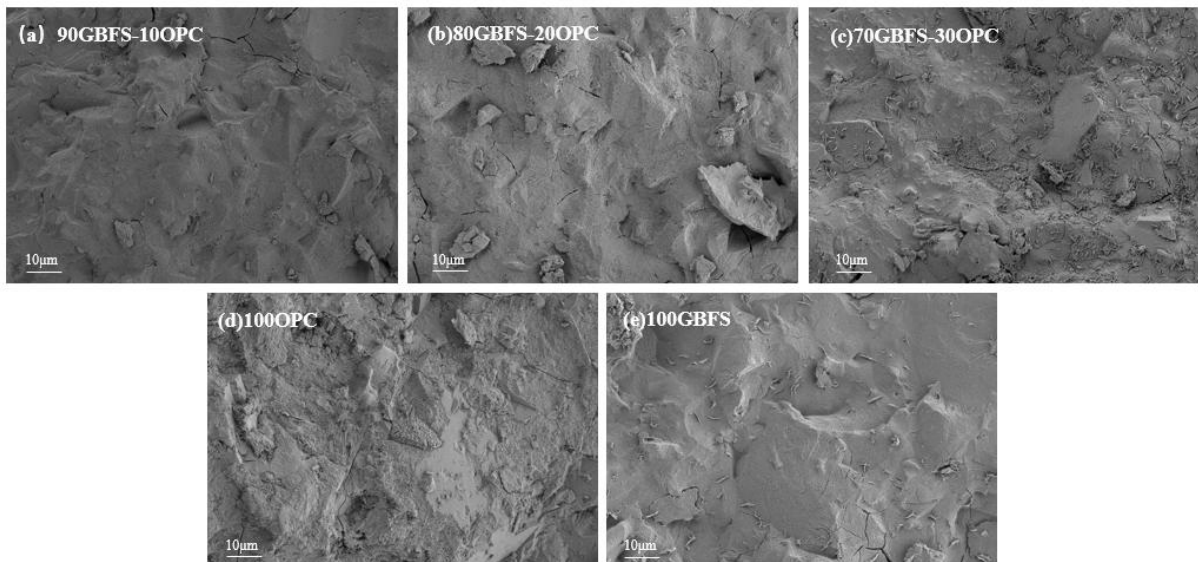


Figure 5-9 SEM images of binder systems activated with 5% Na₂O for 28 days.

Figure 5-7 shows the microstructure images of binder systems after 1 day of curing. As it is shown in SEM images, 90GBFS-10OPC presents more reaction products compared to other binder systems. 70GBFS-30OPC shows loss microstructure, indicates that less reaction products produced, and these results are consistent with the results of compressive strength in Figure 5-1. The same pattern can be observed on the microstructure images at 7 and 28 days of curing. As depicted in the SEM micrographs, the microstructures of all binders become denser and more compact with the increasing curing days. The hydration productions of HAC systems normal have a three-dimensional structure, which is denser and harder compared to two-dimensional C-S-H gel crystal structure (Hadj-sadok et al., 2011, Garcia-Lodeiro et al., 2012). Small cracks have been observed at the samples of 7

and 28 days, especially at the sample of 100GBFS curing at 28 days. Spongy particles are detected in the micrographs of HACs at both 7 and 28 days, which is possibly due to the presence of Hydrated gehlenite (C_2ASH_8) a hydrated product of GBFS activated with Na_2SiO_3 and $NaOH$ (Yang et al., 2012, Shi et al., 2003).

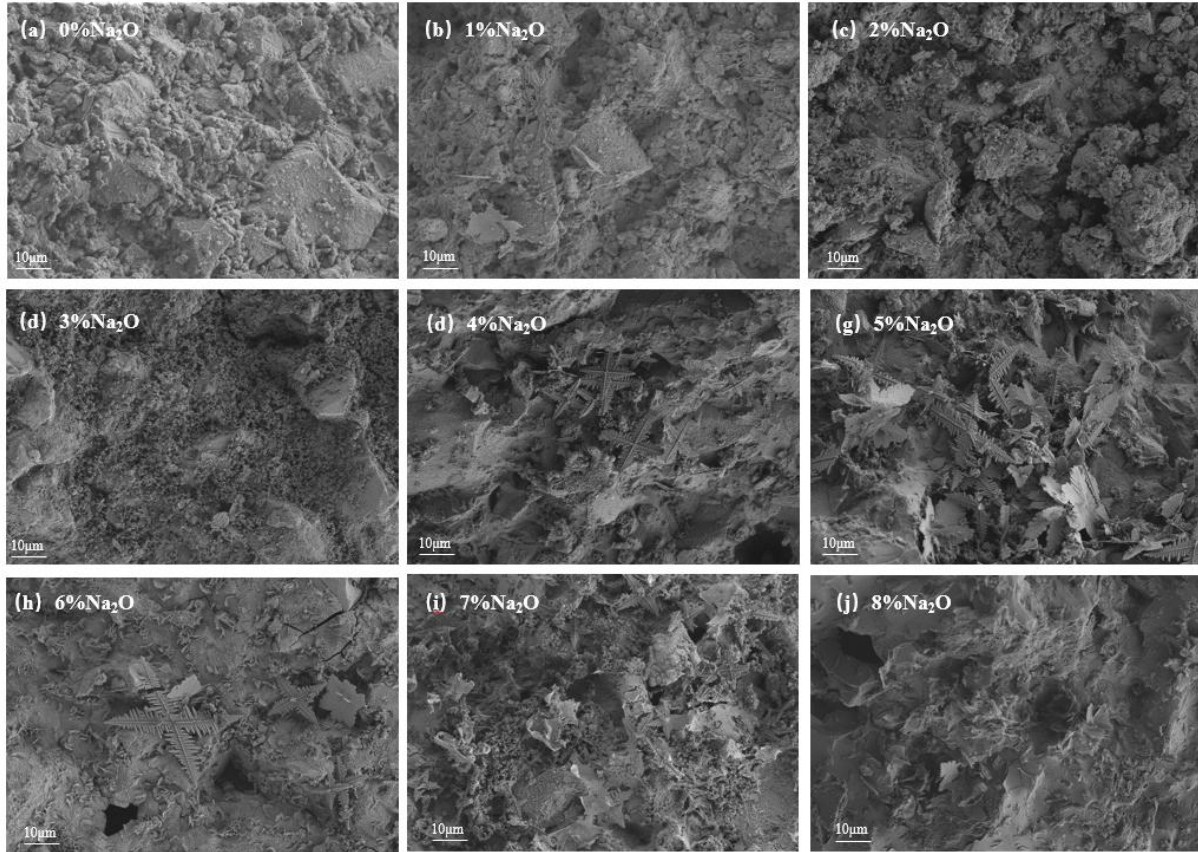


Figure 5- 10 SEM images of HACs with different dosage of Na_2O curing for 1 day.

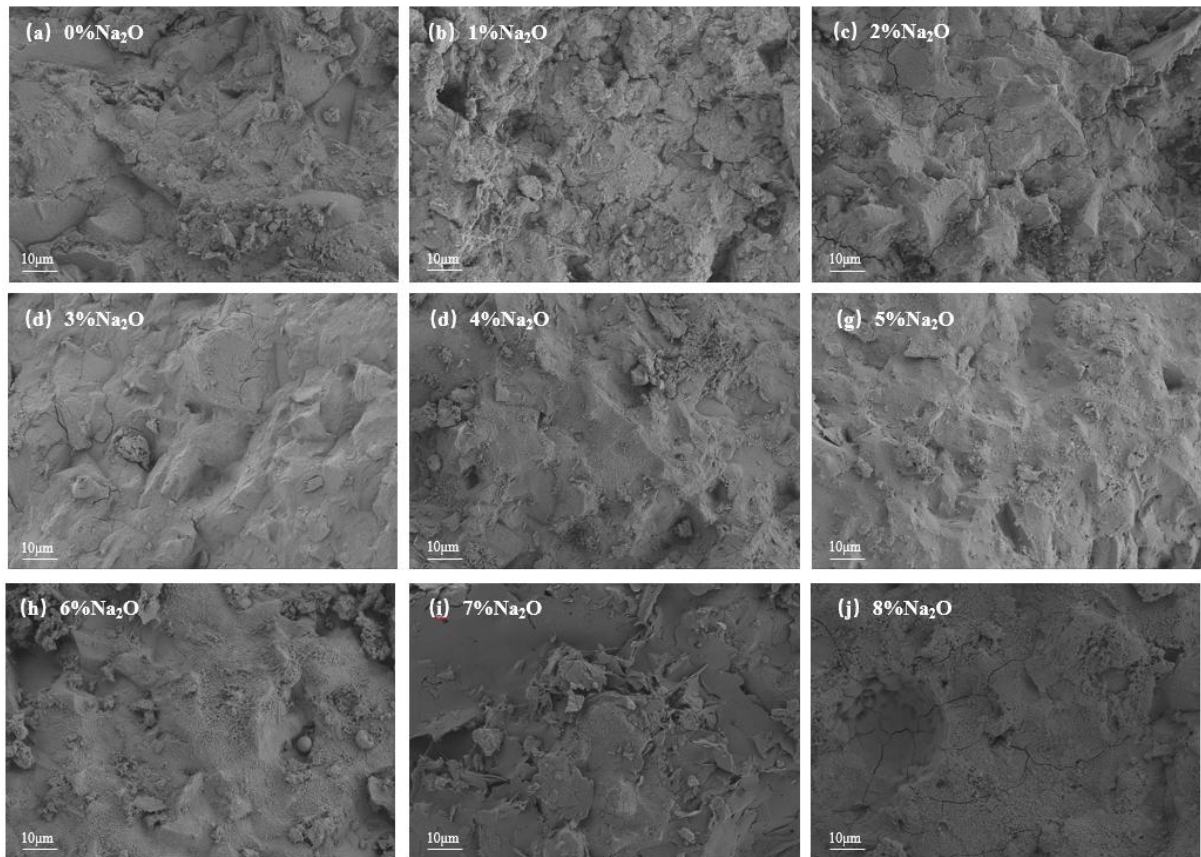


Figure 5- 11 SEM images of HACs with different dosage of Na_2O curing for 7 days

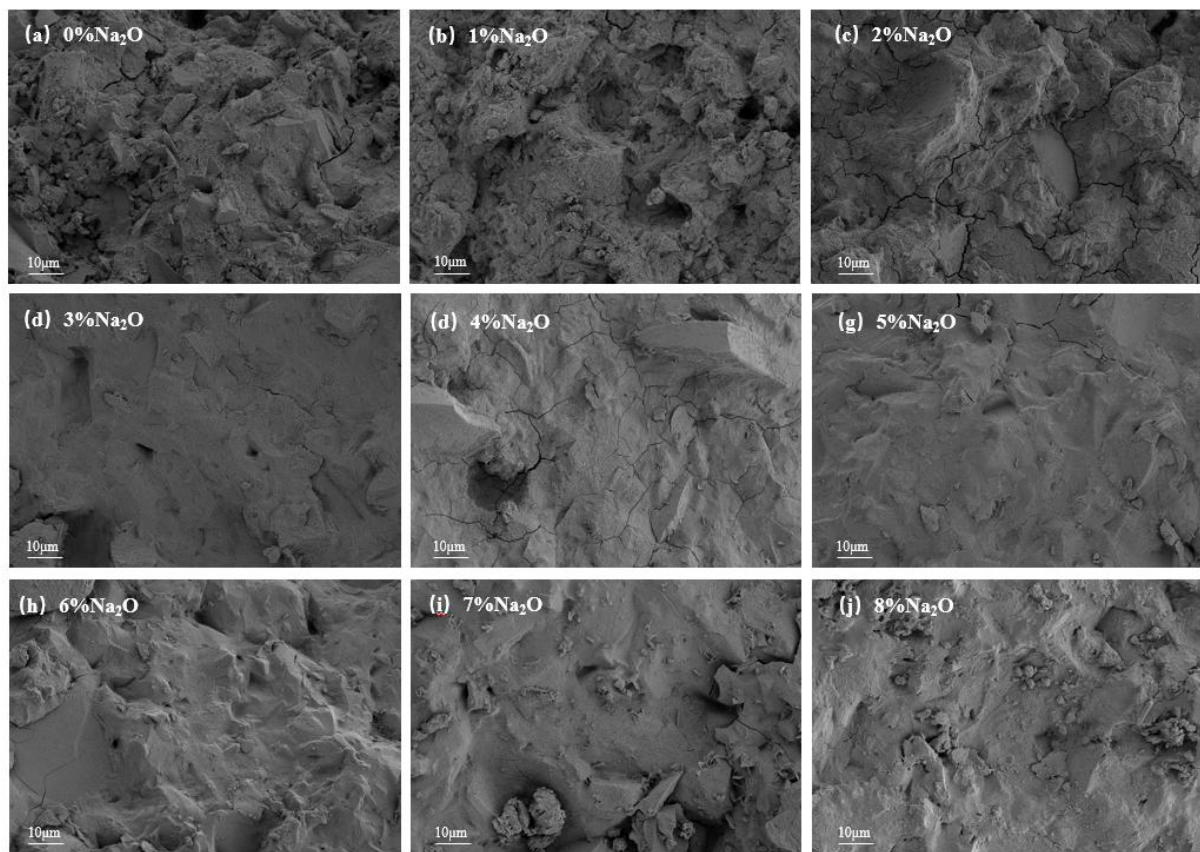


Figure 5- 12 SEM images of HACs with different dosage of Na_2O curing for 28 days.

The outcomes show that the matrix becomes denser with the increasing dosage of $\text{Na}_2\text{SiO}_3 \cdot 9\text{H}_2\text{O}$. As shown in Figure 5- 10 to Figure 5- 12 the binder with 90% GBFS and 10% OPC hydrated by only water looks porous, associated with higher porosity and lower mechanical strength compared to HAC activated by higher dosage of $\text{Na}_2\text{SiO}_3 \cdot 9\text{H}_2\text{O}$. The relatively slow hydration reaction rate of BC produces the slow reaction rate of GBFS compared to OPC (Escalante-Garcia and Sharp, 2001). In BC system, GBFS particles react only after the hydration of OPC (Roy, 1982). Due to the high proportion of GBFS and low ratio of OPC in BC system, the reaction process is very slowly, which results in the lowest compressive strength. As shown in Figure 5- 10, OPC particles normally present bright grey shadows with irregular shapes, and the GBFS particles are relatively dark and the color remains uniform (Nath and Sarker, 2015, Xue et al., 2021a). Unreacted C_3S and C_2S are discernible in the SEM images, which is consistent with the XRD patterns of HACs in Figure 5- 4. Both SEM images Figure 5- 10 to Figure 5- 12 and XRD patterns Figure 5- 4 reveal a gradual decrease in the quantity of C_3S and C_2S with the increasing

dosage of Na_2O content. As seen in Figure 5-10 to Figure 5-12, the gelation matrix becomes denser and more compact with the increasing of Na_2O content. With the increasing dosage of Na_2O content, the pH value in the reaction solution increases gradually. In the alkaline solution, both OPC and GBFS hydration rate have been accelerated. In higher PH solution, the hydration is more quickly, especially for OPC hydration. The rapid rate of Ordinary Portland Cement (OPC) hydration will result in fast setting and an increase in the compressive strength of HAC. However, small cracks can be detected in Figure 5-10 to Figure 5-12, especially at the images by high dosage of Na_2O content which is possibly due to the presence of Hydrated gehlenite (C_2ASH_8) a hydrated product of GBFS activated with Na_2SiO_3 and NaOH (Yang et al., 2012, Shi et al., 2003). This is the primary reason for the decrease in compressive strength in HACs with Na_2O content exceeding 5%.

5.5 Conclusions

HACs with high proportion of supplementary cementitious materials and low proportion of ordinary Portland cement were manufactured with the utilization of alkali activator. The mechanical strength of HAC was affected by many factors, some conclusions can be drawn in the following:

(1) The system 6 (90GBFS-10OPC) activated by 5% Na_2O showed the highest mechanical strength at all the curing ages. The results indicated that HACs can be synthesized flexibly by using different proportion of raw materials. By adjusting the ratio of raw materials, activated by appropriate alkali activator, HACs exhibited good mechanical strength, especially at early age.

(2) The compressive strength of the HAC system demonstrated an increase with the rise in alkali activator dosage. However, an excessive amount of Na_2O content led to the development of cracks in the HAC, resulting in a decrease in compressive strength. It is crucial to incorporate an appropriate dosage of alkali activator in the design and application of HAC.

(3) HACs with varying Na_2O content dosages exhibited no significant alterations in the types of main reaction products at 1 day, 7 days, and 28 days. The quantity of main reaction products increased gradually with the rising curing time and alkali activator dosage in HAC systems. The compressive strength of HACs activated with different Na_2O content dosages was not determined by the types of reaction

products but was more closely related to their quantity.

(4) In all binders, the signal intensity peaks of T_2 gradually shifted left with time, signifying the migration of water to smaller pores. Additionally, compressive strength increased with the extension of curing time. The intensity peaks were at their lowest with an Na_2O content of 5% during the curing period, indicating the production of the most suitable pore structure distribution.

(5) The microstructures of all binders became denser and more compact with the increasing curing time, 90GBFS-10OPC presented more reaction products compared to other binder systems. The gelation matrix became denser and more compact with the increasing of Na_2O content, high dosage of Na_2O content brought cracks and decreased of compressive strength in HACs.

CHAPTER 6: PAPER 3 – THE FACTORS AFFECTING SETTING PROPERTIES OF HYBRID ALKALINE CEMENT BASED ON PORTLAND CEMENT AND GROUND BLAST FURNACE SLAG

6.1 Introduction

Hybrid alkaline cement (HAC) is generally regarded as a new generation of low-carbon binders, which consists of a high ratio of SCMs, a low ration of OPC, activated by appropriate alkali activators. HAC combines the advantages of both alkaline activated material (AAM) and blended cement, shows comparable or even higher mechanical strength and excellent durability performance (Garcia-Lodeiro et al., 2013b, Xue et al., 2021b, Fernandez-Jimenez et al., 2013a, S. Donatello¹, 2014). The incorporation of a chemical activator accelerates the hydration kinetics and enhances the mechanical strength of HAC. However, when HAC is designed with high mechanical strength (high than 60MPa) applications, HAC suffers from poor workability with fast setting and high viscosity, which make it difficult to pump or cast. For example, the initial setting time and final setting time of a HAC paste (70% fly ash and 30% OPC activated by $\text{Na}_2\text{O} \cdot n\text{SiO}_3$ and NaOH) are 13 and 31 min, while the initial setting time and final setting time for OPC generally are 138 and 196 min respectively (Suwan et al., 2014). The optimal initial setting time of a fresh concrete has an important influence on its mixing and pumping process, and effects its strength, durability, and surface quality.

Ning Li et al. explored a method for controlling setting time by altering the composition of alkali activator ions and the degree of silicate polymer in alkaline-activated slag the dosage and alkali modulus of alkali activator, and concluding that properly designed activators can achieve both designable setting time and reasonable compressive strength. Chang et al. (Chang, 2003) studied the setting properties of slag activated by sodium silicate, and found that the PH value of the reaction solution, The dosage and alkali modulus of the alkali activator play an important role in setting properties. Pilehvar et al. (Pilehvar et al., 2020) reported that the setting times of both OPC and AAM paste decreased with the increasing of temperature, due to the accelerated hydration of OPC and geopolymerization of AAM

in high temperature. Some studies found that the ratio of raw materials in HAC system effects setting characters, dramatically(Balun and Karatas, 2023). By now, the factors affecting setting characters of HAC systems have not been fully understood, and the previous studies mainly focused on low-calcium based HAC systems, report about HAC with high mechanical strength and controlled setting times is rare(Millan-Corrales et al., 2020, Fernandez-Jimenez et al., 2019, Alahrache et al., 2016b, Donatello et al., 2013a, Qu et al., 2016, Askarian et al., 2018, Sanchez-Herrero et al., 2019).

Based on the above consideration, this research explores the setting properties of HAC, a series of binder systems were prepared with different ratio of OPC and GBFS, addition with a series of dosage of alkali activator. This study utilizes the heat of hydration testing method to analyze the exothermic behavior during the hydration process of HAC. It employs ^1H NMR technology to investigate changes in capillary water or gel water and to analyze the phases of products after initial and final setting. These approaches provide a theoretical framework for understanding the impact of different parameters on the setting and hardening of HAC. The effects of dosage of activator used and the ration of raw materials on the setting properties of different binder systems were studied.

6.2 Experimental

The binder systems were prepared as shown in Table 6- 1. HAC systems were prepared with 10%-30% OPC, 90%-70% GBFS, and activated by 0-8% alkali activator. OPC hydrated by water was prepared as reference. All binder systems were mixed with the same water-to-solids ratio (w/s) of 0.4. The activator (wt.% of binders) used was $\text{Na}_2\text{SiO}_3 \cdot 9\text{H}_2\text{O}$ in solid condition and blended into ground togetherwith the binders.

Table 6- 1 Composition of binder systems (wt.%)

NO.	System	GBFS	OPC	Activator
1	90GBFS-10OPC	90	10	-
2	90GBFS-10OPC	90	10	1
3	90GBFS-10OPC	90	10	2
4	90GBFS-10OPC	90	10	3
5	90GBFS-10OPC	90	10	4
6	90GBFS-10OPC	90	10	5

7	90GBFS-10OPC	90	10	6
8	90GBFS-10OPC	90	10	7
9	90GBFS-10OPC	90	10	8
10	80GBFS-20OPC	80	20	5
11	70GBFS-30OPC	70	30	5
12	100OPC	-	100	-
13	100GBFS	100	-	5

All samples were made in standard curing (at 20 ± 2 °C and RH > 95 %) in accordance with ISO 1920-3-2004.

6.3 Testing procedure

The testing procedure are introduced in chapter 3 section 3.4.

6.4 Results and discussion

6.4.1 Setting time

Setting times of all binders were tested by vicat in accordance to Chinese standard specified in GBT 1346–2011. In this study, the setting properties of binder pastes were evaluated by the ratio of raw material and the dosage of alkali activator. The effect of the ratio of raw materials and the dosage of alkali activator on setting times of GBFS based binders is shown in Figure 6- 1. Figure 6- 1(a) shows the effect of the proportion of OPC on setting time of binders blended GBFS and/or OPC, with 5% Na₂O content. Both the initial and final setting times of the binders decreased as the ratio of OPC continued to increase in the combined binders. This could be the primary reason for the decrease in setting time as the ordinary Portland Cement (OPC) content increases in the binders. While the setting times of GBFS activated with the same Na₂O content are 62 and 99 min. The results indicate that in alkaline solution, the reaction between OPC and alkaline solution is much faster than that of GBFS. This may be the main reason for the decrease of setting time as the OPC content increases in the binders.

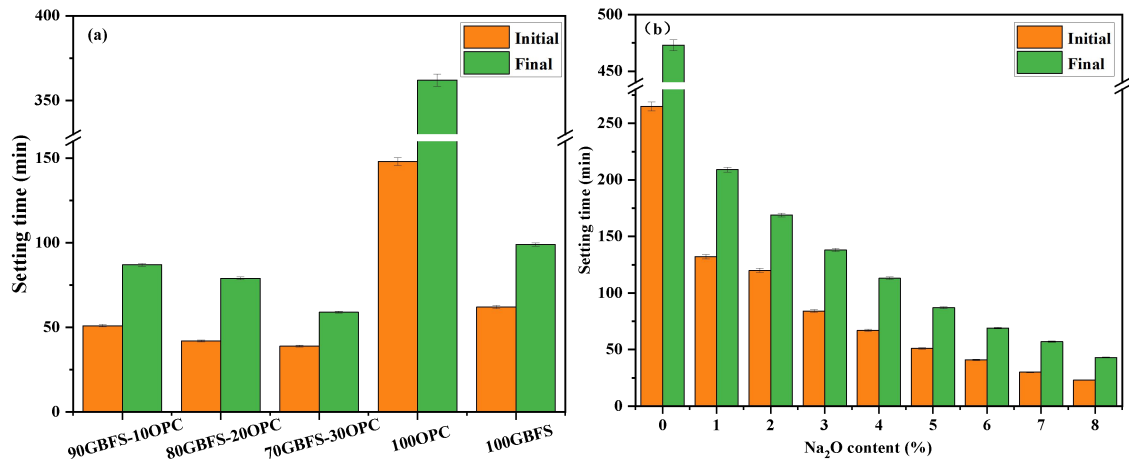


Figure 6- 1 (a) setting time of binder systems; (b) setting time of HACs with different dosage of Na₂O content.

As it is shown in Figure 6-1(b), blended cement (BC, Na₂O content equals to 0) provides the longest setting times 265 min for initial setting and 473 min for final setting. The primary reason is that blast furnace slag, when hydrated solely with water, undergoes a slower hydration rate, resulting in extended setting times and lower early compressive strength compared to OPC (Menéndez et al., 2003, Hoshino et al., 2006, Whittaker et al., 2014, Hlobil et al., 2016, Durdziński et al., 2017). The slow hydration rate of blended cement (Macphée et al., 1988, Pane and Hansen, 2005, Kocaba et al., 2012) produces the reduced reactivity of GBFS compared to OPC (Escalante-Garcia and Sharp, 2001). GBFS particles blended with OPC react only after activation due to the production of OH⁻ produced from OPC hydration (Roy, 1982). The hydration process of this system is as follows: Initially, OPC hydrates to form C-S-H gel and produces calcium hydroxide. As the hydration progresses, GBFS starts to react in an alkaline environment. Due to the relatively low proportion of OPC in this system, the reaction proceeds slowly, resulting in extended setting time and lower early-age compressive strength.

The setting time of HAC systems present a decrease with the increment of Na₂O content. Increasing the alkali content typically shortens the setting time of slag cement due to the alkali's mechanism of action. An alkaline environment promotes the hydration reactions of silicates and aluminates in slag. These reactions produce the C-S-H gel, which facilitates early hardening of the cementitious material. Additionally, alkalis enhance the rate of hydration reactions, accelerating the formation of hydration products and speeding up the overall hydration process. Therefore, increasing alkali content generally significantly shortens the setting time of slag cement, imparting higher early strength and hardening characteristics. When the

dosage of Na_2O content reaches 3%, HAC exhibits initial setting time 84 min (more than 1 hour), and shows 39% decrease (down to 51 min which is less than 1 hour) with the dosage of Na_2O content reaches 5%. The setting time of HAC system shows a decreasing trend with the increase dosage of Na_2O content, which is more obvious in the initial setting time, this decrease in setting time is associated with poor workability for pumping and casting, which is significantly less than that of OPC paste under similar conditions. The initial setting time of HAC reaches 51 min with 5% dosage of Na_2O content, and then a further 55% decreases (down to 23 min) with 8% dosage of Na_2O , which is far less than OPC paste at the same situations.

With the increasing dosage of alkali activator, the pH value in the reaction solution increases gradually. In an alkaline environment (NaOH solution), GBFS rapidly dissolves, releasing silicates (SiO_4^{4-}), aluminates (AlO_2^-), calcium ions (Ca^{2+}), and other components (Garcia-Lodeiro et al., 2012, Barboza-Chavez et al., 2020, Fu et al., 2020). The dissolved silicate and aluminate ions react with water molecules and hydroxide ions (OH^-) in the solution, forming monomeric structures such as sodium silicate (Na_2SiO_3) and sodium aluminate (NaAlO_2). The monomers further polymerize to form dimers. For example, two molecules of silicate monomers can combine through a condensation reaction (Si-O-Si bond formation), releasing water molecules. The dimers continue to polymerize, forming long-chain or three-dimensional network polymers. These polymers are mainly connected by siloxane (Si-O-Si) and aluminate (Al-O-Al) bonds, forming a complex three-dimensional network (Xue et al., 2021a, Fu et al., 2020, Angulo-Ramirez et al., 2018).

As the reaction progresses, the cement slurry gradually coagulates and hardens, forming a hard solid structure. The polymer network acts as a binder and reinforcing agent within the cement matrix. In an alkaline environment, the hydration products of slag mainly include C-S-H gel (calcium silicate hydrate) and C-A-S-H gel (calcium aluminate silicate hydrate) (Millan-Corrales et al., 2020, Fu et al., 2020, Fernandez-Jimenez et al., 2019, Frias et al., 2018). These gels fill the pores within the polymer network, further enhancing the strength and durability of the cement. Throughout the process, the alkaline environment promotes the rapid dissolution and reaction of the slag, aiding in the accelerated formation of monomers, dimers, and polymers. When the dosage of Na_2O reaches 4%, HAC exhibits an initial setting time equivalent to 1 hour, which can meet certain engineering needs, such as precast concrete

components. When the dosage of Na_2O content reaches 5%, the initial setting time of HAC decreases to 51 min, which will be too short for pumping or casting. With the increasing dosage of alkali activator, both initial and final setting time decrease dramatically. Observably, by adding 3% to 5% dosage of alkali activator, HAC performs appropriate setting time and can meet certain needs of practical engineering.

6.4.2 Hydration heat analysis

Thirteen types of binders were designed for testing the hydration heat during the hydration, the details of these binders are shown in Table 6-1. In this thesis, the hydration heat analysis of binder was evaluated by the ratio of raw materials and the dosage of alkali activator.

6.4.2.1 The influence of the ratio of OPC

The heat flow and cumulative heat of binders with different ratios of OPC are illustrated. In HACs, the first exothermic peaks increase with the rising ratio of OPC in the binder system in Figure 6-2. Two significant exothermic peaks are observed on heat flow curves of OPC, the first one appears at the very beginning of the test, which is due to the dissolution of OPC. The second one appears at about 10 hours later, which is attributed to the formation of hydration products. Other binder systems exhibit almost the same pattern of heat release, but with some differences. The binder system of 100GBFS presents the lowest peak. In HACs, the first exothermic peaks increase with the increasing ratio of OPC in binder system. It can be concluded that the first exothermic peak is primarily attributed to the dissolution of OPC in the HAC system. It can be seen that the second exothermic peaks of HACs appear earlier than OPC, and the trend is that the more the ratio of OPC, the earlier exothermic peak it appears. The main reason for this phenomenon is that the hydration of OPC in the HAC system increases the pH value of the reaction solution (Garcia-Lodeiro et al., 2016b), resulting in a faster reaction rate compared to the AAM system. The hydration reaction of OPC is slower than the alkali activation reaction, which may be the reason of longer setting time of OPC than HAC and AAM. The result is consistent with the initial and final setting time of the binder systems in Figure 6-1(a). Analysis to the cumulative heat of the binder systems is shown in

Figure 6-2(b), HAC systems release more heat at first 12 hours, but less as the prolong of hydration process than OPC. AAM presents the lowest cumulative heat in the first 72 hour, and HACs with lower ratio of OPC release less cumulative heat.

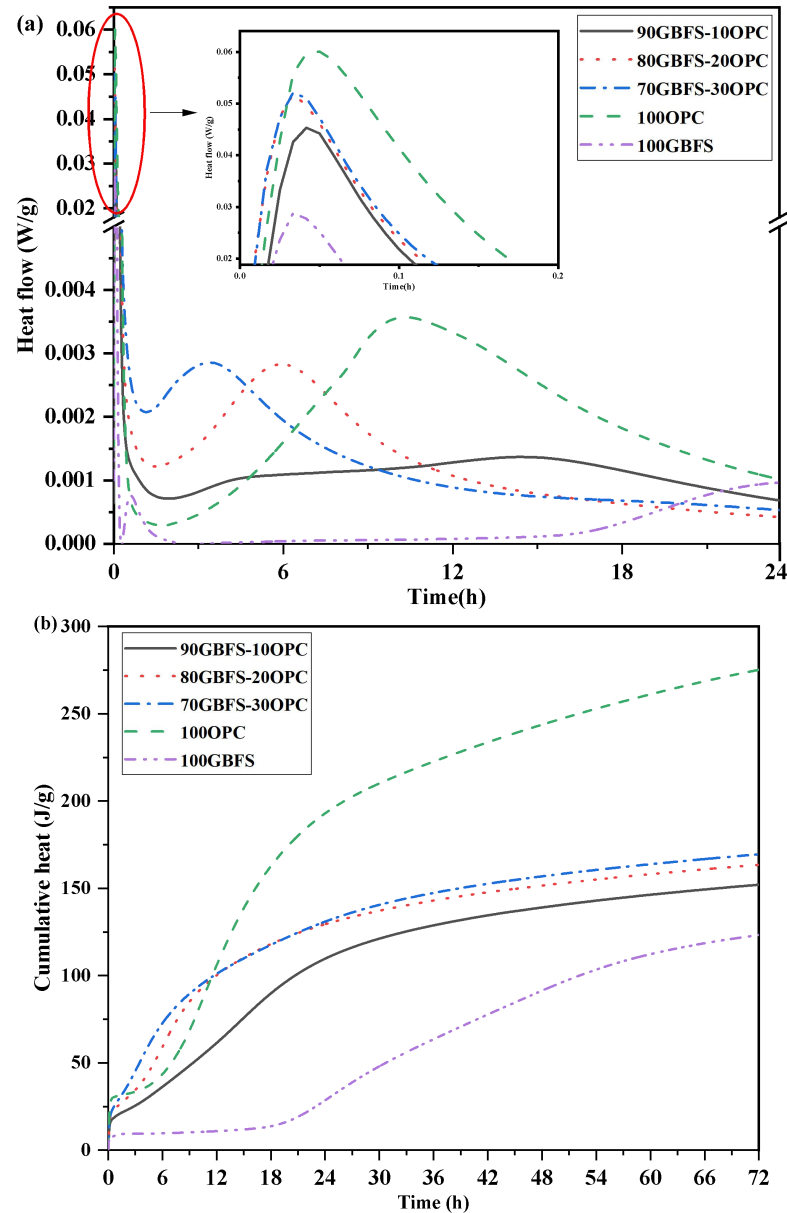


Figure 6-2 (a) Heat flow; (b) Cumulative heat of binders with different ratio of OPC.

6.4.2.2 The influence of the dosage of alkali activator

The heat flow and cumulative heat of HACs with different dosages of alkali activator are depicted in Figure 6-3. The calorimetric curve for HACs has two peaks as the curve of OPC. Two primary peaks are observed in all HAC heat flow curves. The first peaks appear at the beginning of test and almost simultaneously, which is due to the dissolution of raw materials. And it shows a trend of decreasing exothermic peak as the alkali content increases. The second exothermic peaks

appear with a prolonged delay as the alkali content increases, and exhibit almost the same intensity.

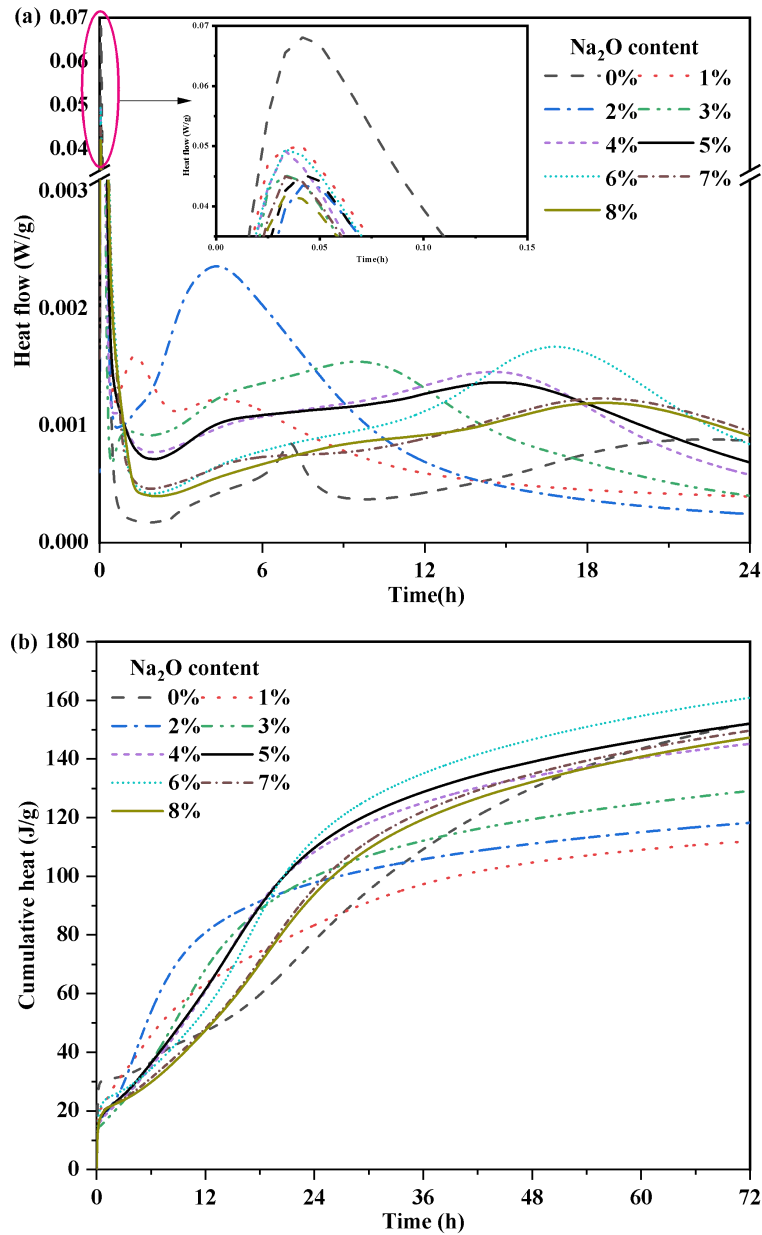


Figure 6-3 (a) Heat flow; (b) Cumulative heat of HACs with different dosage of alkali activator.

The main reason for this phenomenon is that the increase dosage of Na_2O content inhibits the content of CaO in the solution, thereby hindering the formation of reaction products and ultimately delaying the appearance of accelerated reaction peaks. The analysis of cumulative heat curves for HACs is presented in in Figure 6-3(b). The cumulative heat decreases as the increasing dosage of alkali activator at first 18 hours, due to the inhibitory effect of increasing Na_2O content on reaction products. However, the cumulative heat shows an increasing trend with the rising dosage of Na_2O content after 18 hours. However, an interesting phenomenon can be

seen that the cumulative heat does not always increase with the increase of Na_2O content. The cumulative heat reaches the highest when the alkali content reaches 6%, and then decreases with the increasing of alkali content. The result aligns with the compressive strength Figure 5-2 and setting time in Figure 6-1(b). Further analysis need to be done to understanding the setting properties of HACs. In this research the products of the binders at initial and final setting time were analysed with ^1H NMR, TGA and SEM.

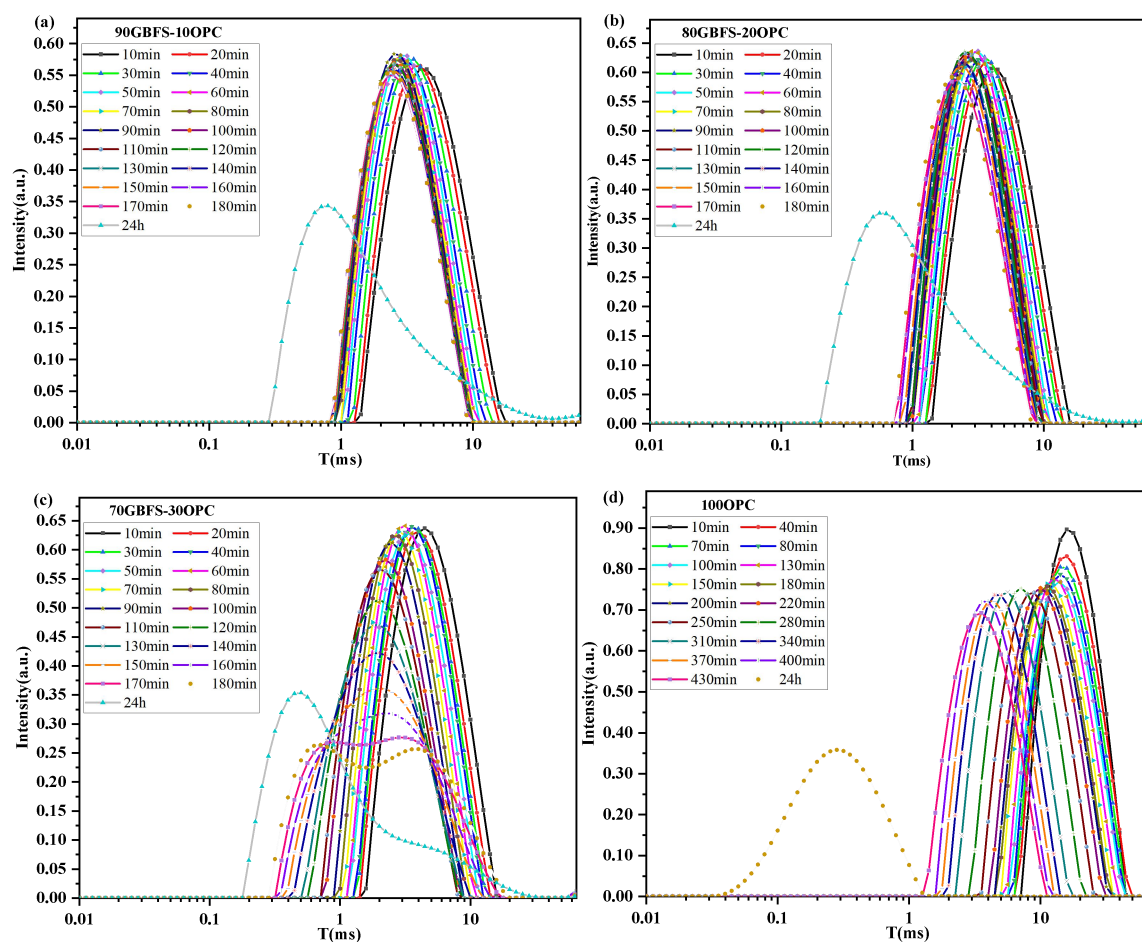
6.4.3 ^1H NMR analysis

In HAC systems, water is an indispensable component. As the alkali-activated reaction progresses, the state of water gradually transitions from free water to physically bound water and chemically bound water. This study utilizes ^1H low-field nuclear magnetic resonance (NMR) to investigate changes in the transverse relaxation time of water during the early stages of the alkali-activated reaction (setting and hardening). By detecting the proton signals of water molecules in different binding states, the study examines the initial and final setting processes of hybrid cement.. The development of transverse relaxation time of T_2 vs signal intensity is evaluated by the different ratio of OPC in the binder systems, and the dosage of Na_2O content in HACs.

6.4.3.1 The influence of the ratio of OPC

The influence of the ratio of OPC on the setting properties is shown in Figure 6-4(a)-(e), and different ratio of OPC present different T_2 vs signal intensity. HAC (90GBFS-10OPC) presents signal intensity peak of T_2 at 4.0ms for the first test (10 min), indicating that the water mainly exists in the form of capillary pore water in the newly blended binder paste. The signal intensity peaks of T_2 shifted left gradually with time, attributed to the majority of water migrating to smaller pores. The signal intensity peak located at $T_2=3.1\text{ms}$ for initial setting time and $T_2=2.5\text{ms}$ for final setting time (corresponding to Figure 6-1). And a weak signal appeared on the intensity curve at $T_2<1.0\text{ms}$, which indicated that some water is converted into gel pore water in the process of setting. The signal intensity shifts to the left gradually, and the peaks continuously decrease after final setting. After 24 hours of hydration, the main peak of T_2 moved left to 0.75ms with significant decreasing of signal

intensity peak, which indicated that most of the water is trapped into gel pore and a lot of hydration products generated during the process of setting. Compared with T_2 of OPC Figure 6-4(d), the main peaks of HACs shift to left much faster, and the signals intensity reduced more significant, these results align with the setting time in Figure 6-1(a). With the increasing ratio of OPC in HAC system, HAC presented a different effect on development T_2 . As shown in Figure 6-4(c), HAC (70GBFS-30OPC) present a series of T_2 vs signal intensity curves that shifted to left more apparent with time.



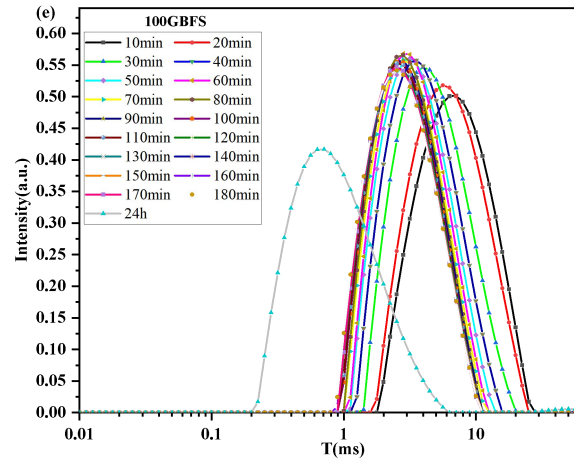


Figure 6-4 T_2 vs. intensity during hydration of binders (a) 90GBFS-10OPC; (b) 80GBFS-20OPC; (c) 70GBFS-30OPC; (d) 100OPC; (e) 100GBFS.

Simultaneously, the intensity peak decreases more rapidly with time. The results indicated that as the increasing ratio of OPC in HAC system, as the alkaline activation reaction progresses, the reaction products increase continuously, and the unreacted evaporable water gradually distributes into smaller pores. The lateral relaxation peaks of the system gradually tend towards shorter relaxation times. In HAC pastes, with increasing OPC content, significant differences in T_2 distributions among various pastes emerge. The T_2 main peak of the 70GBFS-30OPC paste notably shifts leftward, accompanied by the most pronounced intensity decrease. After 3.0 hours of reaction, the T_2 main peaks of the pastes shift leftward to the range of 0.1~5.0 ms. At this point, almost all evaporable water has entered the small pores with short relaxation times, and the water in the paste is primarily gel water and capillary water (Cong et al., 2019, Ji et al., 2017, McDonald et al., 2005). Conclusion can be made that increasing the proportion of OPC in HACs will result in a shortened setting time with the same alkali content. This conclusion is consistent with the setting time which indicated that the water primarily exists in the form of capillary pore water in the fresh binder paste in Figure 6-1(a).

6.4.3.2 The influence of the dosage of alkali activator

The influence of the dosage of Na_2O content in HACs on the setting properties is shown in Figure 6-5(a)-(i), and the increasing dosage of alkali activator in HACs exhibit different setting properties. As shown in Figure 6-5(a), BC (90GBFS-10OPC hydrated by only water) exhibits signal intensity peak of T_2 at 5.0ms for the first measurement (30 min), which indicated that the water mainly exists in the form of

capillary pore water in the fresh binder paste. The intensity peaks shifted to left over time, but the speed of movement is very slow. After 24 hours of hydration, the intensity peak of T_2 moved left slowly to 4.0ms, weak signals are found on the intensity curve at $T_2 < 1.0\text{ms}$, which indicated that a small amount of water was injected into the gel pores, resulting in the formation of few hydration products during the setting process (McDonald et al., 2005, Cong et al., 2019, Muller et al., 2013). The result may be the main reason why blended cement with high proportion of OPC presents long setting time and low compressive strength at early age. With the increasing dosage of Na_2O content in HACs. The other peak at $T_2 > 1.0\text{ms}$ indicates that a proportion of water was trapped in larger pores, the main reason is that with the increase in the activator dosage, the reaction rate of the HAC paste increases continuously during the setting process, leading to the formation of larger pores in the HAC paste due to chemical shrinkage (Cong et al., 2019). Two intensity peaks were detected in HACs with Na_2O content ranged from 1% to 3%, as shown in Figure 6-5(b)-(d). One intensity peak at $T_2 < 1.0\text{ms}$ indicating the formation of hydration products. The other peak at $T_2 > 1.0\text{ms}$, which indicated that a proportion of water was trapped in larger pores. The phenomenon meant that larger pores were produced in HACs with small dosage of alkali activator in the processing of setting.

As the alkali content in High Activation Cements (HACs) continues to increase, the intensity peaks shift left over time. The rate of leftward movement increases with the rise in alkali content, as shown in in Figure 6-5(e)-(i). In tandem with the increase in alkali content, there is a gradual reduction in setting time, as depicted in Figure 6-1(b). At the same time, it is noticeable that the intensity peaks do not exhibit a continuous decrease with the increase in alkali content. The intensity peaks presented the lowest with an alkali content of 5% after 24 hours of hydration, which indicated that the most hydration products were produced. Correspondingly, the compressive strength of HACs present an increase trend with the increasing dosage of alkali activator and then a decrease with the increment of Na_2O content as shown in Figure 5-2.

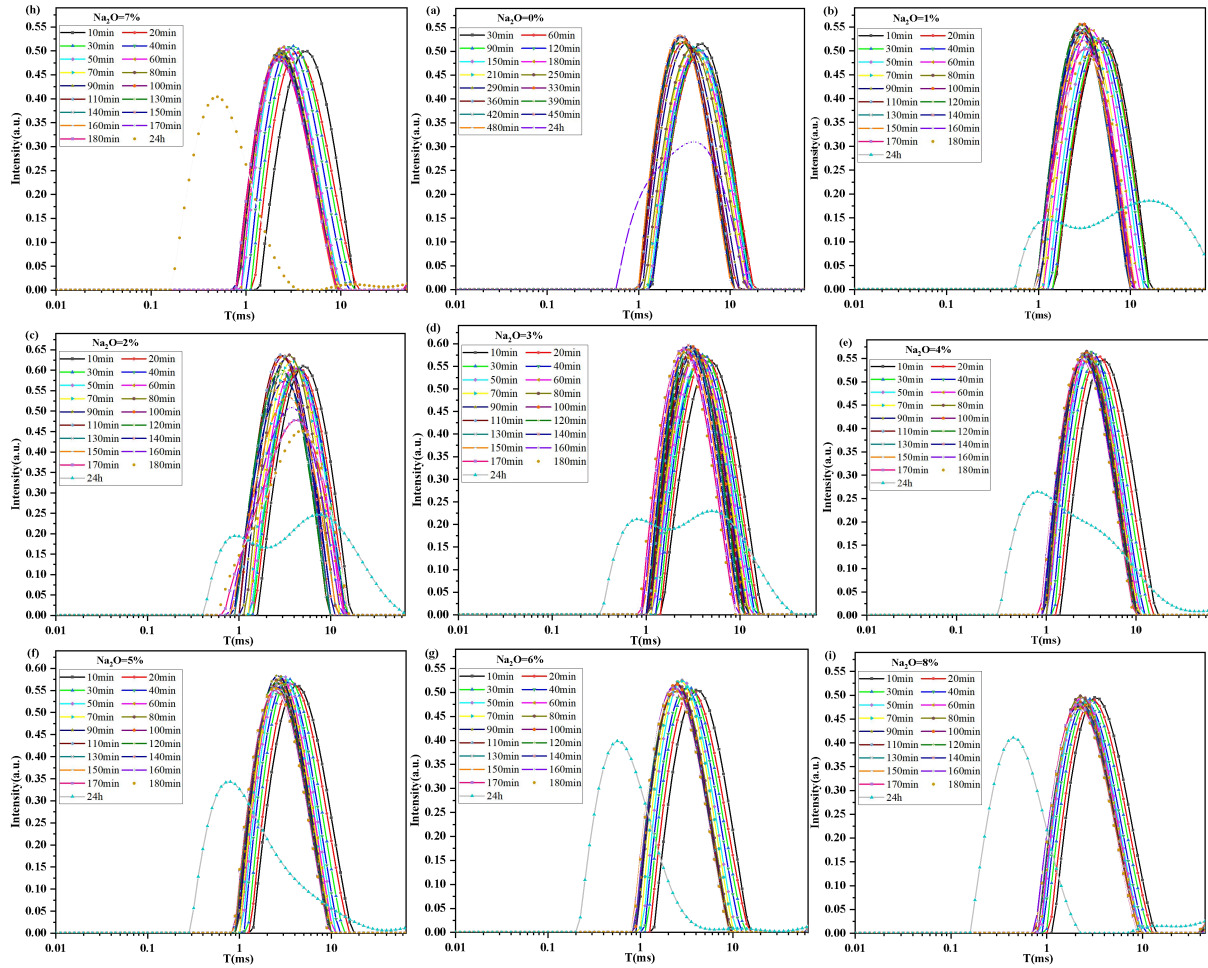


Figure 6-5 T_2 vs. intensity during hydration of HACs with different dosage of alkali activator.

6.4.4 TGA analysis of hydration products

6.4.4.1 The influence of the ratio of OPC on hydration products

TGA and DTG of hydrated binder systems at initial setting time are shown in Figure 6-6. The mass loss of HAC systems from 30°C to 1000°C is about 4.8 % to 6.8%, which is similar to AAM with a mass loss of 4.8 %, while OPC with the least total mass loss of 4% (Figure 6-6a). The increases proportion of OPC in HAC systems increases the total mass loss. Correspondingly, the initial setting time decreases with the increases of proportion of OPC. All binder systems present a quick loss of mass weight between 100 °C and 130 °C. The quick loss of weight is mainly related to the loss of free water from the products of hydration or reaction (Kong and Sanjayan, 2010). OPC exhibits the second quick loss of weight at around 400°C and the third quick loss of mass weight at about 650°C. HACs and AAM present a continuous loss of weight, and a sight quick loss at around 650 °C. HAC

(70GBFS-30OPC) shows a slight decline of mass weight at about 900 °C.

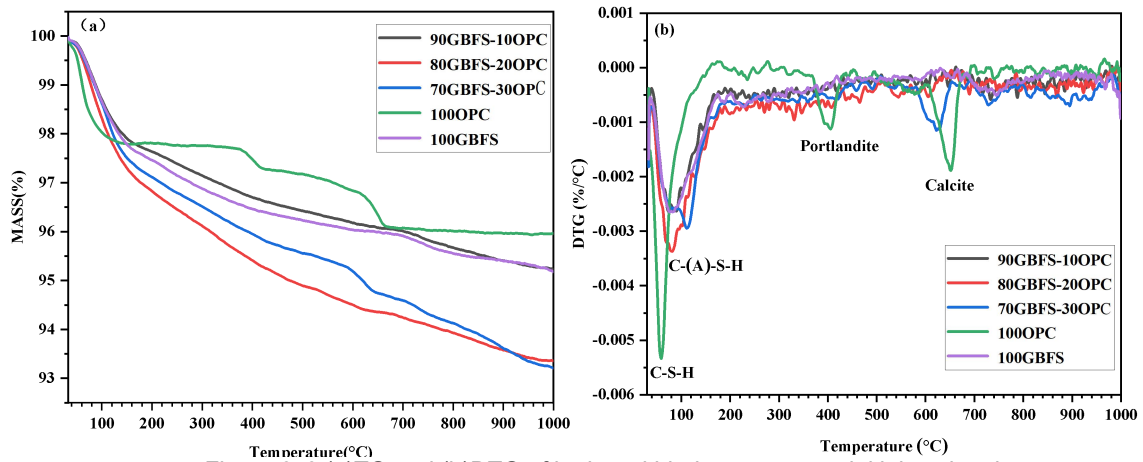


Figure 6-6 (a)TG and (b)DTG of hydrated binder systems at initial setting time.

DTG analysis of hydrated binders at initial setting time are shown in Figure 6-6b. In the DTG curve of OPC, three noticeable endothermic peaks are observed. The first and most significant endothermic peak is observed at about 60 °C is attributed to the loss of water from C-S-H gel (Alahrache et al., 2016a). The second peak at around 400 °C is due to the loss of water from the decomposition of portlandite (Alarcon-Ruiz et al., 2005). At around 650 °C, the last endothermic peak was observed, which is mainly due to the decomposition of calcite (Walkley et al., 2017). In the DTG curve of AAM, there are also three noticeable endothermic peaks are observed. The first endothermic peak is observed at about 80 °C is attributed to the loss of water from C-A-S-H gel. The second peak is slight at around 750 °C. At around 900 °C, the last peak is observed. HAC systems exhibit the first peak at about 70°C to 120 °C, which is due to the loss of water from C-S-H and C-A-S-H gels (Alahrache et al., 2016a). It can be observed that as the increasing proportion of OPC in HAC systems, the endothermic peaks become more significant. The result is consistent with the initial setting time decreases with the increases proportion of OPC.

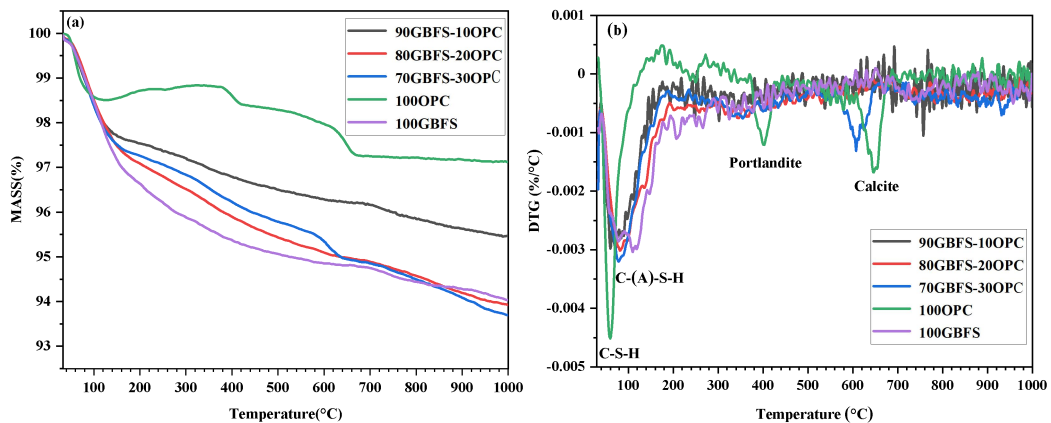


Figure 6-7 (a)TG and (b)DTG of hydrated binder systems at final setting time.

TGA and DTG of hydrated binder systems at final setting time are shown in Figure 6-7. The mass loss of HACs from 30°C to 1000°C is about 4.5 % to 6.3%, which is similar to AAM with a mass loss of 6.0 %, while OPC with the least total mass loss of 2.9% (Figure 6-7a). The total mass loss of HACs increases with the increasing proportion of OPC in HAC systems. In addition, the final setting time decreases with the increases of proportion of OPC in HACs. All binder systems also present a quick loss of weight at 100 °C to 130 °C, which is mainly related to the loss of free water from the products of hydration or reaction (Kong and Sanjayan, 2010). The hydration products of OPC present the second quick decline of total weight at about 400°C and the third quick loss of weight at around 650°C. HAC systems and AAM present a continuous loss of total weight. DTG curves of the binders above at final setting time are shown in Figure 6-7b. As in initial setting time shown in Figure 6-6b, in the DTG curve of OPC, there are also three endothermic peaks are observed. The first peak is at about 60 °C which is due to the loss of water from C-S-H gel (Alahrache et al., 2016a). The second at around 400 °C is attribute to the loss of water from the decomposition of portlandite (Alarcon-Ruiz et al., 2005)., The last is at around 650 °C due to the decomposition of calcite (Walkley et al., 2017). In the curves of HACs and AAM, the most notable endothermic peaks are observed at about 50 °C to 120 °C, which are attributed to the loss of water from C-(A)-S-H gel (Alahrache et al., 2016a). The results show that as the increasing proportion of OPC in HAC systems, the temperature corresponding to the endothermic peaks continuously increases. Meanwhile, alkaline activator can accelerate the hydration reactions of silicates and aluminates in OPC. In HAC systems, the higher the proportion of OPC, the faster these hydration reactions occur, resulting in the production of more hydration products. These hydration products fill the gaps between cement particles, causing the system to transition from liquid to solid more quickly, thereby shortening the setting time. The results also indicate that as the proportion of OPC increases, the final setting time of the binders gradually decreases as shown in Figure 6- 1a.

6.4.4.2 The influence of the dosage of alkali activator on hydration products

TGA and DTG of hydrated HACs with different dosage of alkali activator at initial setting time are shown in Figure 6-8. It can be detected that the mass loss of

BC hydrated by only water is only 1.7%, due to the slow hydration rate of BC hydrated by only water, associated with longer setting time and lower early compressive strength compared to OPC (Menéndez et al., 2003, Hoshino et al., 2006, Whittaker et al., 2014, Hlobil et al., 2016, Durdziński et al., 2017). The total mass loss of HAC systems with different dosage of alkali activator from 30°C to 1000°C is about 3.7 % to 6.6% (Figure 6-8a). The increased dosage of alkali activator can accelerate the hydration reactions of mineral components in HAC, speeding up the formation rate of hydration products such as C-(A)-S-H. This results in the generation of more hydration products, which decompose at high temperatures. TGA analysis detects the decomposition of these products into gases (such as water vapor and carbon dioxide) during heating, leading to an increase in mass loss. Correspondingly, the initial setting time decreases with the rise in Na₂O content in HACs. A quick loss of total mass weight between 100 °C and 130 °C in HAC systems is observed, which is mainly related to the loss of free water from the products of reaction (Kong and Sanjayan, 2010). HACs present a continuous loss of weight, and a sight quick loss at around 650 °C.

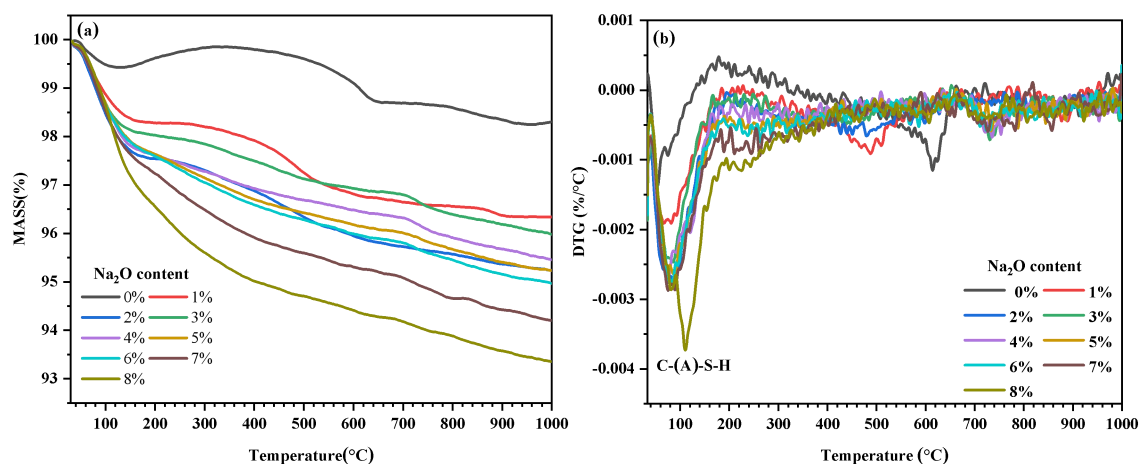


Figure 6-8 (a)TG and (b)DTG of hydrated HACs activated by different dosage of alkali activator at initial setting time.

DTG analysis of HACs at initial setting time are shown in Figure 6-8(b). The most significant endothermic peaks are observed in HAC systems at around 50°C to 110°C, which is due to the loss of water from C-(A)-S-H gels (Alahrache et al., 2016a, Walkley et al., 2017, Kong and Sanjayan, 2010, Alarcon-Ruiz et al., 2005). It can be observed that as the increasing dosage of Na₂O content in HACs, the endothermic peaks become more significant. The result indicates that the C-(A)-S-H gels increase as the Na₂O content increasing in HAC systems. The result is consistent with the initial setting time decreases with the increasing dosage of Na₂O content.

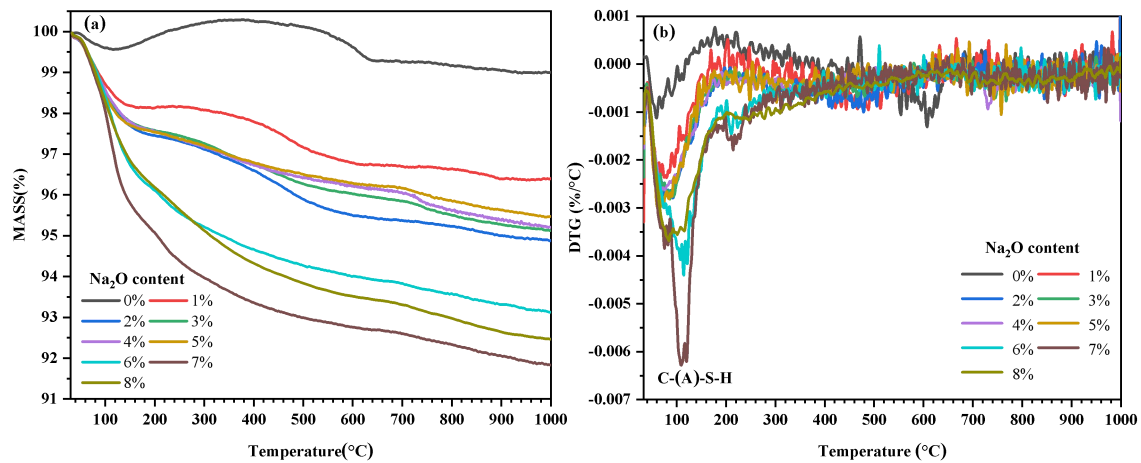


Figure 6-9 (a)TG and (b)DTG of hydrated HACs activated by different dosage of alkali activator at final setting time.

TGA and DTG of HACs activated by different dosage of alkali activator at final setting time are shown in Figure 6-9. The total mass loss of BC hydrated by only water is smallest 1.0%, the main reason is that the hydration rate of BC hydrated by only water is relatively slow, associated with long setting and low early compressive strength (Menéndez et al., 2003, Hoshino et al., 2006, Whittaker et al., 2014, Hlobil et al., 2016, Durdziński et al., 2017). The mass loss of HAC systems at final setting time with increasing dosage of Na_2O content from 30°C to 1000°C is about 3.6 % to 8.2% (Figure 6-9b). Generally speaking, the total loss of weight of HACs is higher than that at initial setting time. The mass loss increases as the increasing dosage of dosage of Na_2O content in HAC systems. In addition, the final setting time decreases with the increases of Na_2O content in HAC systems. Quick decline in the curves are observed between 100 °C and 130 °C in HACs, due to the loss of water from the products of reaction (Kong and Sanjayan, 2010). HACs exhibit a continuous loss of weight in the subsequent test. DTG analysis of HACs activated by increasing dosage of alkali activator at final setting time are shown in Figure 6-9(b). In generally, the results exhibit the same pattern as shown in Figure 6-8. However, the difference lies in the fact that the endothermic peaks do not consistently increase with the increase of Na_2O content. The peak endothermic effect emerges when the Na_2O content equals 7%, and thereafter, the peak actually decreases. In HAC systems, regarding the hydration products at final setting, it was found that the system produced the highest amount of hydration products when the alkali content was 7%. However, as the alkali content increased further to 8%, although it was expected to increase hydration product formation, the actual amount of hydration products in the system started to decrease. This indicates that excessive alkali has a negative impact on hybrid

cement systems.

6.4.5 SEM analysis of hydration products

SEM analysis for binders with different ratio of OPC and different dosage of Na_2O content, at initial and final setting time were shown in Figure 6-10 to Figure 6-13. Analysis of the variations in the micrographs over time and by varying the ratio of OPC and Na_2O content revealed in the following.

The microstructure images of binder systems at initial setting time are shown on Figure 6-10. Figure 6-10(d) shows 100OPC sample hydrated with water at initial setting time, a small amount of gel can be observed in the matrix, together with the unhydrated OPC particles, a loose structure is formed. With the increasing ratio of OPC in HAC systems activated by 5% Na_2O content, more gels can be detected. 70GBFS-30OPC sample presents the most gels as shown in Figure 6-10(c), indicating that a denser structure is formed. 70GBFS-30OPC shows the shortest initial setting time in binder systems. The result is consistent with Figure 6-1(a). It should notice that different microstructures are formed in HACs with different ratio of OPC in binder systems. Reaction products are relatively reduced in 90GBFS-10OPC sample as shown in Figure 6-10(a), and the matrix becomes relatively loose. By adjusting the proportion of OPC in HAC systems, their initial setting time can be adjusted. Reducing the proportion of OPC can extend the initial setting time, which has certain guiding significance for engineering applications.

The microstructure images of binder systems at final setting time are shown on Figure 6-11. Figure 6-11 (d) shows 100OPC sample hydrated with water at final setting time. More hydration products are detected in the matrix, cross-linked C-S-H gels forms a dense microstructure. More reaction products are also observed in HACs at final setting than initial setting time. 70GBFS-30OPC sample presents the densest microstructure as shown in Figure 6-11, indicating that more gels are formed. With the decreasing ratio of OPC in binder systems, less gels can be detected. 90GBFS-10OPC shows the longest final setting time in HAC systems activated by 5% Na_2O content. The result is consistent with Figure 6-1(a). The outcome is also consistent with the analysis at initial setting in Figure 6-10.

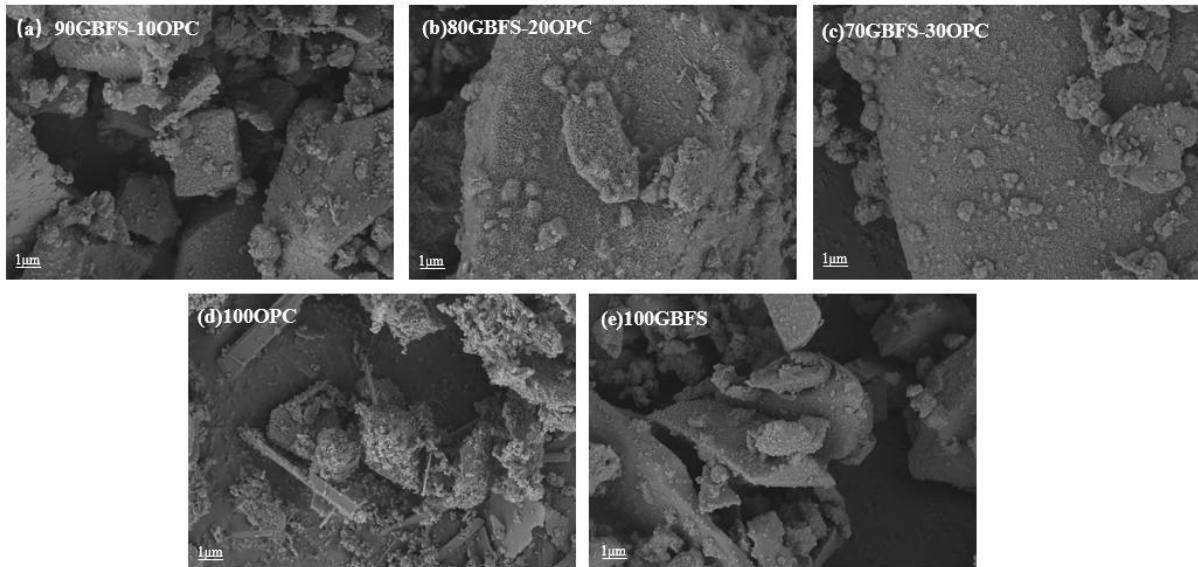


Figure 6- 10 SEM images of binder systems activated with 5% Na₂O at initial setting.

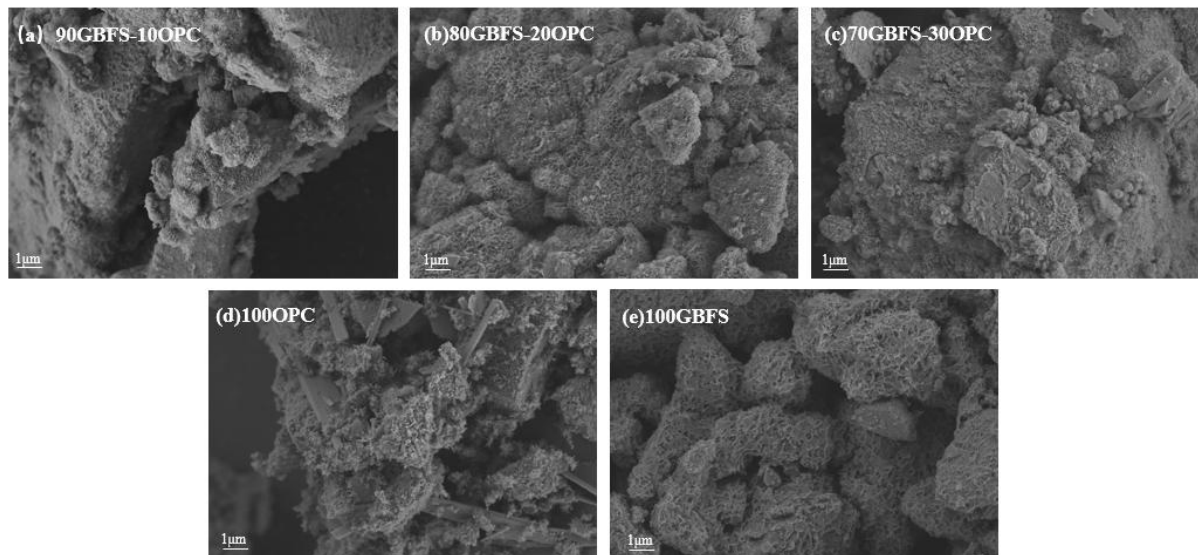


Figure 6- 11 SEM images of binder systems activated with 5% Na₂O at final setting.

The microstructure images of binder systems at initial setting time are shown on Figure 6-12, the matrix becomes denser with the increasing dosage of Na₂SiO₃·9H₂O. 90GBFS-10OPC hydrated by only water looks porous, associated with higher porosity compared to other binders. GBFS reacts only after the formation of hydration products from of OPC (Roy, 1982) in BC system, causing a very slow hydration rate. Due to the high proportion of GBFS and low ratio of OPC in BC system, the reaction process is very slowly, which results in long setting time. As shown in Figure 6-12 and Figure 6-13, OPC particles normally present bright grey shadows with irregular shapes, and the GBFS particles are relatively dark and the color remains uniform(Nath and Sarker, 2015, Xue et al., 2021a). More products were produced with the increasing of Na₂O content. With the increasing dosage of Na₂O content, the

pH value in the reaction solution increases gradually. In the alkaline solution, both OPC and GBFS hydration rate have been accelerated. In higher pH solution, minerals such as silicates and aluminates in HAC dissolve more easily. These dissolved ions can participate more rapidly in hydration reactions, thereby accelerating the reaction rate, especially for OPC hydration. The high rate of OPC hydration will bring fast setting. The outcomes are consistent with the results in Figure 6-1(b), and suitable setting time requires HACs with Na_2O content no more than 5%.

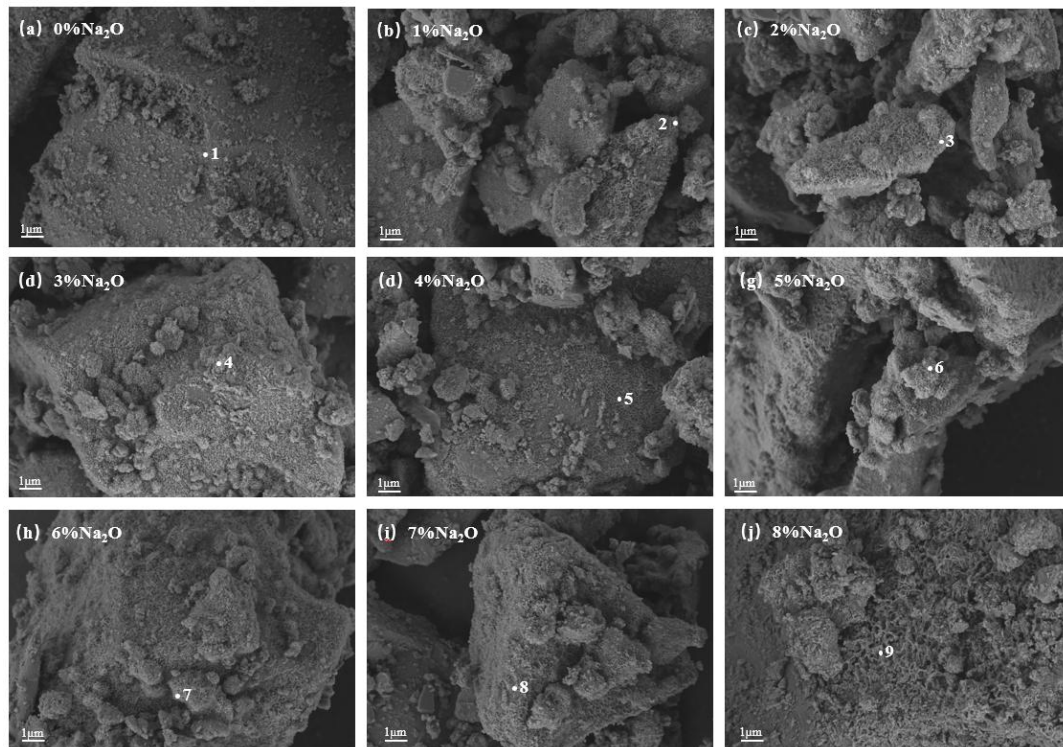


Figure 6-12 SEM images of HACs with different dosage of Na_2O at initial setting.

As shown in Figure 6-12, BESM-EDX spectrum of HAC gels shows the similar reaction products of all HAC systems. The Ca/Si ratio decreases with the increasing of Na_2O content, which is decreased from 4.17 to 1.29, with the Na_2O content increases from 0 to 8%. As the Na_2O content increases (points 1 to 9), the ratio of Ca/Si decreases, suggesting increased polymerization and crosslinking within the product gel (Gebregziabihier et al., 2015, Xue et al., 2021a). The concentration of Na increased with the increased Na_2O content. The elemental ratios of HACs with different dosage of Na_2O at initial setting time are summarized in Table 6-2.

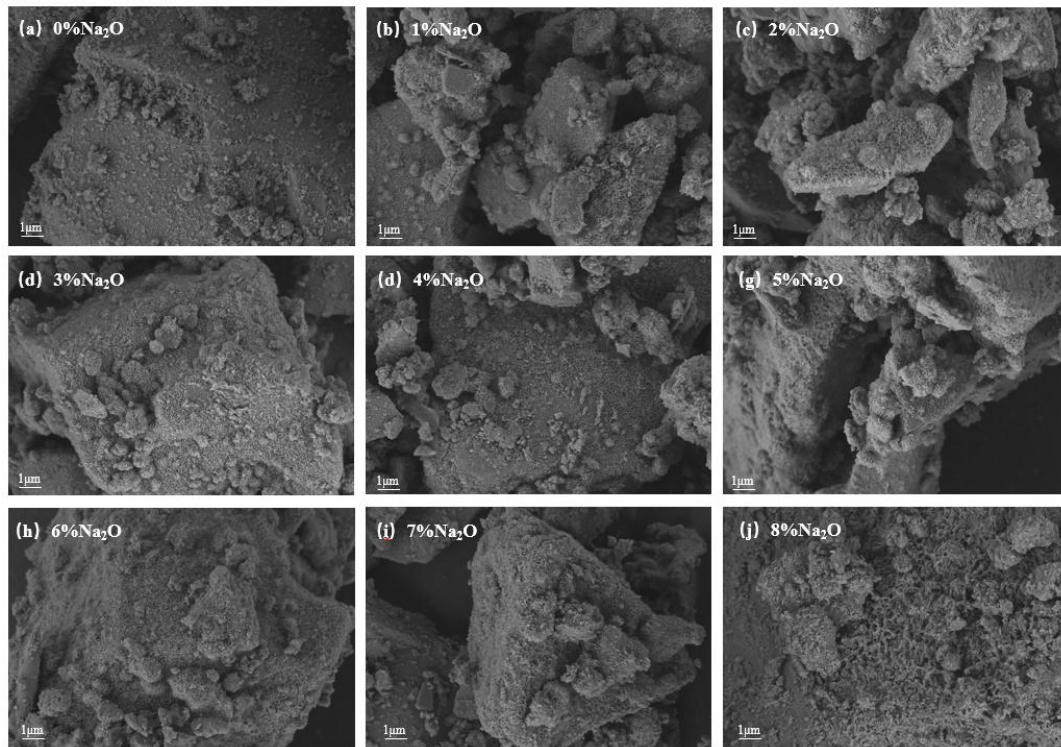


Figure 6-13 SEM images of HACs with different dosage of Na_2O at final setting.

Table 6-2 Elemental ratios of HACs with different dosage of Na_2O at initial setting time.

Point	Ca/Si	Na/Si	Si/Al
1	4.17	0.00	2.08
2	1.79	0.23	2.20
3	1.73	0.28	2.89
4	1.68	0.21	1.91
5	2.02	0.23	2.17
6	1.61	0.26	2.42
7	1.46	0.24	2.10
8	1.50	0.34	1.51
9	1.29	0.67	2.41

The Na/Si ratio increased with the continuously adding of Na_2O content, which is increased from 0.00 to 0.67 with the Na_2O content increases from 0 to 8%. The concentration of aluminum (Al) also shows an increasing trend with the rise in Na_2O content. Ca and Si are the primary reaction products, with the increasing Na and Al as the increasing Na_2O content. These elements contribute to the formation of C-S-H and C-(A)-S-H in alkaline solution.

6.5 Conclusions

This research investigates the effects of activator dosage and the ratio of raw materials on the setting properties of various binder systems. Based on the findings, the following key conclusions can be drawn::

(1) The hydration exothermic peak of HAC appears earlier than that of OPC, and the total heat released within the first 12 hours is also higher for HAC than for OPC. As the proportion of OPC increases, the alkali content increases, causing the exothermic peak to appear earlier and the total heat released within the first 12 hours to increase. The main reason for this phenomenon is that the hydration rate of OPC in the HAC system increases under the action of the alkaline activator, making its reaction rate faster than the hydration of OPC. This may be the main reason why the setting time of HAC is shorter, and decreases further with the increase in OPC proportion and activator dosage.

(2) ^1H NMR test results indicate that as the proportion of OPC in the HAC system increases, the amount of hydration products generated during the setting and hardening process increases, resulting in a shorter setting time. Simultaneously, more water in the paste transitions to gel pore water, leading to an increase in porosity and a decrease in early mechanical strength. Additionally, as the Na_2O content in HAC increases, the T_2 main peak shifts to the left at an accelerated rate over time. This suggests that with the increase in activator dosage in the HAC system, the transition of water in the paste to gel water and capillary water speeds up, accelerating the chemical reaction rate and shortening the setting time. However, when the activator dosage is too high ($\text{Na}_2\text{O} > 5\%$), the rapid chemical reaction causes a significant amount of gel pore water to form during the hardening process of the HAC paste, leading to a sharply shortened setting time and a noticeable decline in the mechanical strength of the hardened material.

(3) Meanwhile, alkaline activator can accelerate the hydration reactions of silicates and aluminates in OPC. In HAC systems, the higher the proportion of OPC, the faster these hydration reactions occur, resulting in the production of more hydration products. These hydration products fill the gaps between cement particles, causing the system to transition from liquid to solid more quickly, thereby shortening the setting time. The increased dosage of alkali activator can accelerate the hydration

reactions of mineral components in HAC, speeding up the formation rate of hydration products such as C-(A)-S-H. This results in the generation of more hydration products, which decompose at high temperatures. TGA analysis detects the decomposition of these products into gases (such as water vapor and carbon dioxide) during heating, leading to an increase in mass loss.

(4) From the SEM analysis, it is evident that different microstructures form in HAC systems with varying OPC proportions. With an increasing OPC proportion in the HAC system, more gel formations are detected, indicating a denser structure. This suggests that as the OPC proportion increases in the HAC system, the reaction rate correspondingly accelerates, leading to shorter initial and final setting times. As the dosage of $\text{Na}_2\text{SiO}_3 \cdot 9\text{H}_2\text{O}$ increases, the matrix of hydration products in HAC paste after initial and final setting becomes denser. This indicates that with an increasing Na_2O content, more hydration products are generated in the HAC paste after setting and hardening, resulting in a faster hydration rate and consequently shorter initial and final setting times.

Based on the comprehensive analysis above: Under the action of alkaline activators, the hydration rate of OPC in HAC systems accelerates significantly, much faster than that of OPC alone, which is the primary reason for HAC's shorter setting time. With increasing proportions of OPC and alkaline activator dosage, the setting time further shortens. Excessive hydration reaction leads to the formation of a significant amount of gel pore water, increasing structural porosity and thereby affecting the mechanical strength after hardening. The study indicates that by adjusting the mineral composition and dosage of alkaline activators in HAC systems, it is possible to achieve setting times that meet practical engineering requirements and obtain relatively good microstructures.

CHAPTER 7: PAPER 4 – DURABILITY OF HYBRID ALKALINE CEMENT BASED ON PORTLAND CEMENT AND GROUND BLASET FURNACE SLAG

7.1 Introduction

Hybrid alkaline cements (HACs) consist of a high amount of SCMs, a low proportion of ordinary Portland cement (OPC), activated by chemical activators at room or elevated temperatures (A. Palomo, 2007, Garcia-Lodeiro et al., 2012, Palomo et al., 2013a). They are generally regarded as a new generation of low-carbon binders for construction industry (Shi et al., 2019b, Xue et al., 2021b, Shi et al., 2011b). The manufacture of the new type of binders is related to reducing energy consumption and decreasing carbon dioxide emission. Meanwhile, HACs perform excellent compressive strength, especially at early ages, and can be hardened at room temperature. However, the reports about the practical engineering applications of this new generation of binders are very few. There are still many challenges, including unstable raw materials, fast setting times, high viscosity, cost implications of alkali activator and lack of industry norms (Shi et al., 2011b, Shi et al., 2019b). In particular, the durability properties of HAC concrete have garnered widespread concern.

Chloride ions could cause corrosion of steel bars in concrete, which can cause oxidation and localized damage to the passivation film of the steel bars (Wang et al., 2019). Sulfate ions penetrate and react with calcium (Ca) and aluminum (Al) species in cement, forming expansion products such as ettringite ($\text{Ca}_6[\text{Al}(\text{OH})_6]_2(\text{SO}_4)_3 \cdot 26\text{H}_2\text{O}$) and gypsum ($\text{CaSO}_4 \cdot 2\text{H}_2\text{O}$) (Yang et al., 2022, Alexander et al., 2013). AAMs suffer from higher alkali content than Portland cements, which increases the risk of potential alkali-silica reaction (ASR)-induced expansions (Fernández-Jiménez et al., 2007, Provis et al., 2015a).

AAMs normally have stronger resistance to sulfate attack and chloride corrosion than OPC, due to 3D structure of N-A-S-H or C-A-S-H in AAMs, which is more compact than 2D structure of C-A-H in OPCs (Monticelli et al., 2016b, Monticelli et al., 2016a, Babaei and Castel, 2016, Tennakoon et al., 2017). In alkali activated materials (AAMs), chloride penetration is significantly dependent on Na_2O content, that is with the increasing of dosage of Na_2O the chloride penetration decreased (Chi,

2012, Lee and Lee, 2016). Some researchers believed that the excellent sulfate resistance of AAMs may be related to the lack of $\text{Ca}(\text{OH})_2$ in AAM activation productions (Donatello et al., 2013b, S. Donatello¹, 2014, Janotka et al., 2014, Bačuvčík et al., 2018). Up to now, the issue of whether ASR-induced expansion occurs in AAMs has always been controversial. San Nicolas et al. (San Nicolas et al., 2014) conducted ASR-induced expansion tests on 7-year-aged high-calcium-based AAM concretes. Their studies demonstrated that slag based AAMs show excellent durability with advanced age, and there on evidence of ASR-induced expansions were found. Shi et al. (Shi et al., 2015b) state that alkali-aggregate reaction (AAR) could cause destructive expansion in AAM mortars and concretes, and influenced by dosage and type of alkali activators, the nature of precursors, and testing methods.

By now, the study on chloride penetration of HAC is rare. Rivera, et al. (Rivera et al., 2014) pointed out that chloride penetration is significantly influenced by the raw materials in HAC systems. Generally, high-calcium materials based HACs perform higher chloride penetration resistance compared with low-calcium materials based HACs, which is associated with difference of C-S-H/C-A-S-H gel and N-A-S-H gel produced in the two different HAC systems. The coexistence of C-S-H/C-A-S-H gel is denser and deeper than N-A-S-H gel. Correspondingly, the denser gels are linked to increased mechanical strength in high-calcium materials based HACs. I. Garcia-Lodeiro et al. (Garcia-Lodeiro et al., 2016a) indicated that the element chloride in the HAC systems (blended with fly ash, bottom ash and OPC clinker) with concentration higher than the existing standard, which could cause corrosion of steel bars in concrete or reinforcement especially HACs are applied to marine or offshore structures. Therefore, it is necessary to systematically and extensively study the factors that the effect of chloride penetration in HAC systems.

Some studies have reported excellent durability of HAC binders in various aggressive environments, including high temperature, sulfate attack, chloride penetration, and alkali-aggregate reaction (Fernandez-Jimenez et al., 2013a, S. Donatello¹, 2014, Zhang et al., 2017, Donatello et al., 2013b). The binders formed with alkaline activation of 80% fly ash and 20% OPC have been demonstrated superior durability performance in aggressive environments, such as high temperature, sulphate attack, chloride penetration, and alkali aggregate reactionn(S. Donatello¹, 2014, Donatello et al., 2013b). HAC mortars, which consist of a blend of

12% OPC +88% GBFS + alkali activator, show higher mechanical strength than controlled OPC mortars after exposed to aggressive media (0.1-N HCl, sodium sulphates and seawater)(Fernandez-Jimenez et al., 2013a). Excellent resistance of HAC to a sulphate attack is demonstrated by the 5-years strength of HAC-mortar. It is reported that when HACs are exposed to aggressive media, their behavior is wholly comparable to the performance of conventional Portland cements.

Until now, a few studies have indicated excellent sulfate resistance of HAC concrete. Donatello et al. (Donatello et al., 2013b) demonstrated good sulfate resistance of HAC pastes and mortars under the a series aggressive solution. HAC binders formed with 80% fly ash and 20% Portland cement clinker, activated by Na_2SO_4 , were immersed in seawater and 4.4% Na_2SO_4 solutions for 90 days. HACs mortars showed satisfactory sulfate resistance to seawater and Na_2SO_4 solutions compared with current sulfate resistant cement requirements(Donatello et al., 2013b, S. Donatello¹, 2014). Some researchers investigated the sulfate resistance of HAC mortars for long age, and the results show that HAC mortars perform superior resistance to sulfate attack for long ages than the reference PC mortars (Janotka et al., 2014, Zhang et al., 2017, Bačuvčík et al., 2018). Fernández-jiménez et al. (Fernandez-Jimenez et al., 2013a) investigated the durability aspects of HACs in aggressive solutions, and concluded that HAC binders (blended 12% Portland clinker, 88% blast furnace slag and alkali activator) shows good sulfate resistance in 4.4% Na_2SO_4 solution.

UP to now, the studies of alkali-silica reaction (ASR) induced expansion in HACs are rare. Some researchers assert that ASR-induced expansion is unlikely to occur in HACs because the alkalis from the chemical activator are bound in alkali activation products (Garcia-Lodeiro et al., 2016b, Palomo et al., 2019).

Donatello et al. (Donatello et al., 2013b) studied the ASR-induced expansion of ordinary Portland cement and HAC based on fly ash in accordance with the method of ASTM 1260. The results show that ASR-induced expansion of the two binders were both less than 0.1% (16 days limit according to ASTM C1260) over 16 days of testing. However, the expansion became distinction along with the testing age, and the HAC mortar bars showed more stability in dimensional expansion. Angulo-Ramírez et al. (Angulo-Ramirez et al., 2018) reported the ASR-induced expansion of ordinary Portland cement, Portland blended cement, and hybrid alkaline

cement based on 80% GBFS AND 20% OPC. And concluded that blended cement performed the smallest expansion to alkali-silica reaction. HAC was followed by with expansion less than 0.1% over 16 days of testing, and less than 0.2% over 30 days of testing. OPC shows the largest dimensional expansion, which was exceed 16 days and 30 days limit. Palomo et al. (Palomo et al., 2019) reported that mortar can stand for over 6 months with ASR-induced expansion less than 0.1%.

Based on the above consideration, this research will explore the durability properties of HAC on compressive strength, chloride penetration, sulphate attack and alkali-aggregate reaction. A series of HAC concrete systems are prepared with 10% of OPC and 90% GBFS, addition with different dosage of alkali activators. The effects of the dosage of activator used, on the durability properties of different HAC systems will be studied.

7.2 Experimental

The HAC and OPC concrete systems are prepared, detailed mixes information is shown in Table 7-1. The system 1 (highly blended cement concrete) and system 10 (OPC concrete) solely hydrated by water are prepared as references. All the concretes are produced with binder (OPC and/or GBFS) of 400 kg/m³, aggregate 1300 kg/m³, sand 690 kg/m³. All the concrete systems are mixed with the same water (free water plus water in alkali activator) to binder ratio (w/s) of 0.38. The dosage of alkali activator is expressed by the wt.% of Na₂O relative to the quality of the binder, and the solid chemical activator is blended into ground together with the binders. The systems have been tested as enabling hybrid alkali activated GBFS/OPC blends to obtain comparable or even higher compressive strength than OPC mortars while retaining acceptable setting times and workability. The dosage of alkali activator in this study is quite low relative to AAM and HAC systems(Bernal et al., 2012, Barboza-Chavez et al., 2020).

All the specimens are cured in standard curing environment (at 20 ± 2 °C and humidity > 95%) in accordance with ISO 1920-3-2004. No signs of carbonation and efflorescence are observed during the ages of this study, which show that the specimens are sufficiently durable to resist to carbonation and efflorescence during the ages of this study.

Table 7- 1 Composition of concrete systems.

NO.	System	GBFS (kg/m ³)	OPC (kg/m ³)	Aggregate (kg/m ³)	Sand (kg/m ³)	Na ₂ SiO ₃ ·9H ₂ O(%) (Na ₂ O wt.% of binder)
1						0
2						1%
3						2%
4						3%
5	90GBFS-10OPC	360	40	1300	690	4%
6						5%
7						6%
8						7%
9						8%
10	80GBFS-20OPC	80	320	1300	690	5%
11	70GBFS-30OPC	120	280	1300	690	5%
12	100OPC	-	400	1300	690	0
13	100GBFS	400	-	1300	690	5%

Table 7- 2 Composition of mortar bar systems.

NO.	System	GBFS (kg/m ³)	OPC (kg/m ³)	Sand (kg/m ³)	Na ₂ SiO ₃ ·9H ₂ O(%) (Na ₂ O wt.% of binder)
1					0
2					1%
3					2%
4					3%
5	90GBFS-10OPC	360	40	900	4%
6					5%
7					6%
8					7%
9					8%
10	80GBFS-20OPC	80	320	900	5%
11	70GBFS-30OPC	120	280	900	5%
12	100OPC	-	400	900	0
13	100GBFS	400	-	900	5%

7.3 Testing procedure

The testing procedure are introduced in chapter 3 section 3.4.

7.4 Results and discussion

In this study, the durability of HAC concretes were evaluated by the dosage of alkali activator.

7.4.1 Compressive strength

The compressive strength results of all concretes are shown in Figure 7-1 and Figure 7-2. The concretes described in Table 7-1 cured at room temperature and tested at 7, 28, 91 and 180 days.

System 6 (90GBFS-10OPC) shows the highest mechanical strength results: 7d 73.9MPa, 28d 97.0 MPa, 91d 97.38 MPa, and 180d 98.1 MPa, higher than OPC at the same periods which is 7d 60.5 MPa, 28d 71.6 MPa, 91d 74.3 MPa and 180d 76.3 MPa. The result assures that HAC system with high proportion (90%) of SCMs can get even higher compressive strength than OPC in long curing time. The result also proves that by adjusting the proportion of raw materials and adding an appropriate dosage of alkali activator, high-strength and durable HAC can be obtained.

System6 exhibits higher compressive strength compared to system 13(100GBFS). This indicates that the HAC shows higher compressive strength than AAM with the same dosage of alkali activator. The main reason for this phenomenon is that the hydration of OPC in the HAC system increases the pH value of the reaction solution(Garcia-Lodeiro et al., 2016b), resulting in a more complete final reaction compared to the AAM system.

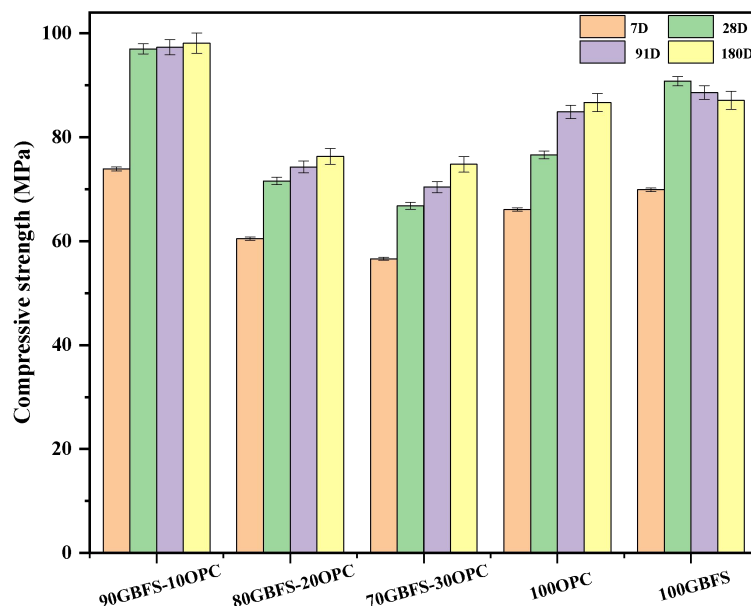


Figure 7-1 Compressive strength of HAC systems activated with 5% Na₂O.

As it is shown in Figure 7-2, blended cement (BC) concretes provide the lowest compressive strength in all the specimens at 7d, 28d, 91d and 180d, especially at early age (19.7MPa at 7d). The main reason is that the hydration

reaction rate is relatively slow, associated with higher porosity, reduced mechanical strength and stiffness compared to OPC concretes (Menéndez et al., 2003, Hoshino et al., 2006, Whittaker et al., 2014, Hlobil et al., 2016, Durdziński et al., 2017). The slow hydration reaction rate of blended cements (Macphee et al., 1988, Pane and Hansen, 2005, Kocaba et al., 2012) produce the reduced reactivity of GBFS compared to OPC (Escalante-Garcia and Sharp, 2001). GBFS particles blended with OPC react only after activation due to the production of OH^- produced from OPC hydration (Roy, 1982). Due to the relatively low proportion of OPC in this experiment, the reaction process relatively slow, which result in the low compressive strength at early age (19.7MPa at 7d), but shows 92% increases at 91d, and 108% increases at 180d. At the same time, the compressive strength of OPC concretes only show 28% increases at 91d, and 31% increases at 180d. The hydration reactions of OPC and GBFS occur simultaneously and interact with each other (Richardson and Groves, 1992, Chen and Brouwers, 2007), Resulting in a very complex combination of different hydration products. Since GBFS contains relatively lower content of calcium than OPC (Lothenbach et al., 2011a), the calcium-silicate-hydrates (C-S-H gel), the most important hydration products of Ordinary Portland Cement (OPC) hydration, known as C-S-H gel, show a lower calcium-to-silicate ratio (C/S) in blended cement as compared to OPC (Richardson and Groves, 1992, Königsberger and Carrette, 2020).

The compressive strength of HAC concretes shows an increase with the rising dosage of alkali activator and then a decrease with the increment of Na_2O content. When the dosage of Na_2O content reaches 4%, HAC exhibits a compressive strength 50.2 MPa at 7 days, and shows 47% increases with the dosage of Na_2O content reaches 5%. The compressive strength of concrete specimens shows an increasing trend with the increase dosage of Na_2O content, which is more obvious in the early age and not obvious in the later age. The compressive strength of HAC concretes reaches 73.9 MPa with a 5% dosage of Na_2O content at 7 days. Subsequently, there is a further 33% increase in compressive strength from 7 to 180 days, surpassing OPC concrete samples at all the ages. However, the compressive strength of HAC concrete samples exhibits a decrease with the increasing dosage of Na_2O content (>5%). Comparing HAC concrete samples with an alkali content of 5% and 8%, the compressive strength of HAC shows a decrease of 28% at 7 days and then a

decrease of 38% at 180 days. The compressive strength of HAC concretes present a decreasing trend with the increase dosage of Na_2O content, which is not obvious in the early age but becomes more pronounced in the later age.

With the increasing dosage of alkali activator, the pH value in the reaction solution increases gradually, thereby accelerating the dissolution of GBFS in alkaline solution and increasing the reaction rate. When the dosage of Na_2O reaches 4%, HAC concrete exhibits a compressive strength equivalent to OPC concrete at 28 days. When the dosage of Na_2O reaches 5%, the compressive strength of HAC reaches the highest point, and then decreases as the dosage of the activator increases. The main reason for this phenomenon is that an excessive amount of Na_2O causes the sample to expand and crack, leading to a decrease in the mechanical strength of HAC concrete. Observably, by adding an appropriate dosage of alkali activator, HAC concrete exhibits higher compressive strength than OPC concrete, both at early age and later ages.

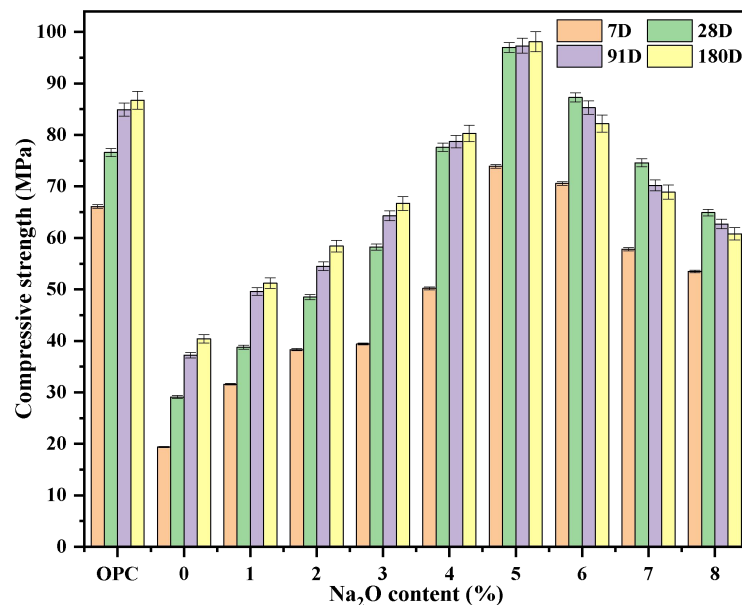


Figure 7-2 Compressive strength of OPC and HACs activated by different dosage of alkali activator.

7.4.2 Resistance to chloride penetration

7.4.2.1 Rapid chloride penetration test

The resistance to chloride penetration of all concretes is measured by rapid chloride penetration test (RCPT), which is obtained according to the total charge passed during the first 6 hours. The resistance to chloride penetration in concretes is evaluated based on five levels: "high, moderate, low, very low, or negligible,"

corresponding to chloride-ion penetrability. The Rapid chloride penetration test (RCPT) results showed in Table 7-3 and Table 7-4 are all the systems, with different ratio of OPC and activated by different dosage of $\text{Na}_2\text{SiO}_3 \cdot 9\text{H}_2\text{O}$, cured at $20 \pm 2^\circ\text{C}$ and $\text{RH} > 95\%$ in accordance with ISO 1920-3-2004 and tested at 28 and 91 days. The system 1 blended cement (90% GBFS+10%OPC without alkali activator) and system 12 (OPC) samples were taken and used as references.

The total charge passed values obtained from the RCPT for all mixes were listed in in Table 7-3 and Table 7-4. The total charge passed values of concrete systems with the same dosage of Na_2O content present an increase trend with the increasing ratio of OPC in concretes. The total charge passed values of OPC concrete is 2211.94 at 28d and 1595.67 at 91d, which shows 28% decrease with the curing days from 28 to 91. At the same situation, the total charge passed values of system 13 (100GBFS) concrete is 655.32 at 28d and 603.89 at 91d, which shows only 30% and 38% compared to OPC at the same at the same curing time. With the increasing ratio of OPC in concrete, the values increase. When the ratio of OPC reaches 30%, system11 exhibits a total charge passed values of 865.87 28 days, 814.28 at 91 days, which is 39% and 51% compared to OPC at the same at the same curing time. The increase trend is more obvious in the later age and not obvious in the early age.

As it is shown in Table 7-3, blended cement concretes show the most total charge passed values in all the specimens at 28d and 91d, that is 2534.84 at 28d and 1697.74 at 91d of total charge passed values, which shows 33% decrease with the curing days from 28 to 91. At the same situation, the total charge passed values of OPC concrete is 2211.94 at 28d and 1595.67 at 91d, which shows 28% decrease with the curing days from 28 to 91. The main reason is that the hydration reaction rate is relatively slow, associated with higher porosity and lower density compared to OPC concretes (Menéndez et al., 2003, Hoshino et al., 2006, Whittaker et al., 2014, Hlobil et al., 2016, Durdziński et al., 2017).

The total charge passed values of HAC concretes present a decrease with the increasing dosage of alkali activator and then an increase with the increment of Na_2O content. When the dosage of Na_2O content reaches 4%, HAC exhibits a total charge passed values of 803.39 28 days, and shows 15% decreases with the dosage of

Na₂O content reaches 5%. The total charge passed values of HAC concrete specimens shows a decreasing trend with the increase dosage of Na₂O content (Na₂O content <5%), which is more obvious in the early age and not obvious in the later age. The total charge passed values of HAC concretes reach 685.99, followed by a further 6% decrease from 28 to 91 days, which is lower than OPC concrete samples at testing period. However, the total charge passed values of HAC concrete sampled show an increase with the increasing dosage of Na₂O content (>5%). Compared HAC concrete samples with an alkali content of 5% and 8%, the total charge passed values of HAC shows an increase of 197% at 28 days and then an increase of 180% at 91 days. The total charge passed values of HAC concrete samples show an increasing trend with the increase in dosage of Na₂O content (Na₂O content >5%).

Table 7-3 Total charge passed values of OPC and HACs at 28 days.

System NO.	Total charge passed values(coulomb)	Relative percentage to OPC(%)	Chlorid-ion penetrability
1	2534.84	115	Moderate
2	1916.43	87	Moderate
3	1327.57	60	Moderate
4	928.43	42	Very low
5	803.39	36	Very low
6	685.99	31	Very low
7	1044.41	47	Moderate
8	1521.08	69	Moderate
9	2038.16	92	Moderate
10	763.42	35	Very low
11	865.87	39	Very low
12	2211.94	100	Moderate
13	655.32	30	Very low

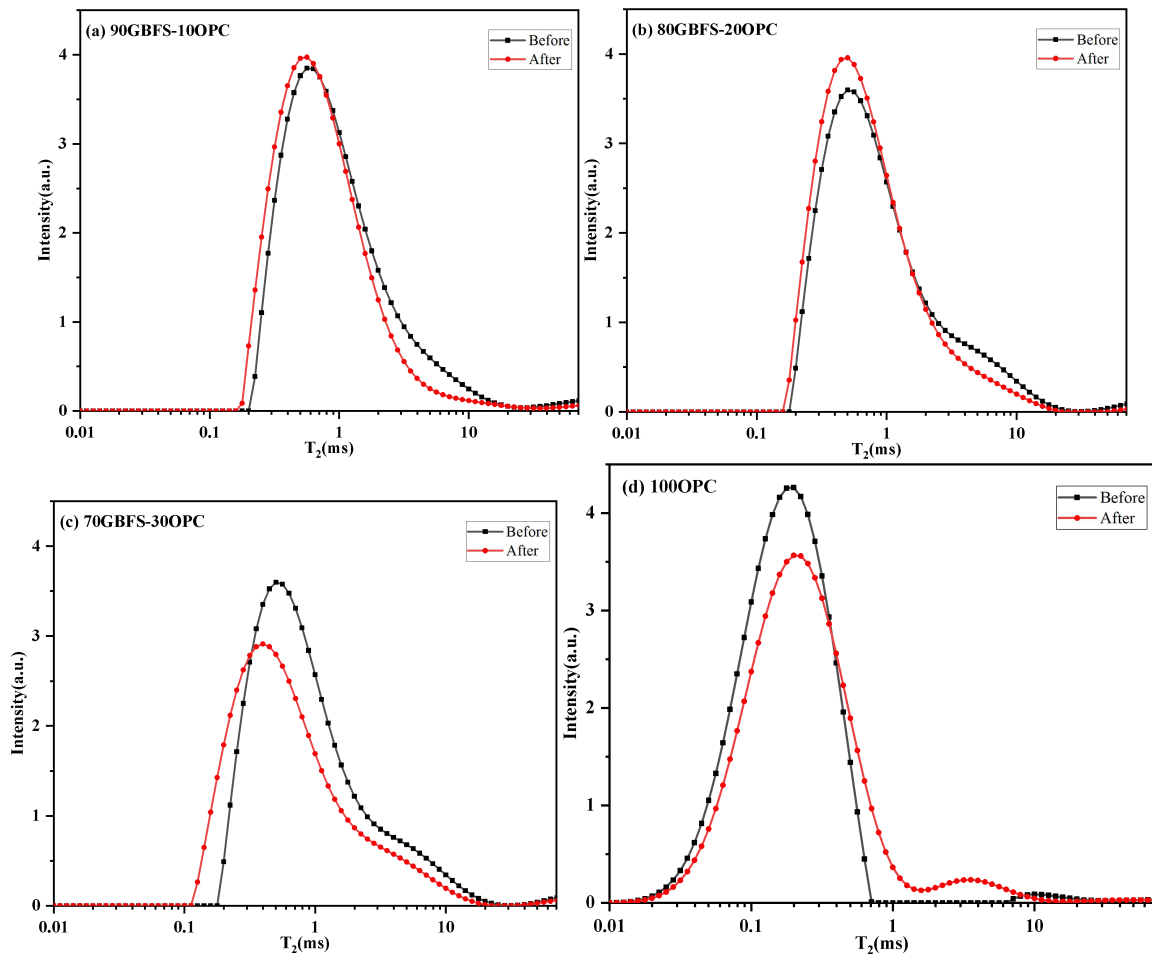
Table 7-4 Total charge passed values of OPC and HACs at 91 days.

System NO.	Total charge passed values(coulomb)	Relative percentage to OPC (%)	Chlorid-ion penetrability
1	1697.74	123	Moderate
2	1364.78	86	Moderate
3	1014.43	64	Moderate
4	851.95	53	Very low
5	735.01	46	Very low
6	644.88	40	Very low
7	1026.82	64	Moderate
8	1361.44	85	Moderate

9	1804.35	113	Moderate
10	712.37	45	Very low
11	814.28	51	Very low
12	1595.67	100	Moderate
13	603.89	38	Very low

7.4.2.2 ^1H NMR analysis

^1H NMR technology was used to explore pore structure of all binder systems before and after chloride penetration. In this ^1H NMR analysis, transverse relaxation time of T_2 vs signal intensity of water in all binders are tested. And, the relationship between water mass and signal intensity has to been established. The development of transverse relaxation time of T_2 vs signal intensity is evaluated by the different ratio of OPC in the binder systems, and the dosage of Na_2O content in HACs.



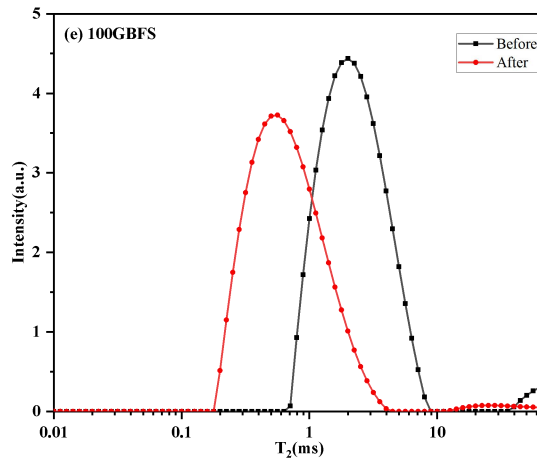


Figure 7-3 T_2 vs signal intensity of binders with ratio of OPC before and after chloride penetration.

T_2 vs signal intensity of binders with ratio of OPC before and after chloride penetration is shown in Figure 7-3, and different ratio of OPC present varying pore structure distributions. The binders with different ratio of OPC present the signal intensity peaks of T_2 shifted left after chloride penetration and the intensity declined or enhanced. AAM (100GBFS) presents signal intensity peak of T_2 from 1.9ms shifted to 0.56 after chloride penetration, indicating a transformation of water from capillary pore water to gel pore water. OPC shows nearly the same signal intensity peak at $T_2 < 0.2$ ms and exhibits a signal intensity peak at around 3.5ms, which indicating that the water is converted into smaller gel pore water after chloride penetration. HACs with different ratio of OPC did not show significant changes after chloride penetration. Generally speaking, AAM preforms best, HACs follow and OPC shows worst after after chloride penetration, the results are consistent with rapid chloride penetration test in Table 7-3 and Table 7-4.

The influence of the dosage of Na_2O content in HACs on pore structure distribution after chloride penetration is shown in Figure 7-4, and the increasing dosage of alkali activator in HACs exhibit different pore structure distributions. As shown in Figure 5-6(a), BC (90GBFS-10OPC hydrated by only water) exhibits signal intensity peak of T_2 from 1.6ms shifted to 1.0ms after chloride penetration, which is the maximum left shift in HAC systems. The intensity peaks shifted left in HACs after chloride penetration, attributed to the majority of water migrating to smaller pores. Meanwhile, it should notice that the intensity peaks do not left shift with the increase of Na_2O content. The intensity peaks show the lowest with an Na_2O content of 5%, which indicated that the most suitable pore structure distribution were produced. However, HAC with high dosage of Na_2O content shows intensity peaks shifted right

(T_2 from 0.4ms shifted to 0.9ms) as shown in Figure 5-6(i). Correspondingly, the compressive strength of HACs exhibits an increasing trend with the growing dosage of alkali activator and subsequently decreases with the increment of Na_2O content, as shown Figure 5-2.

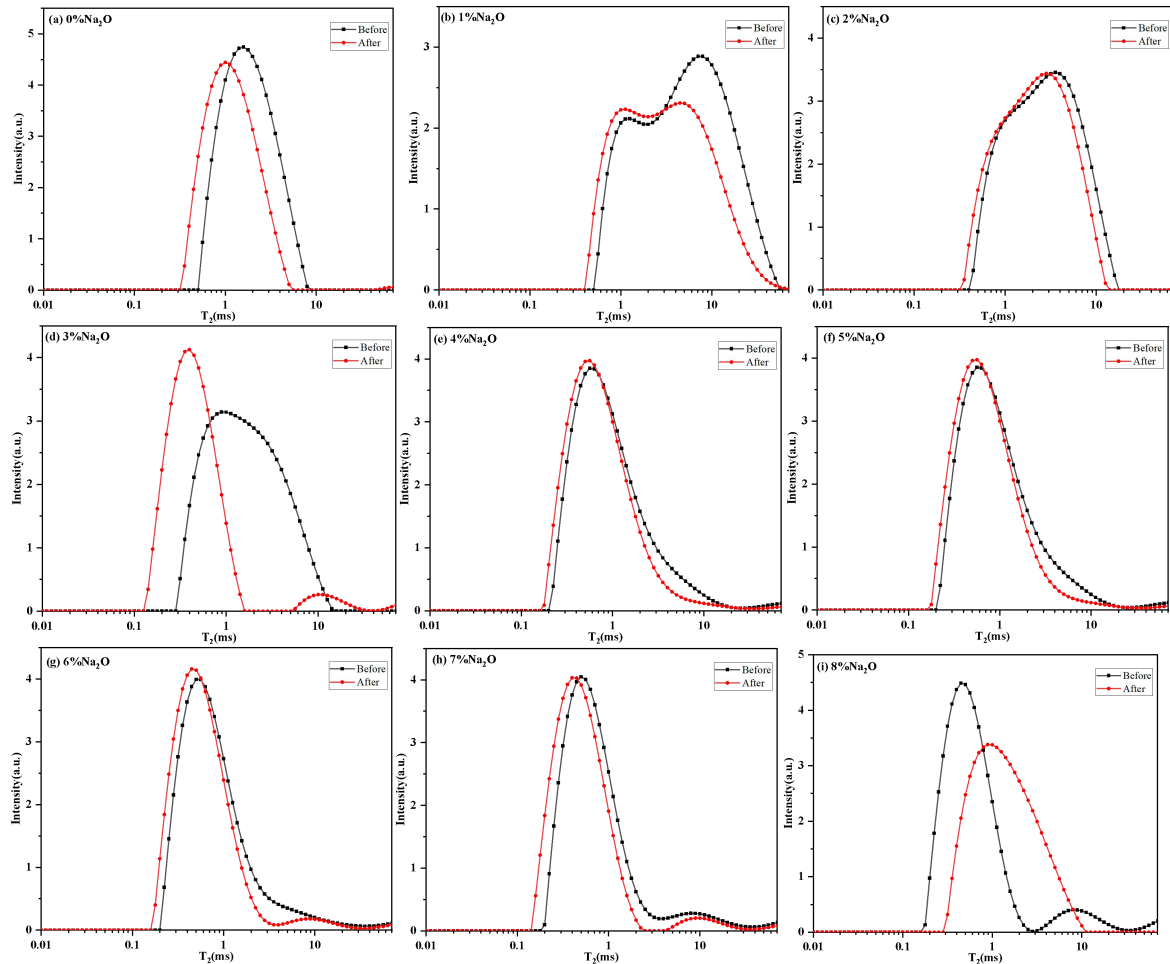


Figure 7-4 T_2 vs signal intensity of HACs with different dosage of Na_2O content before and after chloride penetration.

7.4.3 Sulphate attack resistance

7.4.3.1 sulphate attack resistance of concretes

The results for the sulphate attack resistance of HAC concretes are presented in Table 7-5. It can be seen BC concrete experience the biggest weight loss in all concrete samples. Blended cement concretes lose 2.9% of original weight over 150 times of sulphate attack cycles. Correspondingly, OPC concretes endure only 1.2% of original weight, much lower than that of blended cement concrete. Due to the slow hydration reaction rate of blended cement, resulting in high porosity and low density associated with a loose structural composition (Menéndez et al., 2003,

Hoshino et al., 2006, Whittaker et al., 2014, Hlobil et al., 2016, Durdziński et al., 2017). However, the compressive strength increases 5.4% for blended cement concretes after over 150 times of sulphate attack cycles, meanwhile the compressive strength of Ordinary Portland Cement (OPC) decreases by up to 24.6% under the same sulphate attack conditions. The results indicate that the compressive strength of blended cement concretes is not only decreased during sulphate attack but also increased, showcasing significant advancements in recent years. The main reason is that Na_2SO_4 is a near-neutral salts that can be used as alkali activators in HAC, and has also seen considerable advances in recent years (Donatello et al., 2013a, Donatello et al., 2014, Millan-Corrales et al., 2020, Qu et al., 2020, Garcia-Lodeiro et al., 2018b, Garcia-Lodeiro et al., 2018a, du Toit et al., 2018, Fernandez-Jimenez et al., 2019, Garcia-Lodeiro et al., 2016b). In the alkali activation process proposed for blended cement, three distinct stages are involved: (a) Destruction-Coagulation; (b) Coagulation-Condensation; and (c) Condensation-Crystallization. The main reaction product is an amorphous alkaline aluminosilicate hydrate known as C-A-S-H gel (García-Lodeiro et al., 2012, Garcia-Lodeiro et al., 2012, Garcia-Lodeiro et al., 2016c). The alkali activation only occurs on the surface of blended cement concretes, so the hydration reaction rate is relatively slow, resulting only 5.4% increasing in compressive strength.

It can be seen HAC concretes show the weight loss ranging from 0.6% to 2.2% of original weight over 150 times of sulphate attack cycles, the loss of weight is related to Na_2O content, compressive strength and roughness of the sample surface. Correspondingly, OPC concretes endure only 1.2% of original weight, between the range of 0.6% to 2.2%. The loss of weight of HAC concretes present a decrease with the increasing dosage of Na_2O content and then an increase with the increment of Na_2O content. However, no significant regular trends are observed in the loss of weight. When the dosage of Na_2O content reaches 3%, HAC samples exhibit a loss of weight of 0.6% of original weight, and shows 2.2% loss of weight with the dosage of Na_2O content reaches 2%. AAMs normally have stronger resistance to sulfate attack than OPC, due to 3d structure of N-A-S-H or C-A-S-H in AAMs, which is more compact than 2d structure of C-A-H in OPCs (Monticelli et al., 2016b, Monticelli et al., 2016a, Babaei and Castel, 2016, Tennakoon et al., 2017). HAC is a new type of AAM, also show good sulfate attack resistance. Some researchers believed that the

excellent sulfate resistance of AAMs may be related to the lack of $\text{Ca}(\text{OH})_2$ in AAM activation productions (Donatello et al., 2013b, S. Donatello¹, 2014, Janotka et al., 2014, Bačuvčík et al., 2018). In this study, HAC consists of 90% of GBFS, 10% OPC and Na_2O (ranging from 1% to 8%), which belongs to high calcium alkali excitation system. C-A-S-H gel is considered as the main reaction product in the hydration of HAC (Xue et al., 2023, Xue et al., 2021a).

The Compressive strength of HAC concrete specimens after over 150 times of sulphate attack cycles shows an increasing trend with the increase dosage of Na_2O content (Na_2O content <4%). The compressive strength increases 6.5% for HAC (Na_2O =4%) concretes. However, the compressive strength of OPC concretes decrease up to 24.6% for OPC experienced the same tests. The test results prove that the compressive strength of HAC concretes activated by low Na_2O content is not only decreased during the sulphate attacking but also increased. Na_2SO_4 is proved as an alkali activator in HAC systems (Donatello et al., 2013a, Donatello et al., 2014, Millan-Corrales et al., 2020, Qu et al., 2020, Garcia-Lodeiro et al., 2018b, Garcia-Lodeiro et al., 2018a, du Toit et al., 2018, Fernandez-Jimenez et al., 2019, Garcia-Lodeiro et al., 2016b). The main reaction product is an amorphous alkaline aluminosilicate hydrate known as C-A-S-H gel (García-Lodeiro et al., 2012, Garcia-Lodeiro et al., 2012, Garcia-Lodeiro et al., 2016c). The reaction of HAC with Na_2SO_4 solution only activated on the surface of HAC concretes, producing relatively low increasing in compressive strength. The decline in compressive strength of HAC concretes after over 150 times of sulphate attack cycles showed an increasing trend with the increase Na_2O content (Na_2O > 5%). The reduction in compressive strength for HAC concretes (Na_2O =5%) reaches 10.8% after over 150 times of sulphate attack cycles. And the decline in compressive strength went up to 23.9% for HAC concretes (Na_2O =8%), which was closed to the reduction in compressive strength for OPC concretes withstand the same sulphate attack. The results also indicate that: when the Na_2O content is not sufficient in HAC systems (Na_2O <4%), Na_2SO_4 solution will acted as alkali activator to stimulate the potential strength of the precursors, when the Na_2O content is sufficient in HAC systems (Na_2O content more than 5%), the potential strength of the precursors has been fully utilized, the exposure of HAC concrete to Na_2SO_4 solution induces corrosion, leading to a reduction in compressive strength and a deterioration in quality. Observably, by adding an appropriate dosage

of alkali activator, HAC concrete exhibits higher resistance to sulphate attack than OPC concrete.

Table 7-5 Sulphate attack resistance of OPC and HACs.

System NO.	Weight loss (%)	Compressive strength before sulphate attack (MPa)	Compressive strength after sulphate attack (MPa)	Reduction in compressive strength (%)
1	2.9±0.2	37.2±2.2	39.2±2.3	-5.4
2	1.6±0.1	49.6±2.3	51.5±2.1	-3.8
3	2.2±0.2	54.5±2.5	55.0±2.4	-0.9
4	0.6±0.1	64.3±2.6	67.9±2.4	-5.6
5	1.3±0.1	78.7±2.1	83.8±2.0	-6.5
6	0.8±0.1	97.3±2.0	86.7±2.1	10.8
7	1.0±0.1	85.3±2.2	73.5±2.0	13.8
8	0.9±0.1	70.2±2.1	53.4±2.2	18.6
9	1.1±0.1	62.7±2.2	47.7±2.1	23.9
12	1.2±0.1	84.9±2.2	65.4±2.3	24.6

7.4.3.2 XRD analysis

Figure 7-5(a) presents the XRD patterns of binders with different ratio of OPC before exposed to Na_2SO_4 solution, Figure 7-6(a) shows the XRD patterns of HACs activated by different dosage of Na_2O content before exposed to Na_2SO_4 solution, and Figure 7-5(b) and Figure 7-6(b) show the XRD patterns after exposed to Na_2SO_4 solution. The analysis of XRD of all the binder before exposed to Na_2SO_4 solution can be seen in chapter 4 section 4.4.2. As shown in Figure 7-5(b), Ettringite is observed in 100OPC sample after exposed to Na_2SO_4 solution, with the intensity of portlandite disappeared in the XRD patterns (Yang et al., 2022). Signals of ettringite is also detected in 70GBFS-30OPC and 80GBFS-20OPC samples, however the intensity is relative weak. With the decreasing ratio of OPC in binder systems, very weak intensity signals of ettringite are observed in 90GBFS-10OPC and 100GBFS samples. The results are consistent with the tests of compressive strength after sulphate attack as shown in Table 7-5. In the sample of 90GBFS-10OPC activated by 0% Na_2O content shown in Figure 7-6(b), the signals of ettringite are observed. With the increasing dosage of Na_2O content, no more intensity of ettringite is detected, which is due the lack of portlandite. This phenomenon is similar to findings reported in other studies (Angulo-Ramirez et al., 2017, Bačuvčík et al., 2018, Fernandez-Jimenez et al., 2013a, Xue et al., 2021b), which attribute it to the

relatively low proportion of OPC in HAC system. Additionally, the high alkalinity of the solution can inhibit or delay the hydration rate of OPC, further contributing to this effect (Puertas et al., 2011). Overall, the outcomes are in line with the compressive strength results observed after exposure to sulphate attack, as indicated in Table 7-5.

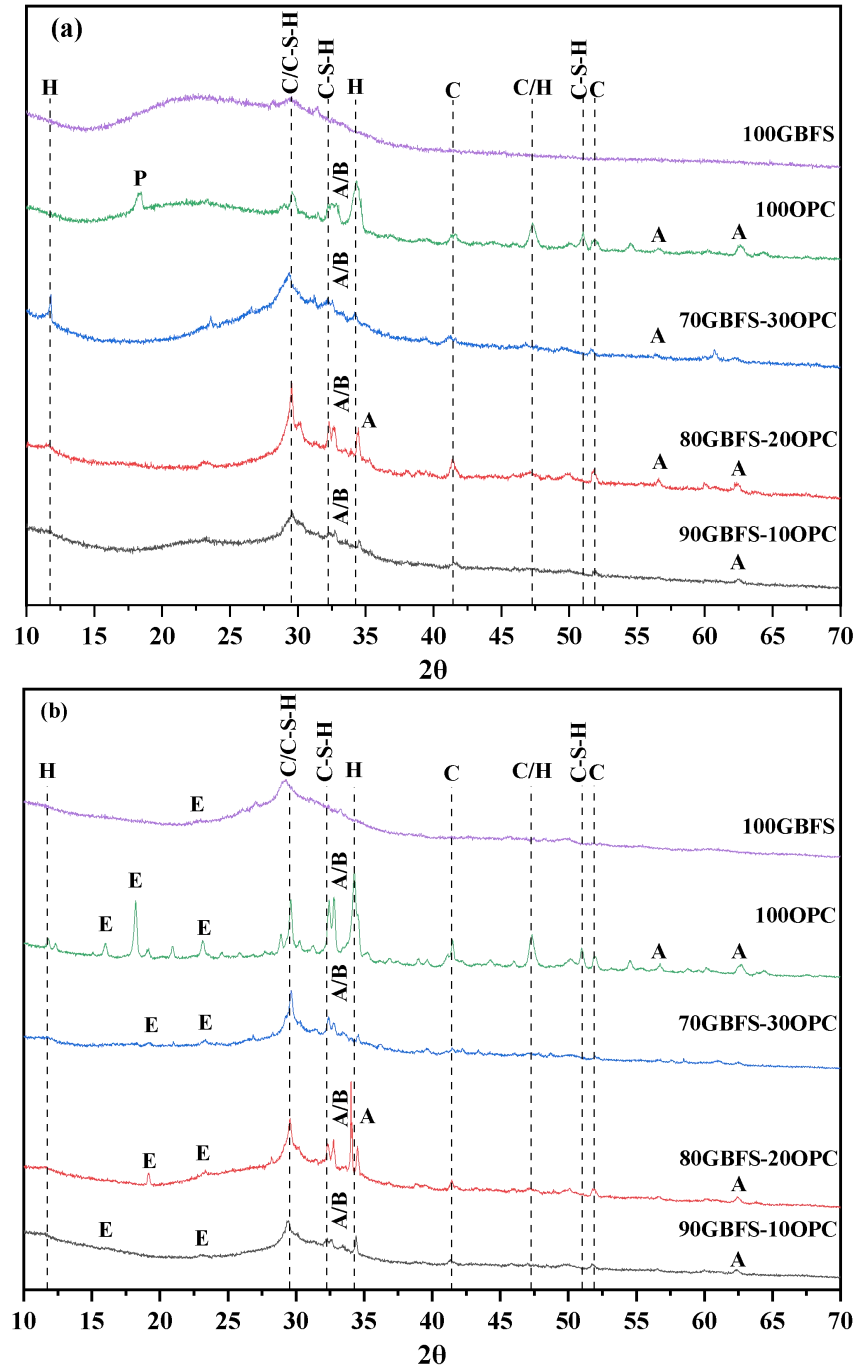


Figure 7-5 XRD patterns of binders with different ratio of OPC before and after sulphate attack. (a) before; (b) after. A: C_3S ; B: C_2S ; C: Calcite; E: ettringite; H: Hydrocaluminte; Ge: hydrated Gehlenite (C_2ASH_8).

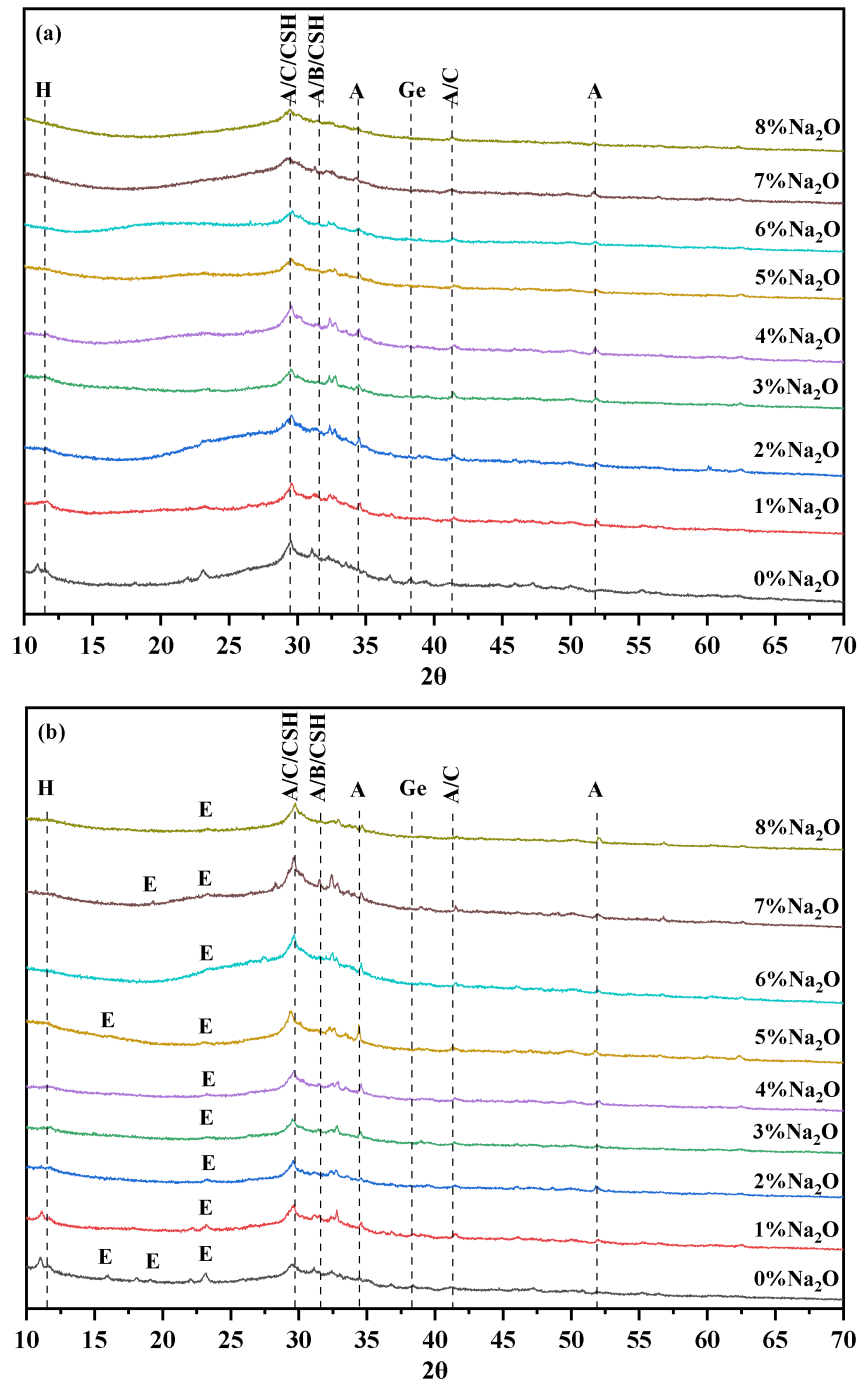


Figure 7-6 XRD patterns of HACs with different dosage of Na_2O content before and after sulphate attack. (a) before; (b) after. A: C_3S ; B: C_2S ; C: Calcite; E: ettringite; H: Hydrocaluminte; Ge: hydrated Gehlenite (C_2ASH_8).

7.4.4 Alkali-aggregate reaction

This study tests the performance to alkali-aggregate reaction of all binder mortar bars as shown in Table 7-2. Alkali-aggregate reaction test of all the mortar bars is carried out. Furthermore, microstructural analysis was performed by scanning electron microscopy. The results of the tests show that BC and HAC exhibit smaller longitudinal expansions compared with OPC.

7.4.4.1 Alkali-aggregate reaction test

Alkali-aggregate reaction test results of all the mortar bars are shown in Figure 7-7 and Figure 7-8 according to ASTM C1260 (Testing and Materials, 2014). The longitudinal expansions are used to evaluate the potential Alkali-aggregate reactivity. The longitudinal expansion of mortar bar is lower than 0.1% within 16 days is indicative harmless to structures according to ASTM C1260 (Testing and Materials, 2014). However, the longitudinal expansion of mortar bar is higher than 0.2% over 16 days, which is indicated of potential destructive expansion aggregates. In this case, no conclusion can be made, when the expansion is longer than 0.1% but lower than 0.2% within 16 days. In this study, the longitudinal expansion test of the mortar bars has been expanded up to 35 days immersed in 1 N NaOH solution at 80°C. The longitudinal expansion of OPC at 16 days is higher than 0.1% but lower than 0.2%, as shown in Figure 7-7. The longitudinal expansion test is extended up to 35 days according to the results.

As shown in Figure 7-7. OPC mortar bars show the greatest longitudinal expansion in all the ages. 70GBFS-30OPC mortar bars are followed by, and 100GBFS mortar bars performed best in the performance to alkali-aggregate reaction. The mortar bars are all immersed in the same 1N NaOH solution curing at 80°C. However, OPC system performs the greatest longitudinal expansion at every age; within 16 days, the longitudinal expansion of OPC mortar bars has exceeded 0.1% (16 days limit according to ASTM C1260). And at 25 days, the longitudinal expansion of OPC mortar bars has already exceeded 0.2% (30 days limit according to ASTM C1260). HAC systems perform longitudinal expansion lower than 0.1% within 20 days in the same 1 N NaOH solution at 80°C, and lower than 0.2% within 35 days. The results suggest that HAC exhibits greater durability than OPC in alkali-aggregate reactions. The test results of HAC system are consistent with the researches of AAMs(Shi et al., 2015c, Krivenko et al., 2014, Fernández-Jiménez and Puertas, 2002). 100GBFS performs the lowest longitudinal expansions compared to OPC and HAC systems, with longitudinal expansions lower than 0.1% to the end of the test (35 days). The longitudinal expansion of AAM mortar bars is much lower than that of OPC mortar bars in the testing period, the result indicates that AAM exhibits better performance in resistance to alkali-aggregate reactions.

AAM systems based on GBFS normally have less alkali-aggregate reaction

influence than OPC system(Gifford and Gillott, 1996, Shi, 1988, Yang et al., 1999). The result can be attributed to the formation of C(N)-A-S-H gels during the alkali reaction of GBFS with alkali activator, where these gels have a lower Ca to Si ratio compared to C-S-H gels(Cyr and Pouhet, 2015, You-zhi et al., 2002, Shi et al., 2015a).The HAC system includes a certain proportion of OPC and uses alkaline activators to stimulate the potential reactivity of raw materials. HAC also exhibits notable resistance to alkali-aggregate reaction attacks(Donatello et al., 2013b, Angulo-Ramirez et al., 2018, Palomo et al., 2019). Some researchers believed that the excellent alkali-aggregate reaction resistance of AAMs may be related to the lack of $\text{Ca}(\text{OH})_2$ in AAM activation productions (Donatello et al., 2013b, S. Donatello1, 2014, Janotka et al., 2014, Bačuvčík et al., 2018). In this study, HAC consists of high ratio GBFS, low ratio of OPC with the help of alkali activator, which belongs to high calcium alkali excitation system. C-A-S-H gel is considered as the main reaction product in the hydration of HAC(Xue et al., 2023, Xue et al., 2021a). This research indicates that alkali-aggregate reaction expansion of HAC systems is mainly influenced by the dosage of alkali activator in the reaction system.

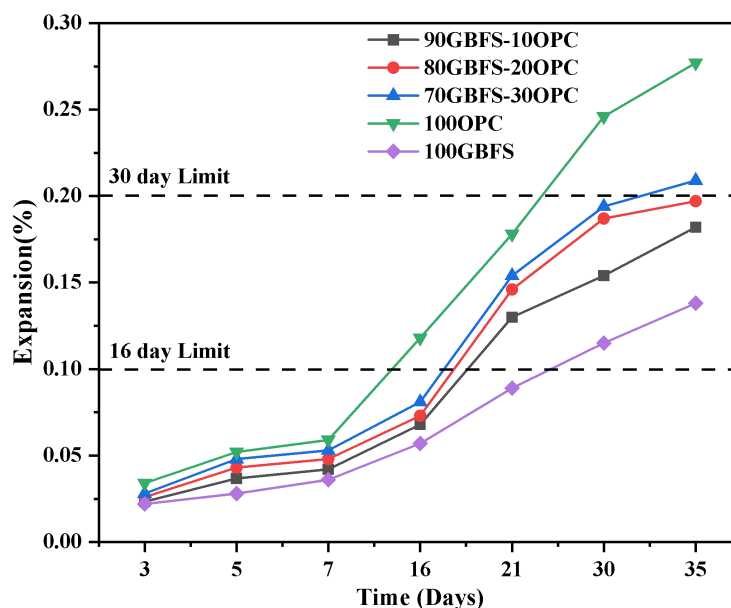


Figure 7-7 Longitudinal expansions of the mortar bars with different ratio of OPC in 1N NaOH at 80°C.

The longitudinal expansion of HAC mortar bars in response to alkali-aggregate reaction is significantly influenced by the Na_2O content. In this study, after determining the proportion of OPC and GBFS in HAC, the formation of hydration products in HAC is primarily influenced by the dosage of alkaline activator. Microscopic test results from Chapter 5 and 6 indicate that increasing the activator

dosage leads to greater formation of C-(A)-S-H gels in hydrated HAC. However, when the activator dosage exceeds a certain threshold (5%), the porosity of hydrated HAC products also increases. These changes affect the outcomes of the longitudinal expansion of HAC mortar bars (Angulo-Ramirez et al., 2018, S. Donatello¹, 2014, Donatello et al., 2013b, You-zhi et al., 2002, Al-Otaibi, 2008, Shi et al., 2015a). The longitudinal expansion of HAC mortar bars show an increase with the increasing dosage of alkali activator. HAC mortar bars exhibit a longitudinal expansion of 0.041% at 16 days with Na₂O content equals 1%, and increase 24% to 0.051% with Na₂O content reaches 8%, both of which are lower than 0.1% (16day limit according to ASTM C1260). As shown in Figure 5, all the HAC systems show expansions much lower than 0.1% (16day limit according to ASTM C1260) with 16 days immersed in 1 N NaOH solution at 80°C. However, the longitudinal expansion of OPC mortar bars reaches 0.118% at 16 days, which is higher than 0.1% (16day limit according to ASTM C1260). The longitudinal expansion of HAC system is lower than that of OPC system in the period of this study, the result indicates that HAC systems with highly proportion of GBFS exhibit better performance in resistance to alkali-aggregate reactions.

The longitudinal expansion HAC mortar bars to alkali-aggregate reaction show an increasing trend with the increasing dosage of Na₂O content, The expansion of HAC mortar bars is more noticeable at later ages but less prominent in the early stages. The longitudinal expansion of HAC mortar bars reach 0.071% at 30 days with Na₂O content equals 1%, and increase 121% to 0.157% with Na₂O content reaches 8%, which is higher than 0.1% but lower than 0.2%. However, the longitudinal expansion of OPC mortar bars reaches 0.247% at 30 days, which is higher than 0.2% (30day limit according to ASTM C1260). The increase in expansion of HAC mortar bars occurs relatively slowly with the rising Na₂O content at early ages. The expansion of HAC mortar bars is 0.021% at 3 days with 1% Na₂O content, and increase 14% to 0.024% at 3 days with 8% Na₂O content. And, the expansion of HAC mortar bars is 0.035% at 7 days with 1% Na₂O content, and increase 9% to 0.038% at 7 days with 8% Na₂O content. However, the expansion of OPC mortar bars reaches 0.034% at 3 days, and 0.059% at 7 days.

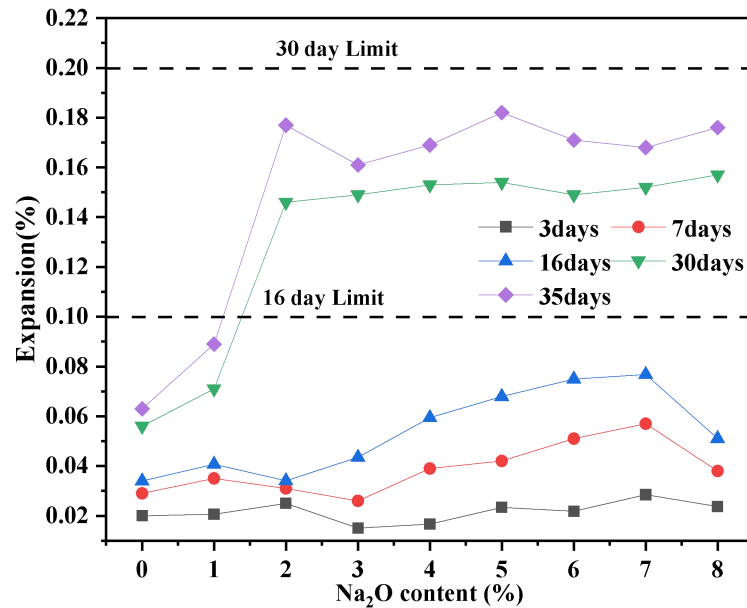


Figure 7-8 Mortar bars of HAC with different dosage of Na₂O content in solution of 1N NaOH at 80°C.

7.4.4.2 Microstructural analysis

SEM and EDS techniques were used to study the effect different ratio of OPC and dosage of Na₂O content on the microstructure of binder systems.

Figure 7-9 shows the SEM micrographs of mortar bar systems with different ratio of OPC activated by 5% of Na₂O content, and 100OPC system was used as reference. For the 90GBFS-10OPC mortar bar as shown in Figure 7-9(a), some small microcracks were detected surrounding the particles of sand and/or binder paste. As shown in Figure 7-9(c), mortar bar of 70GBFS-30OPC exhibits a number of alkali-silica cracks. Small cracks are also found in 100OPC mortar bar as shown in Figure 7-9(d). With the increasing ratio of OPC in binder system, mortar bars exhibit more and wider cracks, and present a increasing trend of Ca in in the matrix of mortar bars. However, little of alkali-silica reaction gel was found. Generally speaking, the results are consistent with Alkali-aggregate reaction test in Figure 7-7.

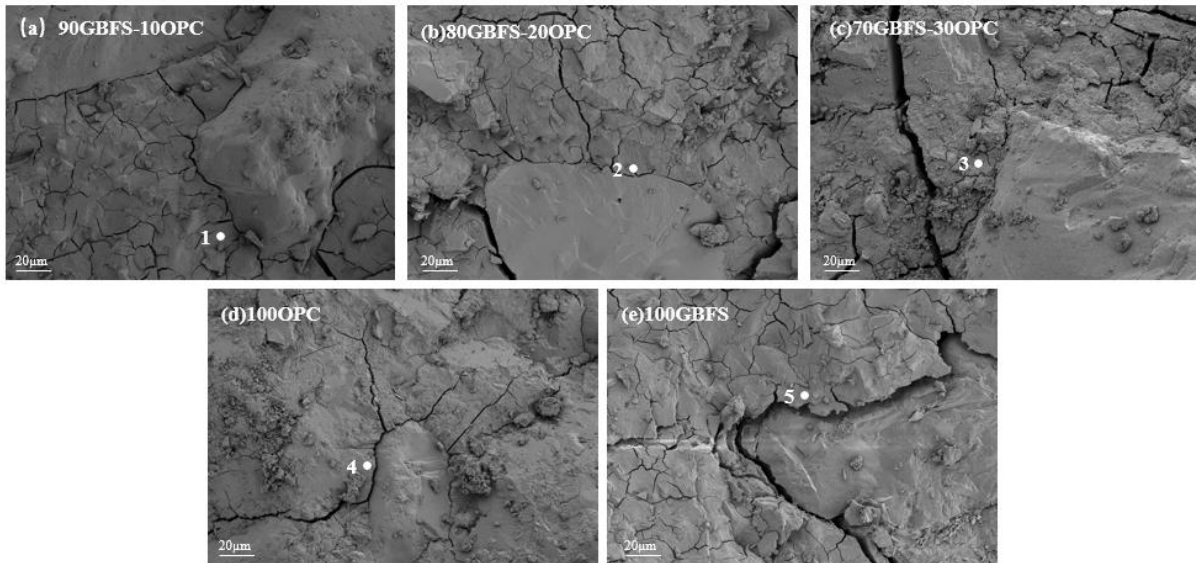
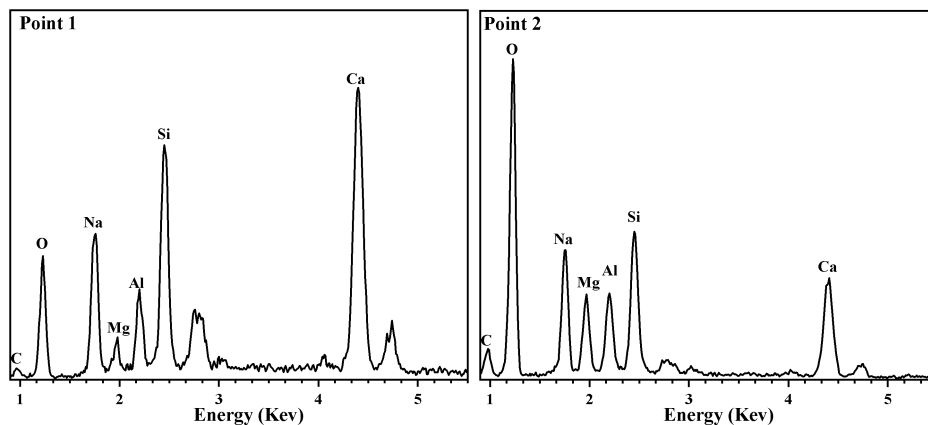


Figure 7-9 SEM images of mortar bars with different ratio of OPC in 1N NaOH at 80°C for 14 days.

The Na_2O content affects the microstructure development of HAC mortar bars in response to alkali-aggregate reactions. In this study, the SEM micrograph of HAC mortar bars based on 90%GBFS and 10%OPC activated by a series dosage of alkali activator is influenced to the dosage of alkali activator. Figure 7-11 shows the SEM micrographs of mortar bar systems activated by different dosage of Na_2O content. However, small cracks can be detected in Figure 7-11 (b) to (e), especially at the images by high dosage of Na_2O content which is possibly due to the presence of Hydrated gehlenite (C_2ASH_8) a hydrated product of GBFS activated with Na_2SiO_3 and NaOH (Yang et al., 2012, Shi et al., 2003). The microcracks of HAC mortar bars to alkali-aggregate reaction show an increasing trend with the increase dosage of Na_2O content. In generally, the results are consistent with alkali-aggregate reaction test in Figure 7-8.



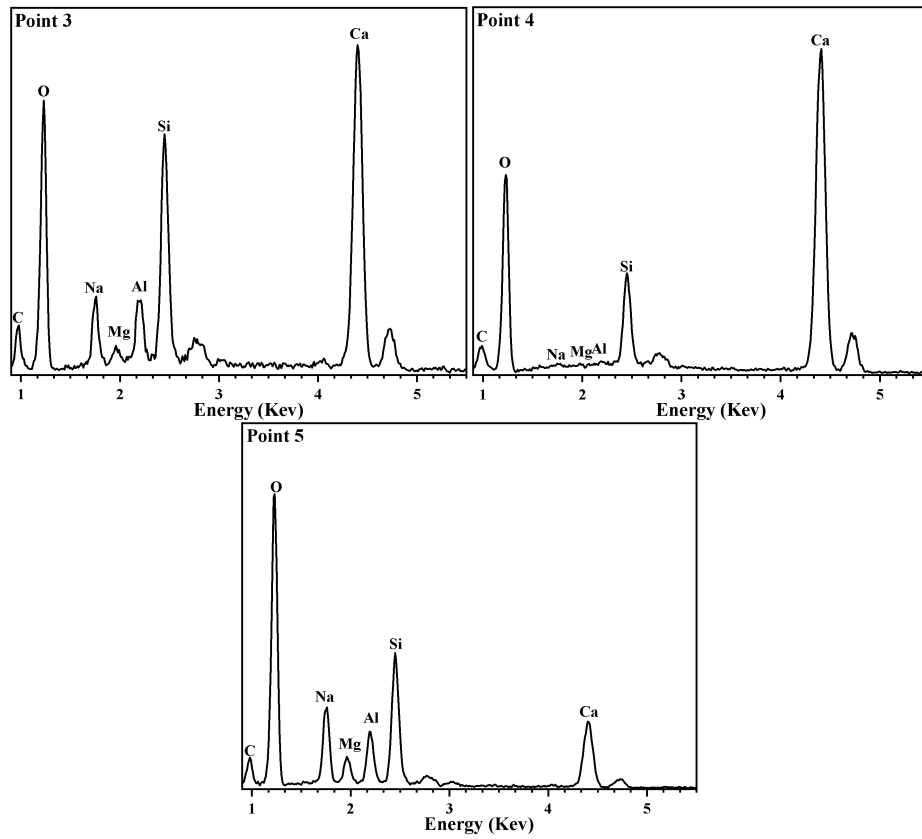


Figure 7- 10 Element distribution in the matrix of mortar bars with different ratio of OPC.

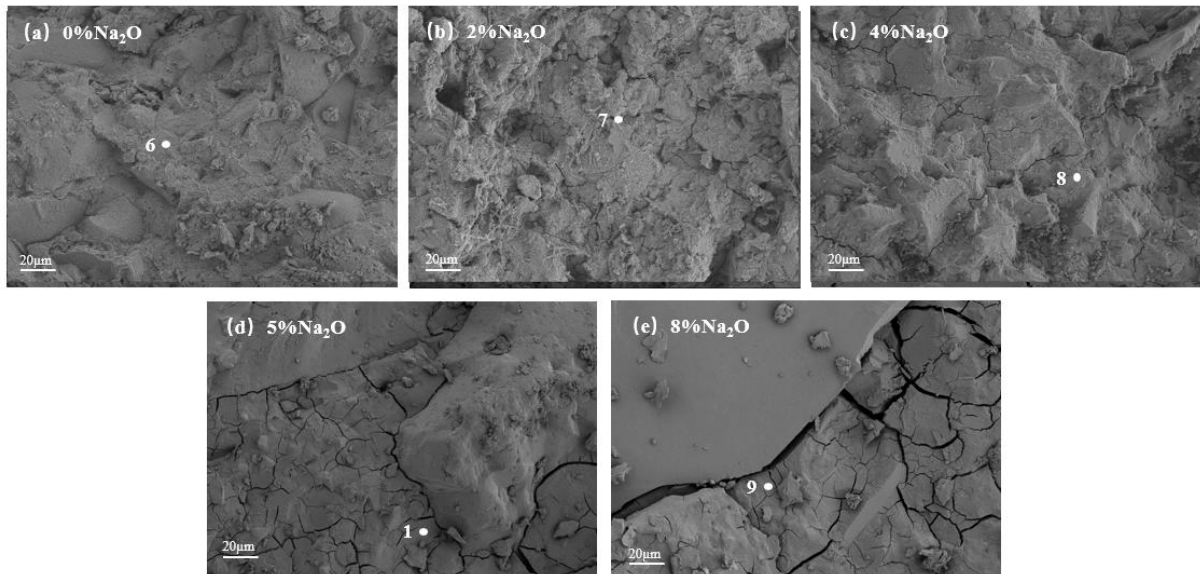


Figure 7- 11 SEM images of HAC mortar bars with different Na_2O content in 1N NaOH at 80°C for 14 days.

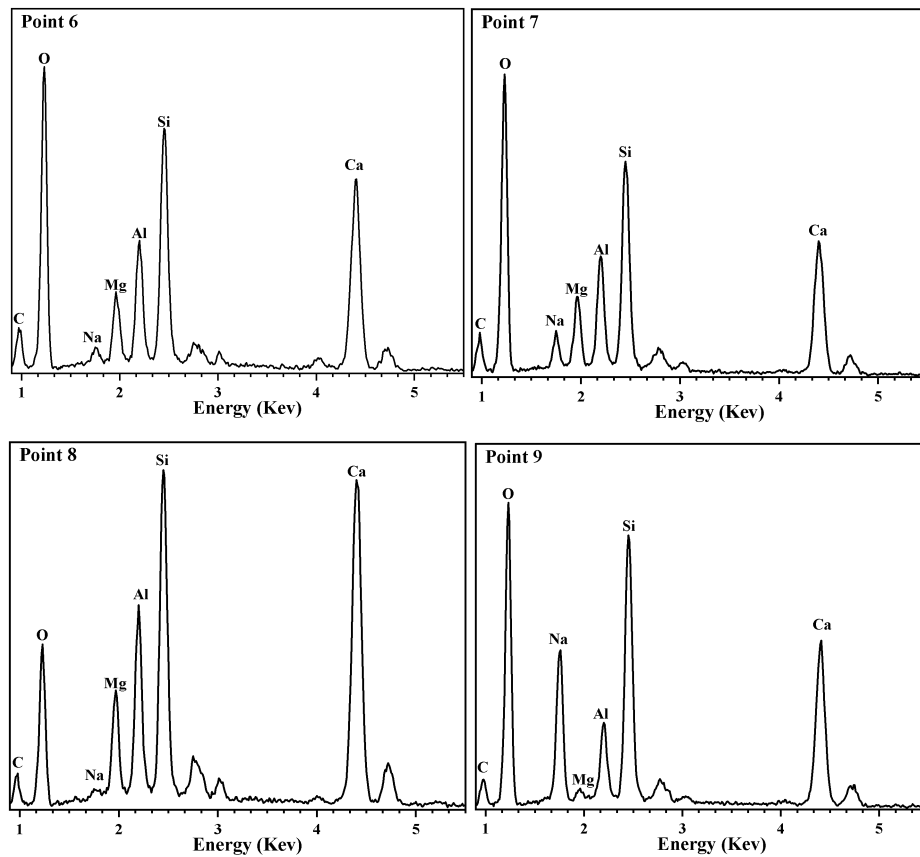


Figure 7- 12 Element distribution in the matrix of HAC mortar bars with different Na₂O content.

7.5 Conclusions

HACs demonstrated excellent durability properties in aggressive environments. The durability of HACs was influenced by many factors. This study investigated the effect of the dosage of alkali activator, leading to the following conclusions:

(1). The proportion of raw materials has a significant impact on the mechanical strength and durability of HAC materials. Reducing the proportion of OPC can notably enhance performance. Additionally, the dosage of alkali activator significantly affects the compressive strength of HAC, especially its long-term compressive strength. An appropriate Na₂O content (less than 5%) can increase early strength, but an excessive Na₂O content (more than 5%) can lead to a decrease in strength, with a more pronounced reduction in long-term strength. Therefore, in practical engineering design, it is crucial to comprehensively consider the proportion of OPC and the dosage of alkali activator to meet specific structural performance requirements.

(2) In an alkaline environment, HAC forms a dense gel phase and microstructure through the action of activators, resulting in low porosity and small

pore size distribution. This dense structure effectively blocks the penetration of chloride ions and the erosion of sulfates, thereby significantly enhancing the material's durability.

(3) During the hardening process, HAC generates the reaction product C-(A)-S-H. This product has excellent chemical durability and acts as a physical barrier, effectively preventing the penetration of chloride ions and sulfate erosion.

(4) The reaction products of HAC do not include the expansive product ettringite, which reduces the expansion caused by AAR. Additionally, HAC typically has a low alkali content, especially in low-calcium systems, which minimizes the presence of soluble alkali ions and thereby lowers the risk of reactions with reactive aggregates.

(5) The quantity of reaction products in HAC and the microstructure of these products are largely influenced by the dosage of the alkali activator. According to the analysis in Chapters 5 and 6, the quantity of reaction products initially increases and then decreases with increasing alkali content, and the microstructure follows the same trend. Selecting an appropriate dosage of the alkali activator is crucial for the durability of HAC materials and is a significant factor in determining their applicability in engineering projects.

CHAPTER 8: CONCLUSIONS AND RECOMMENDATIONS

8.1 Conclusions

The aim of this thesis was to explore the mechanical, setting and durability properties of hybrid alkaline cement based on ground blast furnace slag and ordinary Portland cement. The research works included understanding mechanical strength development of HAC, exploring the factors that affecting setting properties of HAC. After fully understood the factors affecting on mechanical and setting properties of HAC system, this study focused on exploring the influence of the ratio of OPC and the dosage of Na_2O on durability of HAC system, in order to provide a theoretical and experimental foundation for the engineering application of HAC.

This study revealed several key findings. First, it was discovered that HACs with a high proportion of supplementary cementitious materials and a low proportion of ordinary Portland cement can be successfully produced using an alkali activator. Second, the study found that the mechanical strength and setting time of HACs can be effectively controlled by adjusting the ratio of raw materials and selecting the appropriate type and dosage of alkali activators. Finally, it was observed that HACs exhibit excellent performance in aggressive environments.

In Chapter 5, the factors affecting the mechanical properties of HAC were investigated. A series of HACs were prepared with 10-30% OPC and supplementary cementitious materials (granulated blast furnace slag) using 0-8% alkali activator. The samples were then characterized using compressive strength, XRD, SEM, and ^1H NMR technology. The effects of the dosage of activator used, and the ration of raw materials on the mechanical properties of different HACs were studied. It was found that the HACs with high proportion of supplementary cementitious materials, cured at ambient temperature and activated by appropriate dosage of suitable alkali activator perform similar even higher compressive strength than an ordinary Portland Cement.

By increasing the proportion of supplementary cementitious materials and reducing the proportion of ordinary Portland cement, the amount of cement used can be decreased, thus lowering carbon dioxide emissions. Utilizing a higher proportion of supplementary cementitious materials, such as slag, can significantly enhance the long-term strength and durability of hybrid cements. Appropriate types and amounts of alkali activators can effectively activate the potential reactivity of the

supplementary cementitious materials, forming more gel during the hydration reaction and increasing the strength of the cement. Overall, by reasonably adjusting the cement proportion and selecting suitable alkali activators, the strength performance of hybrid cements can be optimized to meet the requirements of various engineering applications.

In Chapter 6, the factors affecting the setting properties of HAC systems were investigated. This study found that increasing the proportion of OPC raises the alkali content in the cement system, accelerating the hydration reaction and causing the hydration peak to appear earlier, thereby shortening the setting time. A higher OPC proportion also produces more hydration products, filling gaps between cement particles and speeding up the liquid-to-solid transition. Additionally, increasing the alkali activator dosage accelerates the transition of water in the cement paste to gel and capillary water, enhancing the chemical reaction rate and further shortening the setting time. However, an excessively high activator dosage (e.g., Na_2O over 5%) can lead to a significant generation of gel pore water during hardening, markedly shortening the setting time but potentially reducing the mechanical strength of the hardened material. Thus, by adjusting the OPC proportion and selecting an appropriate alkali activator dosage, the setting time of hybrid cement can be effectively controlled to meet various engineering application requirements.

Finally, chapter 7 investigated the effect of the ratio of OPC and dosage of alkali activator on durability properties of hybrid alkaline cement concrete. After understanding the mechanical and setting properties of HAC paste and mortars, durability of HAC concrete, which is of vital importance for its application in the construction industry, was investigated.

By reducing the proportion of OPC and increasing the proportion of supplementary cementitious materials, such as slag, the durability of hybrid cement can be enhanced. These supplementary materials can form more stable and denser hydration products under the action of alkali activators, thereby improving the cement's resistance to chemical erosion and long-term durability. While a higher OPC proportion can accelerate early strength growth, it may perform poorly in long-term durability due to OPC hydration products being more susceptible to attack by sulfates and other chemicals. An appropriate amount of alkali activator can effectively activate the supplementary cementitious materials, forming more gel and dense

structures, which improves the permeability resistance and chemical erosion resistance of hybrid cement, thus enhancing its durability. However, excessive use of alkali activators (e.g., Na_2O exceeding 5%) can lead to the rapid formation of a large amount of gel pore water, potentially creating many microcracks during the hardening process. These microcracks can reduce the overall density and durability of the material. In summary, by reasonably adjusting the proportion of OPC and selecting an appropriate amount of alkali activator, the durability of hybrid cement can be significantly improved to meet the needs of various engineering applications.

8.2 Cautions in the development and applications of HACs

This study successfully synthesised a series of ground blast furnace slag and ordinary Portland cement based HACs, which perform designable mechanical, setting and durability properties under laboratory conditions. In the study, two issues that need to be noted: fast initial setting of HAC paste and poor workability of HAC fresh concrete.

8.2.1 Fast initial setting of fresh HAC

Hybrid alkaline cement normally exhibits much shorter setting time than normal ordinary Portland cement, as discussed in Chapter 5. In this research, with the increasing dosage of alkali activator, the pH value in the reaction solution increases gradually, consequently, this accelerates the dissolution of GBFS in an alkaline solution, leading to an increased reaction rate. When the dosage of Na_2O content reaches 5%, the initial setting time of HAC decreases to 51 min, which is too short for pumping or casting. With the increasing dosage of the activator, both initial and final setting time decrease dramatically. The initial setting time of HAC decreases to 23 min, with Na_2O content reaches 8% of the binder, which is too fast to pump or cast.

Both the initial and final setting times of HAC systems present a decrease trend with the increasing of temperature. When the Na_2O content equals to 4%, HAC performs an initial setting time 67 mins at 20°C and 50 mins (shorter than 1 hour) at 35°C, which shows 25% decreases with the elevated temperature from 20°C to 35°C. With the increasing of dosage of alkali activator, the initial setting time of HAC systems decrease. Addition with the elevated temperature, HAC system performs too short setting time for pumping or casting at 35°C with Na_2O content more than 4%.

This means that HAC system with high dosage of alkali activator is not suitable for application in summer environments and high temperature prefabricated production workshop environments.

8.2.2 Workability of HAC fresh concrete

Hybrid alkaline cement normally suffers from poor workability with high viscosity, which makes it difficult to pump or cast. In section 6.2.2, during the preparation of HAC concrete specimens, it was found that the slump of newly mixed HAC concrete was very low, and it is necessary to use a vibration table to compact and shape the concrete sample. Through multiple experiments, it was found that increasing the water to binder ratio cannot improve this situation. Due to the need for studying the new binders and simulating wide application conditions of these cementitious materials, it is becoming important to exploit the fundamental parameters of a fresh concrete: rheology, both in science and technology aspects.

8.3 Recommendations for the future research

Based on the results of this study and the identified cautions related to HACs, there are at least four areas that require further in-depth research, as suggested in the following sections, in order to fully control the manufacturing of HAC and get prepared for its application, this study summarized the following as shown in figure 8-1.

8.3.1 Research on physics and chemistry of raw material

In the production of ordinary Portland cement, the raw material sources and thus the clinker phases are standard and stable. However, both the precursor aluminosilicate materials and alkali activators for HACs need to be able to be purchased over a relatively long period of time through a stable and reliable supply chain to provide the investment return required for establishing production facilities. The current challenge is that the raw materials of HAC are mainly waste or industrial by-products. It is challenging to ensure that these raw materials have a wide range of sources and stable on physics and chemistry. Alternatively, manufacturer must be technically prepared to use various sources of raw materials to produce composite yet stable precursor products.

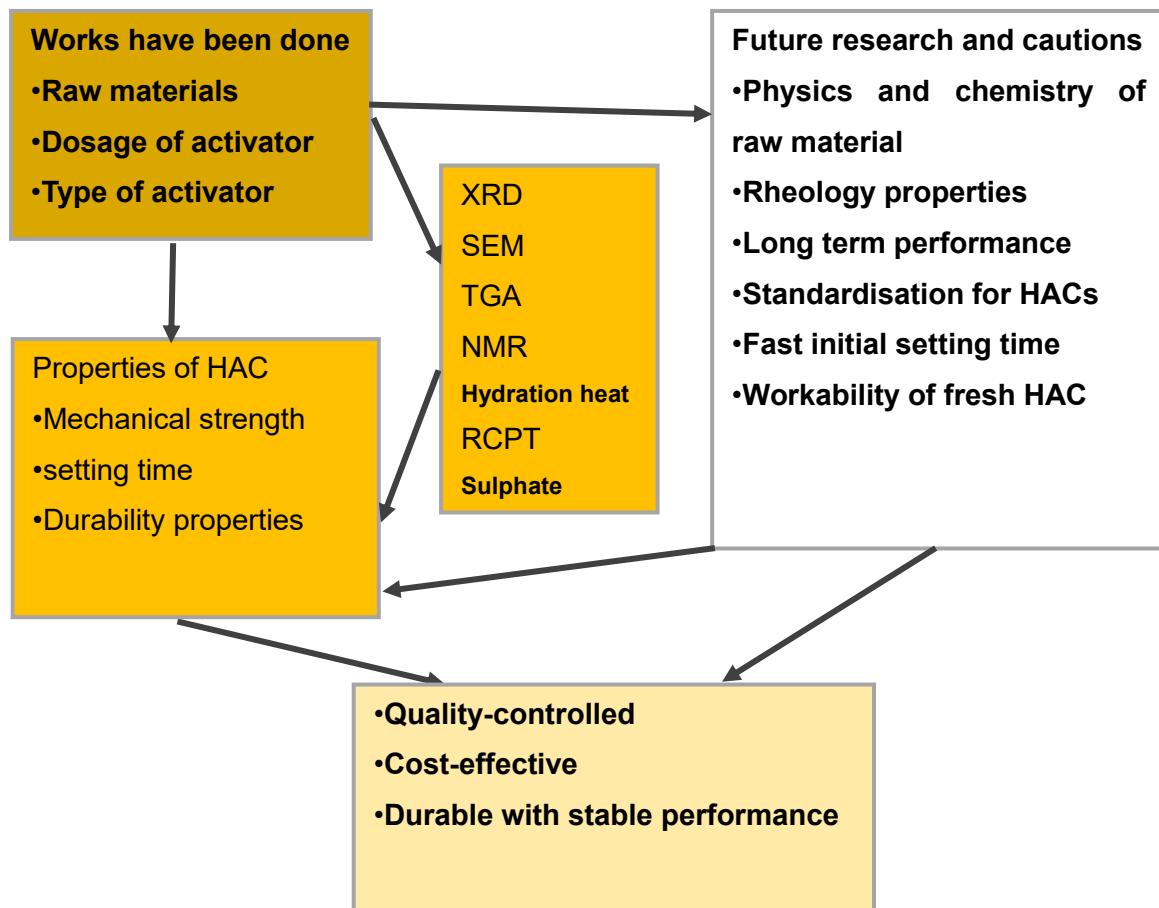


Figure 8- 1 Key Knowledge Concept Map.

8.3.2 Research on rheology properties of HACs

Most evaluations used in practice to qualify the workability of a fresh concrete are of empirical origins, e.g. the slump and slump flow tests. However, empirical tests only represent partial behaviours of a fresh concrete, e.g., the slump test only simulates the low-rate flow; understanding the fundamental parameters of fresh concrete is crucial, especially for higher-rate processes such as mixing and pumping. Due to the need for studying the new binders and simulating wide application conditions of these cementitious materials, it is becoming important to exploit the fundamental parameters of a fresh concrete: rheology, both in science and technology aspects. The rheological characteristics of OPC and AAMs pastes, mortars and concretes have been investigated in depth by a number of studies (Roussel and Coussot, 2005, Roussel et al., 2010, Roussel et al., 2012, Roussel and research, 2005, Roussel and Research, 2006, Alonso et al., 2017, Benavent et al., 2016, Kashani et al., 2015, Mehdizadeh et al., 2018, Palacios and Puertas, 2011, Puertas et al., 2018, Puertas et al., 2014, Shi et al., 2019a, Steins et

al., 2012, Yang et al., 2018). However, studies on the rheological properties of HAC is limited. It is of great importance for a better understanding of the behaviours of HAC-based cements and concretes in view of its potential engineering applications

8.3.3 Research on long term performance of HACs

At present, most methods for evaluating the durability of concrete are accelerated testing methods, which are mainly designed based on OPC materials and are not always applicable to alternative materials such as HACs and AAMs. For the durability testing of HACs and AAMs, researchers need to make reasonable adjustments and modifications to these accelerated testing methods based on material characteristics and practical applications. Another issue that needs to be considered is whether the real environment and structural size effects faced by materials in actual engineering can reflect the real situation in engineering, namely whether the experimental environment and small sample components can reflect the actual situation. This question requires buildings or building components to withstand long-term environmental erosion in the actual environment to achieve. There are also significant differences between small specimens used in the development process of new materials and large components or buildings constructed for practical engineering applications.

8.3.4 Research on standardisation for HACs

In the construction industry, without corresponding standards and certifications, new cement or concrete products will face significant obstacles in entering the market. The preparation of new cement standards is a very difficult process, as it requires the majority vested stakeholders in the standardization committee to reach a final consensus. The stakeholders involved in the assessment and understanding of HAC include producers, construction industry associations, governments, consumer agencies, academia, educational institutions, customers, and certification agencies. These groups or associations are concerned about whether new standards and regulations can ensure the quality and performance of building products, improve the safety of buildings, and be beneficial to environmental health. They are also concerned about whether new standards and regulations can enhance the competitiveness of their own groups. Once manufacturers can provide customers

with building materials with price advantages that meet the safety and durability requirements of buildings, as well as significant environmental advantages, various technical barriers can be easily eliminated.

REFERENCES

- A. PALOMO, A. F. N.-J. N., G. KOVALCHUK L, M. ORDON EZ M. C. NARANJO 2007. Opc-fly ash cementitious systems: study of gel binders produced during alkaline hydration. *Advances in Geopolymer Science & Technology*, 42, 2958–2966.
- ABDELRAHMAN, E. A. & SUBAIHI, A. 2020. Application of Geopolymers Modified with Chitosan as Novel Composites for Efficient Removal of Hg(II), Cd(II), and Pb(II) Ions from Aqueous Media. *Journal of Inorganic and Organometallic Polymers and Materials*, 30, 2440-2463.
- AL-KUTTI, W., NASIR, M., JOHARI, M. A. M., ISLAM, A. B. M. S., MANDA, A. A. & BLAISI, N. I. 2018. An overview and experimental study on hybrid binders containing date palm ash, fly ash, OPC and activator composites. *Construction and Building Materials*, 159, 567-577.
- AL-OTAIBI, S. 2008. Durability of concrete incorporating GGBS activated by water-glass. *Construction and building materials*, 22, 2059-2067.
- ALAHACHE, S., WINNEFELD, F., CHAMPENOIS, J.-B., HESSELBARTH, F. & LOTHENBACH, B. 2016a. Chemical activation of hybrid binders based on siliceous fly ash and Portland cement. *Cement & concrete composites*, 66, 10-23.
- ALAHACHE, S., WINNEFELD, F., CHAMPENOIS, J. B., HESSELBARTH, F. & LOTHENBACH, B. 2016b. Chemical activation of hybrid binders based on siliceous fly ash and Portland cement. *Cement & Concrete Composites*, 66, 10-23.
- ALARCON-RUIZ, L., PLATRET, G., MASSIEU, E. & EHRLACHER, A. 2005. The use of thermal analysis in assessing the effect of temperature on a cement paste. *Cement and concrete research*, 35, 609-613.
- ALEXANDER, M., BERTRON, A. & DE BELIE, N. 2013. *Performance of cement-based materials in aggressive aqueous environments*, Springer.
- ALONSO, M., GISMERA, S., BLANCO, M., LANZÓN, M., PUERTAS, F. J. C. & MATERIALS, B. 2017. Alkali-activated mortars: Workability and rheological behaviour. 145, 576-587.
- ANGULO-RAMIREZ, D. E., DE GUTIERREZ, R. M. & MEDEIROS, M. 2018. Alkali-activated Portland blast furnace slag cement mortars: Performance to alkali-aggregate reaction. *Construction and Building Materials*, 179, 49-56.
- ANGULO-RAMIREZ, D. E., DE GUTIERREZ, R. M. & PUERTAS, F. 2017. Alkali-activated Portland blast-furnace slag cement: Mechanical properties and hydration. *Construction and Building Materials*, 140, 119-128.
- ASKARIAN, M., TAO, Z., ADAM, G. & SAMALI, B. 2018. Mechanical properties of ambient cured one-part hybrid OPC-geopolymer concrete. *Construction and Building Materials*, 186, 330-337.
- ASTM, C. 2007. 1260 Standard test method for potential alkali reactivity of aggregates (mortar-bar method). *Section, 4*, 676-680.
- ASTM, C. 2012. Standard test method for electrical indication of concrete's ability to resist chloride ion penetration. *C1202–18*.
- BABAE, M. & CASTEL, A. 2016. Chloride-induced corrosion of reinforcement in low-calcium fly ash-based geopolymer concrete. *Cement and Concrete Research*, 88, 96-107.
- BAČUVČÍK, M., MARTAUZ, P. & JANOTKA, I. 2018. NTCC 2017: Long-Term Observation of the Resistance of Novel Hybrid Cement Exposed to Sulphate Solution. *Key Engineering Materials*, 761, 163-168.

- BALUN, B. & KARATAS, M. 2023. Factors Affecting the Setting Times of Pumice Based Alkali-Activated Hybrid Cements. *Iranian Journal of Science and Technology-Transactions of Civil Engineering*.
- BARBOZA-CHAVEZ, A. C., GOMEZ-ZAMORANO, L. Y. & ACEVEDO-DAVILA, J. L. 2020. Synthesis and Characterization of a Hybrid Cement Based on Fly Ash, Metakaolin and Portland Cement Clinker. *Materials*, 13.
- BARNETT, S., SOUTSOS, M., MILLARD, S. & BUNGEY, J. 2006. Strength development of mortars containing ground granulated blast-furnace slag: Effect of curing temperature and determination of apparent activation energies. *Cement and Concrete Research*, 36, 434-440.
- BENAVENT, V., STEINS, P., SOBRADOS, I., SANZ, J., LAMBERTIN, D., FRIZON, F., ROSSIGNOL, S., POULESQUEN, A. J. C. & RESEARCH, C. 2016. Impact of aluminum on the structure of geopolymers from the early stages to consolidated material. 90, 27-35.
- BERNAL, S. A., DE GUTIERREZ, R. M. & PROVIS, J. L. 2012. Engineering and durability properties of concretes based on alkali-activated granulated blast furnace slag/metakaolin blends. *Construction and Building Materials*, 33, 99-108.
- BEUSHAUSEN, H., ALEXANDER, M. & BALLIM, Y. 2012. Early-age properties, strength development and heat of hydration of concrete containing various South African slags at different replacement ratios. *Construction and Building Materials*, 29, 533-540.
- BIERNACKI, J. J., BULLARD, J. W., SANT, G., BANTHIA, N., BROWN, K., GLASSER, F. P., JONES, S., LEY, T., LIVINGSTON, R., NICOLEAU, L., OLEK, J., SANCHEZ, F., SHAHSAVARI, R., STUTZMAN, P. E., SOBOLEV, K. & PRATER, T. 2017. Cements in the 21(st) Century: Challenges, Perspectives, and Opportunities. *J Am Ceram Soc*, 100, 2746-2773.
- BIJEN, J. 1996. Benefits of slag and fly ash. *Construction and building materials*, 10, 309-314.
- CAO, Y., WANG, Y., ZHANG, Z., MA, Y. & WANG, H. 2021. Recent progress of utilization of activated kaolinitic clay in cementitious construction materials. *Composites Part B: Engineering*, 211, 108636.
- CHANG, J.-J. 2003. A study on the setting characteristics of sodium silicate-activated slag pastes. *Cement and Concrete Research*, 33, 1005-1011.
- CHEN, W. & BROUWERS, H. 2007. The hydration of slag, part 2: reaction models for blended cement. *Journal of Materials Science*, 42, 444-464.
- CHI, M. 2012. Effects of dosage of alkali-activated solution and curing conditions on the properties and durability of alkali-activated slag concrete. *Construction and Building Materials*, 35, 240-245.
- CONG, X., ZHOU, W., GENG, X. & ELCHALAKANI, M. 2019. Low field NMR relaxation as a probe to study the effect of activators and retarders on the alkali-activated GGBFS setting process. *Cement and Concrete Composites*, 104, 103399.
- CYR, M. & POUHET, R. 2015. Resistance to alkali-aggregate reaction (AAR) of alkali-activated cement-based binders. *Handbook of alkali-activated cements, mortars and concretes*. Elsevier.
- DONATELLO, S., FERNANDEZ-JIMENEZ, A. & PALOMO, A. 2013a. Very High Volume Fly Ash Cements. Early Age Hydration Study Using Na₂SO₄ as an Activator. *Journal of the American Ceramic Society*, 96, 900-906.

- DONATELLO, S., MALTSEVA, O., FERNANDEZ-JIMENEZ, A. & PALOMO, A. 2014. The Early Age Hydration Reactions of a Hybrid Cement Containing a Very High Content of Coal Bottom Ash. *Journal of the American Ceramic Society*, 97, 929-937.
- DONATELLO, S., PALOMO, A. & FERNANDEZ-JIMENEZ, A. 2013b. Durability of very high volume fly ash cement pastes and mortars in aggressive solutions. *Cement & Concrete Composites*, 38, 12-20.
- DU TOIT, G., KEARSLEY, E. P., MC DONALD, J. M., KRUGER, R. A. & VAN DER MERWE, E. M. 2018. Chemical and mechanical activation of hybrid fly ash cement. *Advances in Cement Research*, 30, 399-412.
- DURDZIŃSKI, P. T., HABA, M. B., ZAJAC, M. & SCRIVENER, K. L. 2017. Phase assemblage of composite cements. *Cement and Concrete Research*, 99, 172-182.
- ESCALANTE-GARCÍA, J., GOROKHOVSKY, A., MENDOZA, G. & FUENTES, A. 2003. Effect of geothermal waste on strength and microstructure of alkali-activated slag cement mortars. *Cement and concrete research*, 33, 1567-1574.
- ESCALANTE-GARCÍA, J. & SHARP, J. 2001. The microstructure and mechanical properties of blended cements hydrated at various temperatures. *Cement and Concrete Research*, 31, 695-702.
- ESCALANTE-GARCÍA, J. I. & SHARP, J. 2000. The effect of temperature on the early hydration of Portland cement and blended cements. *Advances in cement research*, 12, 121-130.
- FERNANDEZ-JIMENEZ, A., FLORES, E., MALTSEVA, O., GARCIA-LODEIRO, I. & PALOMO, A. 2013a. Hybrid Alkaline Cements. Part Iii. Durability and Industrial Applications. *Revista Romana De Materiale-Romanian Journal of Materials*, 43, 195-200.
- FERNANDEZ-JIMENEZ, A., FLORES, E., MALTSEVA, O., GARCIA-LODEIRO, I. & PALOMO, A. J. R. J. O. M. 2013b. Hybrid alkaline cements: Part III. Durability and Industrial Applications. 43, 68-73.
- FERNANDEZ-JIMENEZ, A., GARCIA-LODEIRO, I., MALTSEVA, O. & PALOMO, A. 2019. Hydration mechanisms of hybrid cements as a function of the way of addition of chemicals. *Journal of the American Ceramic Society*, 102, 427-436.
- FERNÁNDEZ-JIMÉNEZ, A., GARCÍA-LODEIRO, I. & PALOMO, A. 2007. Durability of alkali-activated fly ash cementitious materials. *Journal of materials science*, 42, 3055-3065.
- FERNÁNDEZ-JIMÉNEZ, A. & PALOMO, A. 2007. Factors affecting early compressive strength of alkali activated fly ash (OPC-free) concrete. *Materiales de Construcción*, 57, 7-22.
- FERNÁNDEZ-JIMÉNEZ, A. & PUERTAS, F. 2002. The alkali-silica reaction in alkali-activated granulated slag mortars with reactive aggregate. *Cement and concrete research*, 32, 1019-1024.
- FRIAS, M., DE LA VILLA, R. V., GARCIA, R., MARTINEZ-RAMIREZ, S. & FERNANDEZ-CARRASCO, L. 2018. New developments in low clinker cement paste mineralogy. *Applied Clay Science*, 166, 94-101.
- FU, J. Y., JONES, A. M., BLIGH, M. W., HOLT, C., KEYTE, L. M., MOGHADDAM, F., FOSTER, S. J. & WAITE, T. D. 2020. Mechanisms of enhancement in early hydration by sodium sulfate in a slag-cement blend - Insights from pore solution chemistry. *Cement and Concrete Research*, 135.
- GARCIA-LODEIRO, I., BOUDISSA, N., FERNANDEZ-JIMENEZ, A. & PALOMO, A. 2018a. Use of clays in alkaline hybrid cement preparation. The role of bentonites. *Materials Letters*, 233, 134-137.

- GARCIA-LODEIRO, I., CARCELEN-TABOADA, V., FERNANDEZ-JIMENEZ, A. & PALOMO, A. 2016a. Manufacture of hybrid cements with fly ash and bottom ash from a municipal solid waste incinerator. *Construction and Building Materials*, 105, 218-226.
- GARCIA-LODEIRO, I., DONATELLO, S., FERNANDEZ-JIMENEZ, A. & PALOMO, A. 2016b. Hydration of Hybrid Alkaline Cement Containing a Very Large Proportion of Fly Ash: A Descriptive Model. *Materials*, 9.
- GARCIA-LODEIRO, I., DONATELLO, S., FERNÁNDEZ-JIMÉNEZ, A. & PALOMO, Á. J. M. 2016c. Hydration of hybrid alkaline cement containing a very large proportion of fly ash: a descriptive model. 9, 605.
- GARCIA-LODEIRO, I., FERNANDEZ-JIMENEZ, A. & PALOMO, A. 2013a. Hydration kinetics in hybrid binders: Early reaction stages. *Cement & Concrete Composites*, 39, 82-92.
- GARCIA-LODEIRO, I., FERNANDEZ-JIMENEZ, A. & PALOMO, A. 2013b. Variation in hybrid cements over time. Alkaline activation of fly ash-portland cement blends. *Cement and Concrete Research*, 52, 112-122.
- GARCIA-LODEIRO, I., FERNANDEZ-JIMENEZ, A. & PALOMO, A. 2015. Cements with a low clinker content: versatile use of raw materials. *Journal of Sustainable Cement-Based Materials*, 4, 140-151.
- GARCIA-LODEIRO, I., FERNANDEZ-JIMENEZ, A. & PALOMO, A. 2018b. Hybrid Alkaline Cements: Bentonite-Opc Binders. *Minerals*, 8.
- GARCIA-LODEIRO, I., MALTSEVA, O., PALOMO, A. & FERNANDEZ-JIMENEZ, A. 2012. Hybrid Alkaline Cements. Part I: Fundamentals. *Revista Romana De Materiale-Romanian Journal of Materials*, 42, 330-335.
- GARCÍA-LODEIRO, I., MALTSEVA, O., PALOMO, Á. & FERNÁNDEZ-JIMÉNEZ, A. J. R. R. D. M. 2012. CIMENTURI HIBRIDE ALCALINE. PARTEA I: FUNDAMENTE*/HYBRID ALKALINE CEMENTS. PART I: FUNDAMENTALS. 42, 330.
- GARCIA-LODEIRO, I., PALOMO, A., FERNANDEZ-JIMENEZ, A. & MACPHEE, D. E. 2011. Compatibility studies between N-A-S-H and C-A-S-H gels. Study in the ternary diagram $\text{Na}_2\text{O}-\text{CaO}-\text{Al}_2\text{O}_3-\text{SiO}_2-\text{H}_2\text{O}$. *Cement and Concrete Research*, 41, 923-931.
- GARCIA-LODEIRO, I., TABOADA, V. C., FERNANDEZ-JIMENEZ, A. & PALOMO, A. 2017. Recycling Industrial By-Products in Hybrid Cements: Mechanical and Microstructure Characterization. *Waste and Biomass Valorization*, 8, 1433-1440.
- GEBREGZIABIHER, B. S., THOMAS, R. & PEETHAMPARAN, S. 2015. Very early-age reaction kinetics and microstructural development in alkali-activated slag. *Cement and concrete composites*, 55, 91-102.
- GIFFORD, P. & GILLOTT, J. 1996. Alkali-silica reaction (ASR) and alkali-carbonate reaction (ACR) in activated blast furnace slag cement (ABFSC) concrete. *Cement and concrete research*, 26, 21-26.
- HADJ-SADOK, A., KENAI, S., COURARD, L. & DARIMONT, A. 2011. Microstructure and durability of mortars modified with medium active blast furnace slag. *Construction and Building Materials*, 25, 1018-1025.
- HAHA, M. B., LE SAOUT, G., WINNEFELD, F. & LOTHENBACH, B. 2011. Influence of activator type on hydration kinetics, hydrate assemblage and microstructural development of alkali activated blast-furnace slags. *Cement and Concrete Research*, 41, 301-310.
- HLOBIL, M., ŠMILAUER, V. & CHANVILLARD, G. 2016. Micromechanical multiscale fracture model for compressive strength of blended cement pastes. *Cement and Concrete Research*, 83, 188-202.

- HOSHINO, S., YAMADA, K. & HIRAO, H. 2006. XRD/Rietveld analysis of the hydration and strength development of slag and limestone blended cement. *Journal of Advanced Concrete Technology*, 4, 357-367.
- JANOTKA, I., BAČUVČÍK, M., MARTAUZ, P. & STRIGÁČ, J. Chemical resistance of novel hybrid cement in various aggressive solutions. Proceed. RILEM international workshop on performance-based specification and control of concrete durability, 2014. 17-24.
- JI, Y., SUN, Z., JIANG, X., LIU, Y., SHUI, L. & CHEN, C. 2017. Fractal characterization on pore structure and analysis of fluidity and bleeding of fresh cement paste based on ¹H low-field NMR. *Construction and Building Materials*, 140, 445-453.
- JUENGER, M. C., SIDDIQUE, R. J. C. & RESEARCH, C. 2015. Recent advances in understanding the role of supplementary cementitious materials in concrete. 78, 71-80.
- KASHANI, A., PROVIS, J. L., VAN DEVENTER, B. B., QIAO, G. G. & VAN DEVENTER, J. S. J. R. A. 2015. Time-resolved yield stress measurement of evolving materials using a creeping sphere. 54, 365-376.
- KOCABA, V., GALLUCCI, E. & SCRIVENER, K. L. 2012. Methods for determination of degree of reaction of slag in blended cement pastes. *Cement and Concrete Research*, 42, 511-525.
- KONG, D. L. Y. & SANJAYAN, J. G. 2010. Effect of elevated temperatures on geopolymer paste, mortar and concrete. *Cement and Concrete Research*, 40, 334-339.
- KONIGSBERGER, M. & CARETTE, J. 2020. Validated hydration model for slag-blended cement based on calorimetry measurements. *Cement and Concrete Research*, 128.
- KRIVENKO, P., DROCHYTKA, R., GELEVERA, A. & KAVALEROVA, E. 2014. Mechanism of preventing the alkali–aggregate reaction in alkali activated cement concretes. *Cement and Concrete Composites*, 45, 157-165.
- LEE, N. K. & LEE, H. K. 2016. Influence of the slag content on the chloride and sulfuric acid resistances of alkali-activated fly ash/slag paste. *Cement & Concrete Composites*, 72, 168-179.
- LI, N., SHI, C. & ZHANG, Z. 2019. Understanding the roles of activators towards setting and hardening control of alkali-activated slag cement. *Composites Part B: Engineering*, 171, 34-45.
- LIU, Y. W., SHI, C. J., ZHANG, Z. H. & LI, N. 2019. An overview on the reuse of waste glasses in alkali-activated materials. *Resources Conservation and Recycling*, 144, 297-309.
- LOTENBACH, B., SCRIVENER, K. & HOOTON, R. 2011a. Supplementary cementitious materials. *Cement and concrete research*, 41, 1244-1256.
- LOTENBACH, B., SCRIVENER, K., HOOTON, R. J. C. & RESEARCH, C. 2011b. Supplementary cementitious materials. 41, 1244-1256.
- MACPHEE, D., ATKINS, M. & GLASSAR, P. 1988. Phase development and pore solution chemistry in ageing blast furnace slag-portland cement blends. *MRS Online Proceedings Library (OPL)*, 127.
- MCDONALD, P., KORB, J.-P., MITCHELL, J. & MONTEILHET, L. 2005. Surface relaxation and chemical exchange in hydrating cement pastes: a two-dimensional NMR relaxation study. *Physical Review E—Statistical, Nonlinear, and Soft Matter Physics*, 72, 011409.
- MEHDIZADEH, H., KANI, E. N. J. C. & MATERIALS, B. 2018. Rheology and apparent activation energy of alkali activated phosphorous slag. 171, 197-204.

- MEJIA, J. M., RODRIGUEZ, E., DE GUTIERREZ, R. M. & GALLEGO, N. 2015. Preparation and characterization of a hybrid alkaline binder based on a fly ash with no commercial value. *Journal of Cleaner Production*, 104, 346-352.
- MENÉNDEZ, G., BONAVETTI, V. & IRASSAR, E. 2003. Strength development of ternary blended cement with limestone filler and blast-furnace slag. *Cement and Concrete Composites*, 25, 61-67.
- MILLAN-CORRALES, G., GONZALEZ-LOPEZ, J. R., PALOMO, A. & FERNANDEZ-JIMENEZ, A. 2020. Replacing fly ash with limestone dust in hybrid cements. *Construction and Building Materials*, 243.
- MONTEIRO, P. J. M., MILLER, S. A. & HORVATH, A. 2017. Towards sustainable concrete. *Nature Materials*, 16, 698-699.
- MONTICELLI, C., NATALI, M., BALBO, A., CHIAVARI, C., ZANOTTO, F., MANZI, S. & BIGNOZZI, M. 2016a. A study on the corrosion of reinforcing bars in alkali-activated fly ash mortars under wet and dry exposures to chloride solutions. *Cement and Concrete Research*, 87, 53-63.
- MONTICELLI, C., NATALI, M. E., BALBO, A., CHIAVARI, C., ZANOTTO, F., MANZI, S. & BIGNOZZI, M. 2016b. Corrosion behavior of steel in alkali-activated fly ash mortars in the light of their microstructural, mechanical and chemical characterization. *Cement and Concrete Research*, 80, 60-68.
- MULLER, A. C., SCRIVENER, K. L., GAJEWICZ, A. M. & MCDONALD, P. J. 2013. Densification of C–S–H measured by ¹H NMR relaxometry. *The Journal of Physical Chemistry C*, 117, 403-412.
- NATH, P. & SARKER, P. K. 2015. Use of OPC to improve setting and early strength properties of low calcium fly ash geopolymer concrete cured at room temperature. *Cement and concrete composites*, 55, 205-214.
- PALACIOS, M., BANFILL, P. F. & PUERTAS, F. J. A. M. J. 2008. Rheology and setting of alkali-activated slag pastes and mortars: effect of organic admixture. 105, 140.
- PALACIOS, M. & PUERTAS, F. J. A. M. J. 2011. Effectiveness of Mixing Time on Hardened Properties of Waterglass-Activated Slag Pastes and Mortars. 108.
- PALOMO, A., FERNÁNDEZ-JIMÉNEZ, A., KOVALCHUK, G., ORDOÑEZ, L. & NARANJO, M. J. J. O. M. S. 2007. OPC-fly ash cementitious systems: study of gel binders produced during alkaline hydration. 42, 2958-2966.
- PALOMO, A., MALTSEVA, O., GARCIA-LODEIRO, I. & FERNANDEZ-JIMENEZ, A. 2013a. Hybrid Alkaline Cements. Part II: The Clinker Factor. *Revista Romana De Materiale-Romanian Journal of Materials*, 43, 74-80.
- PALOMO, A., MALTSEVA, O., GARCIA-LODEIRO, I. & FERNÁNDEZ-JIMÉNEZ, A. J. R. R. D. M. 2013b. Cimenturi hibride alcaline. Partea a II-a: factorul clincher*/hybrid alkaline cements. Part II: the clinker factor. 43, 74.
- PALOMO, A., MONTEIRO, P., MARTAUZ, P., BILEK, V. & FERNANDEZ-JIMENEZ, A. 2019. Hybrid binders: A journey from the past to a sustainable future (opus caementicium futurum). *Cement and Concrete Research*, 124.
- PALOU, M. T., KUZIELOVA, E., ZEMLIČKA, M., BOHAC, M. & NOVOTNY, R. 2016. The effect of curing temperature on the hydration of binary Portland cement. *Journal of Thermal Analysis and Calorimetry*, 125, 1301-1310.
- PANE, I. & HANSEN, W. 2005. Investigation of blended cement hydration by isothermal calorimetry and thermal analysis. *Cement and concrete research*, 35, 1155-1164.

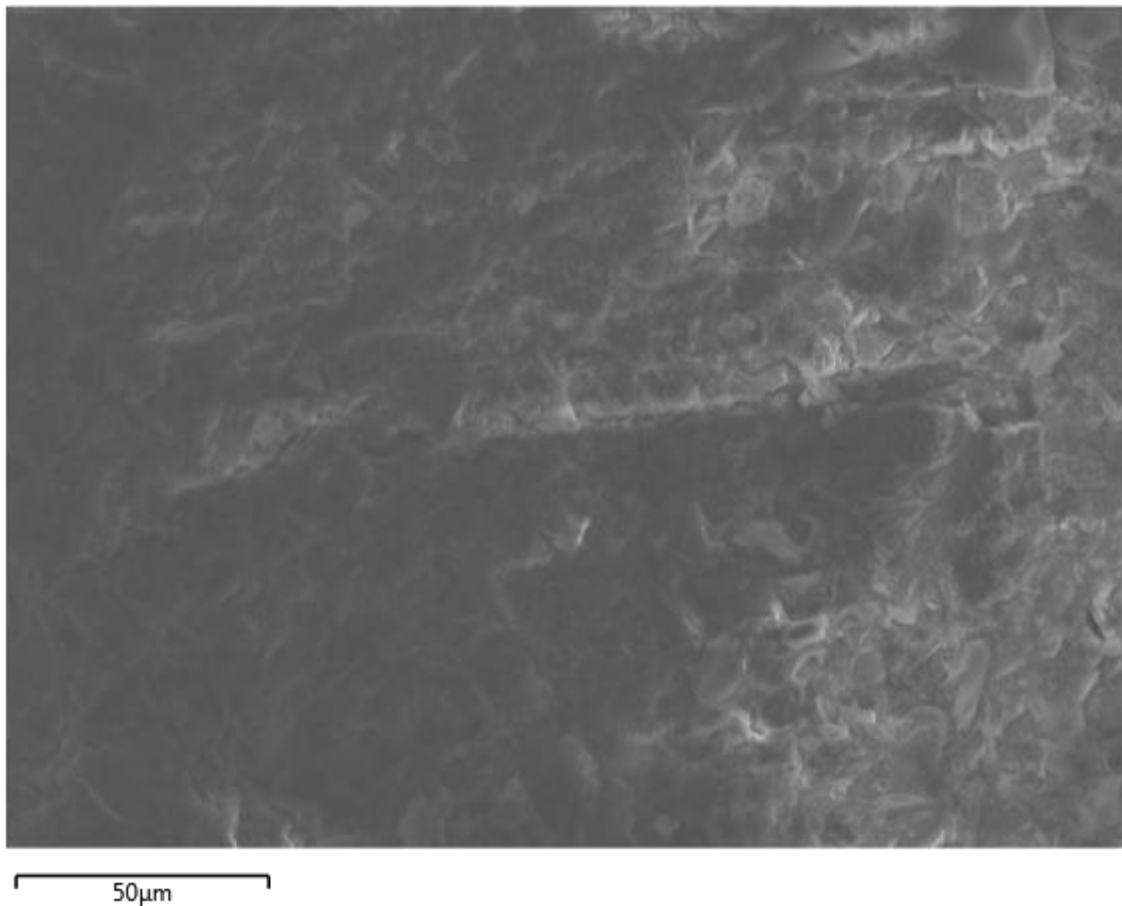
- PILEHVAR, S., SANFELIX, S. G., SZCZOTOK, A. M., RODRÍGUEZ, J. F., VALENTINI, L., LANZÓN, M., PAMIES, R. & KJØNIKEN, A.-L. 2020. Effect of temperature on geopolymer and Portland cement composites modified with Micro-encapsulated Phase Change materials. *Construction and Building Materials*, 252, 119055.
- PROVIS, J. L. & BERNAL, S. A. J. A. R. O. M. R. 2014. Geopolymers and related alkali-activated materials. 44, 299-327.
- PROVIS, J. L., PALOMO, A. & SHI, C. J. 2015a. Advances in understanding alkali-activated materials. *Cement and Concrete Research*, 78, 110-125.
- PROVIS, J. L., PALOMO, A., SHI, C. J. C. & RESEARCH, C. 2015b. Advances in understanding alkali-activated materials. 78, 110-125.
- PUERTAS, F., GONZÁLEZ-FONTEBOA, B., GONZÁLEZ-TABOADA, I., ALONSO, M., TORRES-CARRASCO, M., ROJO, G., MARTÍNEZ-ABELLA, F. J. C. & COMPOSITES, C. 2018. Alkali-activated slag concrete: Fresh and hardened behaviour. 85, 22-31.
- PUERTAS, F., VARGA, C., ALONSO, M. J. C. & COMPOSITES, C. 2014. Rheology of alkali-activated slag pastes. Effect of the nature and concentration of the activating solution. 53, 279-288.
- PUERTAS, F., VARGA, C., PALACIOS, M., PELLERIN, B., EYCHENNE-BARON, C., BABAYAN, D., BOUSTINGORRY, P. & ELKHADIRI, I. Alkali-activation of slag cements: Activation process, microstructure and mechanical properties. Proceedings of 13th International Congress on the Chemistry of Cement, 2011. 3-8.
- QIU, X., SASAKI, K., TAKAKI, Y., HIRAJIMA, T., IDETA, K. & MIYAWAKI, J. 2015. Mechanism of boron uptake by hydrocalumite calcined at different temperatures. *Journal of Hazardous Materials*, 287, 268-277.
- QU, B., JIMENEZ, A. F., PALOMO, A., MARTIN, A. & PASTOR, J. Y. 2020. Effect of high temperatures on the mechanical behaviour of hybrid cement. *Materiales De Construcción*, 70.
- QU, B., MARTIN, A., PASTOR, J. Y., PALOMO, A. & FERNANDEZ-JIMENEZ, A. 2016. Characterisation of pre-industrial hybrid cement and effect of pre-curing temperature. *Cement & Concrete Composites*, 73, 281-288.
- RICHARDSON, I. & GROVES, G. 1992. Microstructure and microanalysis of hardened cement pastes involving ground granulated blast-furnace slag. *Journal of materials science*, 27, 6204-6212.
- RIOS, A., GONZALEZ, M., MONTES, C., VASQUEZ, J. & ARELLANO, J. 2020. Assessing the effect of fly ash with a high SO₃ content in hybrid alkaline fly ash pastes (HAFAPs). *Construction and Building Materials*, 238.
- RIVERA, J. F., DE GUTIERREZ, R. M., MEJIA, J. M. & GORDILLO, M. 2014. Hybrid cement based on the alkali activation of by-products of coal. *Revista De La Construcción*, 13, 31-39.
- ROUSSEL, N. 2011. *Understanding the rheology of concrete*, Elsevier.
- ROUSSEL, N. & COUSSOT, P. J. J. O. R. 2005. "Fifty-cent rheometer" for yield stress measurements: from slump to spreading flow. 49, 705-718.
- ROUSSEL, N., LEMAÎTRE, A., FLATT, R. J., COUSSOT, P. J. C. & RESEARCH, C. 2010. Steady state flow of cement suspensions: A micromechanical state of the art. 40, 77-84.
- ROUSSEL, N., OVARLEZ, G., GARRAULT, S., BRUMAUD, C. J. C. & RESEARCH, C. 2012. The origins of thixotropy of fresh cement pastes. 42, 148-157.
- ROUSSEL, N. J. C. & RESEARCH, C. 2005. Steady and transient flow behaviour of fresh cement pastes. 35, 1656-1664.

- ROUSSEL, N. J. C. & RESEARCH, C. 2006. A thixotropy model for fresh fluid concretes: theory, validation and applications. 36, 1797-1806.
- ROY, D. Hydration, structure, and properties of blast furnace slag cements, mortars, and concrete. *Journal Proceedings*, 1982. 444-457.
- S. DONATELLO¹, I. G.-L., A. FERNANDEZ-JIMENEZ¹ AND A. PALOMO¹. 2014. Some durability aspects of hybrid alkaline cements. *EDP Sciences*, 11.
- SAMAD, S. & SHAH, A. J. I. J. O. S. B. E. 2017. Role of binary cement including Supplementary Cementitious Material (SCM), in production of environmentally sustainable concrete: A critical review. 6, 663-674.
- SAN NICOLAS, R., BERNAL, S. A., DE GUTIERREZ, R. M., VAN DEVENTER, J. S. J. & PROVIS, J. L. 2014. Distinctive microstructural features of aged sodium silicate-activated slag concretes. *Cement and Concrete Research*, 65, 41-51.
- SANCHEZ-HERRERO, M. J., FERNANDEZ-JIMENEZ, A. & PALOMO, A. 2019. Studies About the Hydration of Hybrid "Alkaline-Belite" Cement. *Frontiers in Materials*, 6.
- SEDIRA, N. & CASTRO-GOMES, J. 2020. Effect of activators on hybrid alkaline binder based on tungsten mining waste and ground granulated blast furnace slag. *Construction and Building Materials*, 232.
- SHI, C. 1988. Alkali-aggregate reaction of alkali-slag cements. *Concrete and Cement Products*, 4, 28-32.
- SHI, C., JIMÉNEZ, A. F., PALOMO, A. J. C. & RESEARCH, C. 2011a. New cements for the 21st century: The pursuit of an alternative to Portland cement. 41, 750-763.
- SHI, C., QU, B., PROVIS, J. L. J. C. & RESEARCH, C. 2019a. Recent progress in low-carbon binders. 122, 227-250.
- SHI, C., ROY, D. & KRIVENKO, P. 2003. *Alkali-activated cements and concretes*, CRC press.
- SHI, C., SHI, Z., HU, X., ZHAO, R. & CHONG, L. 2015a. A review on alkali-aggregate reactions in alkali-activated mortars/concretes made with alkali-reactive aggregates. *Materials and Structures*, 48, 621-628.
- SHI, C. J., JIMENEZ, A. F. & PALOMO, A. 2011b. New cements for the 21st century: The pursuit of an alternative to Portland cement. *Cement and Concrete Research*, 41, 750-763.
- SHI, C. J., QU, B. & PROVIS, J. L. 2019b. Recent progress in low-carbon binders. *Cement and Concrete Research*, 122, 227-250.
- SHI, C. J., SHI, Z. G., HU, X., ZHAO, R. & CHONG, L. L. 2015b. A review on alkali-aggregate reactions in alkali-activated mortars/concretes made with alkali-reactive aggregates. *Materials and Structures*, 48, 621-628.
- SHI, Z., SHI, C., ZHAO, R. & WAN, S. 2015c. Comparison of alkali-silica reactions in alkali-activated slag and Portland cement mortars. *Materials and structures*, 48, 743-751.
- SKIBSTED, J. & SNELLINGS, R. 2019. Reactivity of supplementary cementitious materials (SCMs) in cement blends. *Cement and Concrete Research*, 124.
- STEINS, P., POULESQUEN, A., DIAT, O. & FRIZON, F. J. L. 2012. Structural evolution during geopolymerization from an early age to consolidated material. 28, 8502-8510.
- SUWAN, T., FAN, M. J. C. & MATERIALS, B. 2014. Influence of OPC replacement and manufacturing procedures on the properties of self-cured geopolymer. 73, 551-561.
- TAYLOR, R., RICHARDSON, I. & BRYDSON, R. 2010. Composition and microstructure of 20-year-old ordinary Portland cement-ground granulated blast-furnace slag blends containing 0 to 100% slag. *Cement and Concrete Research*, 40, 971-983.

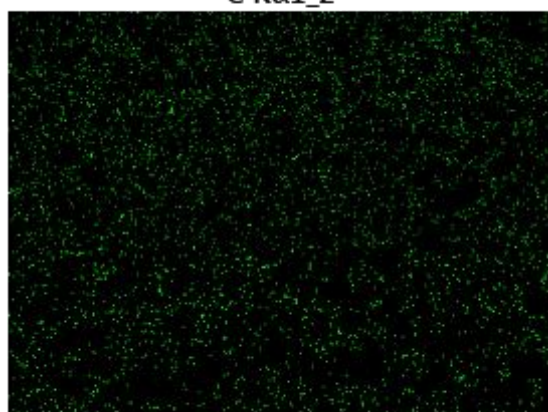
- TENNAKOON, C., SHAYAN, A., SANJAYAN, J. G. & XU, A. 2017. Chloride ingress and steel corrosion in geopolymer concrete based on long term tests. *Materials & design*, 116, 287-299.
- TESTING, A. S. F. & MATERIALS 2014. Standard Test Method for Potential Alkali Reactivity of Aggregates (Mortar-Bar Method), ASTM C1260-14.
- TONIOLO, N., RINCON, A., ROETHER, J. A., ERCOLE, P., BERNARDO, E. & BOCCACCINI, A. R. 2018. Extensive reuse of soda-lime waste glass in fly ash-based geopolymers. *Construction and Building Materials*, 188, 1077-1084.
- TORRES-CARRASCO, M., TOGNONVI, M. T., TAGNIT-HAMOU, A. & PUERTAS, F. 2015. Durability of Alkali-Activated Slag Concretes Prepared Using Waste Glass as Alternative Activator. *Aci Materials Journal*, 112, 791-800.
- VINAI, R. & SOUTSOS, M. 2019. Production of sodium silicate powder from waste glass cullet for alkali activation of alternative binders. *Cement and Concrete Research*, 116, 45-56.
- WALKLEY, B., SAN NICOLAS, R., SANI, M.-A., BERNAL, S. A., VAN DEVENTER, J. S. J. & PROVIS, J. L. 2017. Structural evolution of synthetic alkali-activated CaO-MgO-Na₂O-Al₂O₃-SiO₂ materials is influenced by Mg content. *Cement and concrete research*, 99, 155-171.
- WANG, Y., CAO, Y., ZHANG, P., MA, Y., ZHAO, T., WANG, H. & ZHANG, Z. 2019. Water absorption and chloride diffusivity of concrete under the coupling effect of uniaxial compressive load and freeze–thaw cycles. *Construction and building Materials*, 209, 566-576.
- WHITTAKER, M., ZAJAC, M., HAHA, M. B., BULLERJAHN, F. & BLACK, L. 2014. The role of the alumina content of slag, plus the presence of additional sulfate on the hydration and microstructure of Portland cement-slag blends. *Cement and Concrete Research*, 66, 91-101.
- XUE, L., ZHANG, Z., WALKLEY, B., LIU, H., JIANG, Y. & WANG, H. 2023. Retarding effect of gypsum for hybrid alkali-activated cements (HAACs) at ambient temperature. *Materials Today Communications*, 35, 106182.
- XUE, L., ZHANG, Z. & WANG, H. 2021a. Early hydration kinetics and microstructure development of hybrid alkali activated cements (HAACs) at room temperature. *Cement and Concrete Composites*, 123, 104200.
- XUE, L. L., ZHANG, Z. H. & WANG, H. 2021b. Hydration mechanisms and durability of hybrid alkaline cements (HACs): A review. *Construction and Building Materials*, 266.
- YANG, C., PU, X. & WU, F. 1999. Research on alkali aggregate reaction expansion of alkali-slag mortar. *J*, 1304, 651-657.
- YANG, K.-H., CHO, A.-R., SONG, J.-K. & NAM, S.-H. 2012. Hydration products and strength development of calcium hydroxide-based alkali-activated slag mortars. *Construction and Building Materials*, 29, 410-419.
- YANG, T., GAO, X., ZHANG, J. J., ZHUANG, X. M., WANG, H. & ZHANG, Z. H. 2022. Sulphate resistance of one-part geopolymer synthesized by calcium carbide residue-sodium carbonate-activation of slag. *Composites Part B-Engineering*, 242.
- YANG, T., ZHU, H., ZHANG, Z., GAO, X., ZHANG, C., WU, Q. J. C. & RESEARCH, C. 2018. Effect of fly ash microsphere on the rheology and microstructure of alkali-activated fly ash/slag pastes. 109, 198-207.

- YOU-ZHI, C., XIN-CHENG, P., CHANG-HUI, Y. & QING-JUN, D. 2002. Alkali aggregate reaction in alkali slag cement mortars. *Journal of Wuhan University of Technology-Mater. Sci. Ed.*, 17, 60-62.
- ZHANG, J., SHI, C. J., ZHANG, Z. H. & OU, Z. H. 2017. Durability of alkali-activated materials in aggressive environments: A review on recent studies. *Construction and Building Materials*, 152, 598-613.
- ZHANG, Z. H., PROVIS, J. L., REID, A. & WANG, H. 2014. Geopolymer foam concrete: An emerging material for sustainable construction. *Construction and Building Materials*, 56, 113-127.

APPENDIX A ELEMENTAL DISTRIBUTION MAPPING OF HAC MORTAR BARS IN NaOH AT 80°C FOR 14 DAYS

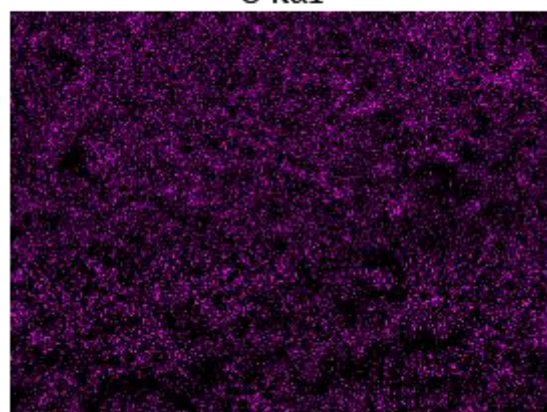


C K α 1_2



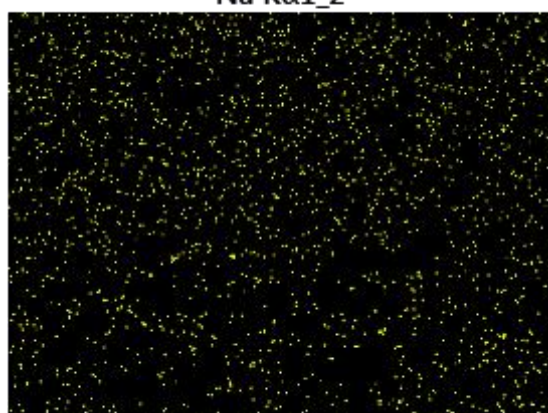
50 μ m

O K α 1



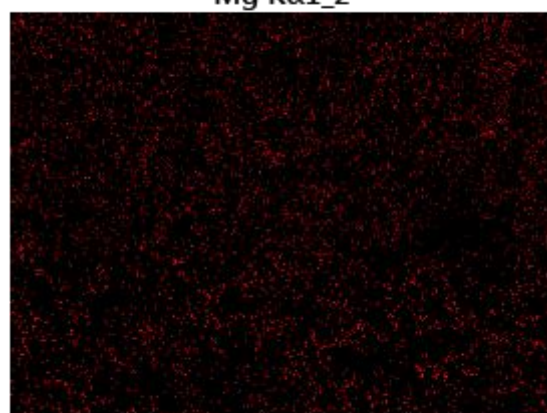
50 μ m

Na K α 1_2



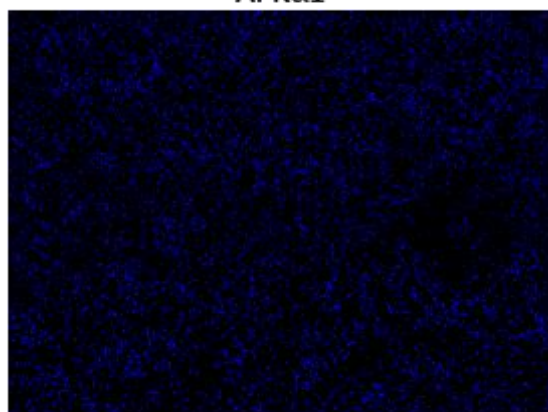
50 μ m

Mg K α 1_2



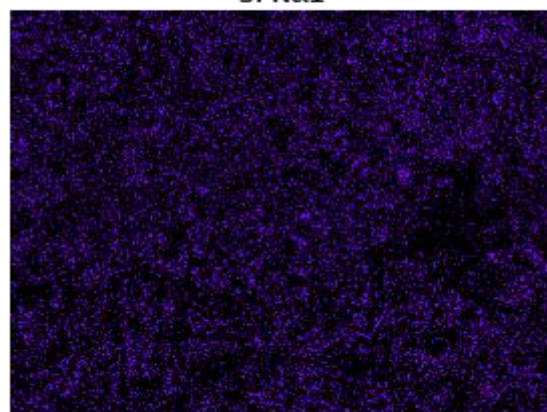
50 μ m

Al K α 1



50 μ m

Si K α 1



50 μ m

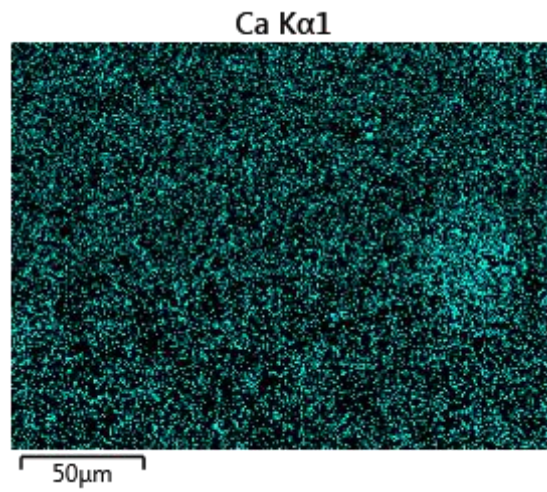
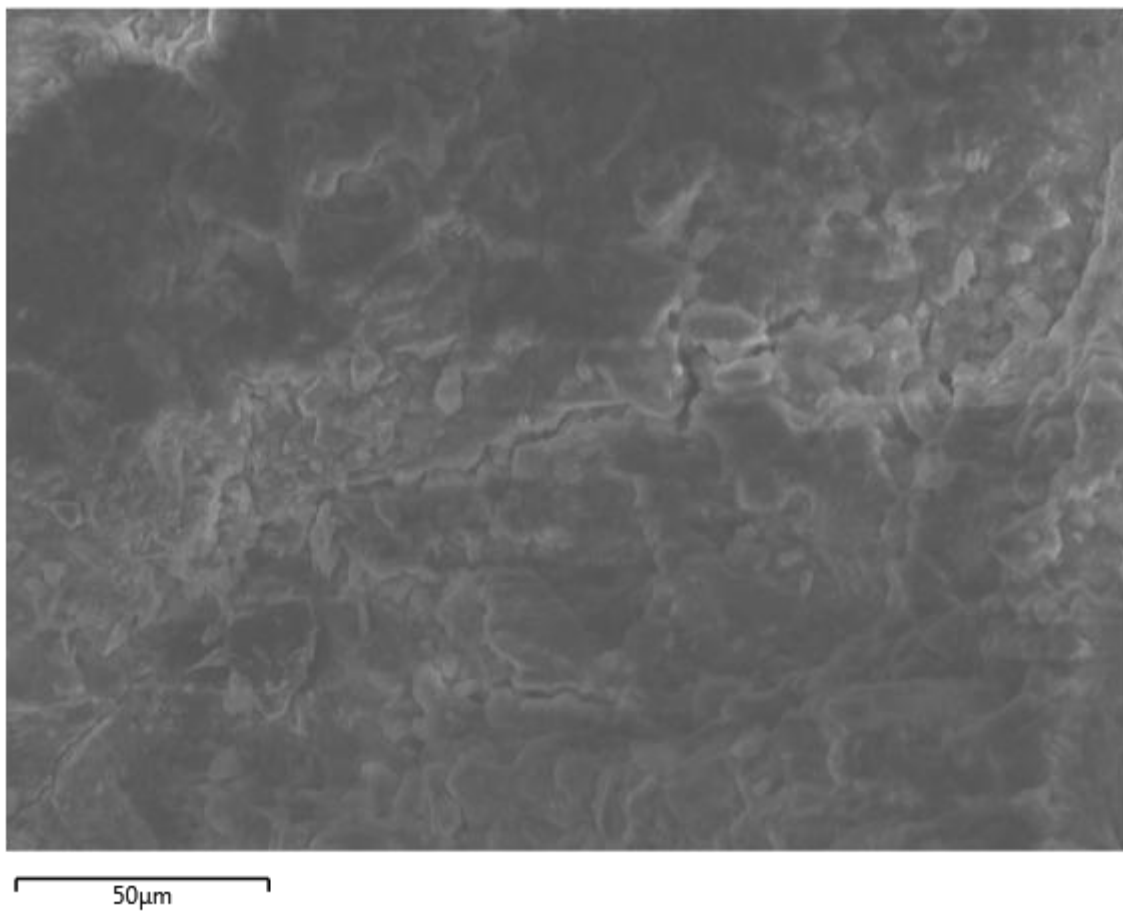
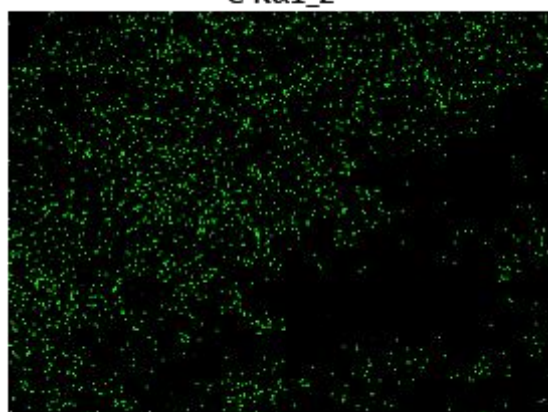


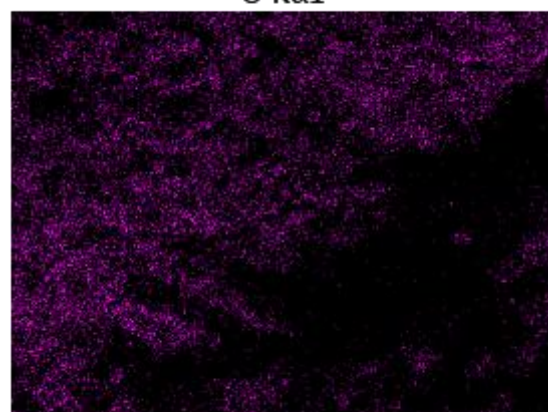
Figure A- 1 Elemental distribution mapping of HAC mortar bars with 0% Na₂O content.



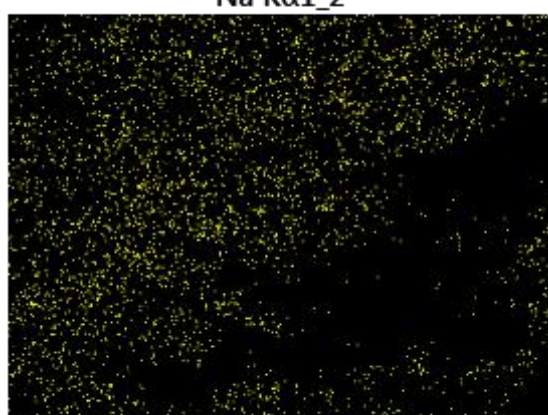
C K α 1_2



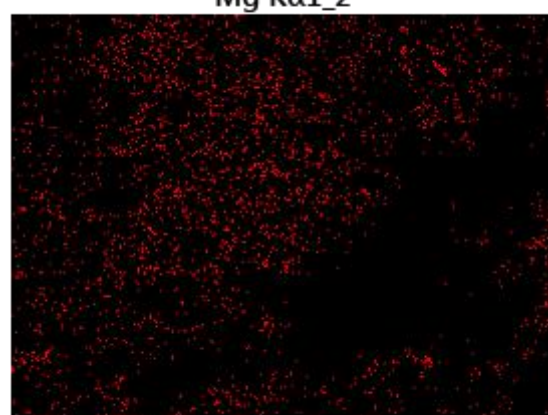
O K α 1



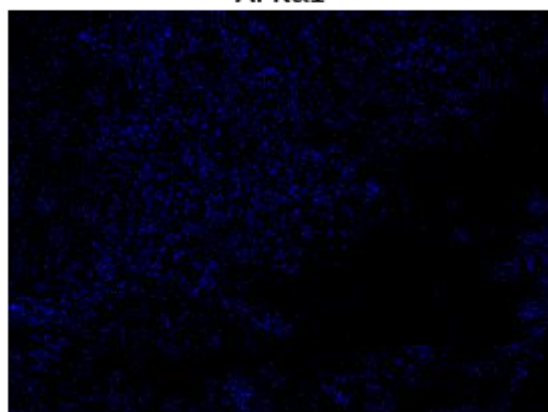
Na K α 1_2



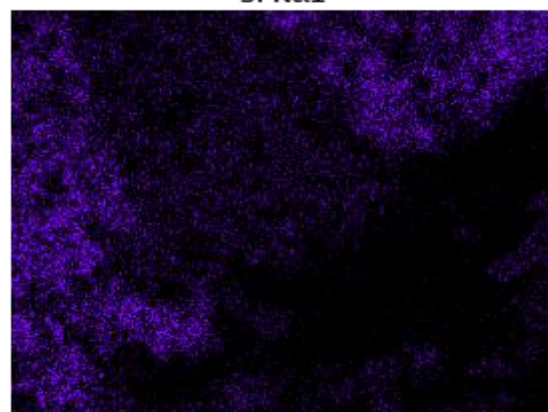
Mg K α 1_2



Al K α 1



Si K α 1



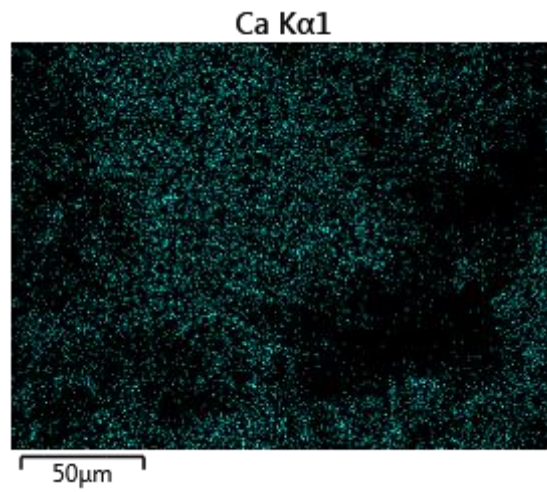
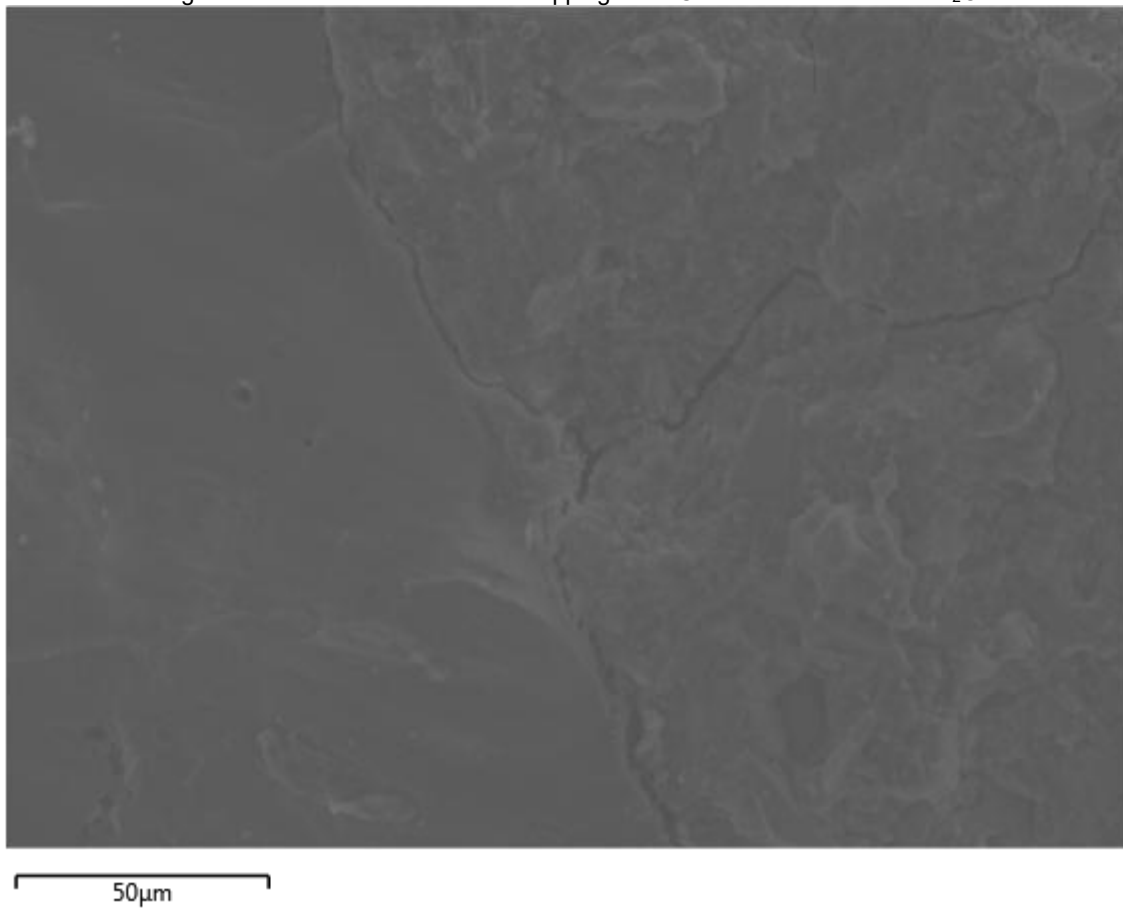
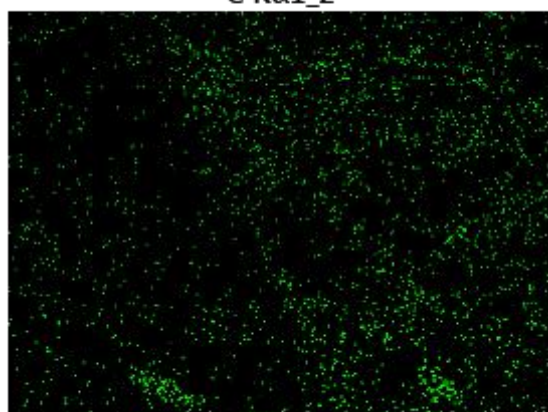


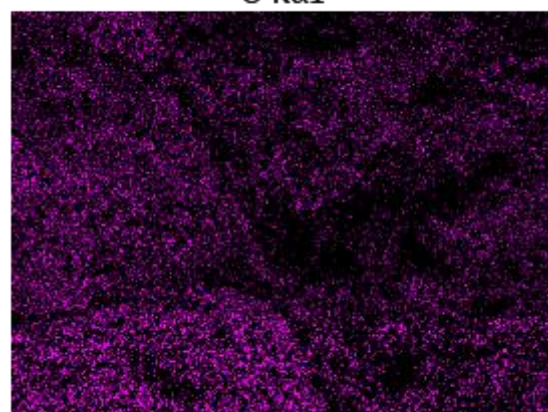
Figure A- 2 Elemental distribution mapping of HAC mortar bars with 2% Na₂O content.



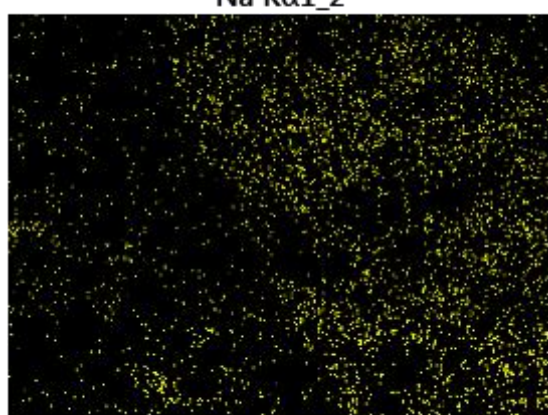
C K α 1_2



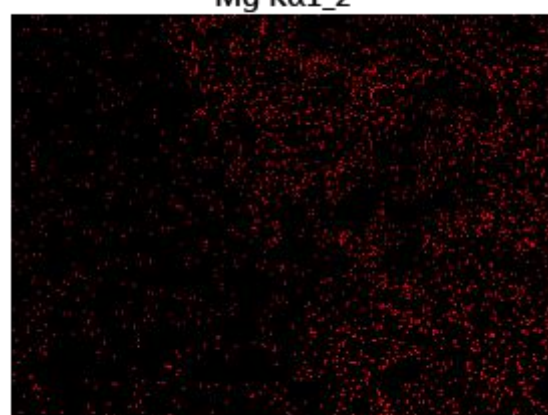
O K α 1



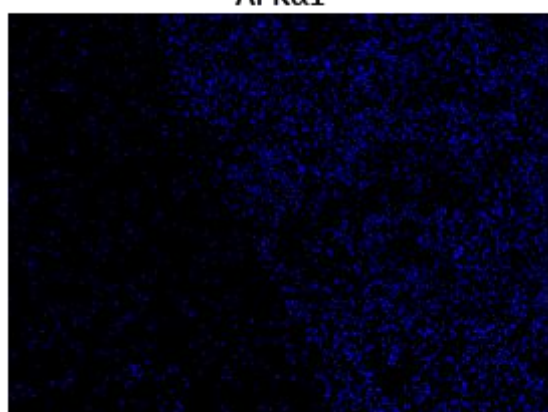
Na K α 1_2



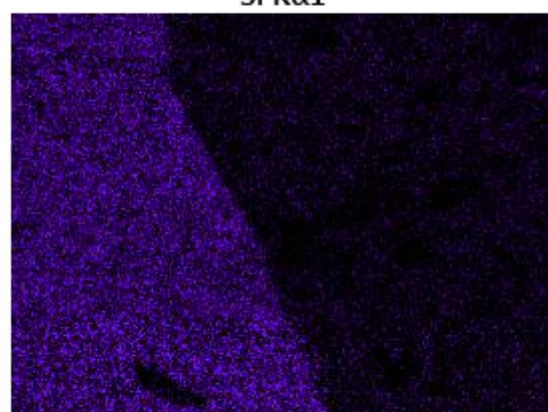
Mg K α 1_2



Al K α 1



Si K α 1



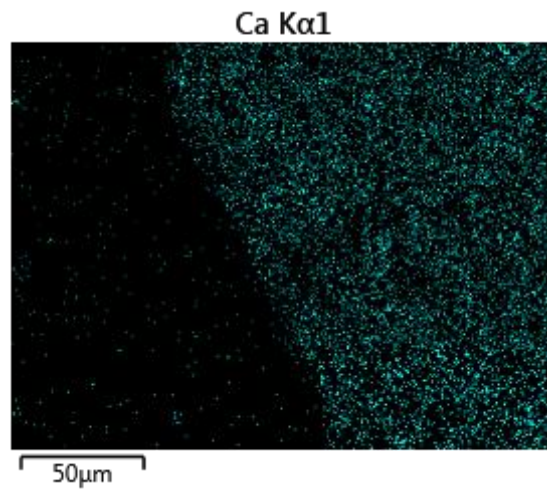
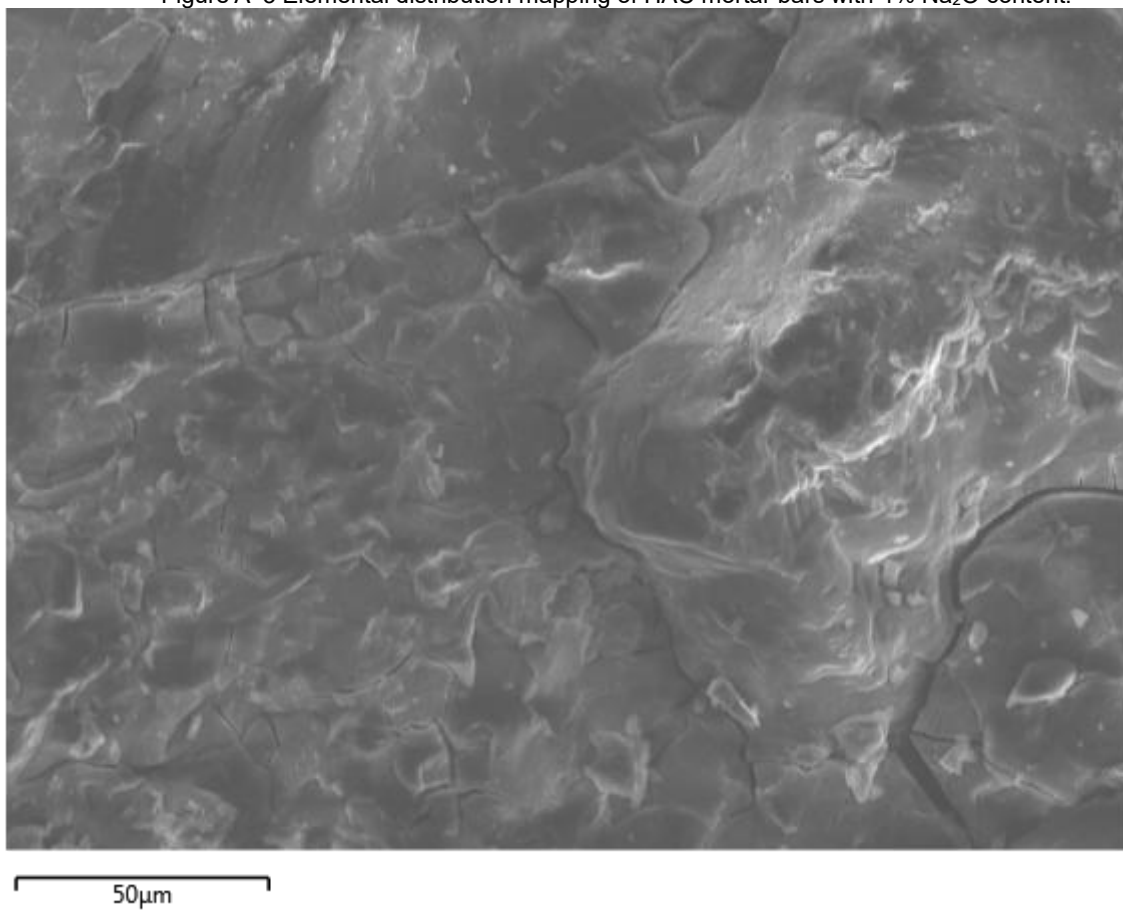
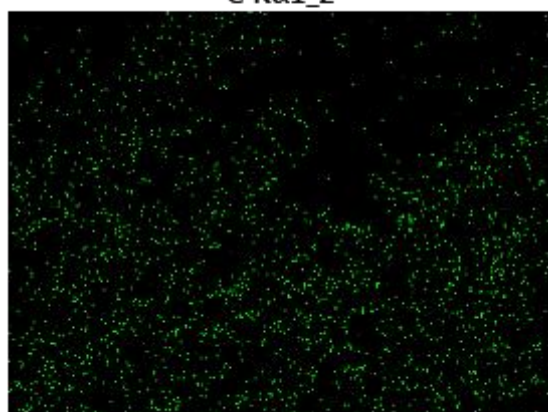


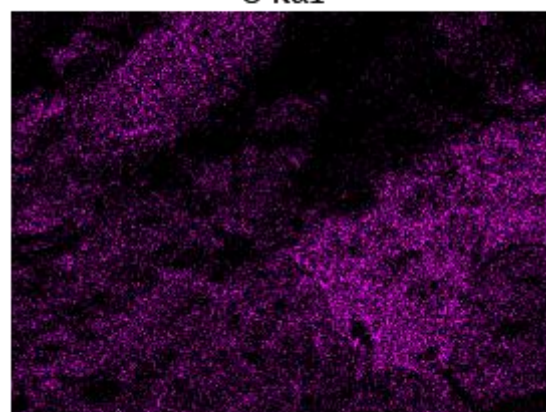
Figure A-3 Elemental distribution mapping of HAC mortar bars with 4% Na₂O content.



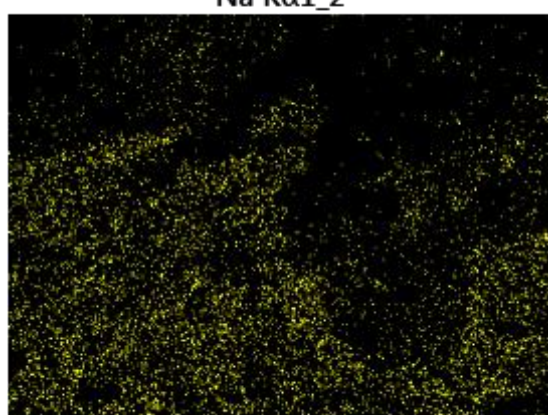
C K α 1_2



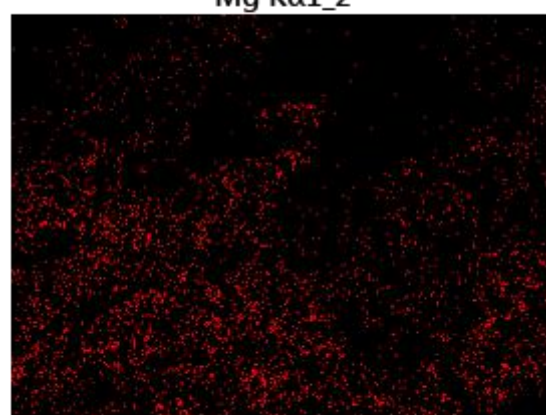
O K α 1



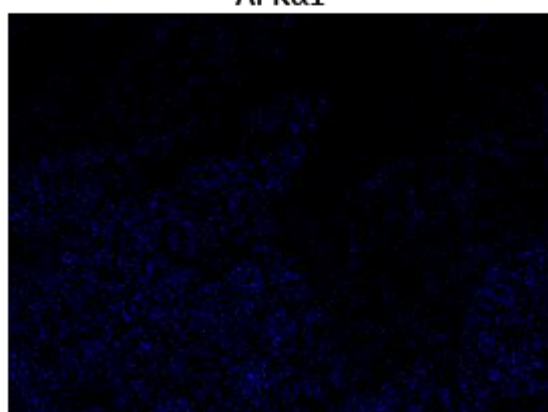
Na K α 1_2



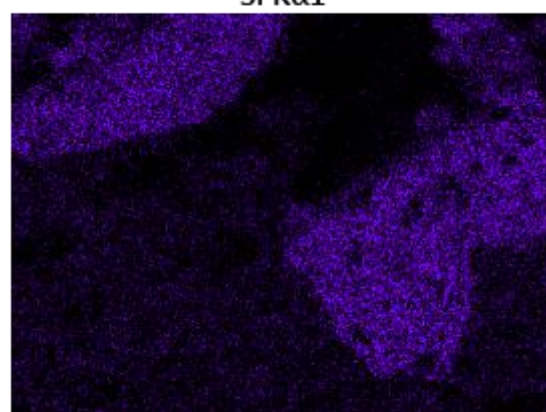
Mg K α 1_2



Al K α 1



Si K α 1



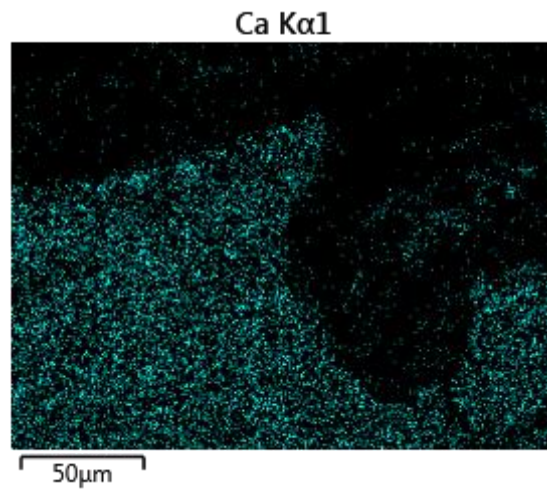
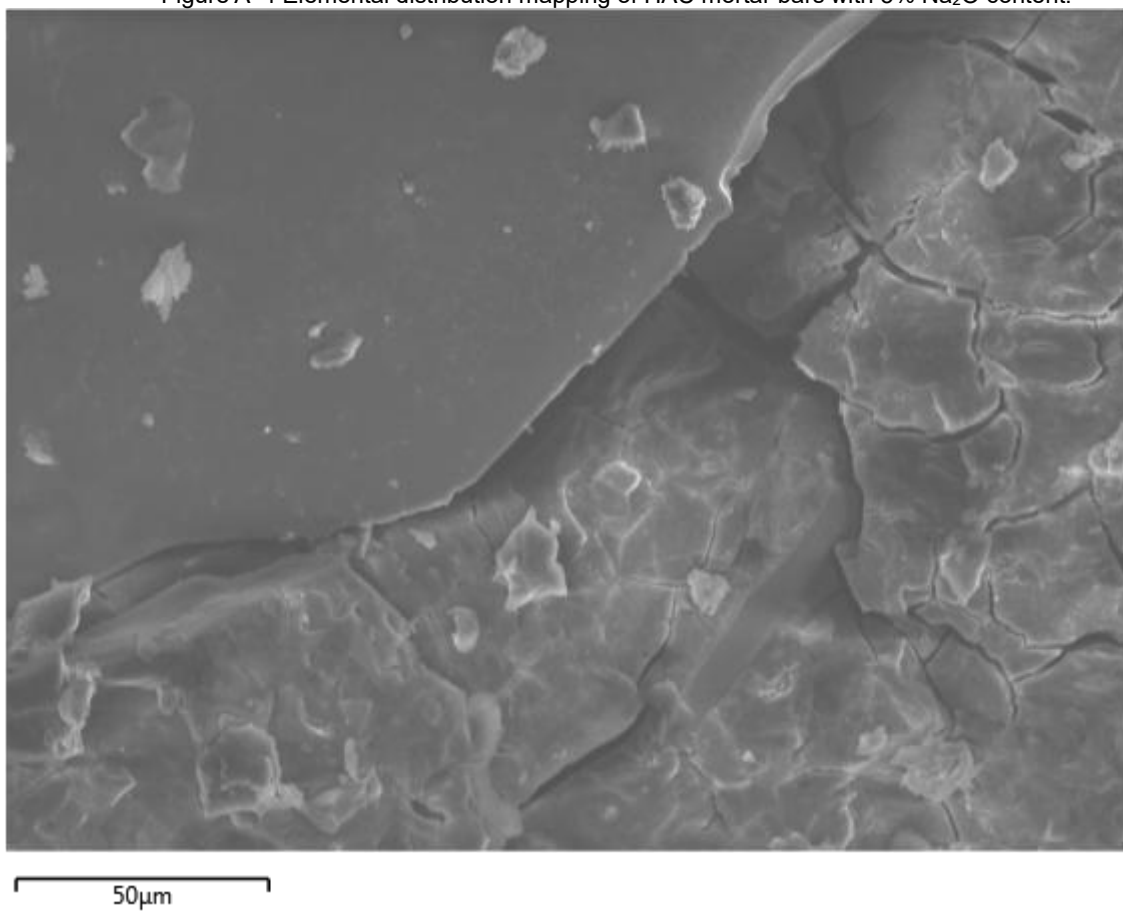
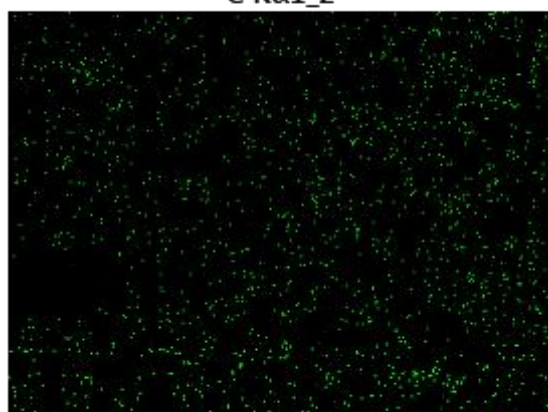


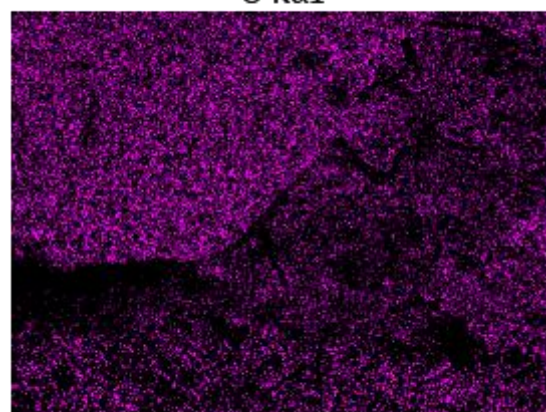
Figure A-4 Elemental distribution mapping of HAC mortar bars with 5% Na₂O content.



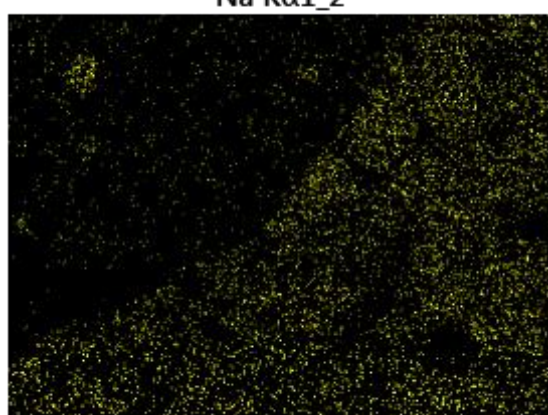
C K α 1_2



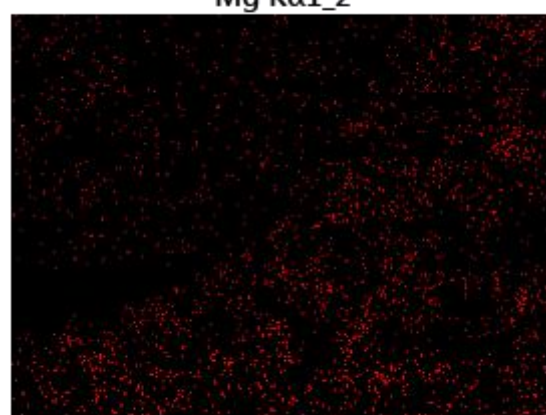
O K α 1



Na K α 1_2



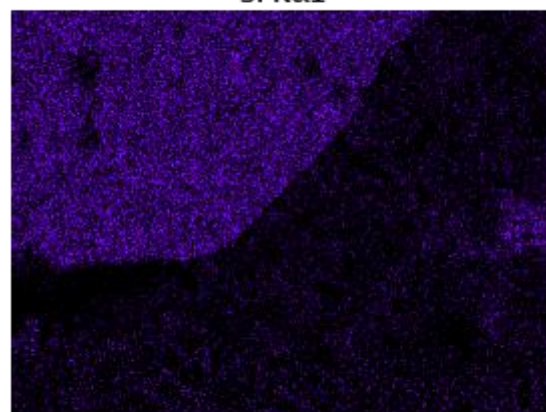
Mg K α 1_2



Al K α 1



Si K α 1



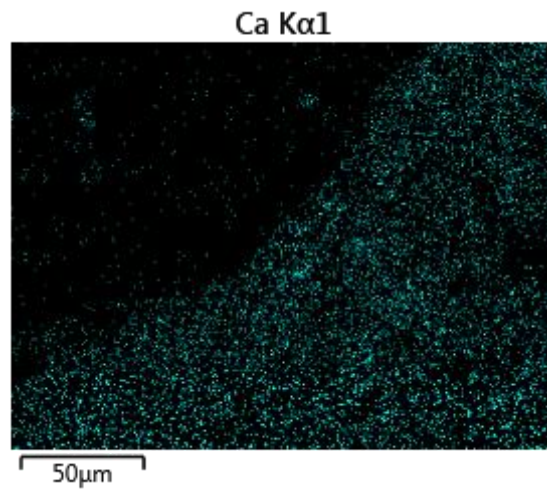
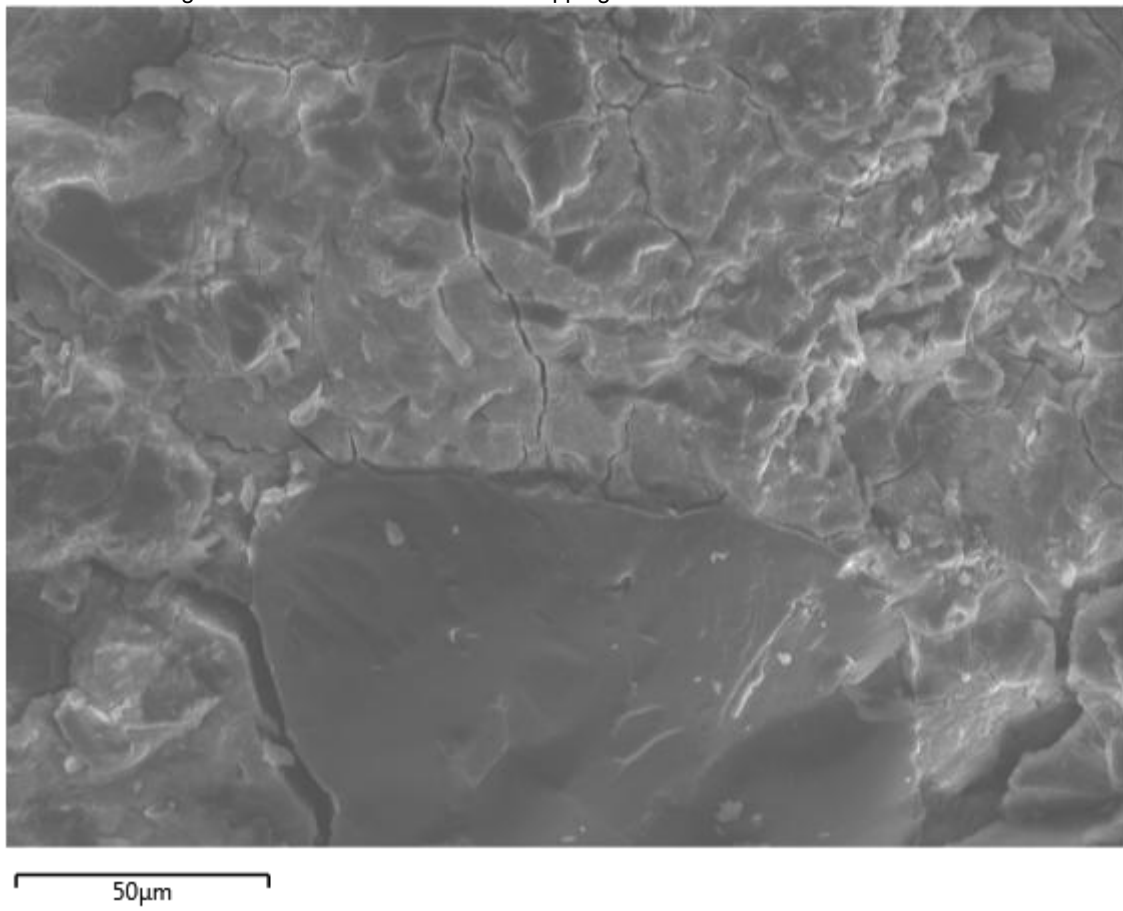
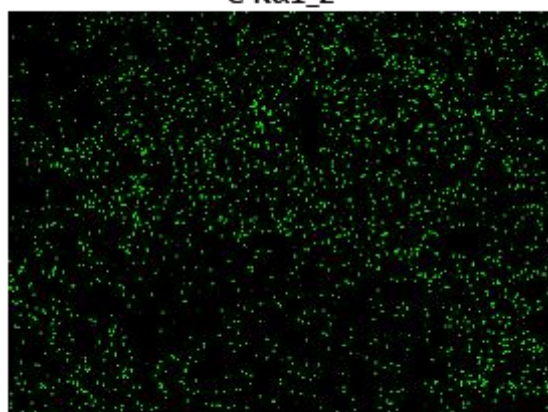


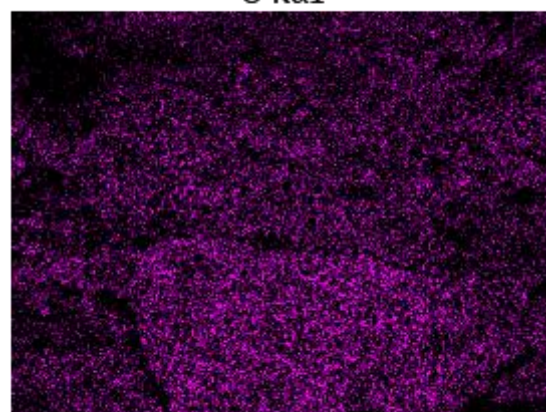
Figure A-5 Elemental distribution mapping of HAC mortar bars with 8% Na₂O content.



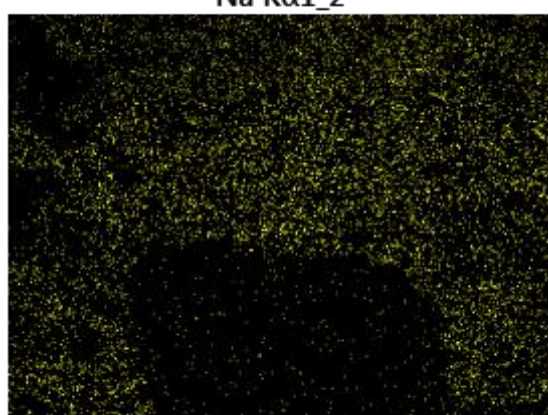
C K α 1_2



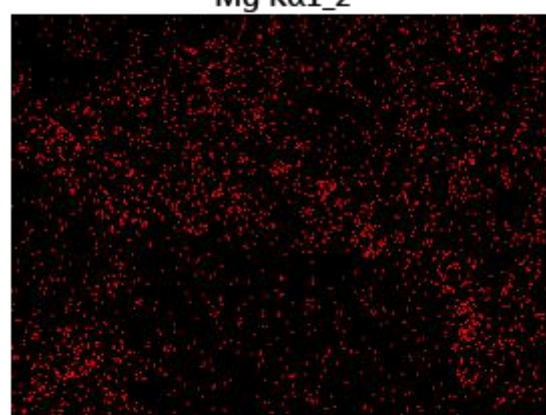
O K α 1



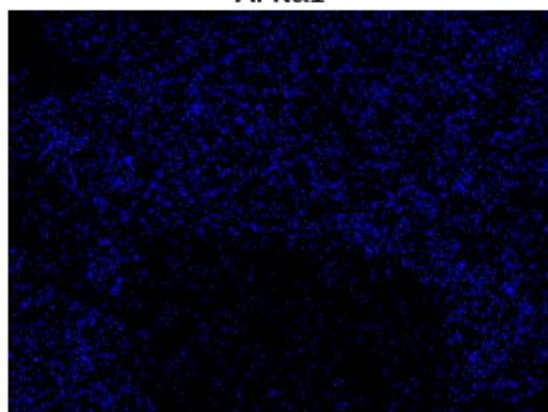
Na K α 1_2



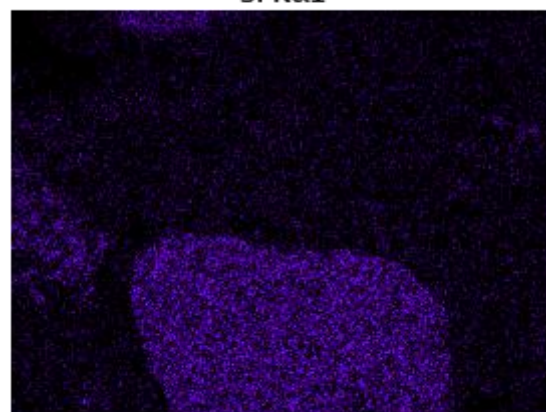
Mg K α 1_2



Al K α 1



Si K α 1



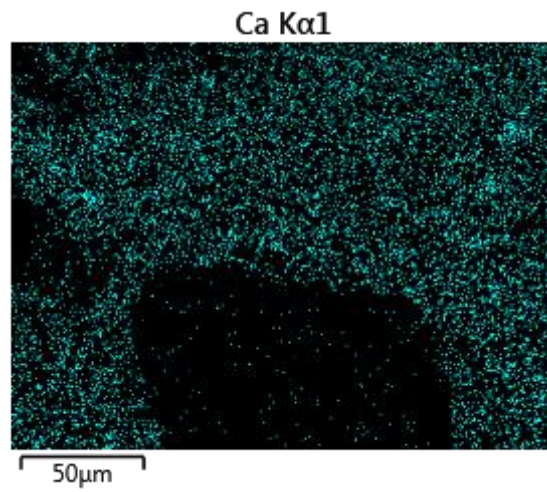
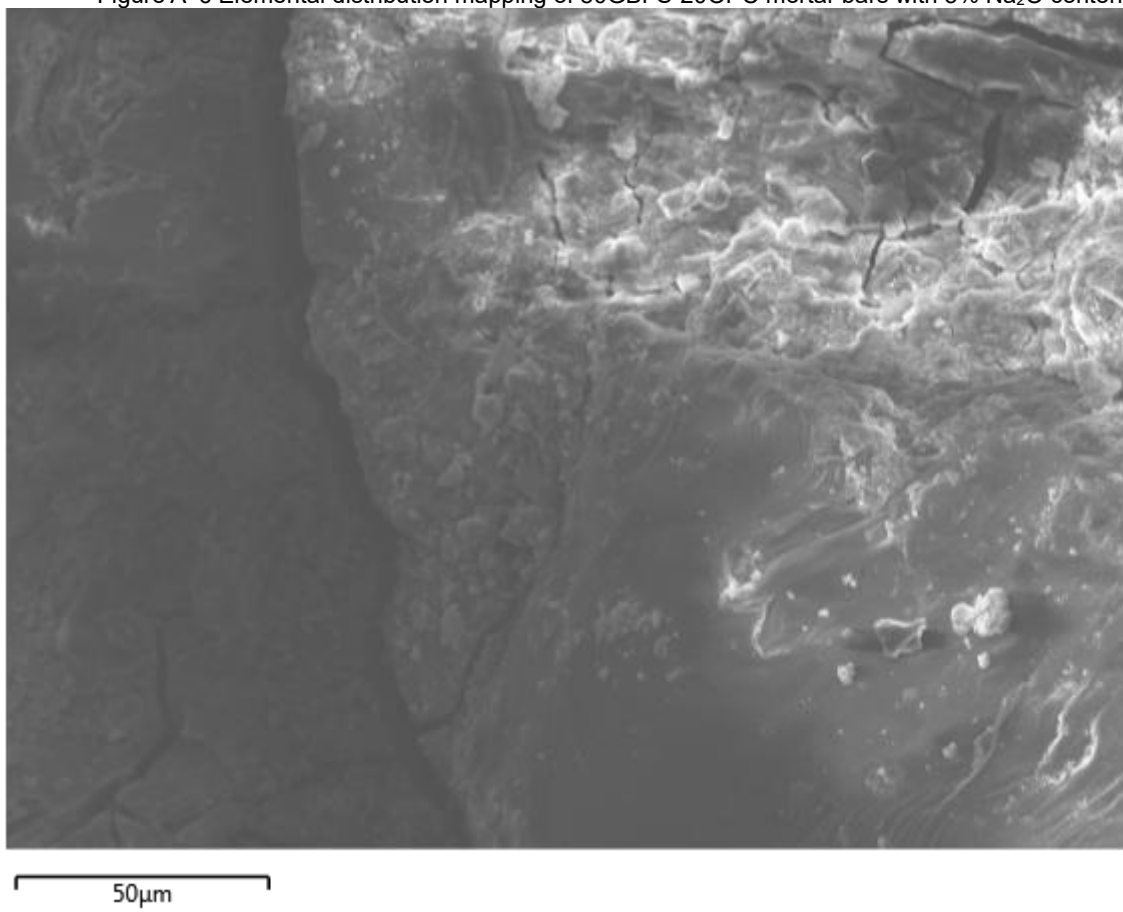
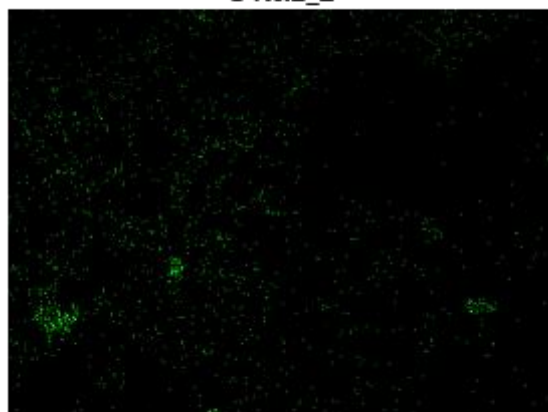


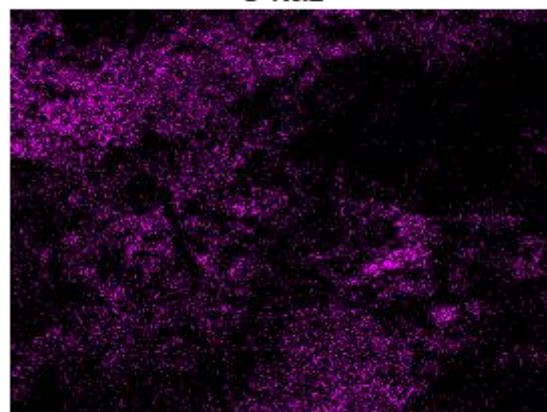
Figure A-6 Elemental distribution mapping of 80GBFS-20OPC mortar bars with 5% Na₂O content.



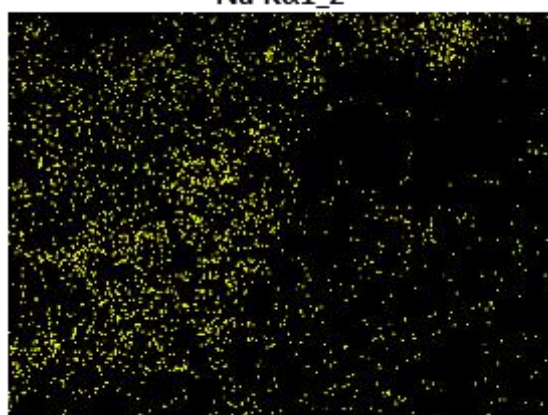
C K α 1_2



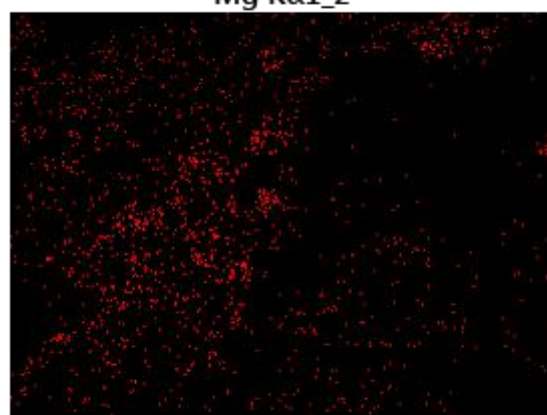
O K α 1



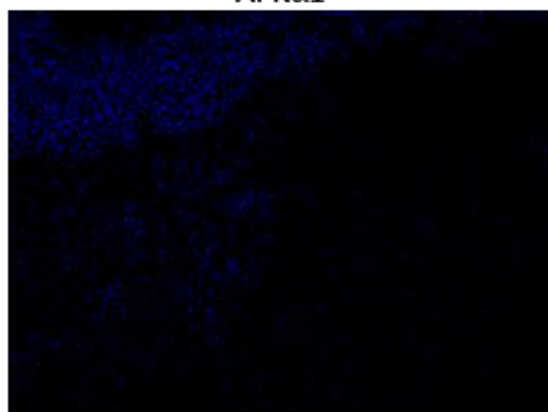
Na K α 1_2



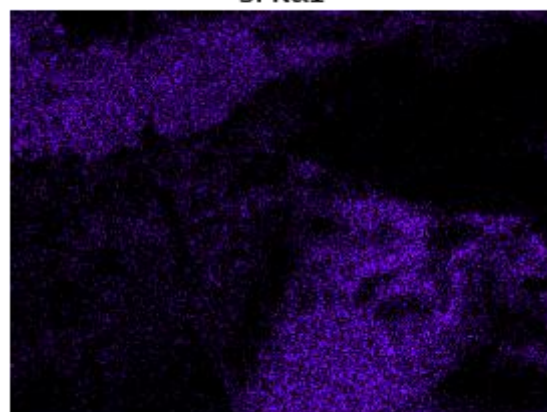
Mg K α 1_2



Al K α 1



Si K α 1



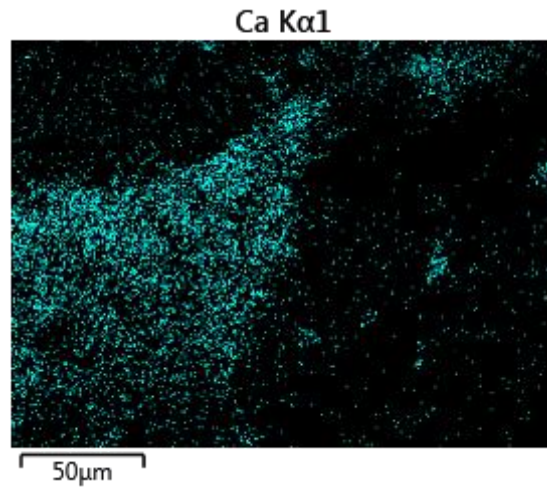
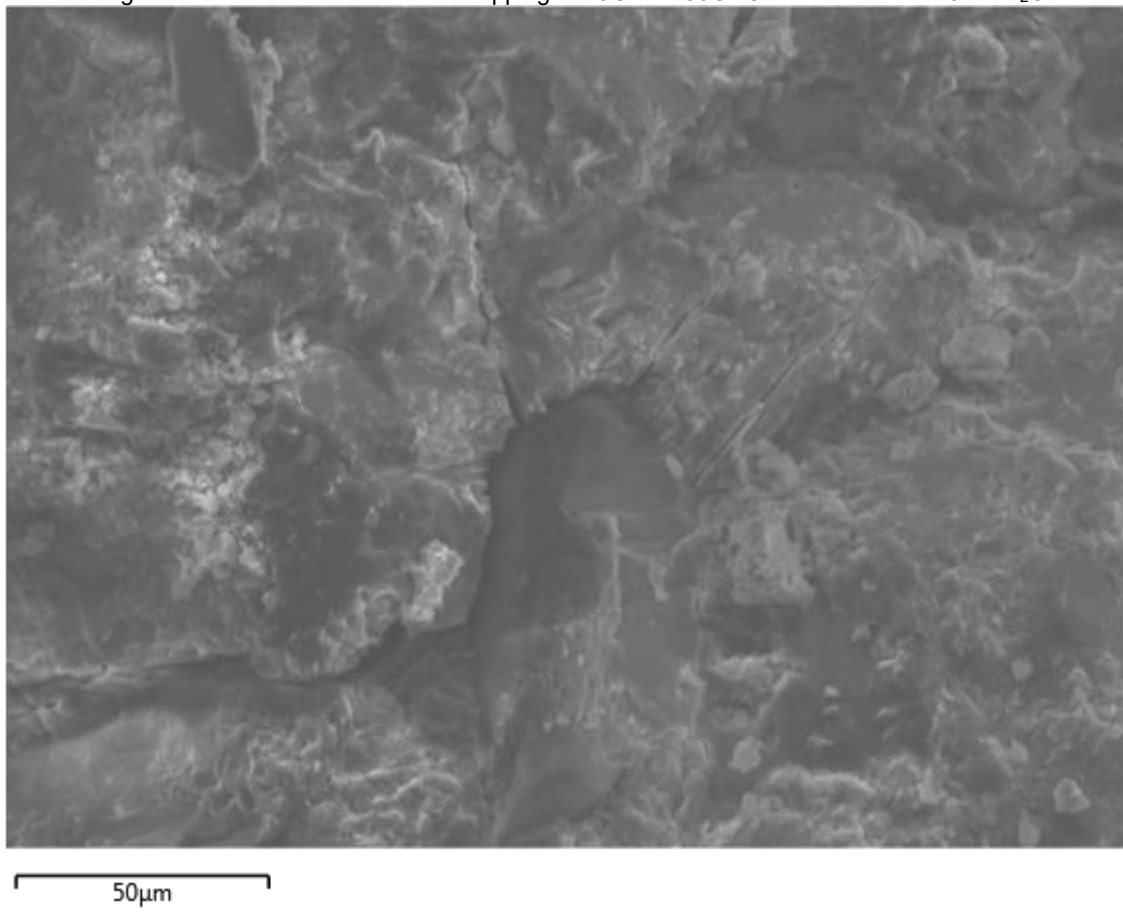
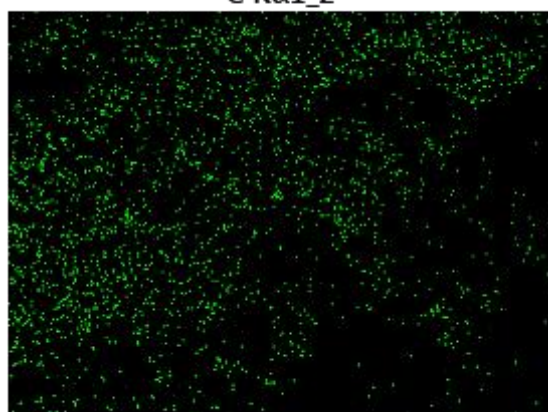


Figure A-7 Elemental distribution mapping of 70GBFS-30OPC mortar bars with 5% Na₂O content

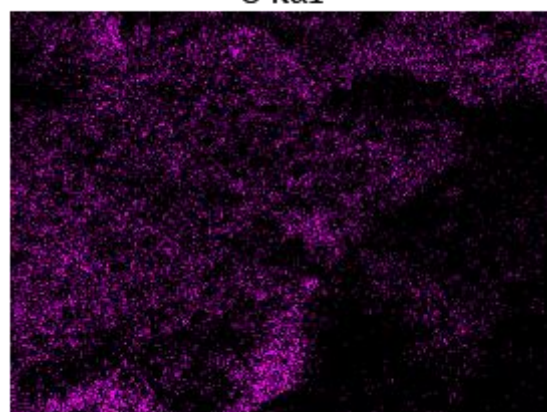


C K α 1_2



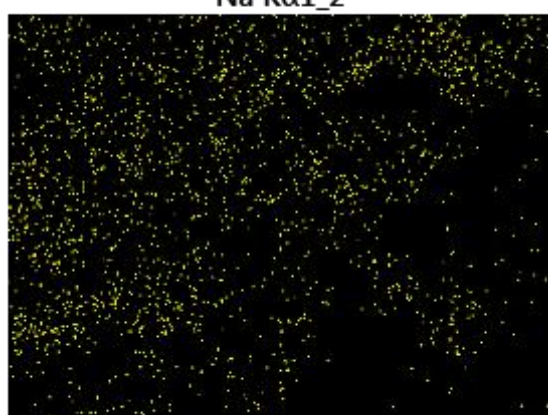
50 μ m

O K α 1



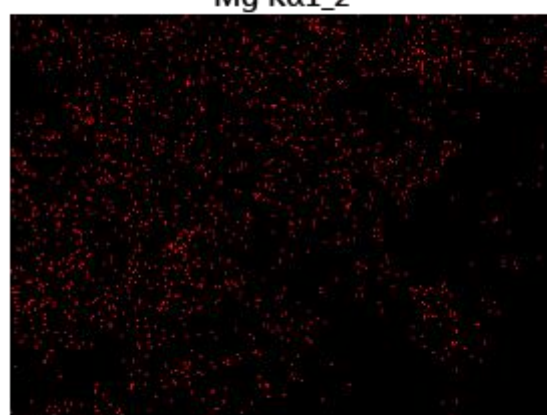
50 μ m

Na K α 1_2



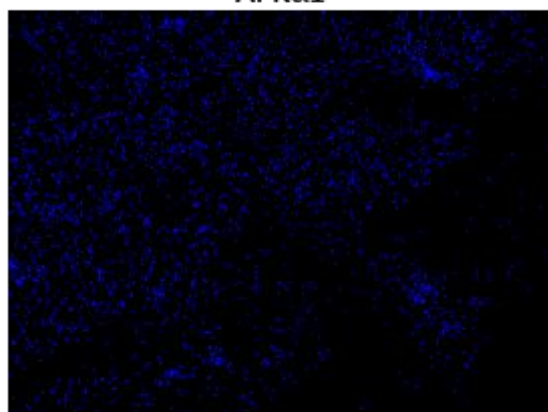
50 μ m

Mg K α 1_2



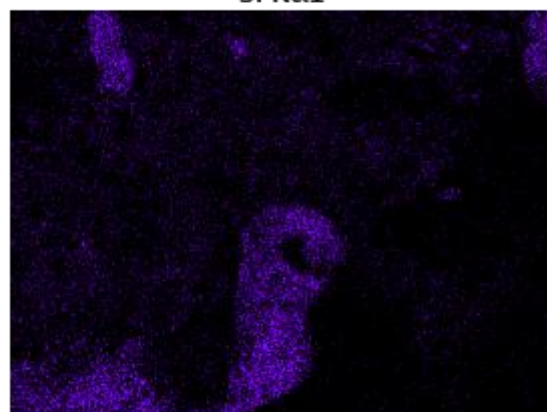
50 μ m

Al K α 1



50 μ m

Si K α 1



50 μ m

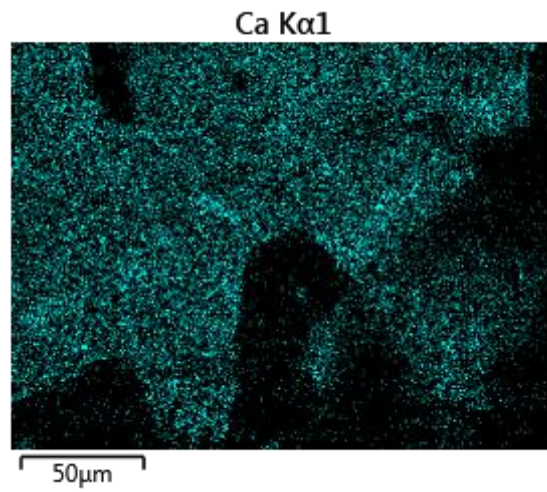
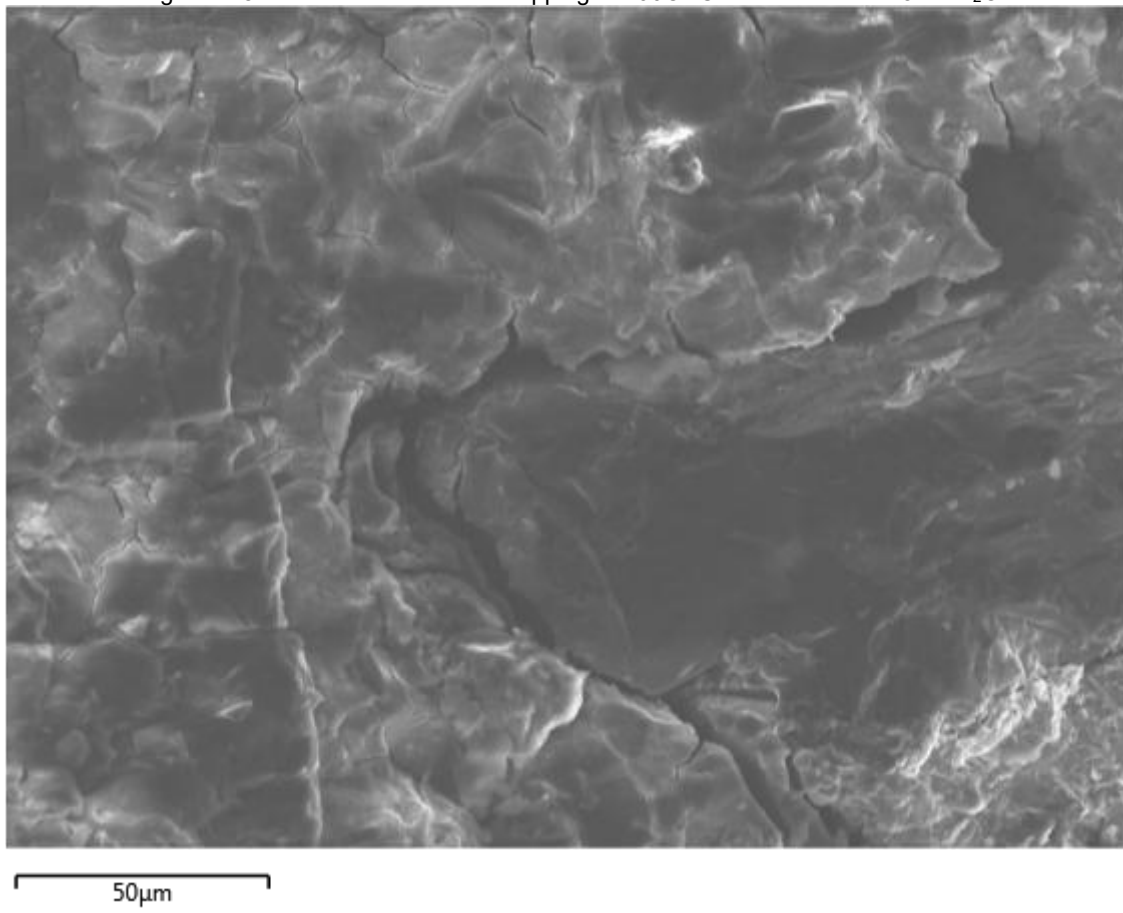
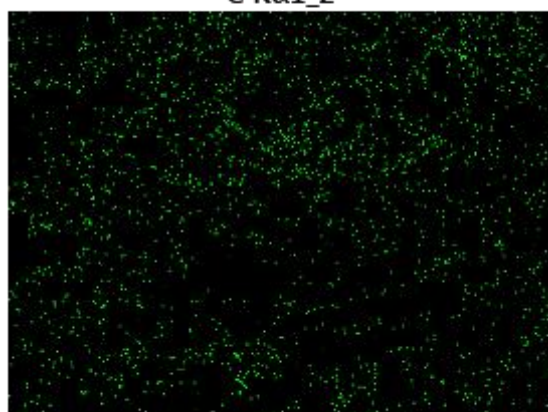


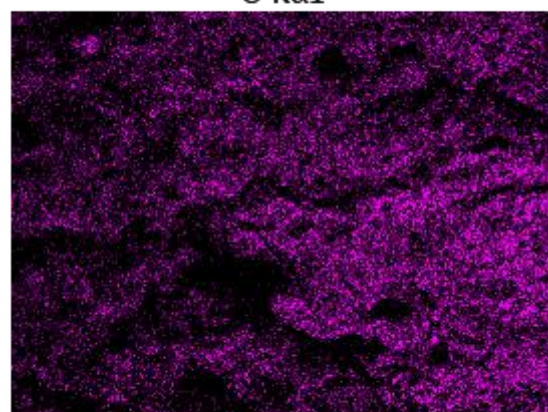
Figure A-8 Elemental distribution mapping of 100OPC mortar bars with 5% Na₂O content.



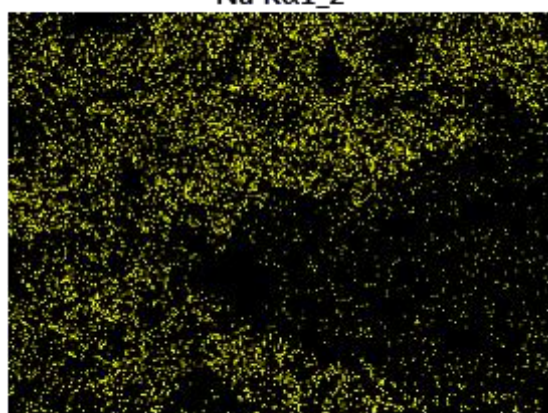
C K α 1_2



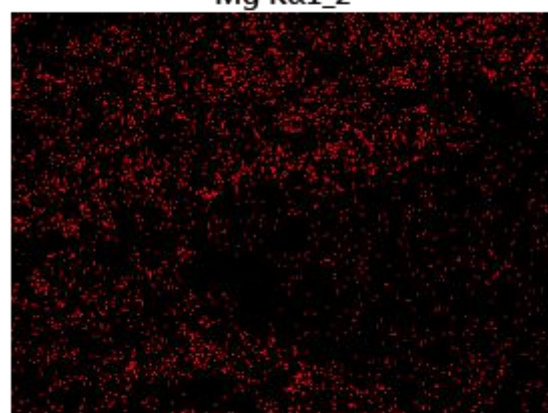
O K α 1



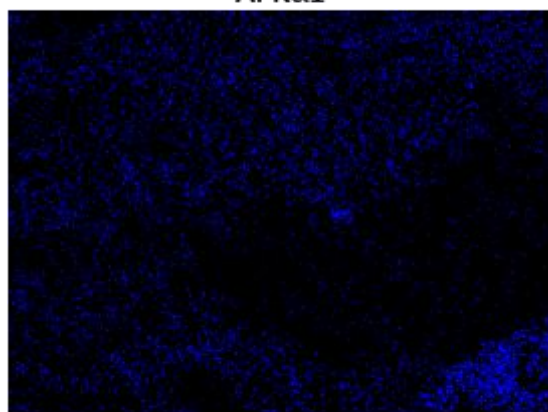
Na K α 1_2



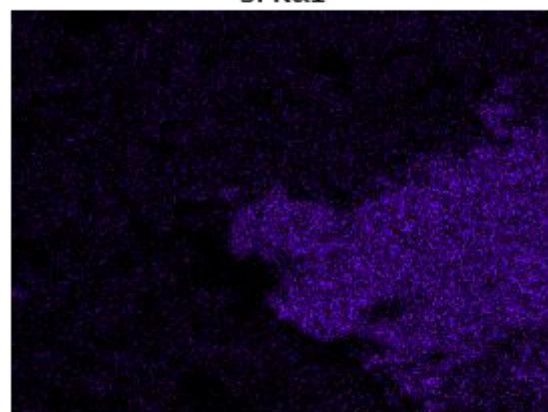
Mg K α 1_2



Al K α 1



Si K α 1



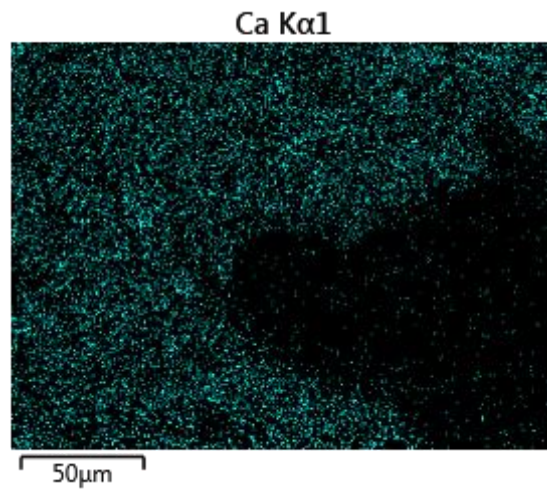


Figure A-9 Elemental distribution mapping of 100GBFS mortar bars with 5% Na₂O content.

APPENDIX B MECHANICAL STRENGTH PREPARATION AND TEST FOR HAC PAST

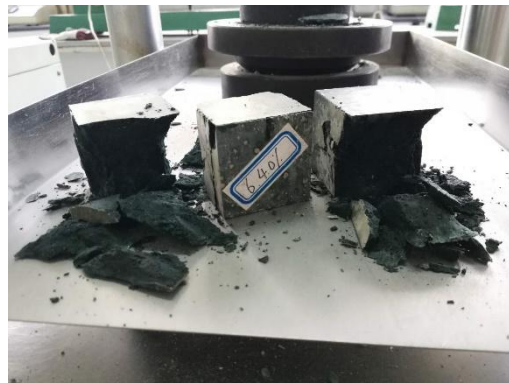
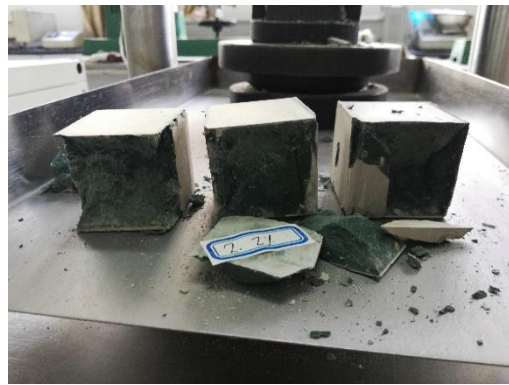




Figure B- 1 Mechanical strength preparation and test for HAC past.

APPENDIX C ^1H NMR TESTING OF ALL BINDER SYSTEMS DURING THE SETTING PERIOD



Figure C-1 ^1H NMR testing of all binder systems during the setting period.

APPENDIX D POOR WORKABILITY OF HAC FRESH CONCRETE



Figure D- 1 Poor workability of HAC fresh concrete.

APPENDIX E DURABILITY OF HAC ON COMPRESSIVE STRESSIV STRENGTH





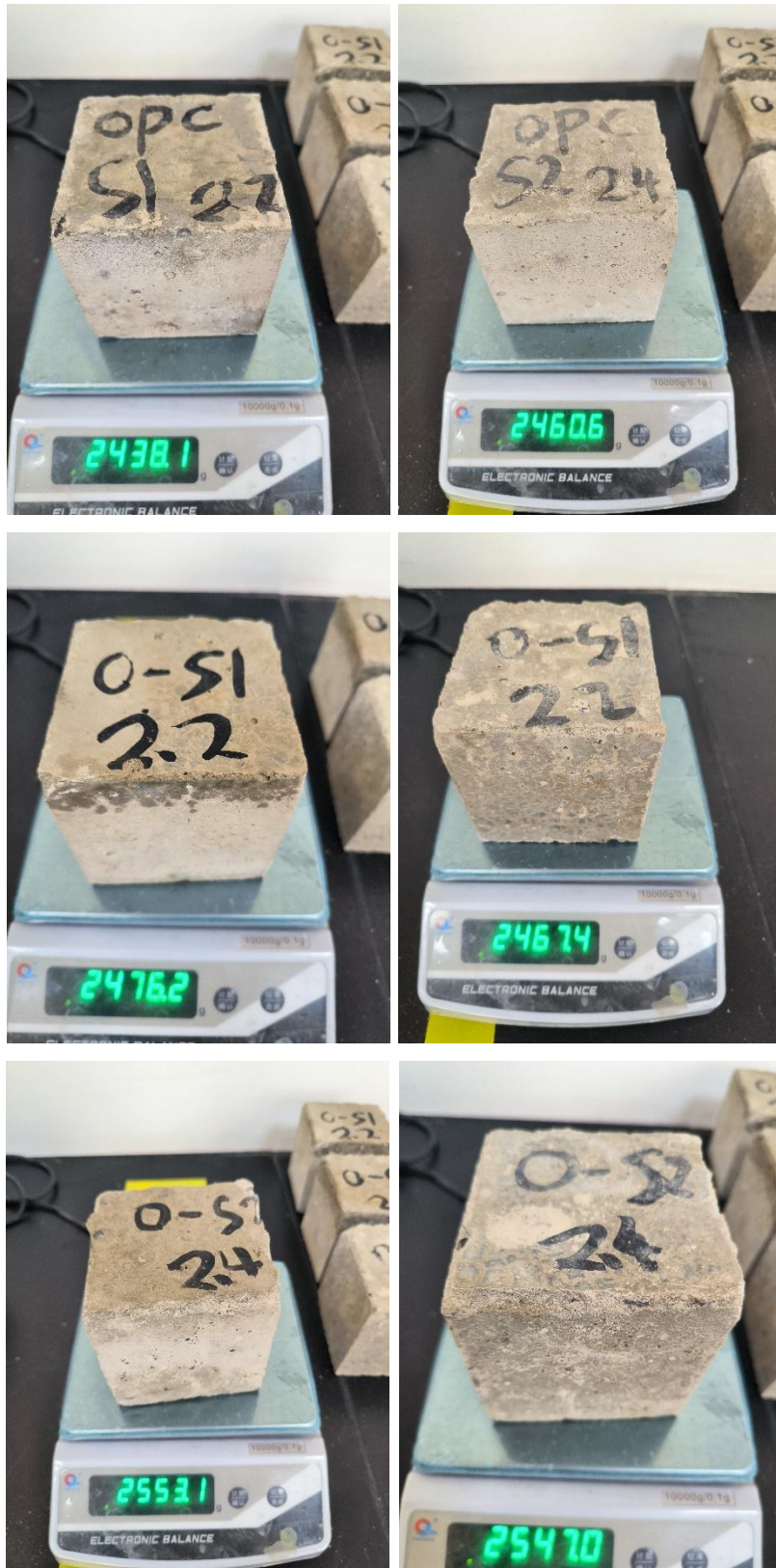
Figure E- 1 Durability of hybrid alkaline cement on compressive strength.

APPENDIX F DURABILITY OF HAC TO CHLORIDE PENETRATION



Figure F- 1 Durability of hybrid alkaline cement to chloride penetration.

APPENDIX G DURABILILTY OF HAC TO SULFHATE ATTACK



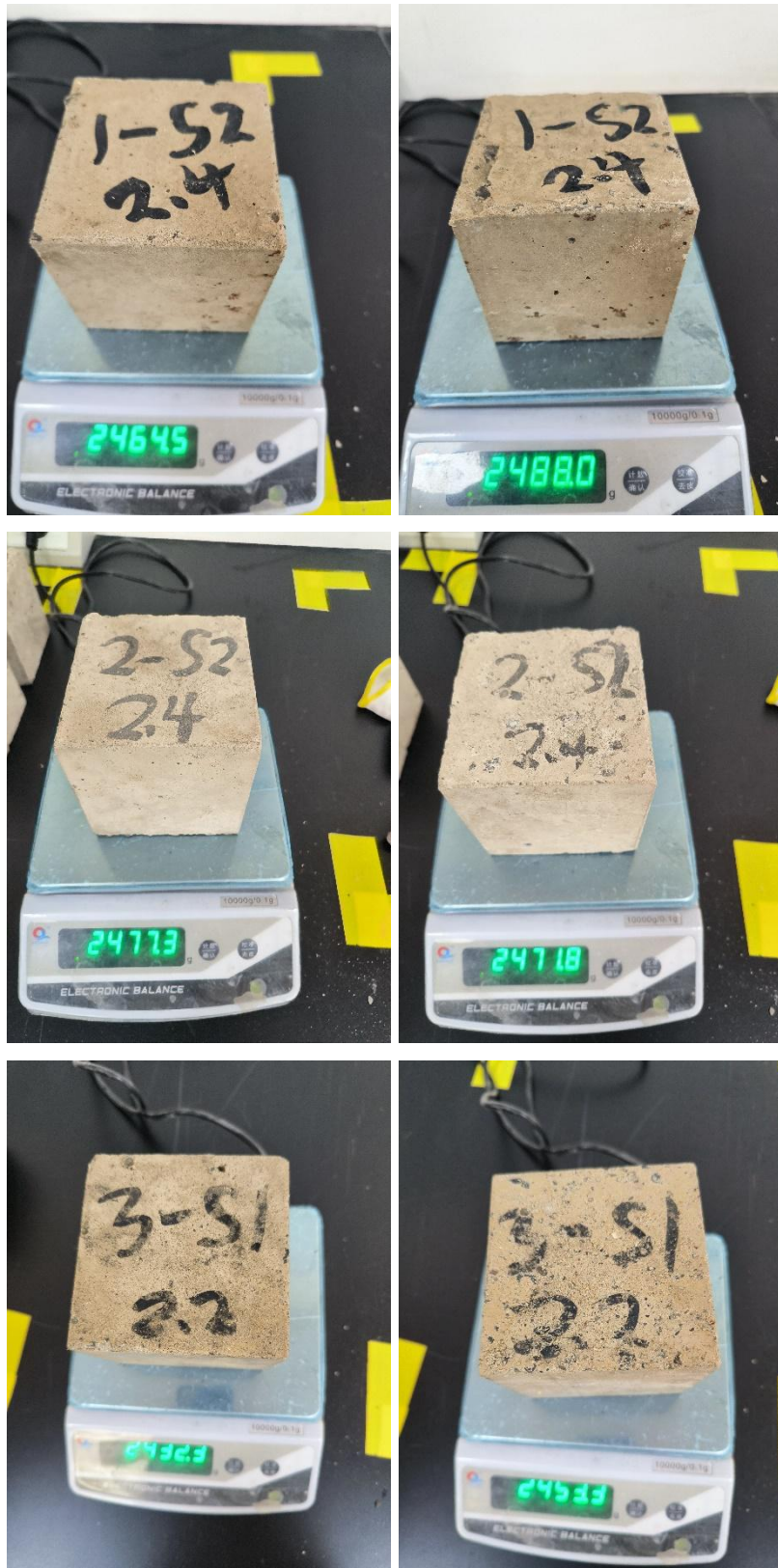


Figure G-1 Durability of hybrid alkaline cement to sulphate attack.

APPENDIX H DURABILITY OF HAC TO ALKALI- AGGREGATE REACTION





Figure H- 1 Durability of hybrid alkaline cement to alkali-aggregate reaction.